Alma Mater Studiorum – Università di Bologna

DOTTORATO DI RICERCA IN

CHIMICA

Ciclo 35

Settore Concorsuale: 03/A1 CHIMICA ANALITICA

Settore Scientifico Disciplinare: CHIM01/ CHIMICA ANALITICA

ANALYTICAL PYROLYSIS TO STUDY MICROPLASTICS AND OTHER POLYMERS IN THE ENVIRONMENT

Presentata da: Irene Coralli

Coordinatore Dottorato

Prof. Luca Prodi

Supervisore

Prof. Daniele Fabbri

Esame finale anno 2023

Abstract

Synthetic polymers constitute a wide class of materials which has enhanced the quality of human life, providing comforts and innovations. Anyway, the increasing production, the abuse and the incorrect waste management, are leading to the widespread occurrence of polymeric materials in the environment, generating concern. In order to understand the extent of this issue, analytical identification and quantification of those polymers hold an essential position. However, standardised methods have not established yet, and additional studies are required to improve the present knowledge. The main aim of this thesis was to provide comprehensive information about the potential of pyrolysis coupled with gas-chromatography and mass spectrometry (Py-GC-MS) for polymers investigation, from their characterisation to their identification and quantification in complex matrices. Water-soluble (poly(dimethylsiloxanes), PDMS, and their poly(ethylene glycol), PEG, copolymers) and water-insoluble polymers (microplastics, MPs, and bioplastics) were studied. The different studies revealed the possibility to identify heterogeneous classes of polymers, fingerprinting the presence of PDMS copolymers and distinguishing chemically different polyurethanes (PURs). The occurrence of secondary reactions in pyrolysis of polymer mixtures was observed as possible drawback. This study resulted in the identification of pyrolysis products indicative of interactions and their reaction mechanisms. Py-GC-MS also revealed its fundamental role for the identification of polymers composing commercial items based on bioplastics. The results aided to identify the chemical nature of non-intentionally added compounds that have the potential to migrate in sea waters. Investigations were not circumscribed to purely laboratorial analyses, but the potential of Py-GC-MS was also tested on environmental samples. Results demonstrated the capability to provide reliable, reproducible and comparable quantitative results about polymers in complex matrices (PEG-PDMS in sewage sludges and PURs and other MPs in road dusts and spider webs), proving the simultaneous quantification of different analytes, within discussed restrictions. Criticisms of Py-GC-MS analyses were especially found in quantitation, such as the selection of polymer standards and reference materials, the construction of reliable calibration protocols and the occurrence of bias due to interferences of polymers with environmental matrices or other polymers. This thesis pursues the greater purpose to develop harmonised and standardised methods for environmental investigations of polymers, that is fundamental to assess the real state of the environment.

Table of contents

1. Introduction 1

1.1. Polymers as emerging environmental contaminants..... 1

1.1.1. Water-soluble polymers.....2

1.1.2. Water-insoluble polymers.....5

1.2. Analytical techniques for the investigation of polymers..... 22

1.2.1. Pyrolysis coupled with gas-chromatography and mass spectrometry 28

1.2.2. Environmental investigation: harmonization is the key 31

2. Aims.....58

3. Experimental results 60

3.1. Applications of Py-GC-MS for the investigation of water-soluble polymers 60

3.1.1. Analytical pyrolysis of poly(dimethylsiloxane) and poly(oxyethylene) siloxane copolymers. Application to the analysis of sewage sludges.....60

3.2. Applications of Py-GC-MS for the investigation of water-insoluble polymers 87

3.2.1. Secondary reactions in the analysis of microplastics by analytical pyrolysis..... 87

3.2.2. Determination of polyurethanes within microplastics in complex environmental samples by analytical pyrolysis 121

3.2.3. Analysis of seawater leachates from bioplastics: an analytical pyrolysis and GC-MS study 159

4. Conclusions 206

1. Introduction

1.1. Polymers as emerging environmental contaminants

Anthropocene Epoch describes the most recent period in Earth's history [1]. The term Anthropocene derives from the Greek word *anthropo* ("man") and *cene* ("new") and it was coined by the biologist Eugene Stormer and the chemist Paul Crutzen in 2000, inspired by the event that identify the epoch: human activity that started having a significant impact on the planet's climate and ecosystems [1–3]. The beginning of Anthropocene is debated, according to a popular theory it began at the start of the Industrial Revolution of the 1800s, when human activity had a great impact on carbon and methane in Earth's atmosphere. Other scientist referred the beginning of Anthropocene to 1945, when humans tested and then dropped atomic bombs on Hiroshima and Nagasaki, Japan, resulting in radioactive particles globally spread [1,3]. Most of the human daily activities produce (intentionally or not) compounds that are release in the environment, differently affecting the ecosystem's dynamisms. Among these compounds, pollutants have regulated emission because the risk that they cause on the environment is verified, whereas emerging contaminants (ECs) pose a challenge for regulatory agencies. Smital (2008), defined emerging contaminants as *"any synthetic or naturally occurring chemical or any microorganism that is not commonly monitored in the environment, but has the potential to enter the environment and cause known or suspected adverse ecological and/or human health effects*" [4]. In this context, the term "emerging" has double meaning, including both contaminants that only recently have appeared in the environment and contaminants already present in the environment, but whose concern has been raised much more recently [5]. According to toxicology, the main characteristics of contaminants are persistence, lipophilicity (preference for fat-tissue, which determines bioavailability), and toxicity (both acute and chronic). ECs usually exhibit pseudo-persistence, meaning that their continuous occurrence in the environment is not due to a persistent behaviour, but to their constant release [6]. Typically, ECs are categorise as: pharmaceuticals and personal care products (PPCPs), surfactants, plasticizers, pesticides, flame retardants and biological ECs [2,4]. Anyway, given the definition of ECs, polymeric materials can be included in the class. The first polymer was invented treating cellulose in 1869 by Jhon Wesley Hyatt who was looking for a substitute of ivory [7]. This revolutionary discovery led to the expanding research of new materials, to create substitutes of traditional materials (protecting natural resources from the destructive forces of human need)

or to create new useful, comfortable and innovative materials. The invention of new materials has continuously increased, leading to improvements in industrial processes, personal care formulations, medical features, technology and so forth, enhancing the quality of human daily life. During the last decades, the environmental investigation of polymers has become of interest, mainly because the surprisingly widespread occurrence. Even though some classes of polymers demonstrate to have no harmful adverse effect on ecosystems, their constant release may represent a concern because of the pseudo-persistent behaviour. Moreover, for most of the existing polymers, environmental behaviour, toxicity and interaction with organisms are still under study. Analytical investigation plays a key role in understanding the extent of the issue, to then formulate regulation and organise mitigation actions.

In the field of environmental pollution, great attention has been paid to solid (water-insoluble) polymeric materials, such as plastics, while the group of water-soluble polymers, has been less considered, partly because they look like "invisible" entities. In this thesis work both categories have been considered.

1.1.1. Water-soluble polymers

Water-soluble polymers are materials that modify the physical properties of aqueous systems by dissolving, dispersing or swelling in water, defining gelation, thickening, emulsification, stabilization by rheology modifications [8,9]. Both natural and synthetic polymers can be part of this class of materials, which include broad arrays of molecular chemistry, structures and sizes [10,11]. To achieve hydrophilicity, polymers must contain specific units in their backbones (such as O and N atoms), that supply lone pair electrons for hydrogen bonding to water, or other hydrophilic functional groups (e.g., OH, NH_2, CO^-_2, SO^-_3) [10,12]. The ultimate properties of the final aqueous system and performances of water-soluble polymers depend on structural characteristics: both the nature of the repeating units (chemical composition, characteristics of the involved bonds, locations and frequency [10,12]) and the spatial configuration of chains (linear, branching, crosslinked, intramolecular effects [8,10,12]) are relevant [13]. Chemical and physical/mechanical properties are expression of those structures, and they can be mainly predicted considering the chemical nature and hydrodynamic volume of the chains while they are in solution [13]. The latter is mainly determined by the polymer's molecular weight (MW) and the conformational rigidity of the chains, mainly influencing the viscosity efficiency [12]. Despite relative abundances of polymer in water solutions are usually low [10], they significantly generate new properties of aqueous systems which can be exploited commercially in a variety

of industrial applications. According to Williams (2007) [10], they play key roles in increasing the viscosity of solutions, forming physical gels, stabilising dispersions and emulsions, inducing particle aggregation to facilitate solid–liquid separation, modifying surface properties to control wetting properties and inhibit deposition, solubilising hydrophobic compounds by complexation and facilitating the controlled release and delivery of active compounds [14]. These aptitudes highlight the extent of the power in using water-soluble polymers in many fields of applications. Nowadays, this polymer class have a broad range of applications including, detergents [15], cosmetics and personal care products [16,17], foods [18], pharmaceuticals [8], paints and other coatings [19], paper [20,21], waste water treatment [22,23], hydraulic fracturing [11], agriculture [24], etc.

An extract of the most commonly produced and used water-soluble polymers is listed in Table 1.1.1-1. Structures, properties and main field of applications are explained in order to show the extent of the potential this class of materials.

Table 1.1.1-1. *Overview on the most commonly used synthetic and natural water-soluble polymers [8,25].*

Polymer	Structure	Properties	Applications	References
Synthetic				
Polyethylene glycol (PEG)	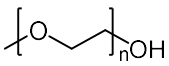	Highly soluble in organic solvents Low toxicity High capability to enhance the solubility of hydrophobic molecules or to prevent aggregations	Applications as lubricants, coatings, osmotic pressure agent, electrolytic solvent, ingredient of cosmetic and personal care products, medical laxatives, nanotechnologies, flocculant in water purification, etc.	[26–29]
Polyvinyl alcohol (PVA)	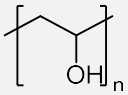	Soluble in highly polar and hydrophilic solvents Non-toxic, non-carcinogenic It presents a rubbery and elastic nature that simulates natural tissue Widely used as a thickening, suspending and emulsion stabilizing agent in low viscosity systems	Applications as ingredient in paper-marking lubricants, bio adhesives, component of pharmaceuticals, drug delivery carriers, textile field, coatings, metal removal, etc.	[30–32]

Polyacrylamides 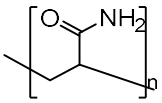	Chemically inert and stable over various conditions (e.g., pH 3 - 11) Non-toxic but controversial ingredient because of its potential ability to secrete acrylamide Gels can have a range of pore size	Used in fractionation of differently sized macro and micro biomolecules, ingredient of cosmetic and personal care products, film former in food applications, medium in electrophoretic techniques, delivery and removal of bioactive macromolecules (e.g., insulin or toxins), etc.	[16,33–35]
Polyacrylic acid (PAA) 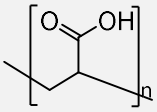	Biodegradable pH modification changes it form, liquid at pH 5 and as a gel at pH 7 It can be hydrophobically modified allowing aggregation followed by an increase in the apparent MW which enhances viscosity of solutions	Applications in super absorbent products (e.g., in disposable nappies), water treatment, medical features, drug delivery carrier, tissues engineering, etc.	[36–40]
Polyethyleneimine (PEI) 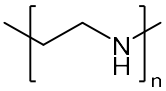	Excellent stability in aqueous solutions Organic polymer with the highest positive charge density potential Two main existing forms, linear and branched Low biodegradability, good safety profile Possibility to create bonds with inorganic matrices (e.g., silica)	Applications in tie-coat adhesives, laminated films, resins and pigment dispersants, paper-making, water purification from heavy metals, acidic gas absorbent, in the drilling and completion of oil and gas wells, ingredient of cosmetics and personal care products, medical applications, etc.	[15,41–45]
Polyvinylpyrrolidone (PVP) 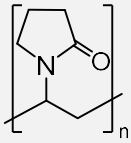	Basic water-soluble polymer that is also soluble in polar solvents Thanks to its universal solubility is widely use in blend with many materials Easily processable with Good electrical properties, environmental stability and excellent optical transparency	Applications in electrical devices, coatings, of pharmaceuticals formulation, cosmetics, lubricants, as a stabilizer, etc.	[46–49]

Natural			
Guar gum 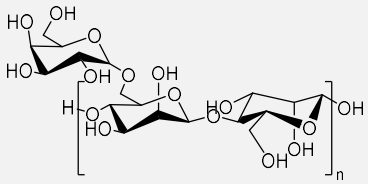	Derive from the endosperm of the guar plant (*Cyamopsis tetragonoloba*), high MW hydrocolloidal polysaccharides	Applications as binder, disintegrant pharmaceutical tablet formulation, stabilizer, emulsifier, thickening, and suspending agent in liquid ingredient in food packaging, cosmetics personal care products and pharmaceutical, drug delivery carrier, etc.	[50–52]
Xanthan gum 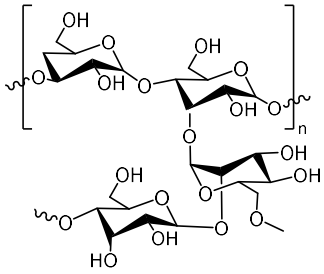	Derive from the fermentation of corn starch (*Xanthomonas* Campestris) Provide viscous solutions at low concentrations, effective thickener and stabilizer Pseudoplastic behaviour	Applications as thickener and stabilizer in personal care products, cosmetics, emulsifier or surfactant in pharmaceuticals, used in most of the ready to eat, semi-prepared foods and convenience foods, acting as stabilizer, etc.	[53–55]
Pectin 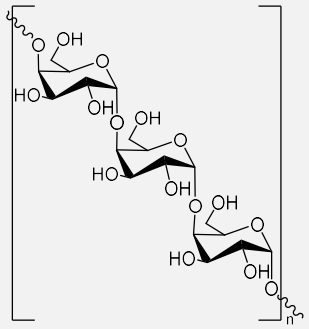	Mixtures of polysaccharide deriving from plants, mainly citrus peel or apple pomades	Applications in pharmaceuticals, cosmetics and personal care ingredient (in form of microspheres), drug delivery carrier, thickening stabilizing and gelling agent stabilizer in food and beverage industry, applications in lead and mercury removal from the gastrointestinal tract and respiratory organs, etc.	[56–58]
Chitosan derivatives 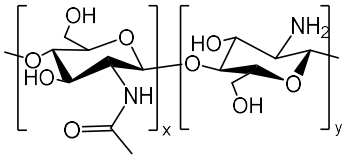	Linear polysaccharide made by treating the chitin shells of shrimp and other crustaceans with an alkaline substance Biodegradable, bio compatible, with low toxicity Usually, modifications are required because it is not easily soluble in water and in neutral pH	Applications in food processing to waste management, medicine, biotechnology for orthopaedic devices and connective tissues, Ingredient in pharmaceutical industry, applications in industrial effluent purification in metal removal, etc.	[59–61]

1.1.2. Water-insoluble polymers

Water-insoluble polymers consist of a broad class of materials that has gained the predilection in human life, mainly composed by plastics and rubbers. Certainly, properties that have led

water-insoluble polymers to this high success are the low production costs, the relatively low density of materials that results in their light weights and the possibility to variate chemical, physical and mechanical properties leading to a wide versatility. In fact, polymer properties can be modulated in manufacturing phase, not only depending on the chemistry of the involved monomers, but also on the basis of distribution of repeating units, the length of the chains (degree of polymerisation that determines the MW) and their architecture (linear, branched, cross-linked). Moreover, for some polymers (e.g., polypropylene, polymethylmethacrylate, polyvinylchloride, etc.) also the isomeric distribution of chains and the whole configurational isomerism generates further differences in properties (such as flexibility or fragility). All these microscopic properties are reflected on the macroscopic ones, defining different mobility of chains and interactions among them that are translated in different physical and mechanical properties (mainly based on the crystallinity degree). Depending on the chemical structure and the synthesis process, polymers can present highly different properties, for examples they can be rigid or flexible, insulators or conductors, thermoplastic or thermos-setting, etc. In the case that modulating of structures is not sufficient, chemicals are added during compounding to meet the needs of the specific applications. Different type of molecules can be added, depending on the purpose. Additives can enhance the polymer transformation (e.g., stabilizers, lubricants, melting promoters), modulate of mechanical properties (e.g., plasticizers, reinforcing charges, tenacity improvers), prevent ageing (e.g., antioxidants, UV stabilizers), modify surface properties (e.g., antistatic agents), change optical properties (e.g., pigments, colourants, nucleating agents), improve fire-resistance (flame retardants, fire extinguisher agents, anti-smoking agents), modify foaming properties (expanding agents). Finally, polymers are very easily shaped into complex forms, allowing the integration of plastic materials in a wide variety of functions. Therefore, it is easy to understand how polymers are widespread in every aspect of our everyday life. In facts, since they have been introduced in society, a real revolution occurred such that our life without plastics is inconceivable [62,63].

Primary plastic production data describe an annual substantial increase from 1950s to 2019. A hard decrease was noticed in 2020 due to Covid-19 pandemic and the most affected field was that of automotive (Figure 1.1.2-1) [64]. A good recovery occurred in 2021, but during the first part of 2022 plastic production seems to be further decreased. Certainly, a first reason can be attributed to the slowdown in global economy, resulting in a lower demand for plastics in primary forms. Moreover, high energy and production costs in Europe have to be taken into account, leading to a reduction of exports [64]. Anyway, plastics compounding companies in Europe are 52000, demonstrating the contribution of the sector to economy, including 1.5 million of employees [65].

According to Plastic Europe, 40.5 % of plastics is addressed to packaging applications, followed by the building and construction (20.4 %), automotive (8.8 %), electrical and electronical sector (6.2 %), etc. (Figure 1.1.2-2). Depending on the field of application, different polymers a preferred, but polyethylene (PE), polypropylene (PP), polyvinylchloride (PVC) and polyethylene terephthalate (PET) are overall predominant. An overview on the most commonly used water-insoluble polymers is shown in Table 1.1.2-1.

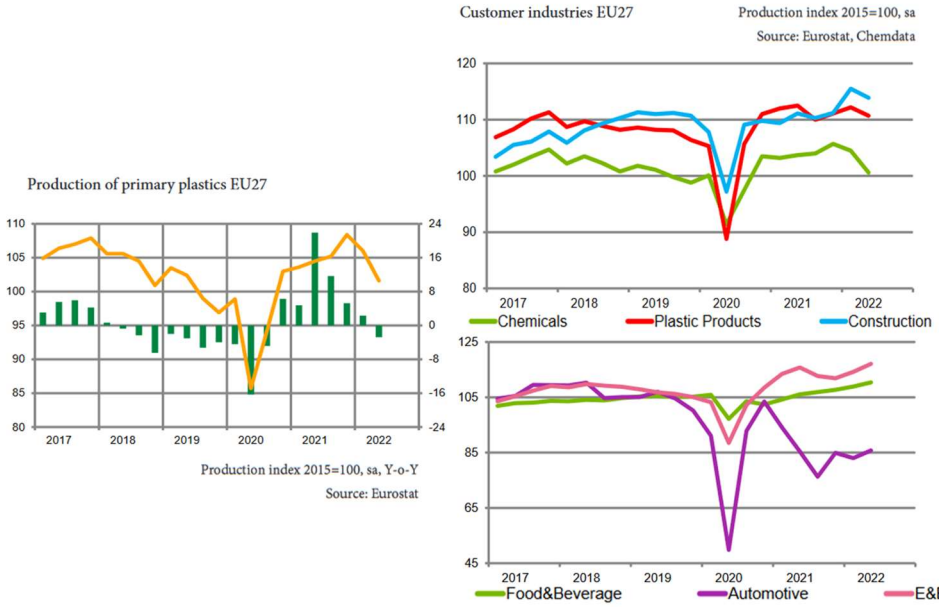

Figure 1.1.2-1. *Tends of production of primary plastics and related costumer industries [64].*

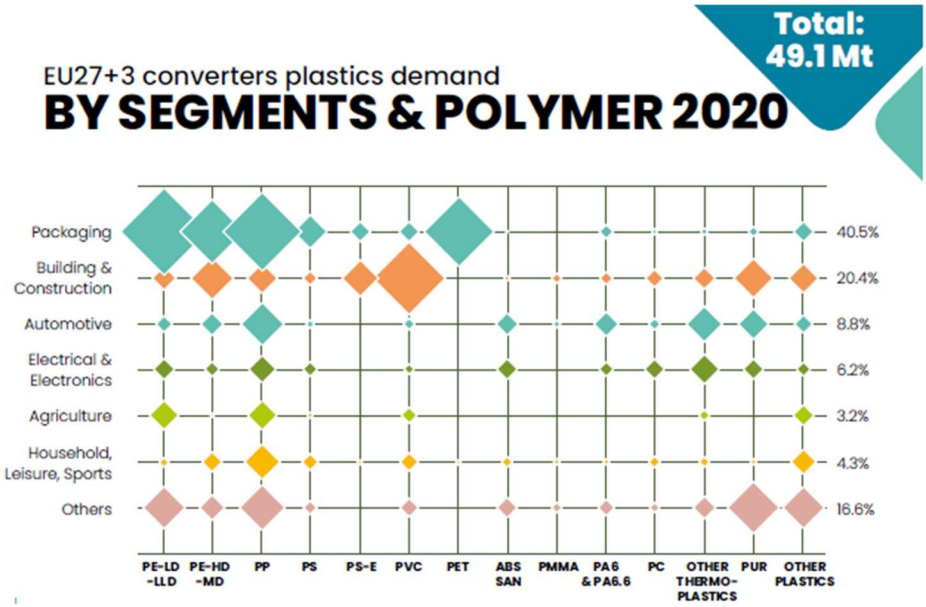

Figure 1.1.2-2. *Polymer application in different fields [65].*

Table 1.1.2-1. *Overview on the most commonly used water-insoluble polymers, plastics [65].*

Polymer	Structure	Properties	Applications	References
Polyethylene (PE)	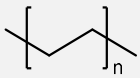	14.9 % of the European plastic production (including high density, HD 6.32 % and low density, LD 8.57%) HDPE: resistant to acid and bases, easy to process and mould, good electrical insulation, waterproof LDPE: high tensile strength, resistant to low temperature, relatively strong and stiff, waterproof, good electrical insulation	Applications of LDPE in reusable bags, trays, food packaging films and containers, agricultural film, Corrosion protection layer for work surfaces, computer hardware covers and packaging etc.; HDPE used for milk, detergent, shampoo bottles, pipes, houseware, fibres for ropes, nets, and industrial fabrics, vehicle fuel tanks, boat parts, pipes and tubing, chairs and tables, playground structures, trash and recycling bins, ice cube containers, toys, ice chests, etc.	[65]
Polypropylene (PP)	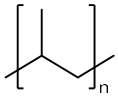	9.7 % of the European plastic production Waterproof and highly resistant to solvents and acids Resistant to thermal stress and moderately resistant to mechanical stress and UV oxidation	Applications in food packaging (e.g., sweet and snack wrappers), kitchen equipment (e.g., hinged caps, microwave containers), fashion industry (e.g., outdoor accessories, reusable bags), buildings (e.g., pipes), automotive parts, medical industry, bank notes, textile, etc.	[65]
Polyvinylchloride (PVC)	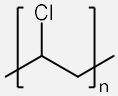	4.7 % of the European plastic production In its pure form is rigid, but plasticisers are usually added to produce flexible forms Rigid: highly stiff, intrinsic flame retardant, suitable for transparent applications, moderate chemical resistance, good electrical insulation Flexible: high impact strength, good resistance to UV, acids, bases, oils, and corrosive chemicals, good electrical insulation, non-flammable	Applications in buildings (e.g., window frames, profiles, floor and wall covering, pipes, cable insulation), packaging (e.g., blister and clamshell packaging for medicines, personal care products), household goods (e.g., raincoats, boots and shower curtains, inflatable pools), medical industry (e.g., blood-collection bag), etc.	[65,66]

Polyethylene terephthalate (PET) 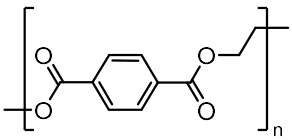	4.1 % of the European plastic production Good chemical resistance to most mineral acids, conventional bleaching agents, cleaning solvents and surfactants High rigidity and hardness, but good creep resistance Lightweight and naturally transparent	Applications in textile (fibres for most of the common synthetic clothes), packaging (e.g., bottles for water, soft drinks, cleaners), automotive (e.g., cases, screen wiper arms and door handles), electronics (e.g., covers, switches, insulation panes), medical industry (e.g., functional parts in drug dosing systems), mechanical engineering (e.g., gears and sliding elements), etc.	[65]
Polyurethanes (PURs) 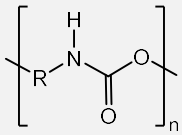	3.8 % of the European plastic production It can be produced in different form: foams, coatings, adhesive, sealant, elastomers… Flexible foams: light durable, supportive, comfortable Rigid foams: most economic and energy efficient insulation, good electrical insulation, good thermal insulation, good noise insulation Coating, adhesive, sealants, elastomers: wide versatility, shining properties, colour durability increaser, flexibility, resistant to corrosive agent	Applications in building (e.g., insulating foams, pillows and mattresses), shoes and clothes (e.g., artificial leather), foam protections for automotive sector (e.g., seat cushioning and cover, internal noise insulation), gym equipment (e.g., handlebar protection), adhesives, sealants, binders, coatings, paints and varnish, etc.	[65,67,68]
Polystyrene (PS) 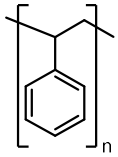	3 % of the European plastic production Highly versatile depending on manufacture: Crystal-clear polystyrene, is a fully transparent, rigid and rather brittle Expanded form is thermally insulating, with high impact resistance and good processability Widely used in copolymers	Applications in food packaging (e.g., dairy, fishery), disposable items (e.g., cups, glasses, dishes), building and insulation (e.g., sheets, foams), electrical & electronic equipment, brush handles, and combs inner liner for fridges, eyeglasses frames, etc.	[65,66]

Polyamides (PA-6 and PA-6,6) 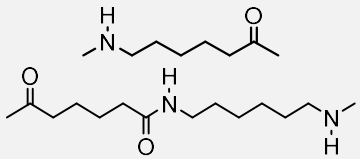	0.85 % of the European plastic production Polyamides are a family with recurring amide groups as integral parts of the polymer backbone High wear resistance and excellent elastic revery behaviour High thermal stability and chemical resistance Very good strength and hardness related to fibres morphology	Applications in textile (fiber for underwear, sport apparels), automotive (e.g., valve covers, airbag containers), food and beverage packaging, robotics (e.g., wire and cable protection), etc.	[65,69]
Polycarbonate (PC) 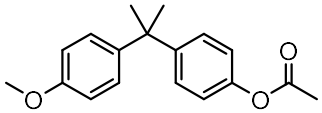	0.73 % of the European plastic production High impact strength, resistance and dimensional stability Transparency and lightness Good electrical properties, thermal stability and chemical resistance	Applications in beverage containers (e.g., baby bottles, refillable water bottles, Sippy cups), automotive (e.g., machine parts and electronic components), buildings (e.g., window, skylight applications), eyeglass lenses, compact discs, sealants (e.g., dental application), plastic dinnerware, room divider, etc.	[65]
Acrylonitrile butadiene styrene (ABS) 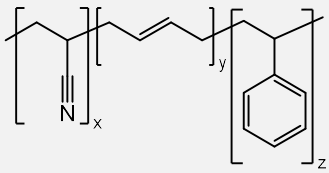	Together with SAN covers 0.83 % of the European plastic production High resistance to impact, abrasion and strain Good tensile strength, surface hardness, rigidity Fire-retardant and heat-resistant and electrical characteristics	Applications in electronic housings, auto parts (e.g., hub caps, dashboard components, door liners and handles, seat belt components), consumer products, plastic construction toys, pipe fittings, etc.	[65]
Styrene-acrylonitrile (SAN) 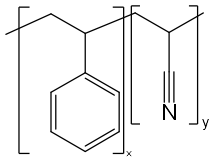	Together with ABS covers 0.83 % of the European plastic production High resistance to grasses, chemicals and stress cracking and crazing Rigid and transparent	Application in kitchen equipment (e.g., mixing bowls, basins, fittings for refrigerators, thermally insulated jugs), food container and storage, office and industrial equipment (e.g., all types of outer covers, printers, calculators, lamps), scales, battery housings, winding cores, etc.	[65]

1.1.2.1. Microplastics

The countless number of benefits, comforts and improvements that plastics have provided to the quality of our life probably lead to think that nowadays living without plastics is inconceivable. Unfortunately, the huge amount of plastic that is in circulation today, together with the future predicted productions and uses, along with an imperfect waste management, put us in front of a serious pollution problem.

According to global estimations, in 2017 about 30 % of the whole plastic produced ever was currently still in use [70]. Given the durability of plastic products, this percentage means that a very large amount of plastics continue to exist in some forms [62,70]. Cumulative plastic waste generation (from plastics and recycled plastics), between 1950 and 2015, was 6300 Mt, where 12 % of plastics have been incinerated, 9 % recycled and only 10 % recycled more than once [70]. More optimistic data showed that 23 % of plastic wastes was disposed in landfills, 42 % was addressed to waste to energy plant and 35 % was recycled in Europe in 2020 [65]. Anyway, given that amount of waste and considering the issue of incorrect waste management, supposedly plastic debris are spread in the environment, threatening soils, fresh water and especially marine environments (where more than 80 % of litter is plastics [71]) . Over the last decade, particular attention was paid on small-size fractions of these debris, the so-called microplastics (MP). Size is the first parameter for their characterisation and, after many definitions expressed over the time, according to Frias and Nash (2019) "*Microplastics are any synthetic solid particle or polymeric matrix, with regular or irregular shape and with size ranging from 1 µm to 5 mm, of either primary or secondary manufacturing origin, which are insoluble in water*" [72]. Later, an ISO regulation limited the size range from 1 µm to 1000 µm [73]. Particles < 1 µm are called nanoplastics, and this size limit was given by the colloidal behaviour that plastics exhibit under this threshold [74]. Trying to relate micro and nano plastics with known and natural components, Figure 1.1.2-3 shows what large MPs are comparable with sand and sediments, but also with some organisms, such as zooplankton, larvae and algae. As regard small MPs, their size is comparable with respirable fractions of particulate (PM_{10}) and, at around 1 µm, particles can potentially cross into cells. This framework gives a first insight on how MP spread can be potentially dangerous.

The second parameter used for MP classification is the origin, defining primary and secondary MPs [75]. Primary MPs are polymeric particles intentionally manufactured within the 1 µm – 1 mm size range. These plastics are generally employed in cosmetic formulations (e.g., scrubs or toothpastes) or used as ingredients in abrasive materials (e.g., in media blasting techniques for rust and paint removal). Over the last few years, in order to mitigate MP emission, the

production of some categories of primary MPs was reconsidered and some regulations have been emitted. Production of microbeads for cosmetic was forbitten in some countries, including United States, United Kingdom and Canada and, European Union (EU) established that rinse-off products containing microbeads were no longer allowed to use the EU ecolabel [76].

Secondary MPs derive from the breakdown of larger plastics and they can be produced while plastics are used or disposed. Plastic items are involved in our daily life therefore, daily actions such as driving car or washing clothes lead to secondary MPs production, for the abrasion of tires or during the centrifuge of synthetic fibres [62,77]. Nevertheless, another important source of secondary MPs is the incorrect management of plastic wastes. When plastic items are released in the environment, they are subjected to many environmental agents which give rise to their degradation. Degradation may be physical, for the mechanical breaking-down of plastics (e.g., due to impacts, dragging, rolling, etc.) but, also oxidative, biological and chemical attacks can occur (e.g., by sun, organisms or pH changes) leading to the weakening of the materials which successively fragmentate [62,76]. Including primary and secondary MPs, many sources of emission can be indicated. Personal care products and cosmetics represent an important source of primary MPs with toothpaste, shaving cream, nail polish scrubs, insect repellents, resin pellets, etc. [78–80]. As mentioned before, this type of primary MPs source is predicted to decrease [76] and the replacement of traditional abrasive materials already started using natural options such as oatmeal, pumice, peanut [81]. MPs from this source are more likely predicted to be found in fresh waters or marine environment because of their domestic use which determinate their release in wastewaters. Another interesting source of domestic MPs is from washing machines [82,83]. These secondary MPs are produced by mechanical (centrifuge phase, powdery detergents rubbing) and chemical stresses (use of detergents, stain removers, softening) that synthetic clothes undergo during a washing process in a laundry machines. A large portion of microfibres was found in marine environment, and due to the recognisable shape of this MPs, the source was easily found [84,85]. To mitigate the impact of washing machines, many researchers are designing and optimising filters to reduce the number of released fibres [86,87]. Microbeads and microfibers from domestic activities are only two examples of the many emission sources of MPs. In addition to domestic sources, industrial, manufacturer, agricultural, fishing, material production or processing activities are source of MPs [62,76–78,83]. Moreover, when plastics are not recycled, even though they are correctly sent to landfills, secondary MPs can be produced, manly from open dumps and mismanaged landfills or plastic burning [88,89] .

Once MPs are released or produced in the environment, they are spread out and the long list of sources and fates gives a framework of the concerning situation [62,70,76,77,90–92].

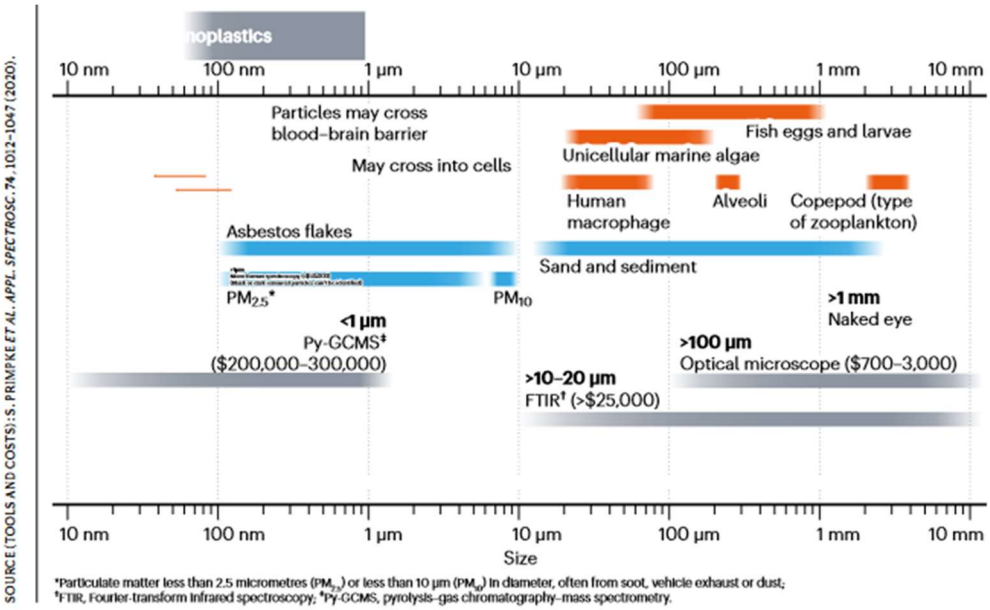

Figure 1.1.2-3. *Size-related comparison between micro and nano plastics to biology and environment [93,94].*

Entering the environment, MPs are inevitably distributed in different compartments and some of the main predicted pathways are shown in Figures 1.1.2-4 and 1.1.2-5. Research working on MPs usually focusing on separate environmental compartments, such as soil, vegetation, water bodies (freshwater and sea) and atmosphere. Nevertheless, it is very important to take into account that MPs are not stationary, but they passively move following environmental dynamisms [92], guided by chemical or physical interactions. To this purpose, Horton and Dixon [95] and Bank and Hansson [96] have introduced the concept of *Plastic Cycle* to indicate the biogeochemical cycle of plastics between environmental compartments [96]. Despite many different circumstances were taken into account to construct the *Plastic Cycle* (Figure 1.1.2-4), the model shows a picture which still simplifies the reality (for example atmospheric transport of MPs is poorly understood [97,98]). However, from this point of view, MP pollution shows how challenging it is. Moving thorough environmental compartments, MPs interacts with biotic and abiotic ecosystem components. For example, MPs enter the food chain by involuntary ingestion (mainly by fish or marine organisms) or by filtration (e.g., by mussels) being then carried in bodies. When animals are preyed, MPs are transferred from preys to by predators, moving within the trophic levels, also reaching humans [91,99]. The presence of MPs in the digestive tract of some animals was notices, but usually this is not a real source of concern, since it is assumed that after consumption, the largest fraction of the is excreted in the feces (> 90 %) [100]. Moreover, digestive tracts are parts usually not consumed but, more serious is the bioaccumulation in crustaceans or mussels, which are filter feeders and their digestive tract is

consumed [90,101]. Mussels and molluscs are usually employed as indicators of marine environment pollution for their filtration, whereas benthic fish usually indicate sediment contamination [90]. MP interactions are not limited to the marine environment, in fact they alter physical and chemical properties of soils [102]. For examples they are responsible to plant root distortions, affecting the nutrient uptake and depleting, they impact on the size of seeds, germination rates and chlorophyll content; when ingested by soil fauna (worms), MPs disrupt the digestive systems, accumulating in living tissue [91,102,103].

Numerous studies have proven the occurrence of MPs in the environment, studying distribution and sources, but the consequences that their presence cause are not fully understood. Definitive explanation on the risk that MPs pose, chemically and physically interacting with organism at different trophic levels, is not provided yet. However, just considering the widespread occurrence and the numerous exposure routs (examples in Figures 1.1.2-4 and 1.1.2-5), this potential risk appears to be more concerning. One additional reason of concert is the potential carrier behaviour of MPs for environmental pollutants (e.g., heavy metals or organic pollutant) and, again, marine environment is the most exposed. It is still not clear how many different molecules MPs are capable to absorb, for example opposite points of view were reported on the absorption of persistent organic pollutants (POPs) [104]. Anyway, it was demonstrate that potential mechanisms of organic pollutants adsorption are several, including hydrophobic interactions, partitioning, electrostatic interactions, other non-covalent actions, and multiple mechanisms are often involved [105,106]. The capability of MPs to absorb chemicals was reported for antibiotics, metals, polychlorinated biphenyls (PCBs), per- and poly-fluoroalkyl substances (PFAS), polybrominated diphenyl ethers (PBDEs), fungicides, herbicides, pesticide [105–110]. Therefore, MPs act as carrier of pollutants delivering them in different environmental compartments, organisms and tissues, with the potential to produce toxicity or endocrine disrupts and to bioaccumulate and bio-magnify [99,106,110]. Given the size of MPs, also microorganisms can be adsorbed on their surfaces, leading to the transportation and delivery of biological contaminants. Studies have reported the capability of algae, bacteria, protozoa, and fungi to rapidly colonise on MP surfaces [111,112]. Being the infective dose of some pathogens very low [113], with respect to chemical pollutants, biological delivery to host bodies might be of larger concern to the health of humans and animals.

Finally, another reason of concern is related to chemical that are already present in plastics in form of additives. Chemicals that are added to plastics during manufacture can potentially leach out under specific environmental conditions (e.g., pH changes, salinity, chemical degradation, etc.). Leaching may occur when MPs are in the environment but also after ingestion by organisms, potentially causing serious health problems [114,115]. For example, phthalates are

widely used as plasticiser and the risk that the exposure to phthalate esters pose on human health is already known [116–118]. Despite validated protocols for the analysis of MP leachates do not exist yet, several distinct methods are under optimisation [114,115,119,120].

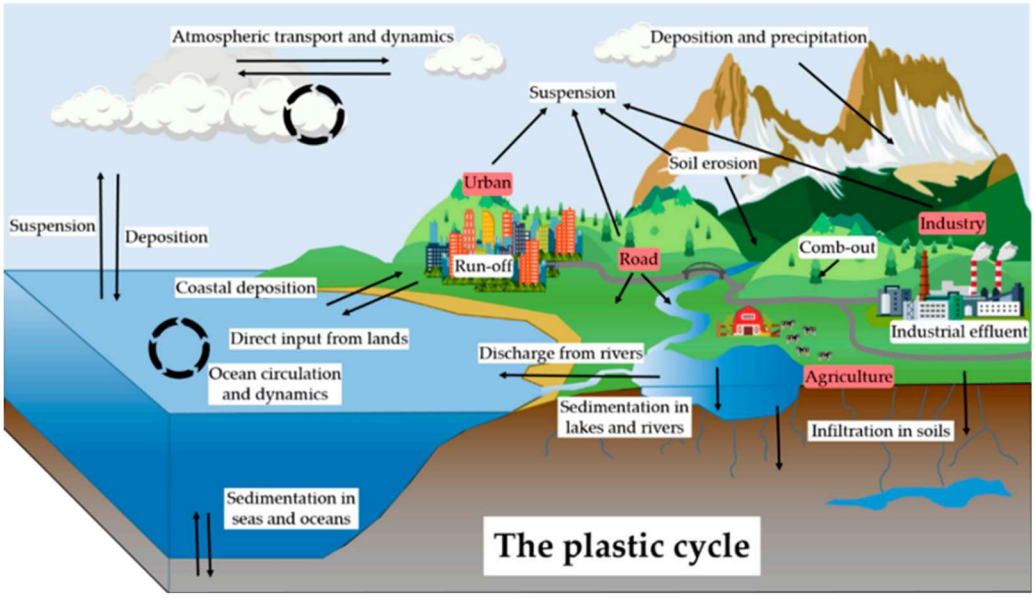

Figure 1.1.2-4. *The Plastic Cycle [92]: biogeochemical cycle of plastics between environmental compartments, introduced by Horton and Dixon [95] and Bank and Hansson [96].*

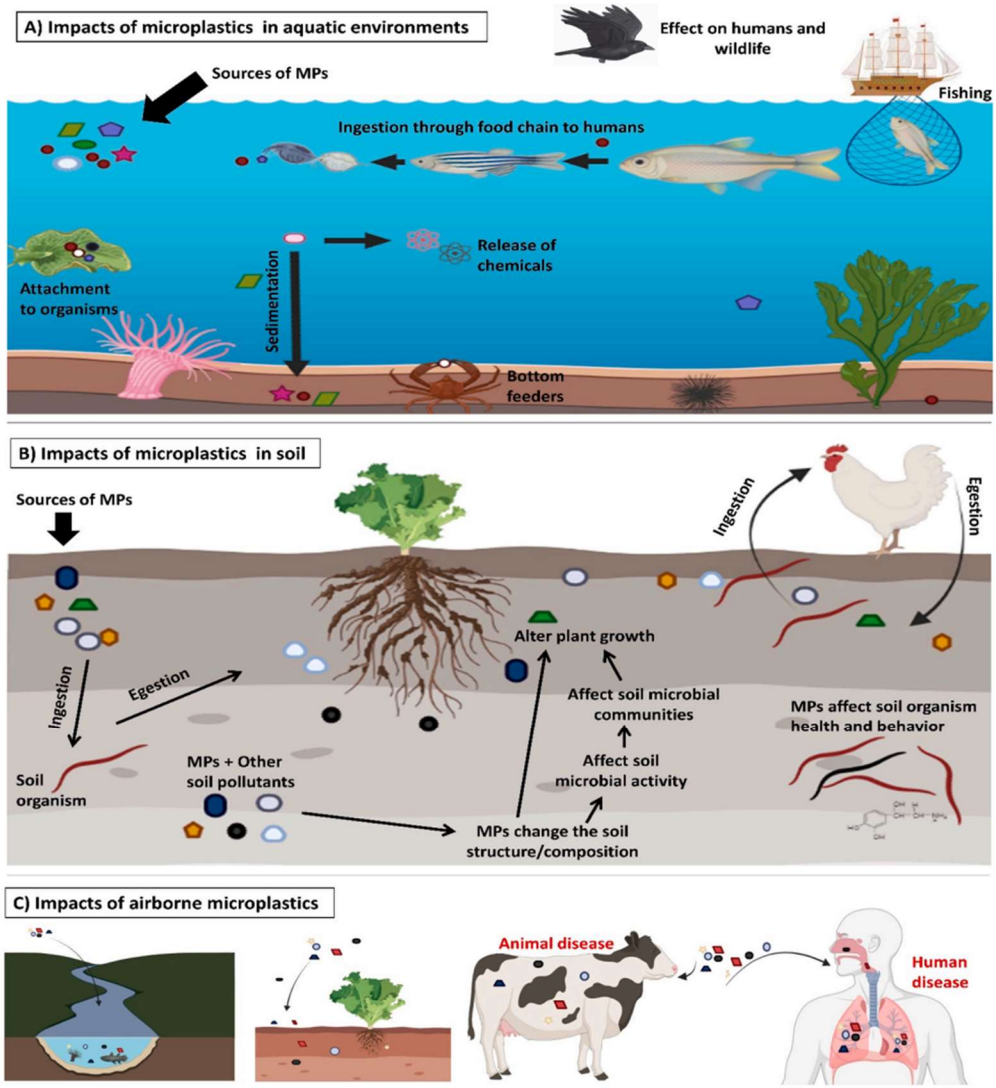

Figure 1.1.2-5. *Pathways and impacts of MPs in different ecosystems, aquatic (a), soil (b) and airborne (c) [91].*

1.1.2.2. Bioplastics

Over the last decades, waste production has become a source of concern and attention is more and more paid on circular economy principles. Circular economy is a zero-waste economy, based on the annulment of the end-of-life of products toward reuse and recycle of materials and energy. Attention must be paid on the origin of raw materials, but also on management and fate of products, according to the principle that while a waste is being generated a new life cycle has to start. In this context, the production of new, more environmental-friendly materials started: the bioplastics. Contrary to conventional fossil-based plastics, bioplastics can be bio-based, biodegradable, or both [121]. Figure 1.1.2-6 shows a scheme which easily allow the identification of bioplastics, depending on the origin of raw materials and biodegradability. Bio-based plastics

are made of polymers which fully or partially derive from renewable sources [121,122]. The definition of bio-based is not related to the nature of the polymer and two categories can be distinguished: natural and synthetic bio-based polymers. Natural bio-based polymers are materials that already exist in the environment in polymeric form. In fact, the manufacture of those polymers only consists in their extraction from the biomass, without any additional polymerisation (green frame in Figure 1.1.2-6) [122]. Natural bio-based polymers are 100 % biobased and biodegradable [121]. This is not the same for synthetic bio-based polymers which substitute the fossil-based conventional polymers (also called *drop ins*), where starting monomers are fully or partially renewables, but artificial polymerisation is necessary. Polymers included in this class present the same properties of their correspondent fossil-based polymers, for this reason they cannot be biodegradable [121,122] (yellow frame in Figure 1.1.2-6). For example, both PET and bio-PET are synthetised by ethylene glycol and terephthalic acid, but bio-PET is made with bio-based ethylene glycol: neither of the two is biodegradable.

Biodegradation is a process that involve the degradation (breaking of polymer chemical bonds leading to MW reduction) operated by enzymes, produced by microorganisms (bacteria, fungi, algae). Enzymes catalyse hydrolysis and oxidation, fragmenting the polymer chain and producing low-MW molecules which can enter the metabolic cycles of microorganisms. Final products of this process are H_2O, CO_2 and biomass [123]. Biodegradable polymers are those that undergo biodegradation, with no relation to the nature of raw materials. Logically, natural bio-based polymers are 100 % biodegradable (naturally occurring in the environment), but also synthetic fossil-based polymers can be designed as biodegradable, becoming part of bioplastics (blue frame in Figure 1.1.2-6).

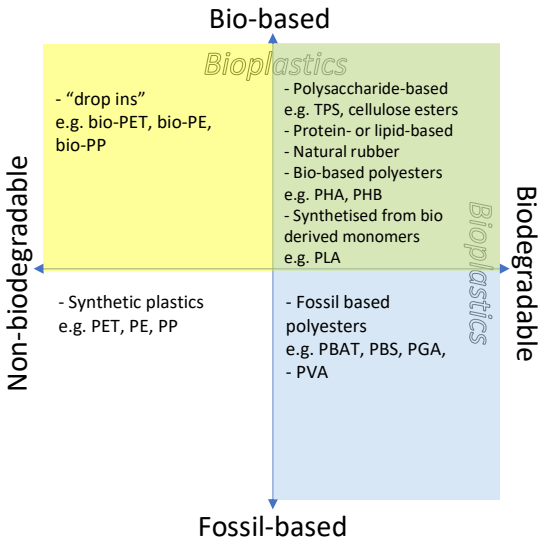

Figure 1.1.2-6. *Polymer categorisation depending on raw materials (bio-based or fossil-based) and biodegradability [121].*

According to Figure 1.1.2-6, talking about bioplastics can be ambiguous and, for this reason, polymers are certified with specific labels which help to understand their nature and biodegradability. Certifications are released by specific accredited institutions (e.g., TÜV Austria, DIN-Geprüft) basing on standard regulations (e.g., ASTM, EN ISO standards). Therefore, a certification is release when a product fits to technical requirements that establish quality specifications. Bio-based content can be evaluated in term of bio-based *carbon* content (ISO 1662-2 [124]) or bio-based *mass* content (ISO 16620-4 [125]) and depending on the measuring method, bio-based contents may variate. The bio-based content gives to consumers indications about the nature of the polymer (Figure 1.1.2-7). Labelling is important also for biodegradability. This property is measured in term of CO_2 released from the biodegradation of a material under specific conditions (temperature, humidity and oxygen) within a specific range of time (ISO 14855 [126]). It is very important to take into account that degradation conditions highly affect the results, leading to specific biodegradation rates within different time ranges. Depending on that, biodegradable polymers need to be distinguished by compostable polymers and the two categories are strictly related to the "environment" where they can achieve biodegradation. Biodegradable materials are those that can biodegrade (90 % of the total) at environmental conditions (20 – 25 °C) within a reasonable range of time which is dependent on the environment (e.g., 6 months in sea water, 2 years in soil). More details are explained in Table 1.1.2-2. Compostable materials need stronger condition to be biodegraded and they are divided in two categories, industrial and domestic composting. To obtain the label as industrial compostable a polymer needs to achieve 90 % of biodegradation at ≈ 60 °C within 6 months, but the same polymer is not domestic compostable if it cannot reach the same biodegradation percentage at ≈ 38 °C within 12 months. Even in this case, labels are very important to understand the behaviour and the fate of polymers: a polymer which is biodegradable in sea water can of course be composable in industry, but not the opposite.

According to European Bioplastics (EUBP), an accelerating growth of bioplastics production is predicted in the next years. Currently, bioplastics cover less than 1 % of the more than 367 Mt of plastic which are annually produced. However, even though the overall plastic production is slightly decreased [65], the bioplastics production capacity is set to increase significantly from around 2.41 Mt in 2021 to approximately 7.59 Mt in 2026 (Figure 1.1.2-8) [129]. This predicted huge increase is due to the competitiveness of performances of bioplastics compared to the conventional plastics. The high developments reached by scientific and engineering research on biopolymers is allowing the sharing of biopolymers, such as PBAT (polybutylene adipate terephthalate) but also PBS (polybutylene succinate) and bio-PAs (bio-based polyamides) as well as a steady growth of polylactic acids (PLAs). In 2018, 56.8 % of the global production capacity

represented the bio-based/non-biodegradable plastics against the biodegradable one (43.2 %). In 2021 the situation was reversed, with the 64.2 % of biodegradable plastics. An overview on the most commonly used natural and synthetic bio-based polymers is shown in Table 1.1.2-3.

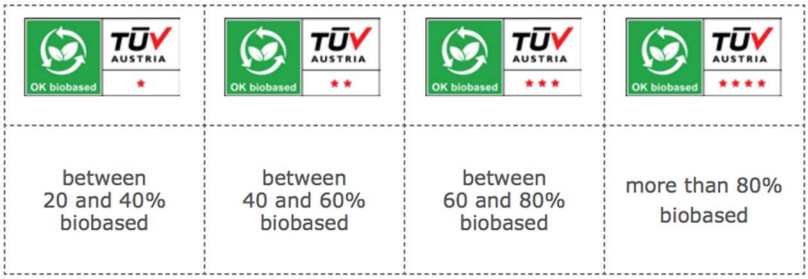

Figure 1.1.2-7. *Examples of labels certifying bio-based content [127].*

Table 1.1.2-2. *Biodegradation conditions according to ISO 14855 [126,128].*

Biodegradation conditions	Temperature	Biodegradation (more than 90 %)	Disintegration (less than 10 % above 2 mm)
Industrial composting	50 – 70 °C	Less than 6 months	Less than 12 weeks
Home composting	20 – 30 °C	Less than 12 months	Less than 6 months
Biodegradation in soil	20 – 25 °C	Less than 24 months	No requirement
Biodegradation in water	20 – 25 °C	Less than 56 days	No requirement
Marine biodegradation	20 – 25 °C	Less than 6 months	Less than 84 days

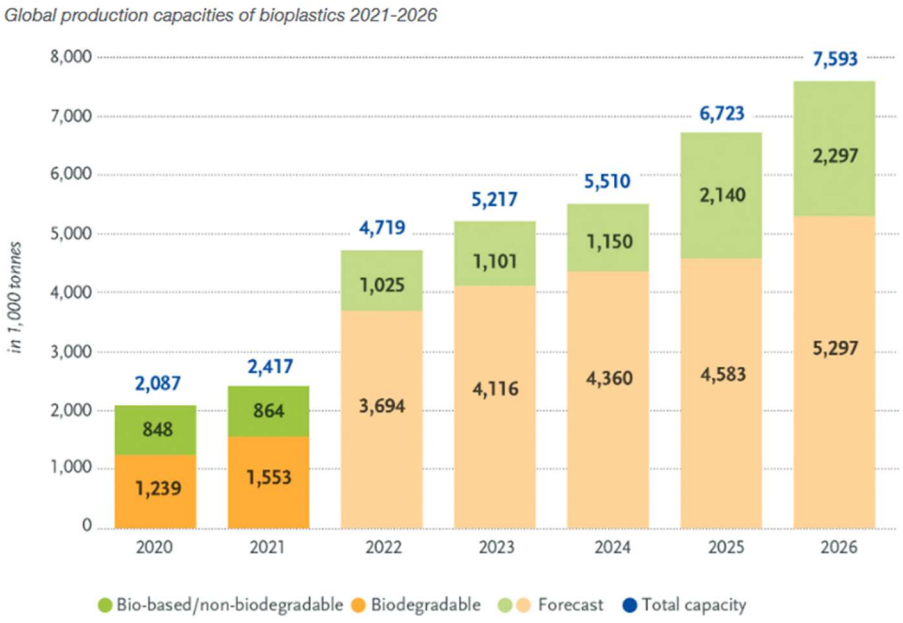

Figure 1.1.2-8. *Prediction of future global production of bioplastics [129].*

Table 1.1.2-3. *Overview on the most commonly used natural and synthetic bio-based polymers [65].*

Polymer	Structure	Properties	Applications	References
Synthetic				
Bio-based polyethylene terephthalate (bio-PET)	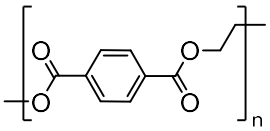	6.2 % of the global production of bioplastics Partially bio-based (≈ 30 % w/w), non-biodegradable The bio-based portion is referred to ethylene glycol which derives from glycerol (obtained from the transesterification and hydrolysis of triglyceride feedstocks)	Applications are the same as fossil-based PET (see Table 1.1.2-1)	[65,129]
Bio-based polyethylene (bio-PE)	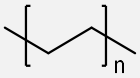	9.5 % of the global production of bioplastics 100 % bio-based, on-biodegradable Ethylene used for synthesis derives from ethanol obtained from yeast fermentation of sugar and starchy feedstocks	Applications are the same as fossil-based PE (see Table 1.1.2-1)	[65,129]
Poly(butylene-co-adipate terephthalate) (PBAT)	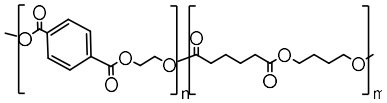	19.2 % of the global production of bioplastics Partially bio-based and biodegradable, but the percentage of aromatic portion has to be limited To achieve specific characteristics is used in combination with other bio-based polymers (PLA, cellulose, star	Applications in packaging (e.g., shopping bags, compost bags), mulch films in agriculture, courier bags, cutlery, etc.	[129–132]

Polylactic acid (PLA) 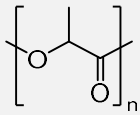	18.9 % of the global production of bioplastics Synthetised from lactic acid, deriving from the bacterial fermentation of sugar and starchy feedstocks Homopolymer 100 % bio-based and biodegradable, not home compostable It can be used in crystalline or amorphous form	Applications in disposable items (e.g., cups, lids, plates, bowls), flexible and rigid packaging (e.g., food containers), 3-D printing, medical devices (e.g., tissue engineering or regenerative medicine), etc.	[129,133]
Poly(butylene succinate) (PBS) 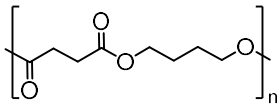	3.5 % of the global production of bioplastics Synthetised from succinic acid and 1,4-butanediol (deriving from the bacterial fermentation of sugar and starchy feedstock) 100 % bio-based and biodegradable, not home compostable	Applications in industries, agriculture (e.g., vegetation net), fishery, forestry and civil engineering, mulching films, compostable bags, disposable food packaging, nonwoven sheets and textiles, catering goods, foams, etc.	[129,131,134]
Natural			
Starch blends 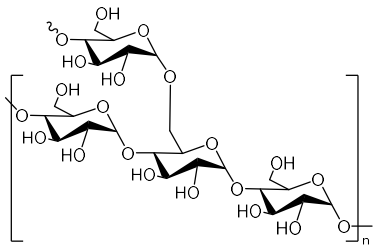	16.4 % of the global production of bioplastics Deriving from starchy feedstocks 100 % bio-based and biodegradable Blends are usually with PLA, PVA, PBAT, PHA	Applications in packaging (e.g., disposable or compostable bags), replacement of LDPE films, water-soluble laundry bags, biomedical and clinical field, electronic devices, membrane material (chemical and automotive industries), etc.	[129,132,135]

Cellulose films 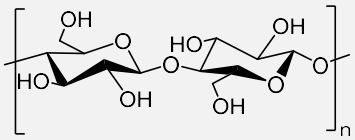	3.2 % of the global production of bioplastics Deriving from plants, is the most abundant biopolymer in the biosphere 100 % bio-based and biodegradable	Applications in food packaging (e.g., Cellophane™)	[129]
Poly(hydroxyalcanoate) (PHA) 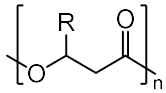	1.8 % of the global production of bioplastics 100 % bio-based and biodegradable	Applications in kitchen equipment (e.g., pots, spoons), packaging (e.g., plastic bags), biomedical engineering and medical devices (e.g., biodegradable surgical staples, screws, bioresorbable suture material and skin staples, wound and burn dressings, membranes for periodontal guided regeneration), etc.	[129,136]

1.2. Analytical techniques for the investigation of polymers

The choice of the analytical technique to be used in polymer investigations mainly depend on the physical properties of the material (e.g., liquid or solid form, solubility, size, colour, etc.) and the aim of the investigation (e.g., study of properties, environmental investigation, etc.). However, the starting point of each polymer investigation is the characterisation of the materials. Properties of interest include MW distribution, molecular structure, morphology, thermal properties, and mechanical properties. Polymer characterisations are mainly categorized as microscopic, rheometric, spectroscopic, chromatographic or thermal.

Microscopic techniques

Microscopic analysis of polymers allows the study and characterisation of the micro and nano-structural features of polymers, which are related to the performances of the material. Scanning

probe, optical and electron microscopy are three different microscopy techniques and allow the visualisation of minor details of extremely small structures and the analysis of polymer morphologies, fundamental in polymer design and optimisation [137–139]. Techniques differ for what they use to explore samples: light for optical microscopy, electrons for electron microscopy and flexible solid probe for scanning probe.

Typical optical microscopes (OM) use multiple lenses and, varying the light sources and the lenses, five basic types of can be established: dark-field, bright-field, differential interference, phase-contrast, and differential interference contrast [137]. Each one of these microscope types has specific characteristics, advantages, and limitations based on applications and functions. In general, OM is widely used for the analysis of soft materials such as membranes, micelles, cells, etc., but it has been applied also for imaging of surface morphology and studies on phase separation of polymer blends and block copolymers [138,140–142].

Electron microscopy has been a fundamental tool for polymer characterisation throughout the history of polymer science, especially for morphological studies of various nanoscale structures [143]. Transmission electron microscopy (TEM) is based on an electron optical apparatus, where a beam of electrons is used to illuminate the specimen [137,143]. TEM can be much more informative than OM, offering 3D morphological information at much higher spatial resolution, thanks to the short wavelength of electrons. On the other hand, the instrument basically works on dried samples under vacuum, otherwise electrons would be scattered by striking air [137]. TEM has found applications in many fields, from material science, engineering, to biological sciences [137,143–145].

Scanning electron microscopy (SEM) is powerful technique useful to many purposes, thanks to its extreme depth of focus, its high resolution, and its capacity to provide X-ray microanalysis [137]. Similar to TEM, SEM produces images of a sample by scanning a probe, a focused beam of electrons, across the sample. On the other hand, the mechanism behind the image formation is very different leading to different information. The electron beam interacts with the atomic level of the sample, generating specific signals which provide information about the composition and surface topography of the sample. Applications of SEM in polymers sciences mainly concern the analysis of surface morphology [146–148].

Microscopic techniques can provide highly informative results about the morphology of samples. They are the most commonly used to examine plastic particles in the context of MP pollution, allowing visual identification and characterisation in term of size, colour and shape [94,149]. In fact, many authors have employed microscopy for MPs investigation in marine environment [150–152], in different types of sediment [153–156], in urban context [157,158], in organisms [159] and so forth. These techniques have been used also for monitoring actions

[160] and for the identification of pollution sources or weathering, highlighted by particle shapes (e.g., fibres form textiles) [84,161–164].

Rheometric analysis

Rheometric analysis provide information about the mechanical properties of polymers in different states. Rheology of polymer is tested to evaluate how much stress or force applied on a material is related to specific deformation or flow. Mechanical properties such as tensile strength, compressive strength, elastic or Young's modulus, viscosity can be calculated and then related to physical/chemical properties of the polymer or polymeric solution structures, such as degree of polymerization, crosslinking, polymer structure, and functionality [139,165]. Mechanical properties of polymers are fundamental in relation with their final applications, and rheometric analyses allow the optimisation of both ultimate products and process conditions [139,166,167].

Rheometric analysis usually developed in polymer engineering and sciences on polymer melts, polymeric solutions, gel or hydrogel to characterise ultimate properties of products [168].

Spectroscopic techniques

Spectroscopic techniques supply precise information about the molecular structure of the polymers and are particularly powerful tools for the characterization of functionalized polymers. Nuclear magnetic resonance (NMR) spectroscopy is an advanced characterisation technique, useful to determine the molecular structure at the atomic level of a sample. In addition to molecular structure, also information about phase changes, conformational and configurational alterations, solubility, and diffusion potential can be obtained. NMR spectroscopy is based on the principle that all nuclei are electrically charged and have multiple spins. When an external magnetic field is applied, it gives rise to the possibility of an energy transfer [169] which occurs from the lower to higher levels. This energy transfer or absorption becomes possible at a specific radio frequency [137,169,170], being a signature of the nucleus type. The most common nuclei examined by NMR are ^{1}H and ^{13}C NMR, due to their sensitivity and their abundance in organic materials. NMR can provide quantitative results about the content different types of functionalities [139,170]. Anyway, NMR experiment may suffer the molecular reorientation, mainly for solid polymers, leading to potential signal loss and inefficient detection [170]. For this reason, the technique is more often use for the characterisation of polymeric solution.

Infra-red (IR) spectroscopy is probably the most widely used technique for the chemical characterisation of materials. It is based on the IR energy absorbed by sample, which generates different type of vibrations at specific wavelengths, depending on the analysed bond. IR region

can be divided into three main areas: far-IR (30 – 400 cm^{-1}), mid-IR (400 – 4000 cm^{-2}), and near-IR (4000 – 4000 cm^{-1}). The mid-IR area is the most informative in polymer characterisation because it is the area where most compounds show characteristic absorption/emission. In mid-IR area, two additional areas can be recognized, functional-group region (4000 – 1400 cm^{-1}) and the fingerprint region (1400 – 400 cm^{-1}) [139,171]. Analysing two different molecules, when spectra show similarity in the first regions, it means that the two materials have similar functional groups. Anyway, their fingerprint region spectra will be different, allowing their discrimination and identification [171].

Fourier-transform infrared (FTIR) spectroscopy has been commonly used to obtain qualitative and information on polymers, being one of the best characterisation methods for identifying molecular structure [94,139].The technique also provides quantitative results based on calibrations protocols of standard materials and according to band intensities [94,171]. Results are based on absorption process due to dipole moment, more exactly on the interference of radiation between two beams, obtaining an interferogram. The source produce one beam which is split in two by mirrors moving and the obtained signal (frequency) is a function of the change of pathlength between the two beams, elaborate by Fourier-transformation mathematical method [171].

Attenuated total reflection (ATR)-FTIR analyse material surfaces, avoiding particular preparation of the analysed materials (e.g., thick layer). It is based on the phenomenon of total internal reflection and analyses occur pressing a crystal on the surface of the material (both in liquid and solid forms), which is then irradiate by an IR beam [94,171]. The beam will undergo the total internal reflection when the angle of incidence at the interface between the sample and crystal is greater than the critical angle (which is a function of the refractive indices of the two surfaces) [171]. The limited portion of the beam which interacts with the tested materials results in an attenuated radiation, giving rise to the absorption spectral characteristics of the sample [94,171].

Raman spectroscopy is usually compared with FTIR, providing the same type of information about molecular structure of materials. Differently form FTIR, Raman is based on light scattering processes [94,172]. Light interacting with molecules, produces the scatter of the majority of the photons at the same energy as the incident photons (elastic scattering). A little portion of these photons will scatter at a different frequency than the incident photons, producing an inelastic scattering (or Raman effect). This effect brings about the deformation of the electron cloud of the molecular bond [172]. Each molecular bond is related to specific energy transition in which polarizability occurs, allowing the user to collect the vibrational signature of a molecule.

Therefore, by spectra interpretation or library search of the resulting vibrational fingerprint, chemical identification of the unknown material is possible.

Spectroscopic techniques are widely used in environmental polymer investigations, providing non-destructive analyses that allow the chemical identification of polymer structures [94,149] and their architecture [173] and the evaluation of degradation state [174]. In the context of MP pollution, FTIR and Raman spectroscopy are the most widely used, both for qualitative and quantitative investigation in many different types of samples. Water has been the most investigated matrix from drinking water samples [175–177] to geographically spread natural waters, such as surface water [178,179], open seawater [180,181], estuary areas [182] or wastewaters [183]. However, spectroscopic techniques have provided results in many other matrices, such as sediments [82,179,184–186], marine organisms [159,187–189], snow [164,190] and so forth. Recently, developments are also focusing on the evaluation of aging, degradation or weathering effect on MPs [163,191,192]

Chromatographic techniques

Chromatographic techniques are used for the separation of molecule mixtures, basing on their distribution between two or more phases. A variety of chromatographic polymer characterisation methods may be used, depending on the analysed material, mainly liquid chromatography (LC), gas chromatography (GC), size exclusion chromatography (SEC) or gel-permeation chromatography (GPC).

LC separations usually require the solubilisation of polymers in polar solvents (e.g., water or methanol), before carrying them out through a solid stationary phase. LC has been a common and important analytical tool for the characterization of functionalized polymers with heterogeneous MW distribution, chain conformation, chemical composition, and microstructure [139,193].

In GC analyses, polymers need to be vaporised before entering the column where an inert gas flow act as a carrier. Separation is primarily based on the boiling points of solute molecules, but it also depends on the affinity of molecules with stationary or mobile phase [139]. Only small molecules, sufficiently volatile pass into the gas phase through heating of the sample, for this reason GC is usually used to characterise residual monomers, oligomers of additives. Anyway, GC can be associated to other techniques which allow the fragmentation of polymer chains, reducing the MW of the analysed molecules (e.g., thermal techniques) [139,194].

SEC and GCP are considered very common, efficient, and fast methods for the characterisation of polymers' MW distribution. The two techniques differ for the solvent type used for the separation (aqueous solvent for GPC), but they are based on the same principles [193].

Macromolecules are separated according to their hydrodynamic volume (size), basing on their partition equilibrium between a mobile phase and the pores of the column packing materials [193,195]. The mechanism is based on steric exclusion of analytes from the pores which compose the column and this partitioning is possible when no significant enthalpic interactions occur between the stationary and mobile phases and the analytes [139,193].

Another technique (not properly chromatographic) that allows separation and the analysis of large molecules and particles is field-flow fraction (FFF). Analytes are introduced into an open channel with laminar flow and they are differently separated by an orthogonal field [137,193]. Like chromatography, FFF is performed injecting samples into an elongated flow chamber, elution is differentiate depending on analyte properties in a laminar flow and an online detection occurs [137]. Nevertheless, retention mechanism is governed by interaction of analyte with an external field which transports analytes to different velocity streams across an open channel. Different FFF techniques can be differentiated depending on the nature of the external field, (such as electric, thermal, gravitational, crossflow, magnetic, dielectrophoretic, etc.), driving separation based on different are physiochemical properties [137,193].

Chromatographic separations are widely used in combination with other techniques. Mass spectrometry (MS) is a powerful tool, providing mass-based chemical information about molecule composition. When chromatography is coupled to MS, high informative results are obtained [94,137,194]. The coupling of LC separations with MS is performed by atmospheric pressure chemical ionization, electrospray ionization, thermo-spray ionization, and particle beam ionization, and GC-MS usually occur by electron ionisation [193,196,197]. Moreover, thermal techniques are usually integrated before the chromatographic separation to provide low-MW thermal degradation products (in gas phase, adsorbed on fibres or trapped in solutions) that can be subsequently separated by chromatography [94,139,194].

Thermal techniques

Thermal analyses represent a group of techniques whereby physical properties of a material are measured as a function of temperature profile and they are widely used in the characterisation and development of new polymeric systems [139]. Differential scanning calorimetry (DSC) and thermal gravimetric analysis (TGA) and are the most common thermal analyses in the field of design on polymers, whereas analytical pyrolysis is used in polymer characterisation and investigations.

In DSC, the amount of heat absorbed or lost by the system is measured to determine changes in the specific heat of a material as a function of temperature. Depending on the heating flow type, exothermic or endothermic processes are related to specific temperature, providing information

about transition temperatures of polymers. Transition temperatures are fundamental in the understanding of physical properties of a polymer, because they are strictly related to polymer structure and architecture (e.g., crystallinity degree). On the other hand, in TGA the mass loss is recorded versus increasing the temperature of the sample, providing information about the thermal stability of the material. Mass loss depends on the degradation/volatilisation of specific components, and category can be defined: loss of volatile components (e.g., water content, absorbed moisture, residual solvents, low-MW additives or oligomers) generally occurring between ambient and 300 °C and generation of volatile degradation products resulting from chain scission that generally require temperatures above 200 °C but not more than 800 °C [198]. Moreover, TGA investigation can also be useful to elaborate the kinetics of these processes, to model and predict cure, thermal stability, and aging due to thermal and thermo-oxidative processes [198]. In the context of environmental investigation, DSC and TGA are usually coupled with other techniques (both chromatographic and spectroscopic, e.g., GC-MS or FTIR). For example, they have been used for the characterisation of polymers within MPs from different types of matrices [199–202].

Analytical pyrolysis is a powerful technique used in material characterisation, capable to provide mass-related information on the chemical composition of a sample [94,139,203]. In contrast other thermal techniques, analytical pyrolysis provides information about the chemical nature of reaction products during heating allowing the study of the formation of products from polymers under heat. To this purpose, pyrolysis is usually coupled with other instrumentation, mainly gas-chromatography and mass spectrometry and the technique is going to be deeply explained in the next section.

1.2.1. Pyrolysis coupled with gas-chromatography and mass spectrometry

Pyrolysis coupled with gas-chromatography and mass spectrometry (Py-GC-MS) is the leading thread of this project, where different polymer types have been investigated by means of this thermoanalytical technique.

Analytical pyrolysis is a technique used for the characterization of a material (or a chemical process) based on the results of chemical degradation reactions induced by thermal energy [203]. The process on the basis of this technique is the pyrolysis, which consists of the chemical degradation of a sample (both solid or liquid) into smaller and volatile molecules, under thermal energy without interacting with oxygen [204]. Pyrolysis usually takes place at temperature

higher than 250 – 300 °C, most commonly between 500 and 800 °C [203]. Heated filament, Curie-Point and microfurnace as the three major types of pyrolyzer and their schematic systems are shown in Figure 1.2.1-1 [94,194]. Depending on the systems, different supports are employed to perform experiments: heating filament pyrolyzer use an open or semi-closed quartz tube, with different inner diameters (Ø 0.2 – 1.3 cm) and length (related to instrument dimension), which is placed into a platinum coil; Curie-Point pyrolyzer use semi-closed ferromagnetic targets (typically Ø 2 mm, 8 mm height); whereas microfurnace pyrolyzer uses stainless steel cups, allowing to analyse higher amount of samples (typical cup dimensions approximately Ø 4 mm, 8 mm height) [94]. Pyrolysis itself, does not provide analytical data unless it is associated with some kind of measurement process. That is, it can be considered a kind of sample pre-treatment prior to instrumental analysis. In this context, Py-GC-MS is the most convenient and complete analytical method, combining thermal degradation at high temperature to products separation and chemical identification. Once volatile pyrolysis products (pyrolyzates) are formed, regardless of the pyrolyzer system, they are heated at specific temperature in an inert atmosphere, usually helium [94,205], to be transferred to GC system where they are separated through the column and finally ionised and detected by MS [203,206]. A schematic representation of the analytical system is shown in Figure 1.2.1-2. Analysing one sample (e.g., PS in Figure 1.2.1-2) information about thermal fragmentation of the polymer, and the chemical nature of the products are all condensed in a so-called pyrogram, which constitute a real fingerprint of the analysed polymer. Exploring the pyrogram, various types of analytical information can be extrapolated, such as qualitative information about pyrolyzates (retention times, mass spectra) that allows to backward reconstruct polymer structure. Further information is obtained by relative abundances of pyrolyzates which give an explanation about the compounds more favourable to be produced, providing an insight on pyrolysis mechanisms [203,206]. Considering specific pyrolysis products, it is possible to build up calibrations by correlating peak areas with the mass of the pyrolysed polymers. Usually, the area integration is not performed on peaks in the total ion current (TIC) chromatogram, because signal to noise ratio of indicator compounds can be incremented by extracting the current for specific fragment ions of the mass spectra of the polymer. This procedure may help also in environmental investigations, where analytes are included into complex samples, which may generate a high signals of background noise [207].

During pyrolysis, pyrolyzates can be directly formed (primary pyrolysis products) or secondary reactions can occur between, producing secondary pyrolysis products. Several types of reactions can take place, the most common are eliminations and rearrangements, but also oxidations, reductions, substitutions, or additions also are possible [203]. The occurrence of unexpected

rearrangements or secondary reactions may lead to error in unknown polymer characterisation. One of the methods useful to obtain less reactive products is derivatisation, that is a well-known technique used in chromatography, allowing a better separation and detection of some compounds. Also in Py-GC-MS derivatisation provides many advantages, not only enhancing chromatographic separation and detection, but also allowing the re-selection of thermal degradation pathway which can improve the pyrolysis products or process, both qualitatively and quantitatively [194]. Derivatisation converts functional groups, modifying pyrolysis products, making them more favourable to be analysed. The most popular derivatisation reagent is tetramethylammonium hydroxide (TMAH) [203]. Thermochemolysis with TMAH gives rise to complementary and more independent reactions in comparison with conventional pyrolysis. Depending on the analysed polymer and the experimental conditions, TMAH improves the chromatographic elution of less volatile or polar compounds, promotes preferable pathway for the formation of products (enhancing the analytical sensitivity) and reduces the reactivity of the whole systems.

Many advantages are provided by Py-GC-MS, allowing sensitive analysis of trace analytes (limit of detection, LOD << 1 µg) with an excellent reproducibility. Moreover, thanks to GC separation and MS recording, the analysis can be extremely selective, simultaneously providing information on the composition of all the organic molecules which compose the sample at once. Analytical pyrolysis is an important technique for the study of natural and synthetic polymers providing qualitative and quantitative information as well as structure exploration [194,203,208].

Environmental applications of analytical pyrolysis are several, encompassing many different complex matrices, including food [209,210], water [177,183,211–214], road dusts [215–217], sediments [184,218], organisms [219–221], airborne [222,223] and so forth.

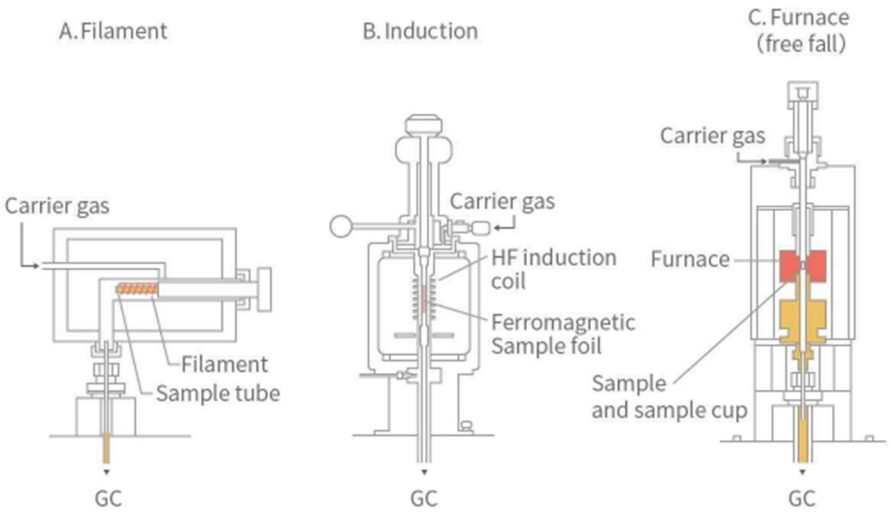

***Figure 1.2.1-1**. Representation of the three typical pyrolyzer; heating filament (A), Curie-Point (B) and micro furnace (C) [205].*

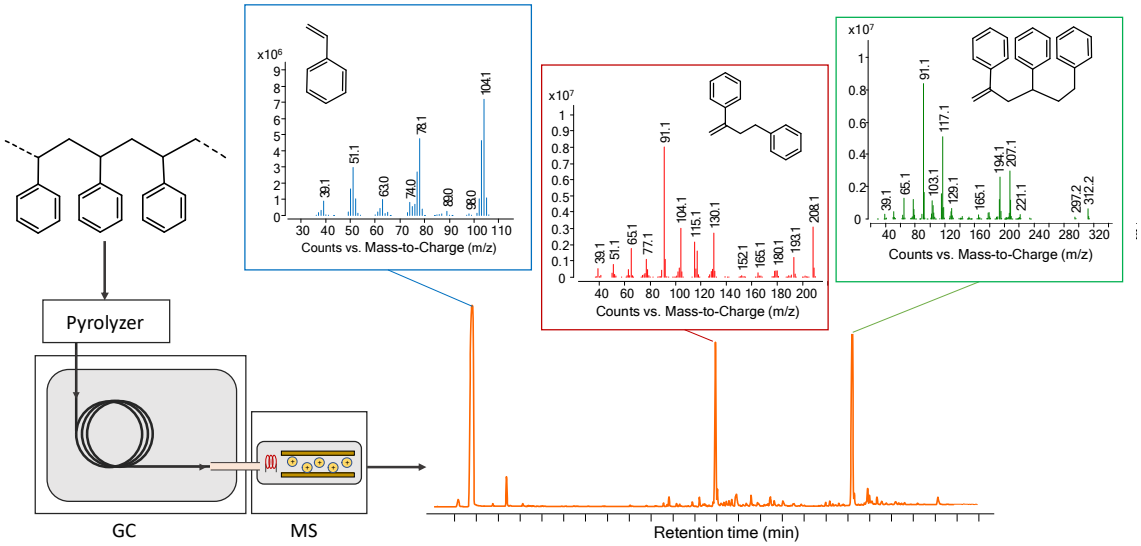

Figure 1.2.1-2. *Schematic flow diagram of Py-GC-MS system with a micro furnace pyrolyzer, example of pyrolysis of polystyrene [206].*

1.2.2. Environmental investigation: harmonization is the key

In previous sections, an overview on the most common analytical techniques employed for the characterisation and the investigation of polymer properties was shown. Moving from laboratory context to environmental samples, many issues arise for the definition of proper procedures to extract and quantify specific polymers, providing reliable results. Depending on the polymer types, on the investigated matrices and on the analytical techniques, procedures for extraction and analysis may be highly different and sometimes they lead to different quantitative information. Reporting of scientific methods and results need to focus on two main purposes: reproducibility and comparability [94,224,225]. These two parameters define the robustness of scientific methods, allowing the use of the obtained data for subsequent evaluations, such as risk assessments or policy supports for the development of mitigation measures or monitoring guidelines [224]. This issue is of particular interest in the context of ECs (emerging contaminants, see Section 1.1), where the lack of knowledge is highlighted already during the definition of the contaminant classes. The delineation of boundaries which categorise a class of contaminants is a crucial starting point for its the correct investigation and it is not always an easy task. The categorisation implies that all the compounds in the same class have specific relations not only in term of morphology and chemical structure, but they necessarily have to present similarity in hazardous properties and environmental behaviour [225].

These issues are common across all scientific fields but, currently, MP research is particularly under focus [224,226] because of the ubiquity of the environmental occurrence of these

contaminants which is growing concerns within societies and governments [94]. During the last two decades, a lot of definition were used to identify MPs, both from scientific and policy fields, resulting in an ambiguous and conflicting communication [225,226]. Moreover, hardly comparable data have been obtained from different studies in, also affecting also risk perception on this environmental pollution issue [227]. Recently, harmonisation on MP definition is under continuous elaboration: Frias and Nash (2019) [72] formulated a consensual definition for the class of contaminants, whereas Hartmann et al. (2019) [225] have proposed seven criteria useful for the categorisation. Figure 1.2.2-1 explains the seven proposed criteria involving physical, chemical, morphological properties and origin, highlighting how misleading can be the recognition of MPs without specific guidelines.

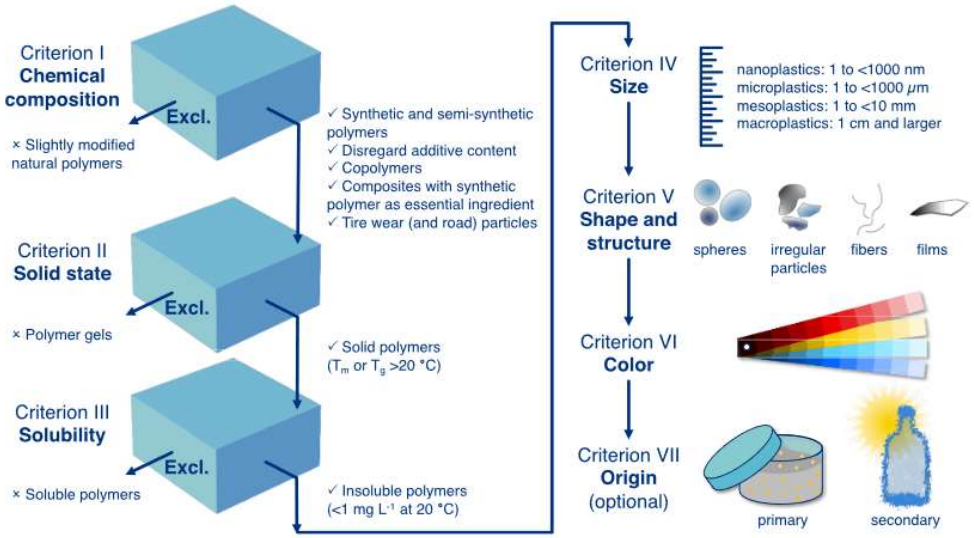

Figure 1.2.2-1. *Proposed definition and categorization framework of MPs, by Hartmann et al. (2019) [225].*

Harmonisation needs to be also spread from definitions to analytical methods and results reporting. MP research field is continuously expanding and new approaches and perspectives emerge every day in the scientific literature. Primpke et al. (2020) provided a comprehensive screening of the most widely used techniques for MP investigation, basing on guidelines, publications and reviews from expert groups. Analytical techniques were compared depending on their performances (e.g., in LOD, expenditure of time), approximate costs and fieldwork capabilities [94]. Table 1.2.2-1 shows a summary of the recovered information, mainly indicating that the perfect and complete analytical technique does not exist. Optical techniques provide important information about the size and the shape of particles, helpful to understand their origin (e.g., microfibers from textiles of microbeads from cosmetics), on the other hand no chemical identification of polymers is possible. To remedy this lack, spectroscopic techniques

(e.g., FTIR and Raman) allow a reliable qualitative chemical identification of polymers, but quantitatively they can only provide particle numbers which is highly time-expensive and also related to not-negligible size of detection limit (Table 1.2.2-1). With Py-GC-MS all the polymers that compose the same sample can be simultaneously identified and quantified in mass units, with highly selective and sensitive analyses. On the other hand, no clues about the shape or size of particles are provided. Each technique shows its potential to provide specific results, but none of them is fully informative.

Calls for standardization of methods for MP detection and quantification are arising, from local level monitoring programs to global level implementation studies, such as NOAA marine debris program (United States of America), GESAMP-WG40 (United Nations), and CleanSeas (European Union) [228–230]. The first obstacle to method standardisation is that not every method is suitable to every laboratory, which sometimes cannot afford to implement high-level and high-cost procedures [231]. Furthermore, the numerous existing analytical techniques provide different type of information, which usually are complementary [94]. Finally, the identification of appropriate methods for MPs extraction from specific matrices can complicate the matter, requiring different processing steps depending on matrix composition and analytical instrumentation. Cowger et al. (2020) elaborated Microplastics Reporting Guidelines sharing a collaborative document and inviting researchers to provide inputs for MP research methods. An interactive check list was used to improve authors connections and the mind map in Figure 1.2.2-2 was elaborated. There, a scheme of the most important analytical steps is described and, despite the developed guidelines includes the shared ideas form a highly limited group of research, it highlights the potential and the importance of the collaboration of scientists of different fields to the same purposes.

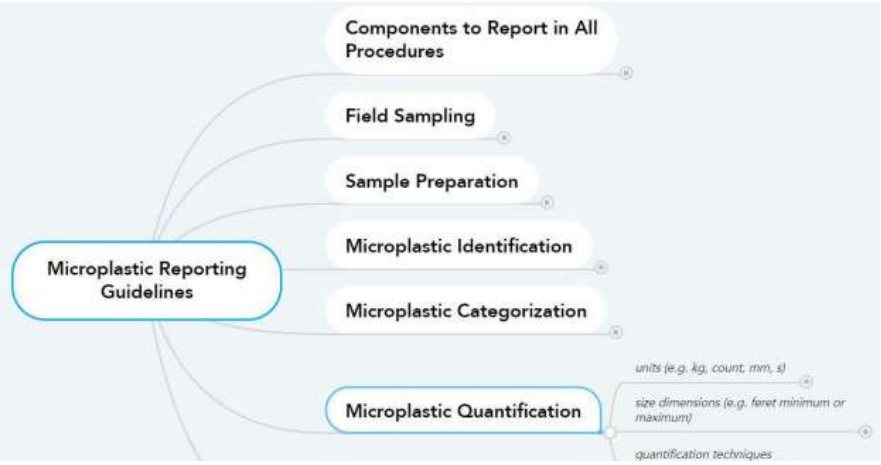

Figure 1.2.2-2. *Mind map elaborated in the context of interactive brainstorming among researchers on MPs from different fields [172].*

The scheme in Figure 1.2.2-2 lists the mains steps to be taken into account for MPs pollution investigation and quantification resulted the most challenging step. Many different analytical protocols, methods and techniques have been developed and applied to environmental samples, but validated standardized methods remain unavailable at this point [94,149,224,228]. Moreover, there is still no consensus on the reporting format of results (EFSA, 2016), such as number of particles per mass of sample, or total mass of particles (or total mass of each polymer) within a given particle size range. To this purpose, few interlaboratory studies (ILSs) on MPs analysis were published, reporting discrepancy in final results [226,229,230]. Van Mourik et al (2021) developed an ILS, involving 34 laboratories from 13 different countries. Laboratories, used different techniques among the currently most widely used, µFTIR, ATR-FTIR, Raman, µRaman and Py-GC-MS. Different samples were provided to laboratories in order to evaluate their performances in the identification of polymers (without sample pre-treatment) and their extraction and quantification. ATR-FTIR was the most commonly applied technique polymer identification (46 %), followed by µFTIR (23 %); whereas microscopy was the most commonly applied method for quantification (36 %), followed by µFTIR (23 %). As general outcomes, the majority of the laboratories reported the correct polymer types, but quantification results were unsatisfactory, reporting an average number of total particles with a relative standard deviation (RSD) from 57 % to 91%. This last result indicates an urgent need towards harmonization and more assessments of harmonization. The need of harmonization was also confirmed by prior ILSs conducted by Isobe et al. (2019) [229], Müller et al. (2020) [230] and Belz et al. (2021) [231], showing a high scattering of result. To this purpose, ILSs delineate an interesting approach which necessarily need to be improved and optimised. The number of involved participants is fundamental to statistically represent the variability of the population of research groups. Secondly, it is important to define a selected range of MP size. According to MP definition, particles range between 1 µm to 1000 µm, but different techniques have different analytical LOD or LOQ (Table 1.2.2-1) leading to results in different size ranges. Moreover, particles of different size behave differently in the environment (being subjected to different transportation processes and posing different risk on ecosystems [92,98]), therefore comparison has to necessarily be performed within the same size ranges. Comparability is also necessary on the type of reported results, which have to indicate polymer types and their quantification. Again, quantitative results will be strictly related to the analytical techniques, in form of counted particles (optical and spectroscopic techniques) of polymer mass measuring (thermal techniques), but to complete results, both information are necessary.

Harmonisation plays a fundamental role in scientific investigation. Even though research is continuously under development, it is necessary for researchers to share the same objectives to focus all the efforts on the comprehension of complex issues, such as MP pollution, moving together towards the same direction: knowledge and quantification.

Table 1.2.2-1. *Comparison of optical, spectroscopic an thermoanalytical techniques for the analysis of MPs [94]. CQ: pyrolysis cubs or quartz tubes; F: filters; IP: isolated particle; LID: limited chemical identification; MO: monitoring; MD: modelling; NoID: no chemical identification; NoM: no mass determination; NoN: no particle number determination; NA: no information available; NoS: no particle sizes determination; R: routine; RA: risk assessment; RE: research; PA/SA: partial analysis/subsampling analysis on filter; P: particle; PD: polymer dependent; PND: particle number dependent; REP: replicates; TA: total absorption.*

Methods	Unit	Naked eye	Optical microscopy	Nile red staining	Flow cytometry	Flow imaging	FT-IR qualitative	Particle based µFT-IR	µFT-IR imaging
LOD		1 mm	100 µm	3–20 µm	500 nm	2 µm	>300 µm	25 µm	10 µm
Instrument costs[a]	$k	<1	2–3	2–50	>50	>130	25–50	100–125	200–250
Special consumables				Dye and solvent	Cleaning solutions	Cleaning solutions		Liquid nitrogen	Liquid nitrogen
Field applicability		Good	Good	No	No	Possible	Handheld	No	No
Limitations		NoID	NoID, NoM, PA/SA	NoID, NoM, PA/SA	NoID, NoM	NoID, NoM		TA, NoM	TA, NoM
Automated data evaluation		No	No	No[d]	No	No	No	Yes	Yes
Measurement time[b]	min	1	60	35	30	30	1	360	240
Data Analysis time[b]	min	NA			5	5	1	60	360
Working time[b]	min	1	60	35	48	48	2	120	60
Typical fractions per sample		50 P	7 F	7 F	3 REP	3 REP	50 P	1 F	1 F
Instrument availability for analysis[c]	d	261	261	261	237	249	250	250–261	250–261
Average working time per sample	min	PND	420	245	144	144	PND	120	60
Field of application		MD, MO	MD, MO, R	MD, MO, R	MD, MO, R	MD, MO, R	MD, MO, R, RA, RE	MD, MO, R, RA, RE	MD, MO, R, RA, RE

Methods	Unit	Raman qualitative	Particle based µRaman	py-GC-MS qualitative	Quantitative py-GC-MS	TED-GC-MS	HIS	SEM-EDX
LOD		>300 µm	1 µm	~1 µg IP	<<1 µg PD	<1 µg PD	NA	nm
Instrument costs[a]	$k	50–100	200–400	>150	>215	>250	40-120	>100
Special consumables				GC-columns and filaments	GC-columns and filaments	GC-columns and filaments		Sample coating
Field applicability		Handheld	No	No	No	No	Device dependent	No
Limitations			PA/SA, NoM		NoN, NoS	NoN, NoS	LID	LID
Automated data evaluation		Yes[e]	Yes	No	No[f]	No[f]	No	No
Measurement time[b]	min	2	2580–>10 000	35–120	120	120	5	120
Data Analysis time[b]	min	1	1	5–10	60[g]	60[g]	5	60
Working time[b]	min	3	60–580	5	30 (qual.) 72 (quant.)[g]	30 (qual.) 72 (quant.)[g]	10	180
Typical fractions per sample		50 P	1 F	50 P	1–5 CQ	1–5 CQ	1 F	1 F
Instrument availability for analysis[c]	d	250–261	250–261	250	250	250	NA	NA
Average working time per sample	min	PND	60	PND	72-216	72-216	10	180
Field of application		MD, MO, R, RA, RE	MD, MO, R, RA, RE	MD, MO, RE	MD, MO, R, RE	MD, MO, R, RE	MO, RE	MD, RA, RE

[a]Raw estimates which may strongly vary dependent on the country. [b]Calculated for one filter/particle per analysis. [c]Working days (normal work hours/days) exclusive instrument maintenance time. [d]Image analysis possible. [e]For Raman microscopes. [f]Autosamplers are available. [g]Calculated based on a micro-furnace system with an average sequence size (6 standards, 10 samples).

References

[1] P. Tschirhart, E.F. Bloomfield, Framing the Anthropocene as influence or impact: The importance of interdisciplinary contributions to stratigraphic classification, Environmental Communication. 14 (2020) 698–711. https://doi.org/10.1080/17524032.2020.1716033.

[2] P.J. Crutzen, E.F. Stoermer, The "Anthropocene," IGBP Global Change. 41 (2020) 17–18.

[3] J. Zalasiewicz, C.N. Waters, E.C. Ellis, M.J. Head, D. Vidas, W. Steffen, J.A. Thomas, E. Horn, C.P. Summerhayes, R. Leinfelder, J.R. McNeill, A. Gałuszka, M. Williams, A.D. Barnosky, D. de B. Richter, P.L. Gibbard, J. Syvitski, C. Jeandel, A. Cearreta, A.B. Cundy, I.J. Fairchild, N.L. Rose, J.A. Ivar do Sul, W. Shotyk, S. Turner, M. Wagreich, J. Zinke, The Anthropocene: comparing its meaning in geology (chronostratigraphy) with conceptual approaches arising in other disciplines, Earth's Future. 9 (2021) e2020EF001896. https://doi.org/10.1029/2020EF001896.

[4] T. Smital, Acute and chronic effects of emerging contaminants, in: D. Barceló, M. Petrovic (Eds.), Emerging Contaminants from Industrial and Municipal Waste: Occurrence, Analysis and Effects, Springer, Berlin, Heidelberg, 2008: pp. 105–142. https://doi.org/10.1007/698_5_105.

[5] S. Sauvé, M. Desrosiers, A review of what is an emerging contaminant, Chem Cent J. 8 (2014) 15. https://doi.org/10.1186/1752-153X-8-15.

[6] P.E. Rosenfeld, L.G.H. Feng, 16 - Emerging Contaminants, in: P.E. Rosenfeld, L.G.H. Feng (Eds.), Risks of Hazardous Wastes, William Andrew Publishing, Boston, 2011: pp. 215–222. https://doi.org/10.1016/B978-1-4377-7842-7.00016-7.

[7] History and future of plastics, Science History Institute. (2016). https://www.sciencehistory.org/the-history-and-future-of-plastics (accessed October 18, 2022).

[8] V.G. Kadajji, G.V. Betageri, Water soluble polymers for pharmaceutical applications, Polymers. 3 (2011) 1972–2009. https://doi.org/10.3390/polym3041972.

[9] Water soluble polymers, MDPI AG, Basel, 2018.

[10] P.A. Williams, ed., Handbook of industrial water soluble polymers, Blackwell Pub, Oxford ; Ames, Iowa, 2007.

[11] J. Du, J. Liu, L. Zhao, P. Liu, X. Chen, Q. Wang, M. Yu, Water-soluble polymers for high-temperature resistant hydraulic fracturing: A review, Journal of Natural Gas Science and Engineering. 104 (2022) 104673. https://doi.org/10.1016/j.jngse.2022.104673.

[12] J.E. Glass, Water-soluble polymers, in: John Wiley & Sons, Inc. (Ed.), Kirk-Othmer Encyclopedia of Chemical Technology, John Wiley & Sons, Inc., Hoboken, NJ, USA, 2000: p. 2301200507120119.a01. https://doi.org/10.1002/0471238961.2301200507120119.a01.

[13] S.W. Shalaby, C.L. McCormick, G.B. Butler, eds., Water-soluble polymers: Synthesis, solution properties, and applications, American Chemical Society, Washington, DC, 1991. https://doi.org/10.1021/bk-1991-0467.

[14] D.Q.M. Craig, The mechanisms of drug release from solid dispersions in water-soluble polymers, International Journal of Pharmaceutics. 231 (2002) 131–144. https://doi.org/10.1016/S0378-5173(01)00891-2.

[15] I.M. Helander, H.-L. Alakomi, K. Latva-Kala, P. Koski, Polyethyleneimine is an effective permeabilizer of gram-negative bacteria, Microbiology (Reading). 143 (Pt 10) (1997) 3193–3199. https://doi.org/10.1099/00221287-143-10-3193.

[16] Safety assessment of polyoxyalkylene siloxane copolymers, alkyl-polyoxyalkylene siloxane copolymers, and related ingredients as used in cosmetics | Cosmetic Ingredient Review, Washington, 2015.

[17] H.-J. Jang, C.Y. Shin, K.-B. Kim, Safety evaluation of polyethylene glycol (PEG) compounds for cosmetic use, Toxicol Res. 31 (2015) 105–136. https://doi.org/10.5487/TR.2015.31.2.105.

[18] M.M. Jayakody, K.G. Kaushani, M.P.G. Vanniarachchy, I. Wijesekara, Hydrocolloid and water soluble polymers used in the food industry and their functional properties: a review, Polym. Bull. (2022). https://doi.org/10.1007/s00289-022-04264-5.

[19] R. Parvani, M.C. Shukla, Water soluble clear coating compositions and their film properties, Pigment & Resin Technology. 20 (1991) 4–7. https://doi.org/10.1108/eb042867.

[20] I. Bicu, F. Mustată, Water soluble polymers from Diels-Alder adducts of abietic acid as paper additives, Macromolecular Materials and Engineering. 280–281 (2000) 47–53. https://doi.org/10.1002/1439-2054(20000801)280:1<47::AID-MAME47>3.0.CO;2-#.

[21] Y. Du, Y.-H. Zang, J. Sun, The effects of water soluble polymers on paper coating consolidation, Progress in Organic Coatings. 77 (2014) 908–912. https://doi.org/10.1016/j.porgcoat.2014.01.007.

[22] V. Vajihinejad, S.P. Gumfekar, B. Bazoubandi, Z. Rostami Najafabadi, J.B.P. Soares, Water soluble polymer flocculants: Synthesis, characterization, and performance assessment, Macromolecular Materials and Engineering. 304 (2019) 1800526. https://doi.org/10.1002/mame.201800526.

[23] B. Chaufer, A. Deratani, Removal of metal ions by complexation-ultrafiltration using water-soluble macromolecules: Perspective of application to wastewater treatment, Nuclear and Chemical Waste Management. 8 (1988) 175–187. https://doi.org/10.1016/0191-815X(88)90025-3.

[24] T. Berninger, N. Dietz, Ó. González López, Water-soluble polymers in agriculture: xanthan gum as eco-friendly alternative to synthetics, Microbial Biotechnology. 14 (2021) 1881–1896. https://doi.org/10.1111/1751-7915.13867.

[25] K. Halake, M. Birajdar, B.S. Kim, H. Bae, C. Lee, Y.J. Kim, S. Kim, H.J. Kim, S. Ahn, S.Y. An, J. Lee, Recent application developments of water-soluble synthetic polymers, Journal of Industrial and Engineering Chemistry. 20 (2014) 3913–3918. https://doi.org/10.1016/j.jiec.2014.01.006.

[26] I.A. Tekko, O.M. Ali, M.F. Chehna, T. Hatahet, Polyethylene glycol-based solid dispersions to enhance eprosartan mesylate dissolution and bioavailability, APPR. 2 (2019) 1–11.

[27] K. Knop, R. Hoogenboom, D. Fischer, U.S. Schubert, Poly(ethylene glycol) in drug delivery: Pros and cons as well as potential alternatives, Angewandte Chemie International Edition. 49 (2010) 6288–6308. https://doi.org/10.1002/anie.200902672.

[28] A.A. D'souza, R. Shegokar, Polyethylene glycol (PEG): A versatile polymer for pharmaceutical applications, Expert Opinion on Drug Delivery. 13 (2016) 1257–1275. https://doi.org/10.1080/17425247.2016.1182485.

[29] J. Chen, S. K. Spear, J. G. Huddleston, R. D. Rogers, Polyethylene glycol and solutions of polyethylene glycol as green reaction media, Green Chemistry. 7 (2005) 64–82. https://doi.org/10.1039/B413546F.

[30] D.H. Reneker, A.L. Yarin, H. Fong, S. Koombhongse, Bending instability of electrically charged liquid jets of polymer solutions in electrospinning, Journal of Applied Physics. 87 (2000) 4531–4547. https://doi.org/10.1063/1.373532.

[31] L.S.C. Wan, L.Y. Lim, Drug release from heat-treated polyvinyl alcohol films, Drug Development and Industrial Pharmacy. 18 (1992) 1895–1906. https://doi.org/10.3109/03639049209046338.

[32] J. Zhang, C. Huang, Y. Chen, H. Wang, Z. Gong, W. Chen, H. Ge, X. Hu, X. Zhang, Polyvinyl alcohol: a high-resolution hydrogel resist for humidity-sensitive micro-/nanostructure, Nanotechnology. 31 (2020) 425303. https://doi.org/10.1088/1361-6528/ab9da7.

[33] S. Raymond, L. Weintraub, Acrylamide gel as a supporting medium for zone electrophoresis, Science. 130 (1959) 711. https://doi.org/10.1126/science.130.3377.711.

[34] J.S. Ahn, L. Castle, Tests for the depolymerization of polyacrylamides as a potential source of acrylamide in heated foods, J Agric Food Chem. 51 (2003) 6715–6718. https://doi.org/10.1021/jf0302308.

[35] M. Syaifudin, Gel electrophoresis: The applications and its improvement with nuclear technology, in: Jakarta, Indonesia, 2021: p. 050008. https://doi.org/10.1063/5.0042067.

[36] G. Saunders, B. MacCreath, A guide to multi-detector gel permeation chromatography, Agilent Technologies, 2012.

[37] L. Bromberg, Polyether-modified poly(acrylic acid): Synthesis and applications, Ind. Eng. Chem. Res. 37 (1998) 4267–4274. https://doi.org/10.1021/ie980358s.

[38] D.Q.M. Craig, S. Tamburic, G. Buckton, J.M. Newton, An investigation into the structure and properties of Carbopol 934 gels using dielectric spectroscopy and oscillatory rheometry, Journal of Controlled Release. 30 (1994) 213–223. https://doi.org/10.1016/0168-3659(94)90027-2.

[39] D. Ayers, J.M. Cuthbertson, K. Schroyer, S.M. Sullivan, Polyacrylic acid mediated ocular delivery of ribozymes, Journal of Controlled Release. 38 (1996) 167–175. https://doi.org/10.1016/0168-3659(95)00117-4.

[40] M. Jafari, G.R. Najafi, M.A. Sharif, Z. Elyasi, Superabsorbent polymer composites derived from polyacrylic acid: Design and synthesis, characterization, and swelling capacities, Polymers and Polymer Composites. 29 (2021) 733–739. https://doi.org/10.1177/0967391120933482.

[41] S. Choi, M.L. Gray, C.W. Jones, Amine-tethered solid adsorbents coupling high adsorption capacity and regenerability for CO2 capture from ambient air, Chemistry-Sustainability-Energy-Materials. 4 (2011) 628–635. https://doi.org/10.1002/cssc.201000355.

[42] C.-C. Hsu, Y.-Y. Chao, S.-W. Wang, Y.-L. Chen, Polyethylenimine-capped silver nanoclusters as fluorescent sensors for the rapid detection of ellagic acid in cosmetics, Talanta. 204 (2019) 484–490. https://doi.org/10.1016/j.talanta.2019.06.047.

[43] S. Wu, G. Li, W. Liu, D. Yu, G. Li, X. Liu, Z. Song, H. Wang, H. Liu, Fabrication of polyethyleneimine-paper composites with improved tribopositivity for triboelectric nanogenerators, Nano Energy. 93 (2022) 106859. https://doi.org/10.1016/j.nanoen.2021.106859.

[44] A.I. Fahira, R. Amalia, M.I. Barliana, V.A. Gatera, R. Abdulah, Polyethyleneimine (PEI) as a polymer-based co-delivery system for breast cancer therapy, BCTT. 14 (2022) 71–83. https://doi.org/10.2147/BCTT.S350403.

[45] H. Xiu, J. Li, H. Wang, Y. Ji, Application of PEI and PAC as anionic trash catcher to improve the paper properties of aspen APMP containing furnish-a case study, 26 (2014) 6.

[46] A. Kuźmińska, B.A. Butruk-Raszeja, A. Stefanowska, T. Ciach, Polyvinylpyrrolidone (PVP) hydrogel coating for cylindrical polyurethane scaffolds, Colloids and Surfaces B: Biointerfaces. 192 (2020) 111066. https://doi.org/10.1016/j.colsurfb.2020.111066.

[47] M. Kurakula, G.S.N.K. Rao, Pharmaceutical assessment of polyvinylpyrrolidone (PVP): As excipient from conventional to controlled delivery systems with a spotlight on COVID-19 inhibition, Journal of Drug Delivery Science and Technology. 60 (2020) 102046. https://doi.org/10.1016/j.jddst.2020.102046.

[48] M. Lens, Recent progresses in application of fullerenes in cosmetics, BIOT. 5 (2011) 67–73. https://doi.org/10.2174/187220811796365707.

[49] D.-H. Kang, W.-Y. Choi, H. Woo, S. Jang, H.-Y. Park, J. Shim, J.-W. Choi, S. Kim, S. Jeon, S. Lee, J.-H. Park, Poly-4-vinylphenol (PVP) and poly(melamine- *co* -formaldehyde) (PMF)-based atomic switching device and its application to logic gate circuits with low operating voltage, ACS Appl. Mater. Interfaces. 9 (2017) 27073–27082. https://doi.org/10.1021/acsami.7b07549.

[50] R.J. Chudzikowski, Guar gum and its application, Journal of Society of Cosmetic Chemistry. (1971).

[51] D. Mudgil, S. Barak, B.S. Khatkar, Guar gum: processing, properties and food applications – A Review, J Food Sci Technol. 51 (2014) 409–418. https://doi.org/10.1007/s13197-011-0522-x.

[52] N. Thombare, U. Jha, S. Mishra, M.Z. Siddiqui, Guar gum as a promising starting material for diverse applications: A review, International Journal of Biological Macromolecules. 88 (2016) 361–372. https://doi.org/10.1016/j.ijbiomac.2016.04.001.

[53] B. Katzbauer, Properties and applications of xanthan gum, Polymer Degradation and Stability. 59 (1998) 81–84. https://doi.org/10.1016/S0141-3910(97)00180-8.

[54] A. Palaniraj, V. Jayaraman, Production, recovery and applications of xanthan gum by Xanthomonas campestris, Journal of Food Engineering. 106 (2011) 1–12. https://doi.org/10.1016/j.jfoodeng.2011.03.035.

[55] A. Kumar, K.M. Rao, S.S. Han, Application of xanthan gum as polysaccharide in tissue engineering: A review, Carbohydrate Polymers. 180 (2018) 128–144. https://doi.org/10.1016/j.carbpol.2017.10.009.

[56] C.D. May, Industrial pectins: Sources, production and applications, Carbohydrate Polymers. 12 (1990) 79–99. https://doi.org/10.1016/0144-8617(90)90105-2.

[57] A. Belkheiri, A. Forouhar, A.V. Ursu, P. Dubessay, G. Pierre, C. Delattre, G. Djelveh, S. Abdelkafi, N. Hamdami, P. Michaud, Extraction, characterization, and applications of pectins from plant by-products, Applied Sciences. 11 (2021) 6596. https://doi.org/10.3390/app11146596.

[58] B.R. Thakur, R.K. Singh, A.K. Handa, Chemistry and uses of pectin – A review, Crit Rev Food Sci Nutr. 37 (1997) 47–73. https://doi.org/10.1080/10408399709527767.

[59] D. Zhao, S. Yu, B. Sun, S. Gao, S. Guo, K. Zhao, Biomedical applications of chitosan and its derivative nanoparticles, Polymers (Basel). 10 (2018) 462. https://doi.org/10.3390/polym10040462.

[60] N. Morin-Crini, E. Lichtfouse, G. Torri, G. Crini, Applications of chitosan in food, pharmaceuticals, medicine, cosmetics, agriculture, textiles, pulp and paper,

biotechnology, and environmental chemistry, Environ Chem Lett. 17 (2019) 1667–1692. https://doi.org/10.1007/s10311-019-00904-x.

[61] Y. Xia, D. Wang, D. Liu, J. Su, Y. Jin, D. Wang, B. Han, Z. Jiang, B. Liu, Applications of chitosan and its derivatives in skin and soft tissue diseases, Frontiers in Bioengineering and Biotechnology. 10 (2022). https://www.frontiersin.org/articles/10.3389/fbioe.2022.894667 (accessed October 12, 2022).

[62] S. Freeman, A.M. Booth, I. Sabbah, R. Tiller, J. Dierking, K. Klun, A. Rotter, E. Ben-David, J. Javidpour, D.L. Angel, Between source and sea: The role of wastewater treatment in reducing marine microplastics, Journal of Environmental Management. 266 (2020) 110642. https://doi.org/10.1016/j.jenvman.2020.110642.

[63] S.N. Akanyange, Y. Zhang, X. Zhao, G. Adom-Asamoah, A.-R.A. Ature, C. Anning, C. Tianpeng, H. Zhao, X. Lyu, J.C. Crittenden, A holistic assessment of microplastic ubiquitousness: Pathway for source identification in the environment, Sustainable Production and Consumption. 33 (2022) 113–145. https://doi.org/10.1016/j.spc.2022.06.020.

[64] Quarterly report Q2/2022 • Plastics Europe, 2022. https://plasticseurope.org/knowledge-hub/quarterly-report-q2-2022/.

[65] Plastics - the Facts 2021 • Plastics Europe, 2021. https://plasticseurope.org/knowledge-hub/plastics-the-facts-2021/.

[66] A large family • Plastics Europe, Plastics Europe. (n.d.). https://plasticseurope.org/plastics-explained/a-large-family/ (accessed October 19, 2022).

[67] A.S. Dutta, Polyurethane foam chemistry, in: Recycling of Polyurethane Foams, Elsevier Inc., 2018. https://doi.org/10.1016/B978-0-323-51133-9.00002-4.

[68] J. Akindoyo, M. Beg, S. Ghazali, M. Islam, N. Jeyaratnam, Y. Ar, Polyurethane types, synthesis and applications – A review, RSC Adv. 6 (2016) 114453–114482. https://doi.org/10.1039/C6RA14525F.

[69] B.L. Deopura, Textile Institute, eds., Polyesters and polyamides, 1. publ, CRC Press, Boca Raton, 2008.

[70] R. Geyer, J.R. Jambeck, K.L. Law, Production, use, and fate of all plastics ever made, Science Advances. 3 (2017) e1700782. https://doi.org/10.1126/sciadv.1700782.

[71] B. Chatain, Parliament and Council agree drastic cuts to plastic pollution of environment, European Parliament, 2018. https://www.europarl.europa.eu/news/en/press-room/20181219IPR22301/parliament-and-council-agree-drastic-cuts-to-plastic-pollution-of-environment.

[72] J.P.G.L. Frias, R. Nash, Microplastics: Finding a consensus on the definition, Marine Pollution Bulletin. 138 (2019) 145–147. https://doi.org/10.1016/j.marpolbul.2018.11.022.

[73] ISO/TR 21960. Plastics – Environmental aspects – State of knowledge and methodologies, 2020. https://www.iso.org/cms/render/live/en/sites/isoorg/contents/data/standard/07/23/72300.html (accessed October 26, 2022).

[74] J. Gigault, A. ter Halle, M. Baudrimont, P.-Y. Pascal, F. Gauffre, T.-L. Phi, H. El Hadri, B. Grassl, S. Reynaud, Current opinion: What is a nanoplastic?, Environmental Pollution. 235 (2018) 1030–1034. https://doi.org/10.1016/j.envpol.2018.01.024.

[75] GESAMP, Sources, fate and effects of microplastics in the marine environment: A global assessment, Joint Group of Expert in the Scientific Aspects of Marine Environmental Protection, 2015.

[76] J.-Q. Jiang, Occurrence of microplastics and its pollution in the environment: A review, Sustainable Production and Consumption. 13 (2018) 16–23. https://doi.org/10.1016/j.spc.2017.11.003.

[77] S.N. Akanyange, Y. Zhang, X. Zhao, G. Adom-Asamoah, A.-R.A. Ature, C. Anning, C. Tianpeng, H. Zhao, X. Lyu, J.C. Crittenden, A holistic assessment of microplastic ubiquitousness: Pathway for source identification in the environment, Sustainable Production and Consumption. 33 (2022) 113–145. https://doi.org/10.1016/j.spc.2022.06.020.

[78] C.L. Waller, H.J. Griffiths, C.M. Waluda, S.E. Thorpe, I. Loaiza, B. Moreno, C.O. Pacherres, K.A. Hughes, Microplastics in the Antarctic marine system: An emerging area of research, Science of The Total Environment. 598 (2017) 220–227. https://doi.org/10.1016/j.scitotenv.2017.03.283.

[79] K. Lei, F. Qiao, Q. Liu, Z. Wei, H. Qi, S. Cui, X. Yue, Y. Deng, L. An, Microplastics releasing from personal care and cosmetic products in China, Marine Pollution Bulletin. 123 (2017) 122–126. https://doi.org/10.1016/j.marpolbul.2017.09.016.

[80] K. Duis, A. Coors, Microplastics in the aquatic and terrestrial environment: sources (with a specific focus on personal care products), fate and effects, Environ Sci Eur. 28 (2016) 2. https://doi.org/10.1186/s12302-015-0069-y.

[81] L.S. Fendall, M.A. Sewell, Contributing to marine pollution by washing your face: Microplastics in facial cleansers, Marine Pollution Bulletin. 58 (2009) 1225–1228. https://doi.org/10.1016/j.marpolbul.2009.04.025.

[82] M.A. Browne, P. Crump, S.J. Niven, E. Teuten, A. Tonkin, T. Galloway, R. Thompson, Accumulation of microplastic on shorelines worldwide: Sources and sinks, Environ. Sci. Technol. 45 (2011) 9175–9179. https://doi.org/10.1021/es201811s.

[83] F. Salvador Cesa, A. Turra, J. Baruque-Ramos, Synthetic fibers as microplastics in the marine environment: A review from textile perspective with a focus on domestic washings, Sci Total Environ. 598 (2017) 1116–1129. https://doi.org/10.1016/j.scitotenv.2017.04.172.

[84] F. De Falco, M.P. Gullo, G. Gentile, E. Di Pace, M. Cocca, L. Gelabert, M. Brouta-Agnésa, A. Rovira, R. Escudero, R. Villalba, R. Mossotti, A. Montarsolo, S. Gavignano, C. Tonin, M. Avella, Evaluation of microplastic release caused by textile washing processes of synthetic fabrics, Environmental Pollution. 236 (2018) 916–925. https://doi.org/10.1016/j.envpol.2017.10.057.

[85] I.E. Napper, R.C. Thompson, Release of synthetic microplastic plastic fibres from domestic washing machines: Effects of fabric type and washing conditions, Marine Pollution Bulletin. 112 (2016) 39–45. https://doi.org/10.1016/j.marpolbul.2016.09.025.

[86] I.E. Napper, A.C. Barrett, R.C. Thompson, The efficiency of devices intended to reduce microfibre release during clothes washing, Science of The Total Environment. 738 (2020) 140412. https://doi.org/10.1016/j.scitotenv.2020.140412.

[87] F. De Falco, E. Di Pace, M. Avella, G. Gentile, M.E. Errico, A. Krzan, H. ElKhiar, M. Zupan, M. Cocca, Development and performance evaluation of a filtration system for washing machines to reduce microfiber release in wastewater, Water Air Soil Pollut. 232 (2021) 406. https://doi.org/10.1007/s11270-021-05342-6.

[88] R.C. Hale, M.E. Seeley, M.J. La Guardia, L. Mai, E.Y. Zeng, A global perspective on microplastics, Journal of Geophysical Research: Oceans. 125 (2020) e2018JC014719. https://doi.org/10.1029/2018JC014719.

[89] P. He, L. Chen, L. Shao, H. Zhang, F. Lü, Municipal solid waste (MSW) landfill: A source of microplastics? – Evidence of microplastics in landfill leachate, Water Research. 159 (2019) 38–45. https://doi.org/10.1016/j.watres.2019.04.060.

[90] K. Cverenkárová, M. Valachovičová, T. Mackuľak, L. Žemlička, L. Bírošová, Microplastics in the food chain, Life. 11 (2021) 1349. https://doi.org/10.3390/life11121349.

[91] E.S. Okeke, C.O. Okoye, E.O. Atakpa, R.E. Ita, R. Nyaruaba, C.L. Mgbechidinma, O.D. Akan, Microplastics in agroecosystems-impacts on ecosystem functions and food chain, Resources, Conservation and Recycling. 177 (2022) 105961. https://doi.org/10.1016/j.resconrec.2021.105961.

[92] A. Bianco, M. Passananti, Atmospheric micro and nanoplastics: An enormous microscopic problem, Sustainability. 12 (2020) 7327. https://doi.org/10.3390/su12187327.

[93] X. Lim, Microplastics are everywhere – But are they harmful?, Nature. 593 (2021) 22–25. https://doi.org/10.1038/d41586-021-01143-3.

[94] S. Primpke, S.H. Christiansen, W. Cowger, H. De Frond, A. Deshpande, M. Fischer, E.B. Holland, M. Meyns, B.A. O'Donnell, B.E. Ossmann, M. Pittroff, G. Sarau, B.M. Scholz-Böttcher, K.J. Wiggin, Critical assessment of analytical methods for the harmonized and cost-efficient analysis of microplastics, Appl Spectrosc. 74 (2020) 1012–1047. https://doi.org/10.1177/0003702820921465.

[95] A.A. Horton, S.J. Dixon, Microplastics: An introduction to environmental transport processes, WIREs Water. 5 (2018). https://doi.org/10.1002/wat2.1268.

[96] M.S. Bank, S.V. Hansson, The Plastic Cycle: A novel and holistic paradigm for the Anthropocene, Environ. Sci. Technol. 53 (2019) 7177–7179. https://doi.org/10.1021/acs.est.9b02942.

[97] R. Dris, J. Gasperi, M. Saad, C. Mirande, B. Tassin, Synthetic fibers in atmospheric fallout: A source of microplastics in the environment?, Marine Pollution Bulletin. 104 (2016) 290–293. https://doi.org/10.1016/j.marpolbul.2016.01.006.

[98] S. Allen, D. Allen, V.R. Phoenix, G. Le Roux, P. Durántez Jiménez, A. Simonneau, S. Binet, D. Galop, Atmospheric transport and deposition of microplastics in a remote mountain catchment, Nat. Geosci. 12 (2019) 339–344. https://doi.org/10.1038/s41561-019-0335-5.

[99] UNEP, Microplastics: Trouble in the food chain, 2016. https://wesr.unep.org/.

[100] F. Pérez-Guevara, P.D. Roy, G. Kutralam-Muniasamy, V.C. Shruti, A central role for fecal matter in the transport of microplastics: An updated analysis of new findings and persisting questions, Journal of Hazardous Materials Advances. 4 (2021) 100021. https://doi.org/10.1016/j.hazadv.2021.100021.

[101] S. Rainieri, A. Barranco, Microplastics, a food safety issue?, Trends in Food Science & Technology. 84 (2019) 55–57. https://doi.org/10.1016/j.tifs.2018.12.009.

[102] W. Wang, J. Ge, X. Yu, H. Li, Environmental fate and impacts of microplastics in soil ecosystems: Progress and perspective, Science of The Total Environment. 708 (2020) 134841. https://doi.org/10.1016/j.scitotenv.2019.134841.

[103] Z. Zhang, Q. Cui, L. Chen, X. Zhu, S. Zhao, C. Duan, X. Zhang, D. Song, L. Fang, A critical review of microplastics in the soil-plant system: Distribution, uptake, phytotoxicity and prevention, Journal of Hazardous Materials. 424 (2022) 127750. https://doi.org/10.1016/j.jhazmat.2021.127750.

[104] J.P. Rodrigues, A.C. Duarte, J. Santos-Echeandía, T. Rocha-Santos, Significance of interactions between microplastics and POPs in the marine environment: A critical overview, TrAC Trends in Analytical Chemistry. 111 (2019) 252–260. https://doi.org/10.1016/j.trac.2018.11.038.

[105] L. Fu, J. Li, G. Wang, Y. Luan, W. Dai, Adsorption behavior of organic pollutants on microplastics, Ecotoxicology and Environmental Safety. 217 (2021) 112207. https://doi.org/10.1016/j.ecoenv.2021.112207.

[106] R. Kumar, N. Ivy, S. Bhattacharya, A. Dey, P. Sharma, Coupled effects of microplastics and heavy metals on plants: Uptake, bioaccumulation, and environmental health perspectives, Science of The Total Environment. 836 (2022) 155619. https://doi.org/10.1016/j.scitotenv.2022.155619.

[107] M. Ahechti, M. Benomar, M. El Alami, C. Mendiguchía, Metal adsorption by microplastics in aquatic environments under controlled conditions: Exposure time, pH and salinity, International Journal of Environmental Analytical Chemistry. 102 (2022) 1118–1125. https://doi.org/10.1080/03067319.2020.1733546.

[108] E. Costigan, A. Collins, M.D. Hatinoglu, K. Bhagat, J. MacRae, F. Perreault, O. Apul, Adsorption of organic pollutants by microplastics: Overview of a dissonant literature, Journal of Hazardous Materials Advances. 6 (2022) 100091. https://doi.org/10.1016/j.hazadv.2022.100091.

[109] D. Barceló, Y. Picó, Microplastics in the global aquatic environment: Analysis, effects, remediation and policy solutions, Journal of Environmental Chemical Engineering. 7 (2019) 103421. https://doi.org/10.1016/j.jece.2019.103421.

[110] K. Mizukawa, H. Takada, I. Takeuchi, T. Ikemoto, K. Omori, K. Tsuchiya, Bioconcentration and biomagnification of polybrominated diphenyl ethers (PBDEs) through lower-trophic-level coastal marine food web, Marine Pollution Bulletin. 58 (2009) 1217–1224. https://doi.org/10.1016/j.marpolbul.2009.03.008.

[111] D. Lobelle, M. Cunliffe, Early microbial biofilm formation on marine plastic debris, Marine Pollution Bulletin. 62 (2011) 197–200. https://doi.org/10.1016/j.marpolbul.2010.10.013.

[112] F.K. Mammo, I.D. Amoah, K.M. Gani, L. Pillay, S.K. Ratha, F. Bux, S. Kumari, Microplastics in the environment: Interactions with microbes and chemical contaminants, Science of The Total Environment. 743 (2020) 140518. https://doi.org/10.1016/j.scitotenv.2020.140518.

[113] S. Yezli, J.A. Otter, Minimum infective dose of the major human respiratory and enteric viruses transmitted through food and the environment, Food Environ Virol. 3 (2011) 1–30. https://doi.org/10.1007/s12560-011-9056-7.

[114] C.S. Kwan, H. Takada, Release of additives and monomers from plastic wastes, in: H. Takada, H.K. Karapanagioti (Eds.), Hazardous Chemicals Associated with Plastics in the Marine Environment, Springer International Publishing, Cham, 2019: pp. 51–70. https://doi.org/10.1007/698_2016_122.

[115] E.L. Teuten, J.M. Saquing, D.R.U. Knappe, M.A. Barlaz, S. Jonsson, A. Björn, S.J. Rowland, R.C. Thompson, T.S. Galloway, R. Yamashita, D. Ochi, Y. Watanuki, C. Moore, P.H. Viet, T.S. Tana, M. Prudente, R. Boonyatumanond, M.P. Zakaria, K. Akkhavong, Y. Ogata, H. Hirai, S.

Iwasa, K. Mizukawa, Y. Hagino, A. Imamura, M. Saha, H. Takada, Transport and release of chemicals from plastics to the environment and to wildlife, Philos Trans R Soc Lond B Biol Sci. 364 (2009) 2027–2045. https://doi.org/10.1098/rstb.2008.0284.

[116] G. Latini, C. De Felice, A. Verrotti, Plasticizers, infant nutrition and reproductive health, Reproductive Toxicology. 19 (2004) 27–33. https://doi.org/10.1016/j.reprotox.2004.05.011.

[117] Y.-S. Lee, J.-E. Lim, S. Lee, H.-B. Moon, Phthalates and non-phthalate plasticizers in sediment from Korean coastal waters: Occurrence, spatial distribution, and ecological risks, Marine Pollution Bulletin. 154 (2020) 111119. https://doi.org/10.1016/j.marpolbul.2020.111119.

[118] M.A. Kamrin, Phthalate risks, phthalate regulation, and public health: A review, Journal of Toxicology and Environmental Health, Part B. 12 (2009) 157–174. https://doi.org/10.1080/10937400902729226.

[119] J. La Nasa, G. Biale, M. Mattonai, F. Modugno, Microwave-assisted solvent extraction and double-shot analytical pyrolysis for the quali-quantitation of plasticizers and microplastics in beach sand samples, Journal of Hazardous Materials. 401 (2021) 123287. https://doi.org/10.1016/j.jhazmat.2020.123287.

[120] J.H. Bridson, E.C. Gaugler, D.A. Smith, G.L. Northcott, S. Gaw, Leaching and extraction of additives from plastic pollution to inform environmental risk: A multidisciplinary review of analytical approaches, Journal of Hazardous Materials. 414 (2021) 125571. https://doi.org/10.1016/j.jhazmat.2021.125571.

[121] EUBP, Fact sheet – What are bioplastics?, European Bioplastics, 2018. www.european-bioplastics.org twitter.com/EUBioplastics.

[122] H. Storz, K.-D. Vorlop, Bio-based plastics: Status, challenges and trends, Landbauforschung - Applied Agricultural and Forestry Research. (2013) 321–332. https://doi.org/10.3220/LBF_2013_321-332.

[123] K. Leja, G. Lewandowicz, Polymer biodegradation and biodegradable polymers – A review, Polish Journal of Environmental Studies. 19 (2010) 255–266.

[124] SO 16620-2:2019. Plastics – Biobased content – Part 2: Determination of biobased carbon content, 2019. https://www.iso.org/cms/render/live/en/sites/isoorg/contents/data/standard/07/24/72474.html (accessed October 26, 2022).

[125] ISO 16620-4:2016. Plastics – Biobased content – Part 4: Determination of biobased mass content, 2016. https://www.iso.org/cms/render/live/en/sites/isoorg/contents/data/standard/06/38/63817.html (accessed October 26, 2022).

[126] ISO 14855-1:2012. Determination of the ultimate aerobic biodegradability of plastic materials under controlled composting conditions – Method by analysis of evolved carbon dioxide – Part 1: General method, 2012. https://www.iso.org/cms/render/live/en/sites/isoorg/contents/data/standard/05/79/57902.html (accessed October 26, 2022).

[127] OK biobased – Certifications, TÜV Austria. (2022). https://www.tuv-at.be/it/green-marks/certificazioni/ok-biobased/ (accessed October 19, 2022).

[128] ISO 14855-2:2018. Determination of the ultimate aerobic biodegradability of plastic materials under controlled composting conditions – Method by analysis of evolved carbon dioxide – Part 2: Gravimetric measurement of carbon dioxide evolved in a laboratory-scale test, 2018. https://www.iso.org/cms/render/live/en/sites/isoorg/contents/data/standard/07/20/72046.html (accessed October 26, 2022).

[129] EUBP, Bioplastic market development – Update 2021, European Bioplastics, 2021. www.european-bioplastics.org twitter.com/EUBioplastics.

[130] J. Jian, Z. Xiangbin, H. Xianbo, An overview on synthesis, properties and applications of poly(butylene-adipate-co-terephthalate) – PBAT, Advanced Industrial and Engineering Polymer Research. 3 (2020) 19–26. https://doi.org/10.1016/j.aiepr.2020.01.001.

[131] V. Siracusa, N. Lotti, A. Munari, M. Dalla Rosa, Poly(butylene succinate) and poly(butylene succinate-co-adipate) for food packaging applications: Gas barrier properties after stressed treatments, Polymer Degradation and Stability. 119 (2015) 35–45. https://doi.org/10.1016/j.polymdegradstab.2015.04.026.

[132] M. Dammak, Y. Fourati, Q. Tarrés, M. Delgado-Aguilar, P. Mutjé, S. Boufi, Blends of PBAT with plasticized starch for packaging applications: Mechanical properties, rheological behaviour and biodegradability, Industrial Crops and Products. 144 (2020) 112061. https://doi.org/10.1016/j.indcrop.2019.112061.

[133] E. Castro-Aguirre, F. Iñiguez-Franco, H. Samsudin, X. Fang, R. Auras, Poly(lactic acid) – Mass production, processing, industrial applications, and end of life, Advanced Drug Delivery Reviews. 107 (2016) 333–366. https://doi.org/10.1016/j.addr.2016.03.010.

[134] S.A. Rafiqah, A. Khalina, A.S. Harmaen, I.A. Tawakkal, K. Zaman, M. Asim, M.N. Nurrazi, C.H. Lee, A review on properties and application of bio-based poly(butylene succinate), Polymers (Basel). 13 (2021) 1436. https://doi.org/10.3390/polym13091436.

[135] K. Encalada, M.B. Aldás, E. Proaño, V. Valle, An overview of starch-based biopolymers and their biodegradability, Ciencia e Ingeniería. 39 (2018) 245–258.

[136] A.P. Bonartsev, G.A. Bonartseva, I.V. Reshetov, M.P. Kirpichnikov, K.V. Shaitan, Application of polyhydroxyalkanoates in medicine and the biological activity of natural poly(3-

hydroxybutyrate), Acta Naturae. 11 (2019) 4–16. https://doi.org/10.32607/20758251-2019-11-2-4-16.

[137] M.I. Malik, J. Mays, M.R. Shah, eds., Molecular characterization of polymers: A fundamental guide, Elsevier, Cambridge, MA, 2021.

[138] H. Coceancigh, D.A. Higgins, T. Ito, Optical microscopic techniques for synthetic polymer characterization, Anal. Chem. 91 (2019) 405–424. https://doi.org/10.1021/acs.analchem.8b04694.

[139] Y. Pakzad, M. Fathi, M. Mozafari, Characterization methodologies of functional polymers, in: Advanced Functional Polymers for Biomedical Applications, Elsevier, 2019: pp. 359–381. https://doi.org/10.1016/B978-0-12-816349-8.00017-5.

[140] J. Joy, K. Winkler, K. Joseph, S. Anas, S. Thomas, Epoxy/methyl methacrylate acrylonitrile butadiene styrene (MABS) copolymer blends: reaction-induced viscoelastic phase separation, morphology development and mechanical properties, New J. Chem. 43 (2019) 9216–9225. https://doi.org/10.1039/C8NJ05653F.

[141] P. Jyotishkumar, C. Özdilek, P. Moldenaers, C. Sinturel, A. Janke, J. Pionteck, S. Thomas, Dynamics of phase separation in poly(acrylonitrile-butadiene-styrene)-modified epoxy/DDS system: Kinetics and viscoelastic effects, J. Phys. Chem. B. 114 (2010) 13271–13281. https://doi.org/10.1021/jp101661t.

[142] M. Vayer, A. Vital, C. Sinturel, New insights into polymer-solvent affinity in thin films, European Polymer Journal. 93 (2017) 132–139. https://doi.org/10.1016/j.eurpolymj.2017.05.035.

[143] H. Jinnai, Electron microscopy for polymer structures, Microscopy. 71 (2022) i148–i164. https://doi.org/10.1093/jmicro/dfab057.

[144] H. Jinnai, R.J. Spontak, Transmission electron microtomography in polymer research, Polymer. 50 (2009) 1067–1087. https://doi.org/10.1016/j.polymer.2008.12.023.

[145] M.R. Libera, R.F. Egerton, Advances in the transmission electron microscopy of polymers, Polymer Reviews. 50 (2010) 321–339. https://doi.org/10.1080/15583724.2010.493256.

[146] J. Parameswaran Pillai, J. Pionteck, R. Häßler, C. Sinturel, V.S. Mathew, S. Thomas, Effect of cure conditions on the generated morphology and viscoelastic properties of a poly(acrylonitrile–butadiene–styrene) modified epoxy–amine system, Ind. Eng. Chem. Res. 51 (2012) 2586–2595. https://doi.org/10.1021/ie2011017.

[147] M. Vayer, T.H. Nguyen, D. Grosso, C. Boissiere, M.A. Hillmyer, C. Sinturel, Characterization of nanoporous polystyrene thin films by environmental ellipsometric porosimetry, Macromolecules. 44 (2011) 8892–8897. https://doi.org/10.1021/ma201497z.

[148] M.A. Poothanari, P. Xavier, S. Bose, N. Kalarikkal, C. Komalan, S. Thomas, Compatibilising action of multiwalled carbon nanotubes in polycarbonate/polypropylene (PC/PP) blends:

phase morphology, viscoelastic phase separation, rheology and percolation, Journal of Polymer Research. 26 (2019). https://doi.org/10.1007/s10965-019-1833-2.

[149] W.J. Shim, S.H. Hong, S.E. Eo, Identification methods in microplastic analysis: A review, Anal. Methods. 9 (2017) 1384–1391. https://doi.org/10.1039/C6AY02558G.

[150] C.A. Choy, B.H. Robison, T.O. Gagne, B. Erwin, E. Firl, R.U. Halden, J.A. Hamilton, K. Katija, S.E. Lisin, C. Rolsky, K. S. Van Houtan, The vertical distribution and biological transport of marine microplastics across the epipelagic and mesopelagic water column, Sci Rep. 9 (2019) 7843. https://doi.org/10.1038/s41598-019-44117-2.

[151] R. Di Mauro, M.J. Kupchik, M.C. Benfield, Abundant plankton-sized microplastic particles in shelf waters of the northern Gulf of Mexico, Environmental Pollution. 230 (2017) 798–809. https://doi.org/10.1016/j.envpol.2017.07.030.

[152] A.L. Lusher, A. Burke, I. O'Connor, R. Officer, Microplastic pollution in the Northeast Atlantic Ocean: Validated and opportunistic sampling, Marine Pollution Bulletin. 88 (2014) 325–333. https://doi.org/10.1016/j.marpolbul.2014.08.023.

[153] R. Sutton, S.A. Mason, S.K. Stanek, E. Willis-Norton, I.F. Wren, C. Box, Microplastic contamination in the San Francisco Bay, California, USA, Marine Pollution Bulletin. 109 (2016) 230–235. https://doi.org/10.1016/j.marpolbul.2016.05.077.

[154] K.A. Willis, R. Eriksen, C. Wilcox, B.D. Hardesty, Microplastic distribution at different sediment depths in an urban estuary, Front. Mar. Sci. 4 (2017) 419. https://doi.org/10.3389/fmars.2017.00419.

[155] M. Claessens, S.D. Meester, L.V. Landuyt, K.D. Clerck, C.R. Janssen, Occurrence and distribution of microplastics in marine sediments along the Belgian coast, Marine Pollution Bulletin. 62 (2011) 2199–2204. https://doi.org/10.1016/j.marpolbul.2011.06.030.

[156] S.M. Abel, S. Primpke, I. Int-Veen, A. Brandt, G. Gerdts, Systematic identification of microplastics in abyssal and hadal sediments of the Kuril Kamchatka trench, Environmental Pollution. 269 (2021) 116095. https://doi.org/10.1016/j.envpol.2020.116095.

[157] R. Dris, J. Gasperi, V. Rocher, M. Saad, N. Renault, B. Tassin, Microplastic contamination in an urban area: a case study in Greater Paris, Environ. Chem. 12 (2015) 592. https://doi.org/10.1071/EN14167.

[158] G.S. Zhang, Y.F. Liu, The distribution of microplastics in soil aggregate fractions in southwestern China, Science of The Total Environment. 642 (2018) 12–20. https://doi.org/10.1016/j.scitotenv.2018.06.004.

[159] S.C. Leterme, E.M. Tuuri, W.J. Drummond, R. Jones, J.R. Gascooke, Microplastics in urban freshwater streams in Adelaide, Australia: A source of plastic pollution in the Gulf St Vincent, Science of The Total Environment. 856 (2023) 158672. https://doi.org/10.1016/j.scitotenv.2022.158672.

[160] F. Corradini, P. Meza, R. Eguiluz, F. Casado, E. Huerta-Lwanga, V. Geissen, Evidence of microplastic accumulation in agricultural soils from sewage sludge disposal, Science of The Total Environment. 671 (2019) 411–420. https://doi.org/10.1016/j.scitotenv.2019.03.368.

[161] C.M. Rochman, A. Tahir, S.L. Williams, D.V. Baxa, R. Lam, J.T. Miller, F.-C. Teh, S. Werorilangi, S.J. Teh, Anthropogenic debris in seafood: Plastic debris and fibers from textiles in fish and bivalves sold for human consumption, Sci Rep. 5 (2015) 14340. https://doi.org/10.1038/srep14340.

[162] R. Dris, J. Gasperi, C. Mirande, C. Mandin, M. Guerrouache, V. Langlois, B. Tassin, A first overview of textile fibers, including microplastics, in indoor and outdoor environments, Environmental Pollution. 221 (2017) 453–458. https://doi.org/10.1016/j.envpol.2016.12.013.

[163] M.J. Nematollahi, B. Keshavarzi, F. Mohit, F. Moore, R. Busquets, Microplastic occurrence in urban and industrial soils of Ahvaz metropolis: A city with a sustained record of air pollution, Science of The Total Environment. 819 (2022) 152051. https://doi.org/10.1016/j.scitotenv.2021.152051.

[164] S. Abbasi, M. Alirezazadeh, N. Razeghi, M. Rezaei, H. Pourmahmood, R. Dehbandi, M.R. Mehr, S.Y. Ashayeri, P. Oleszczuk, A. Turner, Microplastics captured by snowfall: A study in Northern Iran, Science of The Total Environment. 822 (2022) 153451. https://doi.org/10.1016/j.scitotenv.2022.153451.

[165] A.Ya. Malkin, The state of the art in the rheology of polymers: Achievements and challenges, Polym. Sci. Ser. A. 51 (2009) 80–102. https://doi.org/10.1134/S0965545X09010076.

[166] T.K. Goh, K.D. Coventry, A. Blencowe, G.G. Qiao, Rheology of core cross-linked star polymers, Polymer. 49 (2008) 5095–5104. https://doi.org/10.1016/j.polymer.2008.09.030.

[167] K. Moskalova, A. Aniskin, G. Kozina, B. Soldo, The rheometric analysis of the polymer modifier's properties in the environment of hydrated cement, Materials. 14 (2021) 1064. https://doi.org/10.3390/ma14051064.

[168] J. Meissner, Rheometry of polymer melts, Annual Review of Fluid Mechanics. 17 (1985) 45–64. https://doi.org/10.1146/annurev.fl.17.010185.000401.

[169] B. Diehl, NMR applications for polymer characterisation, in: NMR Spectroscopy in Pharmaceutical Analysis, Elsevier, 2008: pp. 157–180. https://doi.org/10.1016/B978-0-444-53173-5.00007-X.

[170] K. Saalwächter, Chapter 1 - Applications of NMR in polymer characterization – An introduction, (2019) 1–22. https://doi.org/10.1039/9781788016483-00001.

[171] B.H. Stuart, Infrared spectroscopy: Fundamentals and applications, in: Analytical Techniques in the Sciences, John Wiley & Sons, Ltd, Chichester, UK, 2005: pp. i–xvi. https://doi.org/10.1002/0470011149.fmatter.

[172] Mettler-Toledo International Inc all rights, Raman spectroscopy, (n.d.). https://www.mt.com/au/en/home/applications/L1_AutoChem_Applications/Raman-Spectroscopy.html (accessed October 17, 2022).

[173] K. Grenda, A. Idström, L. Evenäs, M. Persson, K. Holmberg, R. Bordes, An analytical approach to elucidate the architecture of polyethyleneimines, Journal of Applied Polymer Science. 139 (2022) 51657. https://doi.org/10.1002/app.51657.

[174] M. Edge, Infrared spectroscopy in analysis of polymer degradation, in: Encyclopedia of Analytical Chemistry, John Wiley & Sons, Ltd, 2006. https://doi.org/10.1002/9780470027318.a2013.

[175] D. Schymanski, C. Goldbeck, H.-U. Humpf, P. Fürst, Analysis of microplastics in water by micro-Raman spectroscopy: Release of plastic particles from different packaging into mineral water, Water Research. 129 (2018) 154–162. https://doi.org/10.1016/j.watres.2017.11.011.

[176] B.E. Oßmann, G. Sarau, H. Holtmannspötter, M. Pischetsrieder, S.H. Christiansen, W. Dicke, Small-sized microplastics and pigmented particles in bottled mineral water, Water Research. 141 (2018) 307–316. https://doi.org/10.1016/j.watres.2018.05.027.

[177] I.V. Kirstein, F. Hensel, A. Gomiero, L. Iordachescu, A. Vianello, H.B. Wittgren, J. Vollertsen, Drinking plastics? – Quantification and qualification of microplastics in drinking water distribution systems by µFTIR and *m/z*, Water Research. 188 (2021) 116519. https://doi.org/10.1016/j.watres.2020.116519.

[178] K. Gunaalan, R. Almeda, C. Lorenz, A. Vianello, L. Iordachescu, K. Papacharalampos, C.M. Rohde Kiær, J. Vollertsen, T.G. Nielsen, Abundance and distribution of microplastics in surface waters of the Kattegat/ Skagerrak (Denmark), Environmental Pollution. 318 (2023) 120853. https://doi.org/10.1016/j.envpol.2022.120853.

[179] C. Lorenz, L. Roscher, M.S. Meyer, L. Hildebrandt, J. Prume, M.G.J. Löder, S. Primpke, G. Gerdts, Spatial distribution of microplastics in sediments and surface waters of the southern North Sea, Environmental Pollution. 252 (2019) 1719–1729. https://doi.org/10.1016/j.envpol.2019.06.093.

[180] I. Peeken, S. Primpke, B. Beyer, J. Gütermann, C. Katlein, T. Krumpen, M. Bergmann, L. Hehemann, G. Gerdts, Arctic sea ice is an important temporal sink and means of transport for microplastic, Nat Commun. 9 (2018) 1505. https://doi.org/10.1038/s41467-018-03825-5.

[181] H.K. Imhof, C. Laforsch, A.C. Wiesheu, J. Schmid, P.M. Anger, R. Niessner, N.P. Ivleva, Pigments and plastic in limnetic ecosystems: A qualitative and quantitative study on

microparticles of different size classes, Water Research. 98 (2016) 64–74. https://doi.org/10.1016/j.watres.2016.03.015.

[182] L. Roscher, A. Fehres, L. Reisel, M. Halbach, B. Scholz-Böttcher, M. Gerriets, T.H. Badewien, G. Shiravani, A. Wurpts, S. Primpke, G. Gerdts, Microplastic pollution in the Weser estuary and the German North Sea, Environmental Pollution. 288 (2021) 117681. https://doi.org/10.1016/j.envpol.2021.117681.

[183] L. Roscher, M. Halbach, M.T. Nguyen, M. Hebeler, F. Luschtinetz, B.M. Scholz-Böttcher, S. Primpke, G. Gerdts, Microplastics in two German wastewater treatment plants: Year-long effluent analysis with FTIR and Py-GC/MS, Science of The Total Environment. 817 (2022) 152619. https://doi.org/10.1016/j.scitotenv.2021.152619.

[184] K. Chouchene, T. Nacci, F. Modugno, V. Castelvetro, M. Ksibi, Soil contamination by microplastics in relation to local agricultural development as revealed by FTIR, ICP-MS and pyrolysis-GC/MS, Environmental Pollution. 303 (2022) 119016. https://doi.org/10.1016/j.envpol.2022.119016.

[185] T. Mani, S. Primpke, C. Lorenz, G. Gerdts, P. Burkhardt-Holm, Microplastic pollution in benthic midstream sediments of the Rhine river, Environ. Sci. Technol. 53 (2019) 6053–6062. https://doi.org/10.1021/acs.est.9b01363.

[186] M. Haave, C. Lorenz, S. Primpke, G. Gerdts, Different stories told by small and large microplastics in sediment - first report of microplastic concentrations in an urban recipient in Norway, Marine Pollution Bulletin. 141 (2019) 501–513. https://doi.org/10.1016/j.marpolbul.2019.02.015.

[187] S. Kühn, F.L. Schaafsma, B. van Werven, H. Flores, M. Bergmann, M. Egelkraut-Holtus, M.B. Tekman, J.A. van Franeker, Plastic ingestion by juvenile polar cod (Boreogadus saida) in the Arctic Ocean, Polar Biol. 41 (2018) 1269–1278. https://doi.org/10.1007/s00300-018-2283-8.

[188] X. Sun, T. Liu, M. Zhu, J. Liang, Y. Zhao, B. Zhang, Retention and characteristics of microplastics in natural zooplankton taxa from the East China Sea, Science of The Total Environment. 640–641 (2018) 232–242. https://doi.org/10.1016/j.scitotenv.2018.05.308.

[189] S. Gao, K. Yan, B. Liang, R. Shu, N. Wang, S. Zhang, The different ways microplastics from the water column and sediment accumulate in fish in Haizhou Bay, Science of The Total Environment. 854 (2023) 158575. https://doi.org/10.1016/j.scitotenv.2022.158575.

[190] M. Bergmann, S. Mützel, S. Primpke, M.B. Tekman, J. Trachsel, G. Gerdts, White and wonderful? Microplastics prevail in snow from the Alps to the Arctic, Sci. Adv. 5 (2019) eaax1157. https://doi.org/10.1126/sciadv.aax1157.

[191] L. Simon-Sánchez, M. Grelaud, C. Lorenz, J. Garcia-Orellana, A. Vianello, F. Liu, J. Vollertsen, P. Ziveri, Can a Sediment Core Reveal the Plastic Age? Microplastic Preservation in a

Coastal Sedimentary Record, Environ. Sci. Technol. 56 (2022) 16780–16788. https://doi.org/10.1021/acs.est.2c04264.

[192] K. Bhagat, A.C. Barrios, K. Rajwade, A. Kumar, J. Oswald, O. Apul, F. Perreault, Aging of microplastics increases their adsorption affinity towards organic contaminants, Chemosphere. 298 (2022) 134238. https://doi.org/10.1016/j.chemosphere.2022.134238.

[193] E. Uliyanchenko, S. van der Wal, P.J. Schoenmakers, Challenges in polymer analysis by liquid chromatography, Polym. Chem. 3 (2012) 2313. https://doi.org/10.1039/c2py20274c.

[194] F.C.-Y. Wang, Polymer analysis by pyrolysis gas chromatography, Journal of Chromatography A. 843 (1999) 413–423. https://doi.org/10.1016/S0021-9673(98)01051-6.

[195] T. Chang, Polymer characterization by interaction chromatography, J. Polym. Sci. B Polym. Phys. 43 (2005) 1591–1607. https://doi.org/10.1002/polb.20440.

[196] S. Crotty, S. Gerişlioğlu, K.J. Endres, C. Wesdemiotis, U.S. Schubert, Polymer architectures via mass spectrometry and hyphenated techniques: A review, Analytica Chimica Acta. 932 (2016) 1–21. https://doi.org/10.1016/j.aca.2016.05.024.

[197] C. Wesdemiotis, Multidimensional mass spectrometry of synthetic polymers and advanced materials, Angewandte Chemie International Edition. 56 (2017) 1452–1464. https://doi.org/10.1002/anie.201607003.

[198] J.D. Menczel, R.B. Prime, eds., Thermal analysis of polymers: Fundamentals and applications, John Wiley, Hoboken, N.J, 2009.

[199] D. Sorolla-Rosario, J. Llorca-Porcel, M. Pérez-Martínez, D. Lozano-Castelló, A. Bueno-López, Study of microplastics with semicrystalline and amorphous structure identification by TGA and DSC., Journal of Environmental Chemical Engineering. 10 (2022) 106886. https://doi.org/10.1016/j.jece.2021.106886.

[200] J. Yu, P. Wang, F. Ni, J. Cizdziel, D. Wu, Q. Zhao, Y. Zhou, Characterization of microplastics in environment by thermal gravimetric analysis coupled with Fourier transform infrared spectroscopy, Marine Pollution Bulletin. 145 (2019) 153–160. https://doi.org/10.1016/j.marpolbul.2019.05.037.

[201] S.A. Abdel Ghani, A.A.M. El-Sayed, M.I.A. Ibrahim, M.M. Ghobashy, M.A. Shreadah, S. Shabaka, Characterization and distribution of plastic particles along Alexandria beaches, Mediterranean Coast of Egypt, using microscopy and thermal analysis techniques, Science of The Total Environment. 834 (2022) 155363. https://doi.org/10.1016/j.scitotenv.2022.155363.

[202] Y. Liu, R. Li, J. Yu, F. Ni, Y. Sheng, A. Scircle, J.V. Cizdziel, Y. Zhou, Separation and identification of microplastics in marine organisms by TGA-FTIR-GC/MS: A case study of

mussels from coastal China, Environmental Pollution. 272 (2021) 115946. https://doi.org/10.1016/j.envpol.2020.115946.

[203] S.C. Moldoveanu, Analytical pyrolysis of synthetic organic polymers, Elsevier, Amsterdam Oxford, 2005.

[204] E. Stauffer, J.A. Dolan, R. Newman, Chemistry and physics of fire and liquid fuels, in: Fire Debris Analysis, Elsevier, 2008: pp. 85–129. https://doi.org/10.1016/B978-012663971-1.50008-7.

[205] Pyrolyzer | Pyrolysis-GC/MS | Technical Info, Frontier Laboratories. (2022). https://www.frontier-lab.com/technical-information/methodology/part3/ (accessed October 17, 2022).

[206] S. Tsuge, H. Ohtani, C. Watanabe, Pyrolysis–GC/MS data book of synthetic polymers - Pyrograms, thermograms and MS of pyrolyzates, Elsevier, 2012.

[207] M. Fischer, B.M. Scholz-Böttcher, Simultaneous trace identification and quantification of common types of microplastics in environmental samples by pyrolysis-gas chromatography–mass spectrometry, Environ. Sci. Technol. 51 (2017) 5052–5060. https://doi.org/10.1021/acs.est.6b06362.

[208] Șerban Moldoveanu, Analytical pyrolysis of natural organic polymers, 1st ed, Elsevier, Amsterdam ; New York, 1998.

[209] M. Fischer, I. Goßmann, B.M. Scholz-Böttcher, Fleur de Sel – An interregional monitor for microplastics mass load and composition in European coastal waters?, Journal of Analytical and Applied Pyrolysis. (2019). https://10.1016/j.jaap.2019.104711 (accessed September 9, 2021).

[210] C. Dessì, E.D. Okoffo, J.W. O'Brien, M. Gallen, S. Samanipour, S. Kaserzon, C. Rauert, X. Wang, K.V. Thomas, Plastics contamination of store-bought rice, Journal of Hazardous Materials. 416 (2021) 125778. https://doi.org/10.1016/j.jhazmat.2021.125778.

[211] C. Dibke, M. Fischer, B.M. Scholz-Böttcher, Microplastic mass concentrations and distribution in German bight waters by pyrolysis–gas chromatography–mass spectrometry/thermochemolysis reveal potential impact of marine coatings: Do ships leave skid marks?, Environ. Sci. Technol. 55 (2021) 2285–2295. https://doi.org/10.1021/acs.est.0c04522.

[212] E.D. Okoffo, C. Rauert, K.V. Thomas, Mass quantification of microplastic at wastewater treatment plants by pyrolysis-gas chromatography–mass spectrometry, Science of The Total Environment. 856 (2023) 159251. https://doi.org/10.1016/j.scitotenv.2022.159251.

[213] N. Dimitrov, M. Čurlin, T. Pušić, B. Vojnović, Application of GC/MS pyrolysis for assessment residues of textile composites after filtration of washing and rinsing effluents, Separations. 9 (2022) 292. https://doi.org/10.3390/separations9100292.

[214] M. Halbach, M. Vogel, J.K. Tammen, H. Rüdel, J. Koschorreck, B.M. Scholz-Böttcher, 30 years trends of microplastic pollution: Mass-quantitative analysis of archived mussel samples from the North and Baltic Seas, Science of The Total Environment. 826 (2022) 154179. https://doi.org/10.1016/j.scitotenv.2022.154179.

[215] I. Goßmann, M. Halbach, B.M. Scholz-Böttcher, Car and truck tire wear particles in complex environmental samples – A quantitative comparison with "traditional" microplastic polymer mass loads, Science of The Total Environment. 773 (2021) 145667. https://doi.org/10.1016/j.scitotenv.2021.145667.

[216] J.V. Miller, J.R. Maskrey, K. Chan, K.M. Unice, Pyrolysis-gas chromatography-mass spectrometry (Py-GC-MS) quantification of tire and road wear particles (TRWP) in environmental matrices: Assessing the importance of microstructure in instrument calibration protocols, Analytical Letters. 55 (2022) 1004–1016. https://doi.org/10.1080/00032719.2021.1979994.

[217] S. O'Brien, E.D. Okoffo, C. Rauert, J.W. O'Brien, F. Ribeiro, S.D. Burrows, T. Toapanta, X. Wang, K.V. Thomas, Quantification of selected microplastics in Australian urban road dust, Journal of Hazardous Materials. 416 (2021) 125811. https://doi.org/10.1016/j.jhazmat.2021.125811.

[218] Z. Steinmetz, H. Schröder, Plastic debris in plastic-mulched soil—a screening study from western Germany, PeerJ. 10 (2022) e13781. https://doi.org/10.7717/peerj.13781.

[219] F. Saliu, G. Biale, C. Raguso, J. La Nasa, I. Degano, D. Seveso, P. Galli, M. Lasagni, F. Modugno, Detection of plastic particles in marine sponges by a combined infrared micro-spectroscopy and pyrolysis-gas chromatography-mass spectrometry approach, Science of The Total Environment. 819 (2022) 152965. https://doi.org/10.1016/j.scitotenv.2022.152965.

[220] S.T. Anuar, R.S. Altarawnah, A.A. Mohd Ali, B.Q. Lee, W.M.A.W.M. Khalik, K.M.K.K. Yusof, Y.S. Ibrahim, Utilizing pyrolysis–gas chromatography/mass spectrometry for monitoring and analytical characterization of microplastics in polychaete worms, Polymers. 14 (2022) 3054. https://doi.org/10.3390/polym14153054.

[221] R. Nakano, R.K. Gürses, Y. Tanaka, Y. Ishida, T. Kimoto, S. Kitagawa, Y. Iiguni, H. Ohtani, Pyrolysis-GC–MS analysis of ingested polystyrene microsphere content in individual Daphnia magna, Science of The Total Environment. 817 (2022) 152981. https://doi.org/10.1016/j.scitotenv.2022.152981.

[222] I. Goßmann, R. Süßmuth, B.M. Scholz-Böttcher, Plastic in the air?! – Spider webs as spatial and temporal mirror for microplastics including tire wear particles in urban air, Science of The Total Environment. 832 (2022) 155008. https://doi.org/10.1016/j.scitotenv.2022.155008.

[223] S. O'Brien, E.D. Okoffo, J.W. O'Brien, F. Ribeiro, X. Wang, S.L. Wright, S. Samanipour, C. Rauert, T.Y.A. Toapanta, R. Albarracin, K.V. Thomas, Airborne emissions of microplastic

fibres from domestic laundry dryers, Science of The Total Environment. 747 (2020) 141175. https://doi.org/10.1016/j.scitotenv.2020.141175.

[224] W. Cowger, A.M. Booth, B.M. Hamilton, C. Thaysen, S. Primpke, K. Munno, A.L. Lusher, A. Dehaut, V.P. Vaz, M. Liboiron, L.I. Devriese, L. Hermabessiere, C. Rochman, S.N. Athey, J.M. Lynch, H. De Frond, A. Gray, O.A.H. Jones, S. Brander, C. Steele, S. Moore, A. Sanchez, H. Nel, Reporting guidelines to increase the reproducibility and comparability of research on microplastics, Appl Spectrosc. 74 (2020) 1066–1077. https://doi.org/10.1177/0003702820930292.

[225] N.B. Hartmann, T. Hüffer, R.C. Thompson, M. Hassellöv, A. Verschoor, A.E. Daugaard, S. Rist, T. Karlsson, N. Brennholt, M. Cole, M.P. Herrling, M.C. Hess, N.P. Ivleva, A.L. Lusher, M. Wagner, Are we speaking the same language? Recommendations for a definition and categorization framework for plastic debris, Environ. Sci. Technol. 53 (2019) 1039–1047. https://doi.org/10.1021/acs.est.8b05297.

[226] L.M. van Mourik, S. Crum, E. Martinez-Frances, B. van Bavel, H.A. Leslie, J. de Boer, W.P. Cofino, Results of WEPAL-QUASIMEME/NORMANs first global interlaboratory study on microplastics reveal urgent need for harmonization, Science of The Total Environment. 772 (2021) 145071. https://doi.org/10.1016/j.scitotenv.2021.145071.

[227] T. Backhaus, M. Wagner, Microplastics in the environment: Much ado about nothing? A debate, Global Challenges. 4 (2020) 1900022. https://doi.org/10.1002/gch2.201900022.

[228] L. Mai, L.-J. Bao, L. Shi, C.S. Wong, E.Y. Zeng, A review of methods for measuring microplastics in aquatic environments, Environ Sci Pollut Res. 25 (2018) 11319–11332. https://doi.org/10.1007/s11356-018-1692-0.

[229] A. Isobe, N.T. Buenaventura, S. Chastain, S. Chavanich, A. Cózar, M. DeLorenzo, P. Hagmann, H. Hinata, N. Kozlovskii, A.L. Lusher, E. Martí, Y. Michida, J. Mu, M. Ohno, G. Potter, P.S. Ross, N. Sagawa, W.J. Shim, Y.K. Song, H. Takada, T. Tokai, T. Torii, K. Uchida, K. Vassillenko, V. Viyakarn, W. Zhang, An interlaboratory comparison exercise for the determination of microplastics in standard sample bottles, Marine Pollution Bulletin. 146 (2019) 831–837. https://doi.org/10.1016/j.marpolbul.2019.07.033.

[230] Y.K. Müller, T. Wernicke, M. Pittroff, C.S. Witzig, F.R. Storck, J. Klinger, N. Zumbülte, Microplastic analysis – Are we measuring the same? Results on the first global comparative study for microplastic analysis in a water sample, Anal Bioanal Chem. 412 (2020) 555–560. https://doi.org/10.1007/s00216-019-02311-1.

[231] S. Belz, I. Bianchi, C. Cella, H. Emteborg, F. Fumagalli Sirio, O. Geiss, D. Gilliland, A. Held, U. Jacobsson, R. La Spina, D. Méhn, Y. Ramaye, P. Robouch, J. Seghers, B. Sokull-Kluttgen, E. Stefaniak, J. Stroka, Current status of the quantification of microplastics in water – Results of a JRC/BAM interlaboratory comparison study on PET in water, European Commission - Joint Research Centre.Publications Office, LU, 2021. https://data.europa.eu/doi/10.2760/27641 (accessed October 26, 2022).

2. Aims

Synthetic polymers consist of a wide heterogeneous group of materials which are currently present in our daily life, from basic uses to the most technologically advanced ones. The significance of these materials has been increasingly underlined by the huge number of applications that provide comfort and innovation in many fields, such as medical, engineering, biomedical, technological, agricultural, cosmetics, pharmaceutical, automotive, transportation, electrical and electronics, and so forth. On the other hand, the unnecessarily large use, the abuse and the incorrect waste disposal or management, are determining alert signals in environmental balances. In fact, the occurrence of polymers in the environment is widespread and, depending on polymer types, production data and applications, this occurrence may represent an emerging concern. A first reason of concern is that this pervasive occurrence is predicted to increase due to the worldwide rise of polymer production. The risks posed on human health, organisms and ecosystems are currently under investigation and, even though a possible toxicity has been excluded for some classes of polymers, their environmental occurrence may become pseudo-persistent. On the other hand, some polymers are still under study and a real lack of knowledge is arising. In this context, the identification and quantification of polymers in different matrices hold a fundamental position, allowing the assessment of the state of the environment and serving as a starter in the development of remediation ad mitigation actions.

Pyrolysis coupled to gas-chromatography and mass spectrometry (Py-GC-MS) is gaining increasing importance in the analysis of polymeric materials, both for their characterisation and their investigation in environmental samples. Py-GC-MS allows the univocal chemical identification of materials, regardless of their shape (liquid/solid, irregular shapes, colours, sizes, etc.) or the matrix where they are included (thanks to the high selectivity of GC-MS separation). Moreover, the capability of this thermoanalytical technique to provide results in mass-concentration values, is highly beneficial in a view of the definition of mitigation measures. However, standardised and harmonised methods have not established yet, and additional studies are required to improve the present knowledge on the limits and advantages of Py-GC-MS, especially for less investigated polymers.

The main aim of this PhD thesis is to show the potential of the use of Py-GC-MS for the analysis of polymers occurring in the environment. Both the less investigated liquid water-soluble polymers and the widely studied solid water-insoluble polymers (microplastics, MPs) were taken into account to develop methods for the analysis of environmental contamination. The

development of the project involved two different aspects: (I) the polymer characterisation related to the study of chemical structures and thermal behaviours and (II) the development and application of thermoanalytical methods for the identification and quantification of polymers in complex matrices.

Results section (Chapter 2) is split in two main sections with water-solubility as discernment parameter, showing different applications of Py-GC-MS.

In Section 3 water-soluble polymers are investigated. Poly(dimethylsiloxanes) (PDMS) bearing polyethylene glycol (PEG) side chains were selected as analytes of interest, due to their wide use in cosmetics and personal care products. In Section 3.1.1 the thermal behaviour of PDMS and PEG-PDMS is explained, aiming at the detection and quantification of these polymers in complex matrices, with the development of a method for their extraction from sewage sludges and analysis by Py-GC-MS.

In Section 3.2 attention is focused on plastics and bioplastics as water-insoluble polymers. First of all, attention is addressed to MPs, being of emerging concern in the landscape of environmental pollution. Section 3.2.1 provides a detailed study on the thermal behaviour of common polymers while they are co-pyrolysed, such a guideline for the environmental investigation of MPs by Py-GC-MS; Section 3.2.1 shows an application of Py-GC-MS on environmental samples, mainly focusing on the urban spread of the heterogeneous polymer group of polyurethanes (PURs). In the last Section 3.2.2, bioplastics are investigated with a focus on leaching of organic compounds susceptible to migrate into seawater. Py-GC-MS is used to identify the polymers composing commercial bioplastic items used for biological tests on seawater leachates in a collaborative work. The chemical composition of leachate is investigated and compared with Py-GC-MS data.

3. Experimental results

3.1. Applications of Py-GC-MS for the investigation of water-soluble polymers

3.1.1. Analytical pyrolysis of poly(dimethylsiloxane) and poly(oxyethylene) siloxane copolymers. Application to the analysis of sewage sludges

Published on Journal of Analytical and Applied Pyrolysis (2021). DOI: 10.1016/j.jaap.2021.105236

3.1.1.1. Introduction

Polysiloxanes are inorganic polymers consisting of a backbone of alternating silicon and oxygen atoms, although the term “silicones” is often used to designate polysiloxanes with predominant dimethylsiloxane units. Silicones are uniquely man-made materials that depending on their molecular weight and substituents can appear in different forms and properties. Therefore, they have found applications in a variety of sectors such as agriculture, transportation, construction materials, electronics, energy, healthcare, industrial processes, personal care products and so forth [1–3]. The worldwide production of silicones is several million tons per year; the personal care production presented the third-largest application (industrial processes 35 %, construction materials 26 % and personal care products 17 %) [3]. Geographically, the largest silicon market is Europe and the categories products are toiletries, skin care, hair care, fragrances and make-up [3]. The predominant silicone involved in personal care products is poly(dimethylsiloxane) (PDMS), commercially known as dimethicone according to the International Nomenclature of Cosmetic Ingredients (INCI). Besides the homopolymer PDMS, copolymers bearing poly(oxyalkylated) substituents, especially poly(ethylene glycol) (PEG) and poly(propylene glycol) (PPG) derivatives are widely used in personal care products [4]. They were originally called dimethicone copolyols and the name has been commercially replaced by PEG (or PPG) dimethicone and bis-PEG (or PPG) dimethicone [5]. Depending on the location of the poly(oxyalkylated) substituents, they are classified in three primary configurations: end-capped polysiloxanes, alkoxy-polysiloxane/polysiloxane copolymers and combinations of the latter

[6].In this study, attention was payed to PEG-dimethicones because these copolymers are widely used in pharmaceutical and personal care products [2], principally as emulsifiers [4] thanks to the presence of the water-soluble group (PEG) that makes dimethicones surface active and water-soluble, and because of their low toxicity [7]. Given their large use, it is expected that these products could enter wastewater treatment plants (WWTP). Thus, the knowledge on the occurrence of these polymers in treated wastewaters and sewage sludge is important in order to identify the existence of potential source of contamination in the environment. As other water soluble or liquid polymers, PEG-dimethicones have not attracted the same attention of water insoluble solid polymers, such as microplastics, as potential environmental contaminants. However, water soluble polymers are produced in large quantity and could reach the environment if not efficiently removed by degradation or sorption in WWTP [8]. Moreover, some water-soluble polymers are persistent and should not be ignored just because they do not fall within the category of microplastics [9]. The analytical determination of trace concentrations of polymers in a complex heterogeneous matrix is challenging and requires selective and sensitive techniques as those based on mass spectrometry. In a proof of principle concept, Huppertsberg et al. [8] have identified PEG in wastewater effluents by mass spectrometry with in-source fragmentation technique that convert PEG into distinctive fragment ions ($C_4H_9O_2^+$, $C_6H_{13}O_3^+$, $C_8H_{17}O_4^+$ and $C_{10}H_{21}O_5^+$). Analytical pyrolysis (Py) combined with gas chromatography-mass spectrometry (GC–MS) has demonstrated its validity for the determination of microplastics in various matrices [10–12]. Instead, the potential of Py-GC-MS to the analysis of liquid or water-soluble polymers in environmental samples has not been deeply investigated [13]. A fundamental step in developing new analytical methods by Py-GC-MS is the knowledge of the thermal behaviour of the polymers under investigation. Several articles reported on the analysis of PDMS [14–17] and PEG [18,19] by Py-GC-MS, but to the best of our knowledge no articles have been published dealing with Py-GC-MS of their copolymers (virtually between dimethylsiloxane and methylsiloxane bearing a poly (ethylene glycol) side-chain). The main purposes of this study were (1) to gather information on the molecular composition of pyrolyzates of dimethicone and PEG-dimethicones, (2) evaluate the potential of Py-GC-MS for their quali-quantitative analysis in complex organic matrices such as sewage sludge.

3.1.1.2. PDMS nomenclature

Polysiloxanes are characterised by the structure Si-O-Si and Si atom can also be bonded to C depending on their substituent. In general, the term “siloxanes” indicates compound containing

Si atom bonded to at least one O atom. In order to easily identify organosilicons structures, following sections will use the nomenclature which accords to Rücker and Kümmerer (2015) [2]. The shorthand notation is based on the number of O atoms bonded to each Si atoms and each structure can be identified by a letter (see Figure 3.1.1-1). M stands for monovalent structural unit $Me_3SiO_{1/2}$, D for divalent $Me_2SiO_{2/2}$, T for trivalent $MeSiO_{3/2}$, and Q for quadrivalent $SiO_{4/2}$. Moreover, in order to distinguish cyclic to linear structure, cyclic methylsiloxanes are termed D_n (n is the number of silicon atoms) and linear methylsiloxanes are indicated MD_n-2M or more shortly L_n. Finally, a superscript to the right of a symbol denotes a group that replaced a methyl, thus siloxanol of D_5 is termed D_4D^{OH}.

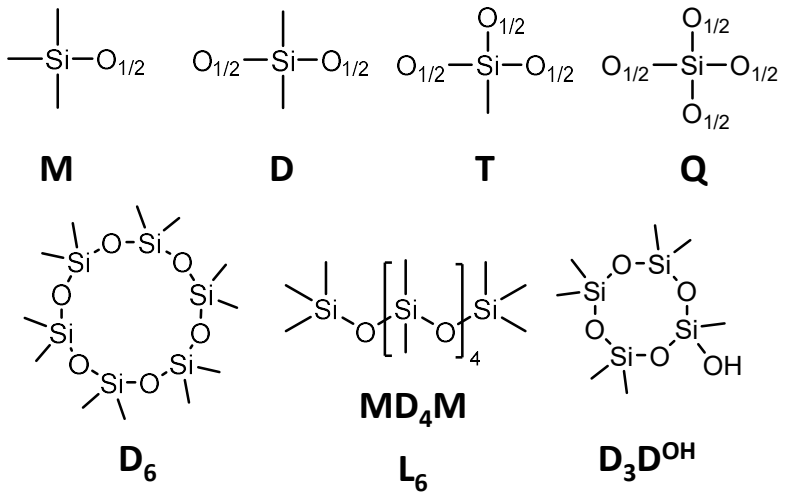

Figure 3.1.1-1 *Shorthand nomenclature notation for methylsiloxanes with examples of structural formulas [20].*

3.1.1.3. Experimental

3.1.1.3.1. Standard materials

Polydimethylsiloxanes from Dow Corning were kindly provided by Prof. Luca Valgimigli, University of Bologna. Namely, INCI name (commercial name): dimethicone (ACESIL 350), PEG-12 dimethicone (XIAMETER® OFX-0193 Fluid), PEG-8 dimethicone (FANCORSIL® LIM- 1), and bis-PEG-18 methyl ether dimethyl silane (DOWSIL™ 2501 Cosmetic Wax) (see Figure 3.1.1-2). These PDMS were selected because they are widely used in formulation of personal care products, therefore they can be representative of the domestic pollution which reach WWTPs. Dimethicone and copolyols were dissolved in tetrahydrofuran (THF, Sigma Aldrich) to prepare solutions with increasing concentrations in the 0.02-13 mg mL^{-1} range. These solutions were initially used for the characterisation of polymers, then they were employed for the construction

of calibration curves. Tetrakis(trimethylsiloxy)silane (M_4Q, trisiloxane, 1,1,1,5,5,5-hexamethyl-3,3-bis[(trimethylsilyl)oxy]-, Sigma Aldrich) was employed as internal standard (IS); a solution of 100 mg L^{-1} (corresponding to 0.112 µg mg^{-1}) of M4Q was prepared in THF.

Standard solutions of $L_{2\text{-}5}$, $D_{3\text{-}6}$ and PEG-200 (Sigma Aldrich) were prepared in THF at concentrations of 1 mg mL^{-1}. These solutions were useful for the correct identification of peaks in PDMS and copolymer pyrograms.

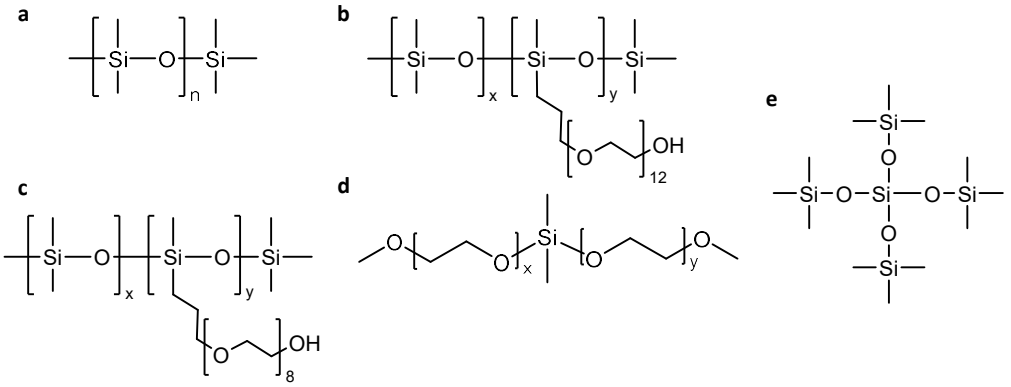

Figure 3.1.1-2. *Structures of standard polydimethylsiloxanes and copolymers analysed: (a) dimethicone, (b) PEG-12 dimethicone, (c) PEG-8 dimethicone, (d) bis-PEG-18 methyl ether dimethyl silane and (e) trisiloxane, 1,1,1,5,5,5-hexamethyl-3,3-bis[(trimethylsilyl)oxy]-, M_4Q (IS).*

3.1.1.3.2. Complex matrices: sewage sludges

Matrices employed to validate the method were sewage sludges from the municipal WWTP of Ravenna. Sewage sludges were sampled in different steps of the depuration process: oxidized sludge (pre-treatment step), thick (primary settling), dewatered (biological thick sludge dewatered at the WWTP by centrifuges).

3.1.1.3.3. Py-GC-MS

Py-GC-MS analyses were used for polymer characterisation, construction of calibration curves and analysis of the extracted samples. All the experiments were conducted following the same procedure and instrumental conditions resumed in Table 3.1.1-1. Pyrolysis temperature was selected as higher than the maximum evolution rate of volatiles from PDMS [21] and PEG [22]. For each experiment 5 µL of THF standard solution or extract and 5 µL, exactly weighed (± 0.01 mg), of IS solution were injected inside the pyrolysis cup (Eco-cup LF, Frontier Lab) which free-fell into the pyrolyzer furnace. As split ratio is inversely related to the amount of products entering the column, relatively low split ratios or even splitless conditions have been used in trace analysis of plastics [23]. In this study, a split ratio 20 was selected to favour polymer

detection avoiding mass spectrum saturation of extracted samples. Compound identification was based on injection of pure volatile methyl siloxanes (L_{2-5} and D_{3-6}), pyrolysis of PEG-200, NIST14 library match, and comparison with literature.

Table 3.1.1-1. *Instrumental conditions for Py-GC-MS analyses of standard PDMS and copolymers, calibration solutions and extracted samples from sewage sludges.*

Pyrolyzer	**Multi-Shot Pyrolyzer (EGA/PY-3030D) - Frontier Lab**	
	Furnace temperature	500 °C
	Interface temperature	300 °C
Gas chromatograph	**Agilent 7890B**	
	Column	Agilent 19091S-433UI HP-5ms Ultra Inert 30 m x 250 µm x 0.25 µm
	Carrier gas	He
	Column flow	1 mL min^{-1}
	Split	1:20
	Injector	300 °C
Oven programmed temperature	Initial temperature	40 °C
	Temperature hold time	5 min
	Temperature rate	10 °C min^{-1}
	Maximum temperature	300 °C
	Temperature hold time	10 min
Mass spectrometer	**Agilent 5977B**	
	MS source temperature	230 °C
	MS quad temperature	150 °C
	Mass scan	35 – 600 *m/z*
	Ionization energy	70 eV

3.1.1.3.4. Spectroscopic characterisation

Standards were also characterized using by spectroscopic analyses to obtain complementary information. Analyses were conducted with a FT-IR spectrometer (Cary 630 FT-IR Spectrometer, Agilent, USA) with ATR diamond crystal. Experimental conditions are described in Table 3.1.1-2.

Table 3.1.1-2. *Instrumental conditions for FTIR-ATR analyses.*

Cary 630 FTIR Spectrometer with ATR diamond crystal	
Spectral range	650 – 4000 cm^{-1}
Background scans	32
Sample scans	32
Resolution	8 cm^{-1}

3.1.1.3.5. PDMS and copolymers extraction procedure

Wet sludges were manually homogenised and then transferred into porcelain crucibles and placed in an oven at 105 °C until complete drying. The quantity of solid matter originally present was calculated by the difference in weight with original sludges, resulting in 1.0, 3.5 and 22.8 % for oxidized, thick and dewatered sludge, respectively. About 1 g, exactly weighed, of dried sewage sludge sample was extracted with 25 mL THF for 2 h under reflux. THF is a good solvent for the extraction of PDMS [24]; preliminary tests showed that PEG-dimethicones were readily dissolved in THF. After solvent extraction, the mixture was centrifuged at 5000 rpm for 5 min, the supernatant was withdrawn and concentrated by rotary evaporation. The resulting solution was transferred into a 1.5 mL glass vial (previously weighted) and concentrated to ≈ 0.5 mL by a gentle nitrogen stream. The weight of the sample was calculated by difference in order to know the volume of sample, which was estimated assuming the sample as THF (density = 0.888 g mL^{-3}). Therefore, it was also possible to estimate the exact amount of IS injected in each analysis. The vials were capped with PTFE caps composed of a central silicon septum protected internally by an aluminium foil and stored at -20 °C prior to Py-GC-MS analyses. Three replicate analyses were performed on each leachate sample.

3.1.1.3.6. Method validation

Peak areas A were determined by integration of the peak in the extracted ion chromatogram of a single specific ion. Calibration protocol was constructed in the form of the Equation 3.1.1.-1.

$$\frac{A_x Q_{IS}}{A_{IS}} = aQ_x + b \qquad \textbf{Equation 3.1.1-1}$$

A_x is the peak area of the pyrolytic marker integrated at a specific *m/z*, A_{IS} the peak area of IS (integrated at *m/z* 281), Q_x the mass (µg) of the pyrolysed polymer, Q_{IS} the mass of the IS (µg, around 0.45 µg exactly calculated from the mass of the injected solution); a the slope (sensitivity) and b the intercept.

Recovery was determined by spiking the already THF-extracted sewage sludge samples with a known quantity of PEG-12 dimethicone (see Table 3.1.1-3) The amount of copolymer was calculated on the basis of the final copolymer in the pyrolyzer, to be in around 20 µg. On the spiked sludges, the overall analytical procedure was applied. The limit of detection (LOD) was estimated as the quantity calculated to give a signal to noise ratio S/N = 3 at the retention time of the pyrolytic marker. Procedural and instrumental blank analyses were run periodically to check for potential contamination by environmental or instrumental (septum/column) contamination. Quantitative data were expressed as mean and percentage relative standard deviation (RSD) from three replicate analyses. RSD values were determined for repeatability estimates with calibration solutions of dimethicone (10 µg) and PEG-12 dimethicone (16 µg).

Table 3.1.1-3. *Recovery samples. Amount PEG-12 dimethicone (mg) added to spike pre-extracted dried sludges (g); concentrations of PEG-12 dimethicone in concentrated-extracted samples (mg mL^{-1}); pyrolysed volume (µL) of each extracted sample was calculated by weighting the injected solutions.*

	Aliquots of pre-extracted dried sludges (g)	**PEG-12 dimethicone added (mg)**	**PEG-12 dimethicone concentrations in extracted samples (mg mL^{-1})**	**Pyrolysed volume (µL)**
Recovery #1	0.98	13.9	4.1	4.63
Recovery #2	0.98	10.5	3.9	4.42
Recovery #3	0.95	10.5	3.8	4.51

3.1.1.4. Results

3.1.1.4.1. PDMS and copolymers characterisation by Py-GC-MS

3.1.1.4.1.1. Pyrolysis products from the siloxane chain

The mass spectra of some methylsiloxanes belonging to different groups (cyclic, linear and with hydroxyl groups) identified in the pyrolyzates of the investigated polymers are presented in Figure 3.1.1-3. The pyrograms of dimethicone (see Figure 3.1.1-4) were dominated by cyclic methyl siloxanes (D_n) in agreement with literature data on the pyrolysis of PDMS [16,21]. It has been reported that the proportion of the various D_n formed upon thermal degradation decreases from D_3 to higher molecular species in a way which is not dependent on temperature and the type of chain ends (trimethyl or hydroxyl) [21]. The identification of D_3-D_6 was confirmed by the injection of pure standards (Table 3.1.1-4). The D_7 could be identified by the $[M-103]^+$ ion at *m/z* 415 following the elimination of methyl radical (15 u) from the molecular ion and the subsequent neutral loss of $Si(Me)_4$ (88 u) after skeletal rearrangement. $D_{>7}$ could be identified by

published mass spectra [25]. In general, mass spectra of D_n are characterised by the absence of the molecular ion $M^{\bullet+}$, the presence of $[M-15]^+$ ion for smaller rings, cyclic siloxanes without a methyl group ($[D_n-15]^+$ at *m/z* 207, 281, 355, 429) and linear $[Me_3Si(OSiMe_2)_{n=0-4}]^+$ ions (*m/z* 147, 221, 295, 369) produced from skeleton rearrangement [1,25]. It is worth noting that the mass spectra of cyclic siloxanes and linear α-ω diols are identical due to the loss of CH_3 and H_2O (33 u) [24]. The diol with n Si atoms typically elutes between D_{n+1} and D_{n+2} [26]. On this basis, the α,ω-dioloctamethyltetrasiloxane ($M_{OH}D_2M_{OH}$) was identified. According to the fact that chain scission is not considered a dominant process in PDMS pyrolysis, linear dimethylsiloxanes (L_n or $MD_{n-2}M$) were barely or not even detected in the pyrolyzates of dimethicone in accordance to literature [21,26,27]. The formation of linear siloxanes was ascribed to secondary reactions involving ring-opening of cyclic siloxanes catalysed by impurities on the walls of the pyrolysis reactor [27]. On the opposite, the pyrolyzates of PEG-12 dimethicone (Figure 3.1.1-5) was featured by the evident occurrence of linear siloxanes. The presence of L_{3-5} was confirmed by the analysis of pure compounds (Table 3.1.1-4). Higher molecular weight (HMW) L_n species were tentatively identified by mass spectrum interpretation, order of elution and comparison with literature data [28]. Analogously to cyclic siloxanes, the identification of linear siloxanes by mass spectral interpretation is cumbersome due to the absence of $M^{\bullet+}$ and rearrangement reactions that lead to the formation of common ions. In addition, many of the isomeric siloxane products have the same mass spectra with a high risk of misinterpretation [24]. As an example, the mass spectrum of the internal standard (M_4Q) was identical to that of MD_3M. The ion at *m/z* 221 resulted the second most abundant ion after the $(CH_3)_3Si^+$ ion (*m/z* 73) in the mass spectra of linear dimethylsiloxanes (Figure 3.1.1-3) and can be used to highlight the presence of linear siloxanes with more than five Si atoms. Similarly to PEG-12 dimethicone, the pyrograms of PEG-8 dimethicone were featured by the presence of linear dimethylsiloxanes (Figure 3.1.1-6) even though dominated by HMW species (L_8, L_9). L_n were not detected in the pyrolyzates of bis-PEG-18 methyl ether dimethyl silane (Figure 3.1.1-7). The much higher proportion of evolved L_n from the co-polymers in comparison to dimethicone indicates that the pyrolytic behaviour of the siloxane chains was influenced by the presence of the PEG side chains. The formation of cyclic compounds involving "back-biting" reactions was probably less favoured than chain scission leading to linear species, probably due to steric hindrance. A similar explanation was advocated to explain higher proportion of linear over cyclic siloxanes from the pyrolysis of polysilalkylenesiloxanes [29]. By comparing Figures 3.1.1-5 and 3.1.1-6, it is evident a different peak pattern between the pyrograms of PEG-12 and PEG-8 dimethicone. This difference can be due to the different length of the two blocks (x and y in the structural formulas of Figure 3.1.1-2), which may assume different values in several commercial products [5] The higher relative

proportion of PEG pyrolysis products in the pyrograms of PEG-8 dimethicone could also be due to residual PEG reagent. PEG dimethicones are synthesised by hydrosilylation of the Si-H groups of a siloxane copolymer precursor, and excess reagent (allyl alcohol ethoxylate) could remain in the final product [5].

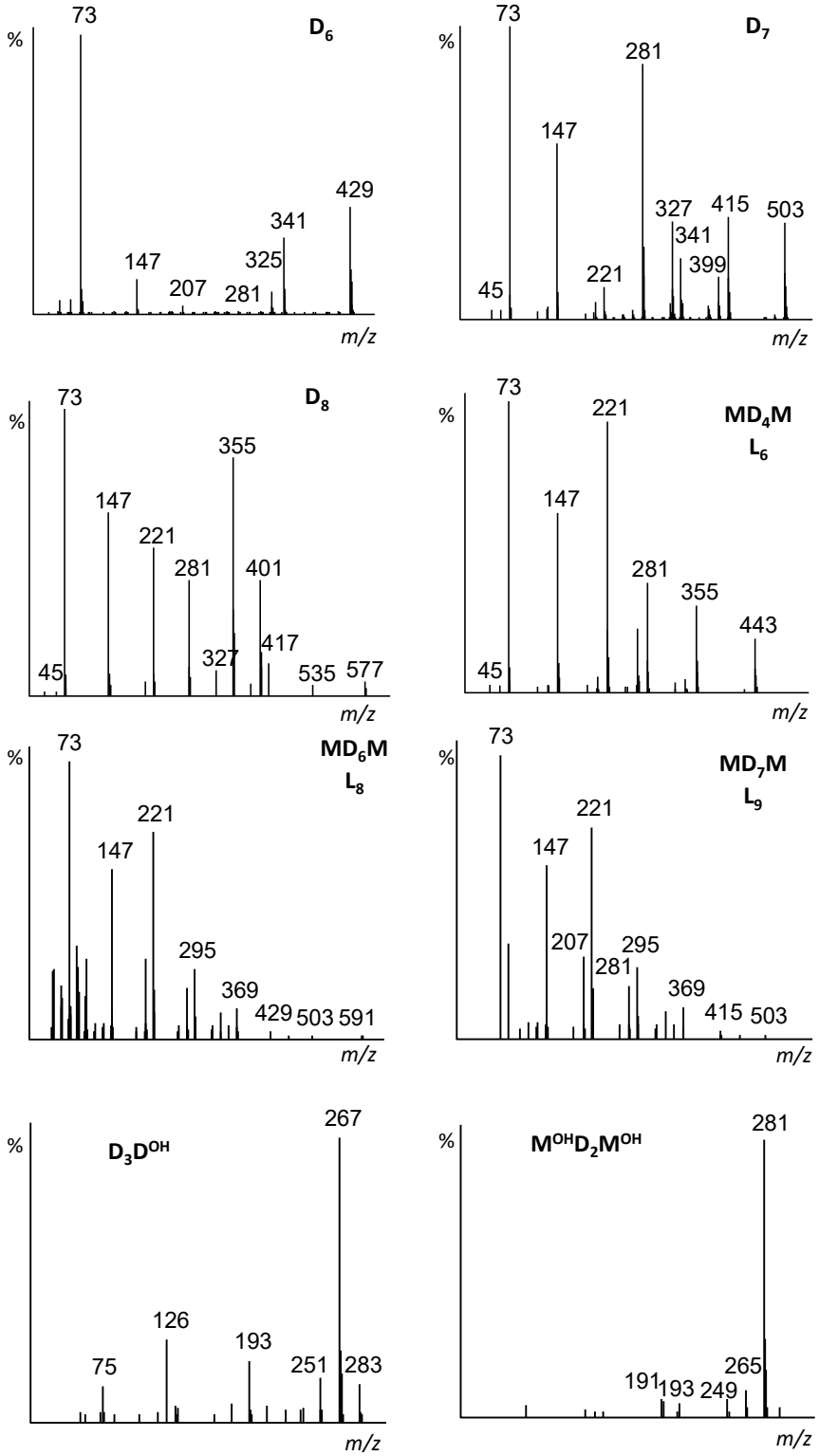

Figure 3.1.1-3. *Mass spectra of some methylsiloxanes in the pyrolyzates of dimethicone and PEG-12 dimethicone [20].*

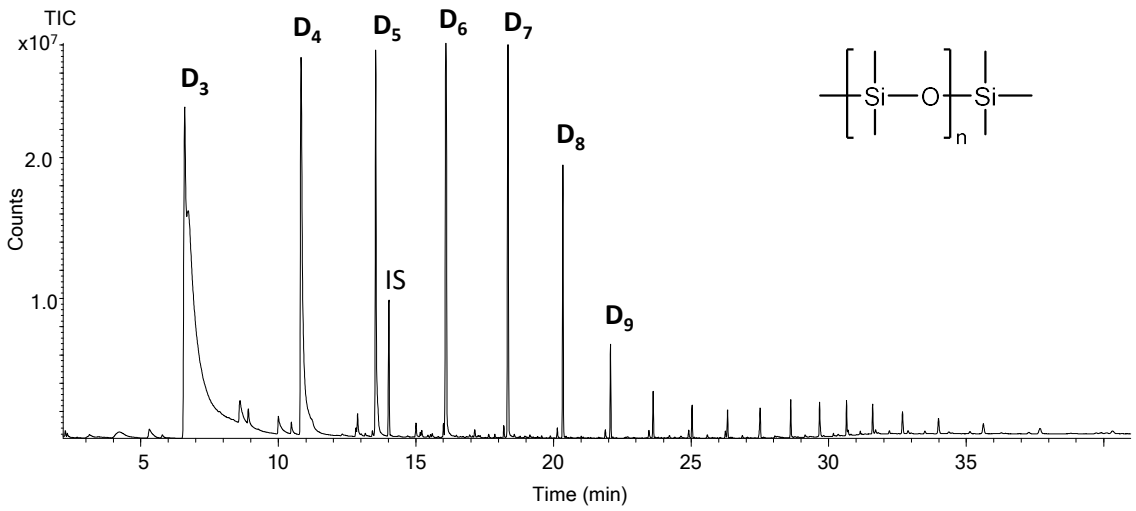

Figure 3.1.1-4. *TIC-pyrogram of dimethicone (45 µg), IS: internal standard, M4Q [20].*

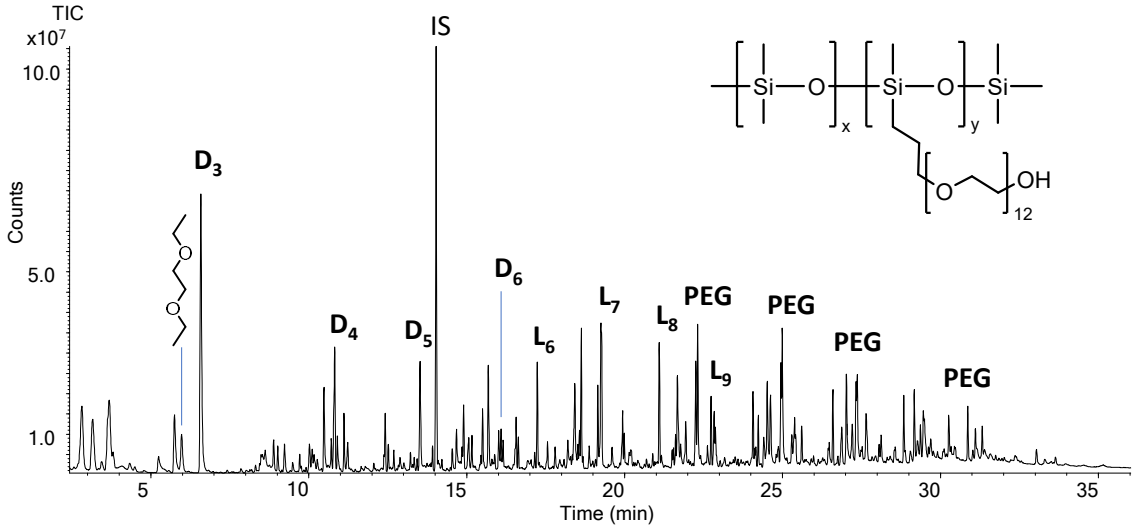

Figure 3.1.1-5. *TIC-pyrogram of PEG-12 dimethicone (40 µg). PEG: peak clusters from PEG pyrolysis. IS: internal standard. In the chemical structure, x and y are unknown [20].*

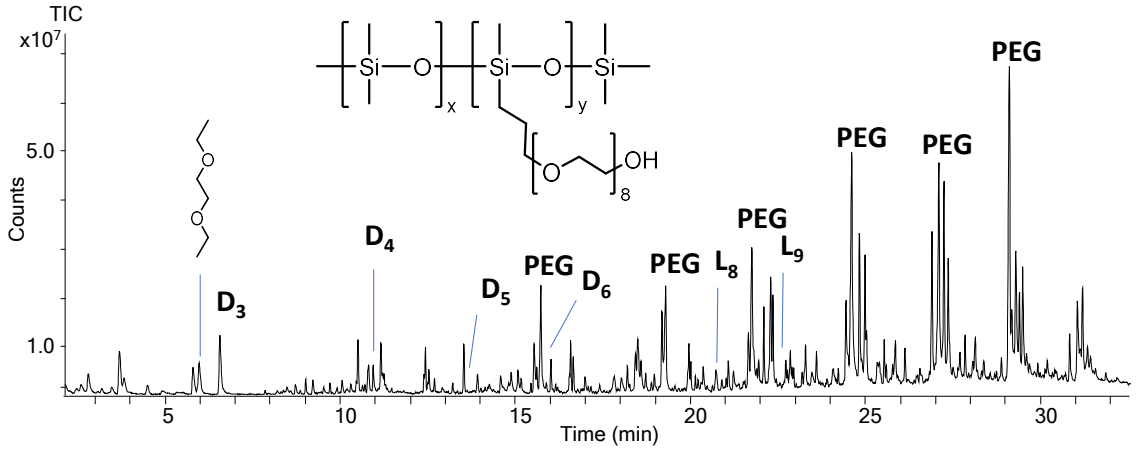

Figure 3.1.1-6. *TIC-pyrogram of PEG-8 dimethicone. PEG: peak clusters from PEG pyrolysis. In the chemical structure, x and y are unknown [20].*

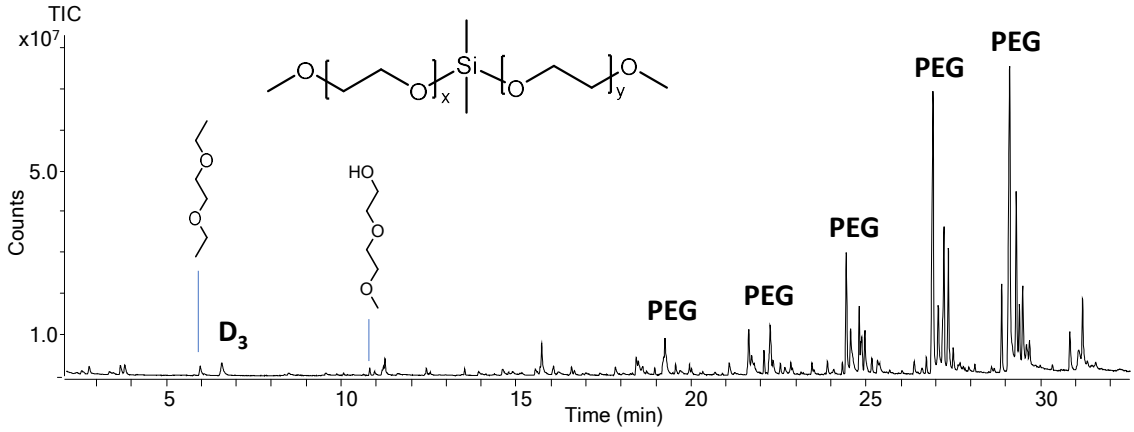

Figure 3.1.1-7. *TIC-pyrogram of bis-PEG-18 methyl ether dimethyl silane. PEG: peak clusters from PEG pyrolysis. In the chemical structure, x and y are unknown [20].*

Table 3.1.1-4. *Siloxanes formed upon flash pyrolysis of dimethicone and/or PEG-dimethicone. RT, retention time; ions, bold base peak; ID, identification based on "St.d" analyses of pure compound, "interpr." interpretation of mass spectrum or literature [20].*

Compound	Abbr	RT (min)	MW	ions *m/z*	ID
hexamethyldisiloxane	L_2	2.89	162	73, 131, **147**	St.d
hexamethyl cyclotrisiloxane	D_3	6.58	222	96, 191, **207**	St.d
octamethyltrisiloxane	L_3	8.2	236	73, 103, 133, **221**	St.d
unknown-1	–	9.23		193, **207**, 221	
unknown-2	–	10.48		191, **207**, 223	
unknown-3	–	10.71		133, 191, 193, **207**	
unknown-4	–	10.79		96, 193, **207**	
octamethylcyclotetrasiloxane	D_4	10.81	296	133, 249, 265, **281**	St.d
decamethyltetrasiloxane	L_4	12.06	310	73, 191, **207**, 295	St.d
heptamethylhydroxy cyclotetrasiloxane	D_3D^{OH}	12.97	298	126, 193, 251, **267**, 283	[26]
unknown-5	–	13.52		193, 281, 309	
decamethylcyclopentasiloxane	D_5	13.54	370	73, 267, **355**	St.d
Internal Standard, tetrakis(trimethylsiloxy)silane	M_4Q, IS	14.03	384	**73**, 147, 281, 369	IS
dodecamethyl pentasiloxane	L_5	14.9	384	73, 147, **281**, 369	St.d

α,ω-dioloctamethyltetrasiloxane	$M^{OH}D_2M^{OH}$	15.89	314	133, 249, 265, **281**	[24]
unknown-6		16.01		**73**, 267, 281, 355	
dodecametylcyclohexasiloxane	D_6	16.09	444	**73**, 325, 341, 429	St.d
unknown-7	–	16.14		**73**, 267, 28, 341	
tetradecamethylhexasiloxane	L_6	17.23	458	**73**, 147, 221, 443	[28]
tetradecamethyl cycloheptasiloxane	D_7	18.34	518	**73**, 147, 281, 415, 503	[25]
hexadecamethyl heptasiloxane	L_7	19.27	532	**73**, 147, 221, 517	Interpr.
hexadecamethyl cyclooctasiloxane	D_8	20.36	592	73, 221, **355**, 577	[25]
octadecamethyl octasiloxane	L_8	21.09	606	**73**, 147, 221, 591	Interpr.
octadecamethyl cyclononasiloxane	D_9	22.07	666	**73**, 147, 429	[25]
eicosamethyl nonasiloxane	L_9	22.73	680	**73**, 147, 221	Interpr.
eicosamethyl cyclodecasiloxane	D_{10}	23.6	740	**73**, 147, 221	[25]

3.1.1.4.1.2. Pyrolysis products from the PEG chain

As expected, the pyrograms of PEG-12 and PEG-8 dimethicones were featured by pyrolysis products formed by the thermal degradation of PEG side chains (Figures 3.1.1-5 and 3.1.1-6). It is known that the thermal degradation of PEG occurs at relatively low temperatures with the homolytic cleavage of the C–O bonds and H transfer reactions leading to oligomeric pyrolysis products containing $–(CH_2–CH_2–O)_n–$ units terminated with hydroxyl and/or ethoxyl end groups; the strongest C–C bonds are cleaved at higher temperatures with formation of methoxyl end groups, while the dehydration of hydroxyl ends brings about the formation of vinyl ether end groups [22,30].Besides linear species, pyrolysis products with a cyclic ether end group [18] and crown ethers [19] were also formed. This molecular complexity became evident in the pyrograms of PEG copolymers and the polymer bis-PEG-18 methyl ether dimethyl silane (constituted by a silicon atom with two PEG substituents) that were characterised by clusters of several peaks separated by 2 – 4 min. The structural assignment of the various oligomer families was difficult because PEG pyrolysis products display very similar mass spectra lacking molecular ion [30]. The PEG structural unit $–CH_2–CH_2–O–$ is preserved in the structure of the pyrolysis products and after ionization is responsible for the loss of 44 u (ethylene oxide). As said above,

the various pyrolysis products differ in their end groups X–(O–CH_2–CH_2–)$_n$ namely hydroxy (X = H), methoxy (X = CH_3), ethoxy (X = CH_3–CH_2), vinyl ether (X = –CH_2=CH). The aldehyde group is also a possible end group even though generally not abundant [31]. Pyrolysis products with two different end groups (e.g., methyl and ethyl ethers) exhibit both the ion series of each terminal group complicating the identification. Common intense ions of linear and cyclic species were found at *m/z* 45 (–CH_3–CH_2–O^+), *m/z* 59 (–CH_3–CH_2–O–CH_2^+), *m/z* 73 (–CH_3–CH_2–O– CH_2–CH_2^+) and *m/z* 89 (–CH_3–CH_2–O–CH_2–CH_2–O^+) [32]. Some of PEG-derived pyrolysis products tentatively identified in the pyrolyzates of copolymers are listed in Table 3.1.1-5. As an example, pyrolysis products eluting in the first portion of the pyrogram of PEG-12 dimethicone are evidenced in Figure 3.1.1-8.

Table 3.1.1-5. *GC–MS data of pyrolysis products of PEG-12 and PEG-8 dimethicone. A, B end groups in the formula: A-(CH_2-CH_2-O)$_x$-B, CE cyclic ether (crown ether). Tentative structural assignment based on the analysis PEG200 (for diols HO- (CH_2-CH_2-O)$_x$-H), library match (> 80 % without background correction), elution order on the same GC stationary phase ([18,19]) [20].*

A	B	X	Formula	RT (min)	*m/z*
CH_3-CH_2-O	CH_3-CH_2	1	$C_6H_{14}O_2$	5.9	59, 74, 45
CH_3-O	H	2	$C_5H_{12}O_3$	9.5	45, 59, 90
HO	H	2	$C_4H_{10}O_3$	10.1	45, 75, 76
CH_3-CH_2-O	H	2	$C_6H_{14}O_3$	10.9	45, 59, 72
CH_2=CH-O	H	2	$C_6H_{12}O_3$	11.1	45, 89, 101
CH_3-CH_2-O	CH_3-CH_2	2	$C_8H_{18}O_3$	11.2	45, 72(73), 59
CH_2=CH-O	CH_2=CH	2	$C_8H_{14}O_3$	12.5	45, 117, 73
HO	H	3	$C_6H_{14}O_4$	15.0	45,89, 58
CH_3-CH_2-O	H	3	$C_8H_{18}O_4$	15.5	45, 72(73), 59
–	–	4	(CE) $C_8H_{16}O_4$	15.7	45, 89, 43
CH_3-CH_2-O	CH_3-CH_2	3	$C_{10}H_{22}O_4$	16.5	45, 73(72), 59
–	–	4	(CE ester) $C_8H_{14}O_5$	17.6	102,45, 103
HO	H	4	$C_8H_{18}O_5$	18.4	45, 89, 58
CH_3-CH_2-O	H		$C_{10}H_{22}O_5$	19.1	45, 72(73), 59
–	–	5	(CE) $C_{10}H_{20}O_5$	19.2	45, 89, 43
CH_3-O	H	5	$C_{11}H_{24}O_6$	21.6	45, 59, 89
HO	H	5	$C_{10}H_{22}O_6$	21.8	45, 89, 58
CH_3-CH_2-O	H	5	$C_{12}H_{26}O_6$	22.2	45, 73, 59
–	–	6	(CE) $C_{12}H_{24}O_6$	22.3	45, 89, 73
CH_3-CH_2-O	CH_3-CH_2	4	$C_{12}H_{26}O_5$	22.8	45, 73(72), 59
–	–	6	(CE ester) $C_{12}H_{22}O_6$	24.0	45, 103, 43
CH_3-O	H	6	$C_{13}H_{28}O_7$	24.4	45, 59, 89
HO	H	6	$C_{12}H_{26}O_7$	24.5	45, 89, 59

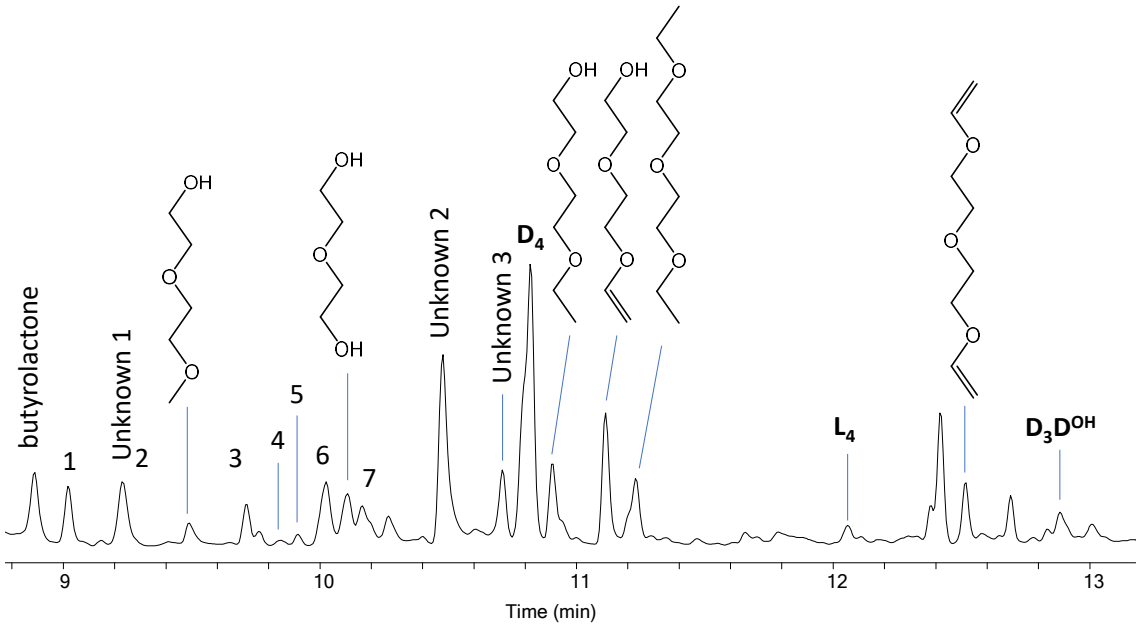

Figure 3.1.1-8. *TIC-pyrogram of PEG-12 dimethicone in the 8.8-13.2 min elution region. GC–MS data of Unknown 1-4 refers to Table 3.1.1-4, PEG derived products to Table 3.1.1-5 and peak numbers to Table 3.1.1-6 [20].*

Table 3.1.1-6. *Unidentified peaks in the pyrograms of PEG-8 and PEG-12 dimethicones. Peak numbers correspond to the peak labels of Figure 3.1.1-8 [20].*

#	RT (min)	*m/z* (% abundance)
1	9.05	119 (77), 133 (100), 145 (31), 173 (84), 188 (26)
2	9.24	133 (100), 147 (29), 177 (74)
3	9.71	133 (100), 147 (15), 175 (40)
4	9.76	101 (100), 116 (58), 145 (28), 160 (17)
5	9.94	133 (100), 149 (15), 177, (36)
6	10.0	193 (100), 209 (52)

3.1.1.4.1.3. Other pyrolysis products

Distinctive pyrolysis products of the PEG dimethicones containing both siloxane and ethylene oxide moieties could not be identified with a reliable degree of certainty. As explained above, linear siloxanes were evidence for the presence of the PEG side chains. GC–MS data of unknown pyrolysis products of PEG-8 and PEG-12 dimethicone, not detected in the pyrolyzates of PDMS and bis-PEG-18 methyl ether dimethyl silane, are reported in Table 3.1.1-4 (unknowns) and Table 3.1.1-6. Four pyrolysis products of Table 3.1.1-6 (# 1, 2, 3 and 5) were characterized by mass spectra exhibiting a base peak at *m/z* 133. An ion at *m/z* 133 occurred only at relatively

low abundance in the mass spectra of a few dimethylsiloxanes (Table 3.1.1-4). The *m/z* 133 ion is the base peak in the mass spectrum of dimethyldiethoxysilane ($[M–CH_3]^+$)and the second most abundant peak of the mass spectrum of methyltriethoxysilane ($[M–OCH_2–CH_3]^+$) [1], thus it is assigned to $(CH_3)Si(OCH_2CH_3)_2^+$. On this ground, the empirical formula of *m/z* 133 could be $C_5H_{13}O_2Si^+$, while other possibilities are $C_4H_9O_3Si^+$ and $C_4H_{13}OSi_2^+$.These pyrolysis products are tentatively assigned to the fragmentation of methyl-propyloxy PEG siloxane units or secondary reactions between dimethylsiloxane and PEG fragments. An interesting compound of this family was the compound eluting at 9.05 min with a mass spectrum presenting an even ion at *m/z* 188.

3.1.1.4.2. PDMS and copolymers characterisation by FTIR-ATR

The spectroscopic analysis was selected as a further characterisation of the starting materials, in order to obtain complementary information to the thermal ones. According to [33], the siloxane backbone can be easily identified depending on the structural units that compose the polymer and main bands are summarised in Table 3.1.1-7. Many bands identify PEG chain since the polymer is mainly composed by the less characteristic C—H bond. However, vibration and bending of this bond are featured by C—H, C—O—H and O—H helping in the univocal identification of PEG side chains (Table 3.1.1-8).

Table 3.1.1-7. *Reference bands for the characterisation of PDMS from FTIR-ATR data (wavenumbers, bond type assignment, band description).*

Wavenumber (cm^{-1})	Bond type	Description	Reference
Polydimethylsiloxane			
1245 – 1275		Strong and sharps band that moves from lower wavenumber when the Si-CH_3 is included in M units, to higher values for D and T units.	[33]
800 – 760	Si—CH_3	Another sharp band features the first one. This band shifts depending on the structural units. For M and T units it is at lower wavenumber value, whereas for D units it moves to 800 cm^{-1}	[33]
840 – 860		Blocks of D units (PDMS chains) show a relatively weak band at 860 cm^{-1}. In many copolymers containing dimethyl D units and for M units the 860 cm^{-1} band shifts to 845 cm^{-1}, becoming stronger.	[33]

1010 – 1020 1080 – 1090	PDMS	PDMS chains are characterised by two strong and distinct bands of about equal intensity	[33]
1000 – 1300	O—Si—O	Siloxane chains produce a band which is as broader as long the chain is. Usually, bands different bands overlap in this region.	[33]

Table 3.1.1-8. *Reference bands for the characterisation of PEG chains from FTIR-ATR data (wavenumbers, bond type assignment).*

Wavenumber (cm^{-1})	Bond type	Reference
Polyethylene glycol		
2800 – 3000	C—H stretching	[34,35]
1456 – 1470	C—H bending	[34,35]
1350 – 1360	C—H deforming	[34,35]
1094 – 1279	O—H bending and C—O—H	[34,35]
1080 – 1100	C—O stretching	[34,35]
843 – 962	C—C	[34,35]
3000 – 3700	O—H stretching	[34,35]

According to literature, the standard PDMS and copolymers were characterised. Figure 3.1.1-9 shows the IR spectrum recorded for dimethicone. According to the structure (Figure 3.1.1-2a), D units compose the whole polymer. IR spectrum confirmed this structure with a sharp band at 1260 cm^{-1}, accompanied by a weak band at 860 cm^{-1} and another strong one at around 800 cm^{-1}. Another fingerprint for PDMS is given by two strong and distinct bands at around 1010-1020 cm^{-1} and 1080-1090 cm^{-1} (1015 cm^{-1} and 1081 cm^{-1} in Figure 3.1.1-9) of about equal intensity. The same region is also representative of the Si—O—Si bond, defining a band which is broader as longer is the chain [33]. Finally, other two regions can be noticed in the IR spectrum of dimethicone, with two bands at around 1430 cm^{-1} (1422 cm^{-1} and 1455 cm^{-1} in Figure 3.1.1-9) and other two at around 2950 cm^{-1} (2906 cm^{-1} and 2965 cm^{-1} in Figure 3.1.1-9). Those regions are usually representative of alkanes because they are related to the C-H bond, the one which appear around 3000 cm^{-1} represents the C—H stretching, whereas the other the C—H bend [34]. Contrary to what emerged from characterisation by Py-GC-MS, IR spectra of PEG-12 and PEG-8 dimethicone were very similar (blue line and green line in Figure 3.1.1-10, respectively). The siloxane structure was confirmed by the same bands that were recorded for dimethicone, but some little differences were noticed due to the PEG side chains. First of all, the fingerprint region

was more crowded, suggesting an increase of C—C and C—O bonds, and confirming the presence of structures which are not in the PDMS backbone. Moreover, bands which represents C—H stretching and bending were more intense and broader than the ones dimethicone, confirming again the presence of additional chains to the PDMS one. Finally, a strong and broad band appeared in the 3000 – 3700 cm^{-1} range. This prominent band explains the presence of O—H bonds, confirming the PEG side chain structures showed in Figure 3.1.1-2b and c.

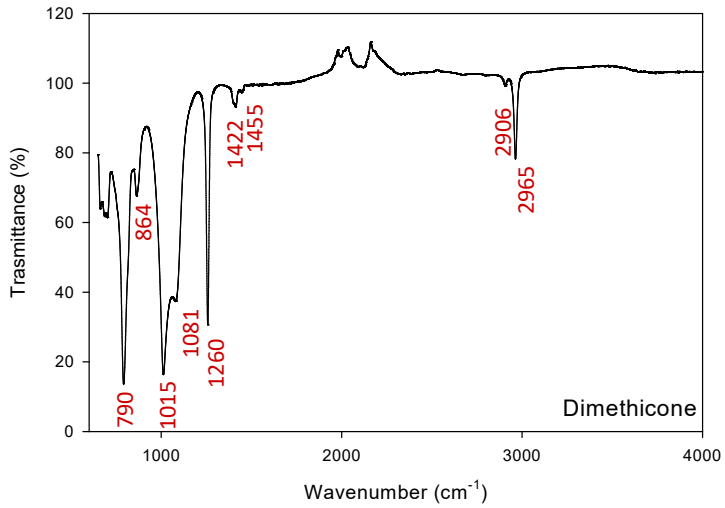

Figure 3.1.1-9. *IR spectrum of dimethicone, polymer structure in Figure 3.1.1-2a.*

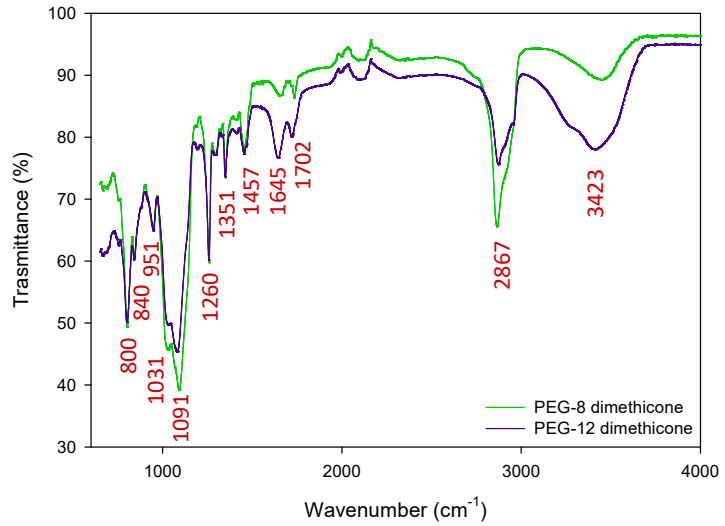

Figure 3.1.1-10. *IR spectrum recoded PEG-12 and PEG-8 dimethicones, polymer structure in Figure 3.1.1-2b and c respectively.*

3.1.1.4.3. Quantitative analysis

The determination of the polymer quantity in a given sample by Py- GC–MS is typically carried out from the peak area of a pyrolysis product characteristic of the polymer. This approach is followed for instance in the analysis of microplastics where polymer-specific pyrolytic markers were utilised for quantitation (for example, styrene trimer for polystyrene, terminal *n*-alkadienes for polyethylene, and 2,4-dimethyl hept-1-ene for polypropylene [10,12]). The potential of the same approach in the case of PEG-12 dimethicone was investigated in this study exploiting the results shown in Section 3.1.1.4.1. Dimethicone and its PEG-copolymers produced cyclic dimethylsiloxane (D_n) upon pyrolysis. The calibration curves of the most intense species $D_{3\text{-}6}$ exhibited different linearity (R^2 from 0.905 to 0.976) for dimethicone in the investigated concentration range (0.09 – 3.7 µg, n = 6). D_6 is proposed for quantitation in real samples because lower MW cyclic species were occasionally found in blank analyses and gave the lower R^2 values. When D_6 was applied as quantitation marker for PEG-12 dimethicone the linearity, evaluated in the 0.75 – 58 µg range (n = 5), was satisfactory (R^2 = 0.995). The sensitivity was much higher for dimethicone (from Equation 3.1.1-1, a = 9.0 10^{-3}) than PEG-12 dimethicone (a = 0.25 10^{-3}) in accordance with the fact that the copolymer contains less D units for the same mass of polymer. This relevant difference in sensitivity between polymer types indicates that D_6 cannot be adequately used for the quantitation of silicones as a family. Besides, D_6, the following pyrolytic markers were investigated for PEG-12 dimethicone: the linear siloxanes L_6, L_8, and L_9, and the triethyleneglycol monoethyl ether (TGE, $C_8H_{18}O_4$). These markers were chosen because relatively intense, successfully identified and eluted in a time region less impacted by products evolved from the sewage sample matrix. The ions at *m/z* 221 for $L_{6,8,9}$ and *m/z* 45 for $C_8H_{18}O_4$ were selected for calculating the calibration protocols and evaluate the method performance. The GC peak of L_7 overlapped with that of the antioxidant 2,6-di-*tert*-butyl-4-methylphenol that exhibits an intense satellite ion at *m/z* 221; due to this interference L_7 was not selected for quantitation. The obtained figures of merit of the method using the pyrolytic markers $L_{6,8,9}$ and TGE are presented in Table 3.1.1-9. Calibration curves gave R^2 = 0.993 for L_6, R^2 = 0.999 for $L_{8,9}$ and R^2 = 0.992 for TGE. The repeatability by analysing a calibration solution (17 µg) was rather good, in general below 10 % in accordance with the typical precision of Py-GC-MS [15]. In comparison to D_6, the sensitivity of TGE and L_6 were similar, while those of L_8 and L_9 slightly lower. The sensitivity of these markers was lower for PEG-8 than PEG-12 dimethicone. The PEG-8/PEG-12 sensitivity ratios of TGE, L_8 and L_9 (L_6 was not detected in PEG-8 dimethicone pyrolyzates) were 0.79 ± 0.04, 0.21 ± 0.01 and 0.029 ± 0.01, respectively. The pyrograms of PEG-12 and PEG-8 dimethicones presented differences in the relative distribution of D/L products,

probably due to the different length of the blocks in the original copolymers. However, this hypothesis cannot be confirmed as x and y in the structural formulas of Figures 3.1.1-5 and 3.1.1-6 are unknown. The pyrolytic markers could not be detected in the pyrolyzate of 0.07 µg of sample, whereas the pyrogram from 0.75 µg exhibited distinct peaks of $L_{6,8,9}$ and TGE successfully identified by mass spectral match after background correction. The LOD estimated from the analyses of the calibration solutions (S/N = 3 criterion) occurred in the 0.04 – 0.4 µg range (Table 3.1.1-9). When the quantity of analysed sample is 1 g, as in this study, the procedural LOD would be less than 0.4 $\mu g_{PDMS}\ g^{-1}$ corresponding to 0.15 $\mu g_{Si}\ g^{-1}$ in terms of silicon when considering the $(CH_3)_3SiO$ unit of 74 u. The LOD by Py-GC-MS is comparable to that of other analytical methods. For instance, the LOD by SEC-ICP-HR/MS and ICP-MS were reported to be 1.2 $\mu g_{Si}\ g^{-1}$ [26] and 0.1 $\mu g_{Si}\ g^{-1}$ [36], respectively. However, these methods did not provide molecular speciation. The recovery, determined by analysing spiked sewage samples previously extracted with THF, was 75 % using L_6 as pyrolytic marker. This value can be considered acceptable for trace contaminants in complex matrices providing support to the validity of the Py-GC-MS procedure.

Table 3.1.1-9. *Figures of merit of the Py-GC-MS procedure in the analysis of PEG-12 dimethicone for each selected marker (TGE: CH_3CH_2-O-(CH_2- CH_2-O)$_3$-H); m/z quantitation ion in bold; coefficient of determination, sensitivity (slope, a), LOD and precision (RSD%) calculated on calibrations; Recovery results with related deviations RSD%) for method validation [20].*

Marker	RT (min)	*m/z* (% abundance)	R^2	*a*	LOD (µg)	RSD (%)	Recovery (%)	RSD (%)
D_6	16.1	73 (100), 341 (100), **429** (20), 342 (15), 147 (14)	0.995	0.0025	0.4	20	76	2
TGE	15.5	**45** (100), 72 (30), 73 (27), 59 (20), 89 (21)	0.992	0.0028	0.1	10	69	5
L_6 (MD_4M)	17.2	73 (100), **221** (83), 147 (73), 281 (29), 443 (4)	0.993	0.0022	0.04	15	76	4
L_8 (MD_6M)	21.1	73 (100), **221** (75), 147 (56), 207 (28), 296 (23)	0.999	0.0015	0.1	4	66	6
L_9 (MD_7M)	22.7	73 (100), **221** (81), 147 (58), 207 (27), 295 (26)	0.999	0.0012	0.2	2.7	68	5

3.1.1.4.4. Py-GC-MS of sewage sludges extracts

3.1.1.4.4.1. Polysiloxanes

Pyrograms of oxidized, thick and dewatered sludges, previously dried and extracted in THF, were mainly dominated by fatty acids, alkanes, alkenes, sterols and sterenes from the matrix. An example is shown in Figure 3.1.1-11. The chemical nature of the pyrolyzate indicates that lipids constituted the main chemical family extracted by THF. Cyclic dimethyl siloxanes from D_3 to D_7 could be revealed by retention time and mass spectrum matching. The $[M-15]^+$ ions were particularly distinctive for the rapid individuation of cyclic dimethylsiloxanes in the extracted ion chromatogram mode. Volatile cyclic siloxanes are known to be present in sewage sludges [2], however, their presence in the pyrolyzates was excluded because the samples were dried before extraction and any volatile D_n would have been eliminated by volatilisation. Hence, D3-D7 were pyrolysis products indicative of the occurrence of polysiloxanes. Pyrolysis products of PEG could not be detected. Analogously, putative PEG-PDMS pyrolysis products (Table 3.1.1-6) could not be revealed, with the exception of the compound eluting at 9.23 min (Table 3.1.1-4). By assuming that D_6, one of the possible pyrolytic markers selected for quantitation in Section 3.1.1.4.3, was released solely from the pyrolysis of dimethicone (PDMS), the concentrations calculated from the calibration protocol were 99, 105 and 61 µg g_{dw}^{-1} for the oxidized, thick and dewatered sludge samples, respectively. The corresponding RSD (n = 3) were 14, 16 and 17 %, respectively. The concentration values were within the ranges reported in other studies [36–39] using different analytical techniques (see Table 3.1.1-10). The absence of pyrolytic markers of PEG units in the analysed sludge samples may suggest that PEG-dimethicones were not present in the matrices at levels detectable by the method. Nonetheless, recovery experiments showed that the copolymer at the level of 17 µg g^{-1} in spiked samples could be successfully identified and quantified (Section 3.1.1.4.3). This level is much lower than those typically reported for silicones in sewage samples (Table 3.1.1-10) evidencing the good performance of the method for the requested application. As PEG is highly biodegradable [7] and microorganisms in sewage sludges degrade PEG [40–43], it is probable that the PEG side chain of dimethicone copolyols could have been degraded. Degradation could result in copolymers with shorter PEG-chains. Another hypothesis is that the copolymer was totally distributed in the water phase (wastewater) due to its water-solubility. However, water was not eliminated by centrifugation before drying, so any copolymer present in the water phase should have ended up in the dried sample. Notably, the occurrence of the L_6 pyrolytic marker of PEG-12 dimethicone could be revealed in all the samples at the correct retention time in the extracted ion chromatograms at

m/z 221. All the characteristic ions of the mass spectrum obtained from the analysis of the standard PEG-12 dimethicone were detected, as exemplified in the inset of Figure 3.1.1-11. Although the identification of PEG-dimethicone copolymers could not be confirmed by PEG markers, the linear siloxanes were considered indicative for the presence of dimethicone copolymers. In order to give a rough estimation of the level of their occurrence, the concentrations of copolymers were calculated from the calibration protocol for PEG-12 dimethicone using the L_6 pyrolytic marker. The obtained values were 245 µg g_{dw}^{-1} (± 15 % RSD), 289 µg g_{dw}^{-1} (± 14 %) and 225 µg g_{dw}^{-1} (± 8 %) for the oxidized, thick and dewatered sludge samples, respectively. Although these values could not be reliably assigned to original PEG-dimethicones, they suggest that dimethicone copolymers could be a significant fraction of total polysiloxanes in sewage sludge. This hypothesis was further supported by looking at the L_6/D_6 GC peak area ratios at *m/z* 221 to *m/z* 429. These ratios were in the range 0.1 – 0.3 for real samples, significantly higher than that of dimethicone (0.001), indicating that the level of linear siloxanes could not be solely assigned to the pyrolysis of the PDMS homopolymer (dimethicone). Nevertheless, the ratios were lower than those found in the analysis of standard PEG- 12 dimethicone in spiked sewage samples (7 ± 3 % RSD). These findings suggest that the investigated sewage samples contained both PDMS homopolymers and copolymers. The nature of these copolymers could not be definitively associated to PEG due to the absence of PEG markers. Different factors make it difficult the quantitation of polysiloxanes as a whole family by using a single standard material: different sensitivity of pyrolytic markers in different polymers, commercial copolymers having different composition, contamination by residual reagents. In addition, ionization and fragmentation efficiencies [8] and peak areas are dependent on the molecular weight of the polymers [15]. Nevertheless, taking into account these limitations, Py-GC-MS can find application in screening studies aimed at estimating the level of contamination and the efficiency of abatement of silicones in WWTPs.

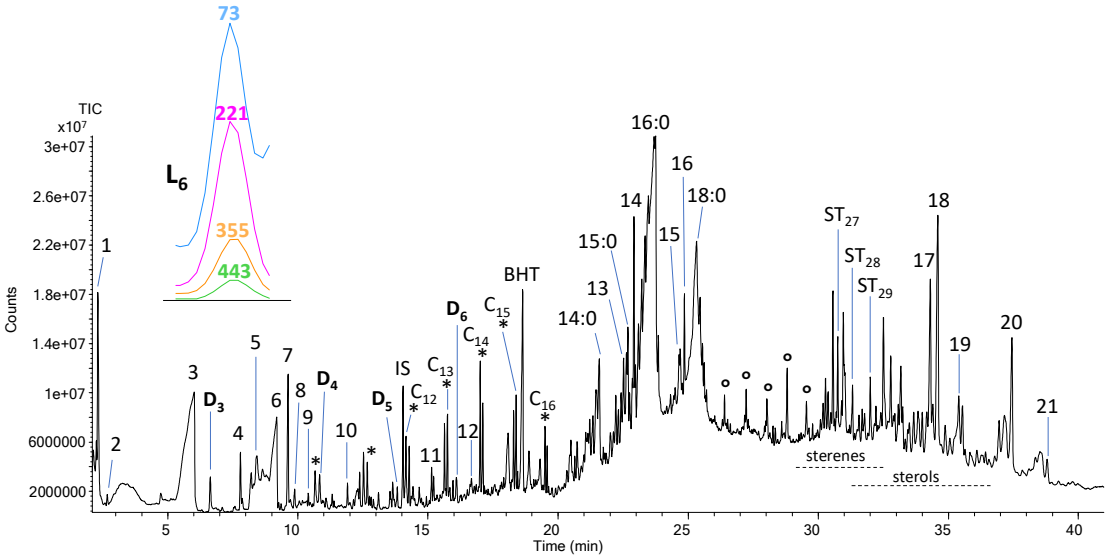

Figure 3.1.1-11. *TIC-pyrogram of sewage sludge thick. Tentative identification: 1: THF; 2: benzene; 3: tetrahydrofuranol; 4: xylene; 5:styrene; 6: butyrolactone; 7: m/z 41, 74, 102 m/z (unknown); 8: C3-benzene; 9: m/z 64, 78, 106 (1,2-dithiolane); 10: C4-benzene; 11: C6-benzene; 12: heptylbenzene; 13: galaxolide; 14: 2-heptadecanone; 15: galaxolide lactone; 16: 3-octadecanone; 17: m/z 249, 389, 404 (unknown); 18: 16-hentriacontanone; 19: hexadecanoic acid hexadecyl ester; 20: octadecanoic acid, hexadecyl ester; 21: 9-octadecenoic acid, hexadecyl ester. BHT: butylated hydroxytoluene (THF additive). 14:0, 15:0, 16:0, 18:0 fatty acids; ST_{27}, ST_{28}, ST_{29}: C_{27}, C_{28} and C_{29}-sterenes; S_{27}: cholestane; (*): n-1-alkene, n-alkanes; (◦): m/z 57,71, 239. In the inset, extracted ion chromatograms at m/z 73, 221, 355 and 443 at the retention time of L_6 (17.2 min) [20].*

Table 3.1.1-10. *Examples of concentrations of siloxanes in sewage sludges reported in the literature with different methods (μg_{Si} were converted into μg_{PDMS} using the 74/ 28 conversion factor) [20].*

Input source of WWTP	Country	Analytical technique	Concentration $\mu g_{PDMS}\ g_{dw}^{-1}$	Reference
Domestic	Australia	ICP-AES	360	[35]
Domestic	Japan	ICP-AES	144	[33]
Domestic and industrial	Maryland	FAAS	254 ± 14	[36]
Domestic and industrial	USA Canada	GCP-ICP-AES	1124 ± 1367	[34]
Domestic	Italy	Py-GC-MS	61 – 105[1] 225 – 289[2]	Present study

[1] From calibration with dimethicone using D_6.
[2] From calibration with PEG-12 dimethicone using L_6.

3.1.1.4.4.2. Additional information on personal care products

Interestingly, a closer insight into the pyrograms of sewage sludges revealed the occurrence of ingredients of personal care products and cosmetics in all the analysed samples. The fragrance galaxolide was identified at retention time 22.6 min and mass spectrum matching with that of injected pure standard (Figure 3.1.1-12). Its degradation product lactone-galaxolide was further tentatively identified at 25.7 min (*m/z* 257, 272). Here, for the first time these cosmetic

ingredients were revealed by Py-GC-MS. Triclosan was also tentatively identified at 25.0 min (*m/z*: 146, 218, 288, 290). These compounds were typically reported in samples from WWTP by GC–MS [44–46].

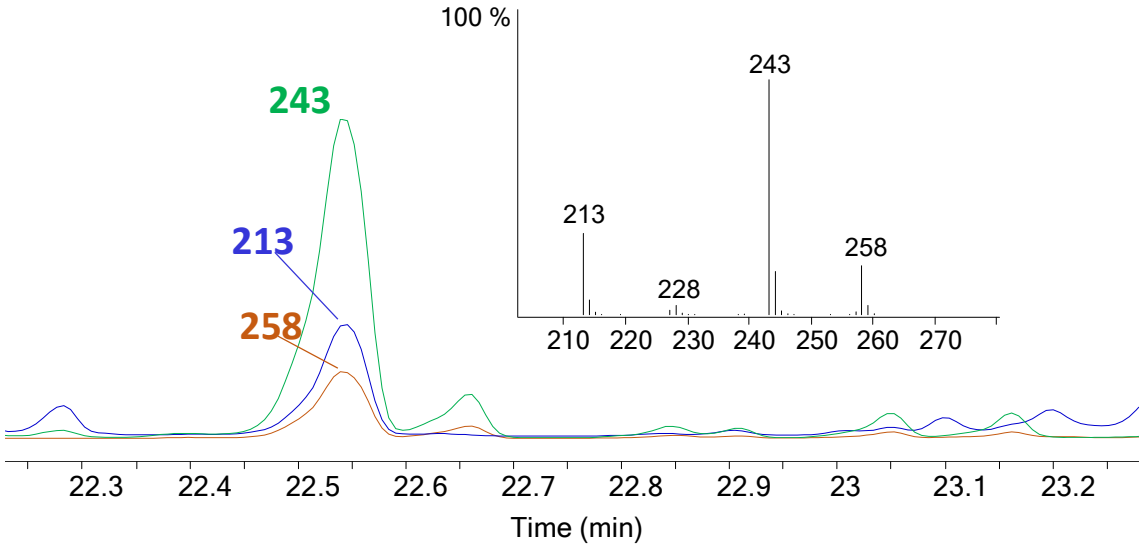

Figure 3.1.1-12. *Py-GC-MS of oxidised sludge. Extracted ion chromatograms at m/z 213, 243 and 258 and mass spectrum at 22.46 min attributed to galaxolide [20].*

3.1.1.5. Conclusions

Flash pyrolysis of PEG dimethicones produced cyclic dimethyl siloxanes and ethylene oxide derivatives evolved from the PDMS and PEG chains, respectively. In addition, linear dimethyl siloxanes were produced which were proposed as pyrolytic markers of siloxane copolymers as they were not present in the pyrolyzates of the homopolymer. The chemical structure of pyrolysis products indicative of the polyoxyethylene methylsiloxane moiety remained elusive. Even though not specific of PEG dimethicones, linear dimethyl polysiloxanes were selected for the development of a novel Py-GC-MS procedure for the analysis of siloxane copolymers in sewage sludges. The satisfactory values of precision, recovery, sensitivity, limit of detection and its performance in the analysis of sewage sludge samples demonstrated the potential of the Py-GC-MS method for complex matrices. Lipids were extracted by the organic solvent concurrently with siloxanes causing an important matrix effect. Thus, further improvements of the Py-GC-MS method will require clean-up steps to separate lipids from siloxanes. Incidentally, the occurrence of galaxolide fragrance and biocide triclosan was revealed by Py-GC-MS showing that the technique can be extended to the determination of a wide range of personal care products with a single analysis.

References

[1] A.L. (Editor) Smith, Winefordner, J. D. (Series Editor), Kolthoff, I. M., Chemical analysis: A series of monographs on analytical chemistry and its applications BeckerThe analytical chemistry of silicones, Jhon Wiley & Sons, Inc, 1991. https://www.wiley.com/en-us/The+Analytical+Chemistry+of+Silicones-p-9780471516248 (accessed January 3, 2020).

[2] C. Rücker, K. Kümmerer, Environmental chemistry of organosiloxanes, Chem. Rev. 115 (2015) 466–524. https://doi.org/10.1021/cr500319v.

[3] Global Silicones Council, Socio-economic evaluation of the global silicones industry, Amec Foster Wheeler Environment & Infrastructure UK Limited, 2016.

[4] J. Nikitakis, B. Lange, International cosmetic ingredient dictionary and handbook, 16th edition, Personal Care Products Council, Washington, DC, 2016.

[5] A.J. O'Lenick, Silicones for personal care, 2nd ed, Allured Pub, Carol Stream, III, 2008.

[6] Safety assessment of polyoxyalkylene siloxane copolymers, alkyl-polyoxyalkylene siloxane copolymers, and related ingredients as used in cosmetics | Cosmetic Ingredient Review, Washington, 2015.

[7] F. Kawai, Biodegradation of polyethers (polyethylene glycol, polypropylene glycol, polytetramethylene glycol, and others), Biopolymers Online. (2005). https://doi.org/10.1002/3527600035.bpol9012.

[8] S. Huppertsberg, D. Zahn, F. Pauelsen, T. Reemtsma, T.P. Knepper, Making waves: Water-soluble polymers in the aquatic environment: An overlooked class of synthetic polymers?, Water Research. 181 (2020) 115931. https://doi.org/10.1016/j.watres.2020.115931.

[9] H.P.H. Arp, H. Knutsen, Could we spare a moment of the spotlight for persistent, water-soluble polymers?, Environ. Sci. Technol. 54 (2020) 3–5. https://doi.org/10.1021/acs.est.9b07089.

[10] J. La Nasa, G. Biale, B. Ferriani, M.P. Colombini, F. Modugno, A pyrolysis approach for characterizing and assessing degradation of polyurethane foam in cultural heritage objects, Journal of Analytical and Applied Pyrolysis. 134 (2018) 562–572. https://doi.org/10.1016/j.jaap.2018.08.004.

[11] R. Peñalver, N. Arroyo-Manzanares, I. López-García, M. Hernández-Córdoba, An overview of microplastics characterization by thermal analysis, Chemosphere. 242 (2020) 125170. https://doi.org/10.1016/j.chemosphere.2019.125170.

[12] N. Yakovenko, A. Carvalho, A. ter Halle, Emerging use thermo-analytical method coupled with mass spectrometry for the quantification of micro(nano)plastics in environmental samples, TrAC Trends in Analytical Chemistry. 131 (2020) 115979. https://doi.org/10.1016/j.trac.2020.115979.

[13] M. Julinová, L. Vaňharová, M. Jurča, Water-soluble polymeric xenobiotics – Polyvinyl alcohol and polyvinylpyrrolidon – And potential solutions to environmental issues: A brief review, Journal of Environmental Management. 228 (2018) 213–222. https://doi.org/10.1016/j.jenvman.2018.09.010.

[14] J.C. Kleinert, C.J. Weschler, Pyrolysis gas chromatographic-mass spectrometric identification of poly(dimethylsiloxane)s, Anal. Chem. 52 (1980) 1245–1248. https://doi.org/10.1021/ac50058a020.

[15] C.J. Weschler, Polydimethylsiloxanes associated with indoor and outdoor airborne particles, Science of The Total Environment. 73 (1988) 53–63. https://doi.org/10.1016/0048-9697(88)90186-6.

[16] J.P. Lewicki, B.P. Mayer, C.T. Alviso, R.S. Maxwell, Thermal degradation behavior and product speciation in model poly(dimethylsiloxane) networks, J Inorg Organomet Polym. 22 (2012) 636–645. https://doi.org/10.1007/s10904-011-9625-0.

[17] J. Maurer, K. Buffaz, G. Massonnet, C. Roussel, C. Burnier, Optimization of a Py-GC/MS method for silicone-based lubricants analysis, Journal of Analytical and Applied Pyrolysis. 149 (2020) 104861. https://doi.org/10.1016/j.jaap.2020.104861.

[18] X. Han, Y.H. Hu, Z.K. Lin, S.F. Li, F.Q. Zhao, Z.R. Liu, J.H. Yi, L.Y. Zhang, X.N. Ren, Effects of fullerenes on thermal behaviors of polyethylene glycol, J Therm Anal Calorim. 93 (2008) 927–932. https://doi.org/10.1007/s10973-007-8715-2.

[19] Z. Lin, T. Wang, X. Han, D. Han, S. Li, Comparative studies on low-temperature pyrolysis products of pure PEG and PEG/nano-Co3O4 by Py-GC/MS, Journal of Analytical and Applied Pyrolysis. 81 (2008) 121–126. https://doi.org/10.1016/j.jaap.2007.09.010.

[20] I. Coralli, A.G. Rombolà, C. Torri, D. Fabbri, Analytical pyrolysis of poly(dimethylsiloxane) and poly(oxyethylene) siloxane copolymers. Application to the analysis of sewage sludges, Journal of Analytical and Applied Pyrolysis. 158 (2021) 105236. https://doi.org/10.1016/j.jaap.2021.105236.

[21] N. Grassie, I.G. Macfarlane, The thermal degradation of polysiloxanes – I. Poly(dimethylsiloxane), European Polymer Journal. 14 (1978) 875–884. https://doi.org/10.1016/0014-3057(78)90084-8.

[22] R. P. Lattimer, Mass spectral analysis of low-temperature pyrolysis products from poly(ethylene glycol), Journal of Analytical and Applied Pyrolysis. 56 (2000) 61–78. https://doi.org/10.1016/S0165-2370(00)00074-7.

[23] L. Hermabessiere, C. Himber, B. Boricaud, M. Kazour, R. Amara, A.-L. Cassone, M. Laurentie, I. Paul-Pont, P. Soudant, A. Dehaut, G. Duflos, Optimization, performance, and application of a pyrolysis-GC/MS method for the identification of microplastics, Analytical and Bioanalytical Chemistry. 410 (2018) 6663–6676. https://doi.org/10.1007/s00216-018-1279-0.

[24] S. Varaprath, D.H. Stutts, G.E. Kozerski, A primer on the analytical aspects of silicones at trace levels-Challenges and artifacts – A review, Silicon Chem. 3 (2006) 79–102. https://doi.org/10.1007/s11201-006-9005-8.

[25] G.R. Pickering, C.J. Olliff, K.J. Rutt, The mass spectrometric behaviour of dimethylcyclosiloxanes, Organic Mass Spectrometry. 10 (1975) 1035–1045.

[26] F. Chainet, L.L. Meur, C.-P. Lienemann, J. Ponthus, M. Courtiade, O.F.X. Donard, Characterization of silicon species issued from PDMS degradation under thermal cracking of hydrocarbons: Part 2 – Liquid samples analysis by a multi-technical approach based on gas chromatography and mass spectrometry, Fuel. 116 (2014) 478–489. https://doi.org/10.1016/j.fuel.2013.08.010.

[27] G. Camino, S.M. Lomakin, M. Lageard, Thermal polydimethylsiloxane degradation. Part 2. The degradation mechanisms, Polymer. 43 (2002) 2011–2015. https://doi.org/10.1016/S0032-3861(01)00785-6.

[28] V.Y. Orlov, Dissociation of methylsiloxane under electron bombardment, Zhurnal Obshchei Khimii. 37 (1967) 2300–2307.

[29] D. Allan, S.C. Radzinski, M.A. Tapsak, J.J. Liggat, The thermal degradation behaviour of a series of siloxane copolymers – A study by thermal volatilisation analysis, Silicon. 8 (2016) 553–562. https://doi.org/10.1007/s12633-014-9247-6.

[30] K. Voorhees, S. Baugh, D. Stevenson, An investigation of the thermal-degradation of poly(ethylene glycol), J. Anal. Appl. Pyrolysis. 30 (1994) 47–57. https://doi.org/10.1016/0165-2370(94)00803-5.

[31] H. Arisawa, T.B. Brill, Flash pyrolysis of polyethyleneglycol Part I: Chemometric resolution of FTIR spectra of the volatile products at 370–550°C, Combustion and Flame. 109 (1997) 87–104. https://doi.org/10.1016/S0010-2180(96)00124-1.

[32] M.M. Fares, J. Hacaloglu, S. Suzer, Characterization of degradation products of polyethylene oxide by pyrolysis mass spectrometry, European Polymer Journal. 30 (1994) 845–850. https://doi.org/10.1016/0014-3057(94)90013-2.

[33] B. Arkles, G.L. Larson, Silicon compounds: silanes and silicones, Gelest, Morrisville, PA, 2013.

[34] L.G. Wade, Organic chemistry, 8. ed., internat. ed, Pearson, Boston, Mass. Munich, 2013.

[35] K. Shameli, M. Bin Ahmad, S.D. Jazayeri, S. Sedaghat, P. Shabanzadeh, H. Jahangirian, M. Mahdavi, Y. Abdollahi, Synthesis and characterization of polyethylene glycol mediated silver nanoparticles by the green method, IJMS. 13 (2012) 6639–6650. https://doi.org/10.3390/ijms13066639.

[36] N. Watanabe, T. Nakamura, E. Watanabe, E. Sato, Y. Ose, Distribution of organosiloxanes (silicones) in water, sediments and fish from the Nagara River watershed, Japan, Science

of The Total Environment. 35 (1984) 91–97. https://doi.org/10.1016/0048-9697(84)90371-1.

[37] N.J. Fendinger, D.C. Mcavoy, W.S. Eckhoff, B.B. Price, Environmental occurrence of polydimethylsiloxane, Environ. Sci. Technol. 31 (1997) 1555–1563. https://doi.org/10.1021/es9608712.

[38] G.E. Batley, J.W. Hayes, Polyorganosiloxanes (silicones) in the aquatic environment of the Sydney region, Mar. Freshwater Res. 42 (1991) 287–293. https://doi.org/10.1071/mf9910287.

[39] R. Pellenbarg, Environmental poly(organosiloxanes) (silicones), Environ. Sci. Technol. 13 (1979) 565–569. https://doi.org/10.1021/es60153a013.

[40] E.L. Fincher, W.J. Payne, Bacterial utilization of ether glycols, Applied Microbiology. 10 (1962) 542–547.

[41] C. Borstlap, C. Kortland, Effect of substituents in the aromatic nucleus on the biodegradation behavior of alkylaryl sulfonates, Journal of the American Oil Chemists Society. 44 (1967) 295–297. https://doi.org/10.1007/BF02635617.

[42] S.J. Patterson, C.C. Scott, K.B.E. Tucker, Nonionic detergent degradation: III. Initial mechanism of the degradation, Journal of the American Oil Chemists' Society. 47 (1970) 37–41. https://doi.org/10.1007/BF02541454.

[43] N. Obradors, J. Aguilar, Efficient biodegradation of high-molecular-weight polyethylene glycols by pure cultures of Pseudomonas stutzeri., Applied and Environmental Microbiology. 57 (1991) 2383–2388.

[44] M. Biel-Maeso, C. Corada-Fernández, P.A. Lara-Martín, Removal of personal care products (PCPs) in wastewater and sludge treatment and their occurrence in receiving soils, Water Research. 150 (2019) 129–139. https://doi.org/10.1016/j.watres.2018.11.045.

[45] A.M. Peck, Analytical methods for the determination of persistent ingredients of personal care products in environmental matrices, Anal Bioanal Chem. 386 (2006) 907–939. https://doi.org/10.1007/s00216-006-0728-3.

[46] S. Ramos, V. Homem, L. Santos, Development and optimization of a QuEChERS-GC–MS/MS methodology to analyse ultraviolet-filters and synthetic musks in sewage sludge, Science of The Total Environment. 651 (2019) 2606–2614. https://doi.org/10.1016/j.scitotenv.2018.10.143.

3.2. Applications of Py-GC-MS for the investigation of water-insoluble polymers

3.2.1. Secondary reactions in the analysis of microplastics by analytical pyrolysis

Published on Journal of Analytical and Applied Pyrolysis (2021). DOI: 10.1016/j.jaap.2021.105377

3.2.1.1. Introduction

MPs are emerging contaminants of great concern because of their pervasive occurrence in the environment, predicted to increase due to worldwide rise of plastic production [1]. MPs constitute a heterogeneous class of contaminants which is difficult to define [2,3]. This factor, in combination with their low concentration in chemically complex matrices, makes their analysis a challenge. Most of our present knowledge on the potential exposure to MPs was obtained by microscopic observation and vibrational spectroscopy, but in the last years thermoanalytical techniques are gaining increasing importance [4–7]. Pyrolysis combined with gas chromatography and mass spectrometry (Py-GC-MS), non-reactive or in the presence of the methylating reagent tetramethylammonium hydroxide TMAH (thermally assisted hydrolysis and methylation, THM), has been applied to the quali-quantitative analysis of MPs in different matrices such as drinking waters [8], sea waters [9], sea salts [10], biosolids [11], sediments [12], seafood [13] and miscellaneous [14–17]. The main advantages of analytical pyrolysis over optical-spectroscopic techniques reside in its capability to provide concentration values on mass units instead of particle number [17] and in its high selectivity due to the combination of chromatographic and mass spectrometric separation[18]. In addition, Py-GC-MS does not have constraints due to different shape (e.g., fibre or sphere), colour or size of the polymer particles. The pyrolysis products characteristic of a given polymer type (pyrolytic markers) are separated by GC and the ions generated in the mass spectrometer are separated and quantified. Selected pyrolytic markers and their associated ions are used for quantitation based on calibration protocols. Calibration is generally constructed by pyrolysing different quantity of standard polymers, but this procedure is not immune from flaws. Calibration protocols are based on the investigation of linear response for polymers pyrolysed individually [8,11,12,17,18] or in their mixture [9,10,14–16], simulating real conditions. A main drawback is matrix effect due to concomitants in the sample that may alter the pyrolytic behaviour of the polymer, in comparison

to the isolated form, or create interfering peaks [15,19]. When concomitants are constituents of the matrix, other than MPs, the problem can be solved by proper sample treatments. The selectivity of Py-GC-MS enables the analysis of mixture of MPs, avoiding the need of isolating single particles. However, different polymer types can interact leading to secondary reactions that may affect analytical results [20]. In the literature several studies have been published on the pyrolysis of polymers and their mixtures, particularly in the field of plastic waste recycling [21–31]. Nevertheless, there are very limited studies on polymer interactions concerned with the analysis of MPs [20]. It has been shown that polyethylene terephthalate (PET) can cause interference in the analysis of polyurethane (PUR) when the diisocyanate was used as pyrolytic marker for quantitation [20]. The explanation given by the authors was that benzoic acid produced from the pyrolysis of PET catalysed the hydrolysis of the diisocyanate into the corresponding amine. Procedural strategy can be adopted to tackle the problem of interference as performing calibration with polymers mixtures [32]. Nevertheless, identifying the occurrence of polymer interactions and understanding fundamental aspects on the chemistry of interactions are important to identify and solve possible bias. The investigation on polymer interaction is normally performed by co-pyrolysing different polymers and comparing the results with those obtained from single polymers pyrolysed under the same conditions. This approach has been followed in this study that aimed at confirming previous studies and providing novel information on the formation of secondary pyrolysis products from the co-pyrolysis of plastic particles of different types. Different polymer types were selected among the most common synthetic polymers found in the environment. The attention was focused to PET as this polymer exhibited the most important interactions. Benzoic acid, a relevant pyrolysis product of PET, was pyrolysed in the presence nitrogenated compounds in order to gain a better understanding of the interactions between polyesters and polyamides.

3.2.1.2. Experimental

3.2.1.2.1. Materials

Common polymeric items were selected instead of pure standard polymers in order to mimic situations closer to real environmental samples. Small fragments in the range of 10 – 120 µg (an example in Figure 3.2.1-1h) were obtained by cutting with a scalpel different polymers: high-density polyethylene (HDPE) from a bottle cap (Figure 3.2.1-1a), polyethylene terephthalate (PET) from a disposable plastic clear bottle (Figure 3.2.1-1b), polypropylene (PP) from a lid of a food container (Figure 3.2.1-1c), polystyrene (PS) from a disposable glass (Figure 3.2.1-1d),

polyvinylchloride (PVC) from a pipe connector (Figure 3.2.1-1e) and polyamide-6 (nylon-6, PA-6) from standard pellets (Figure 3.2.1-1f). Afterward, to further explore mixtures, polyamides-6,6 (nylon 6,6, PA-6,6) from a tie wrap (Figure 3.2.1-1g) was included among the analysed polymers., Benzoic acid, caprolactam, hexan-1-amine, hexan-1,6-diamine for additional investigations were purchased from Sigma-Aldrich.

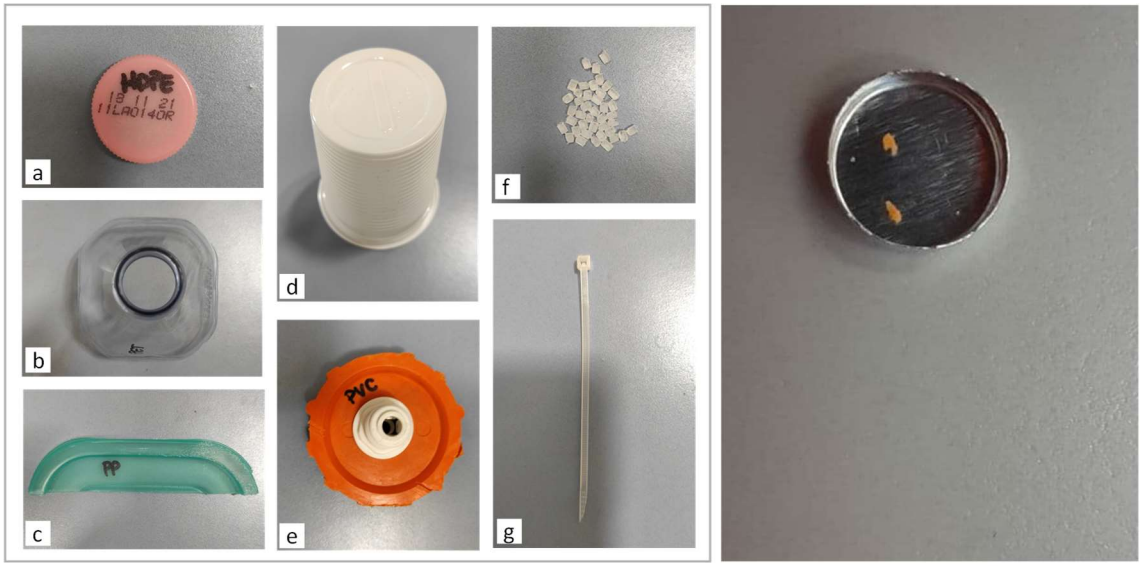

Figure 3.2.1-1. *Polymers selected from commercial items. HDPE bottle cap (a); PET disposable plastic clear bottle (b); PP lid of a food container (c); PS disposable glass (d); PVC pipe connector (e); PA-6 standard pellets (f); PA-6,6 tie wrap (g); plastic particles in a TGA sample pan, inner diameter 6 mm (h).*

3.2.1.2.2. Py-GC-MS

Pyrolyses were performed on single polymers and their mixtures. PET and PA or PVC particles were also pyrolysed separated by a piece of quartz filter (Whatman® Q-MA). Benzoic acid was pyrolysed alone and in mixture with hexan-1-amine or hexan-1,6-diamine. Analyses of single polymers, their mixture, binary mixture and standard compounds were all performed under the same Py-GC-MS experimental conditions, showed in Table 3.2.1-1. The oven programmed temperature was selected to better separate and recognise pyrolyzates while polymers were analysed together.

Table 3.2.1-1. *Instrumental conditions for Py-GC-MS analyses of single polymers, mixtures and standard compounds.*

Pyrolyzer	**Multi-Shot Pyrolyzer (EGA/PY-3030D) - Frontier Lab**	
	Furnace temperature	500 °C
	Interface temperature	280 °C
Gas chromatograph	**Agilent 7890B**	
	Column	Agilent 19091S-433UI HP-5ms Ultra Inert 30 m x 250 µm x 0.25 µm
	Carrier gas	He
	Column flow	1 mL min^{-1}
	Split	1:20
	Injector	280 °C
Oven programmed temperature	Initial temperature	50 °C
	First temperature rate	3.7 °C
	First temperature step	160 °C
	Second temperature rate	20 °C min^{-1}
	Maximum temperature	310 °C
	Temperature hold time	3 min
Mass spectrometer	**Agilent 5977B**	
	MS source temperature	230 °C
	MS quad temperature	240 °C
	Mass scan	35 – 600 *m/z*
	Ionization energy	70 eV

3.2.1.2.3. Additional characterisation by spectroscopic analysis

The identity of commercial polymers was also confirmed by spectroscopic characterisation, in order to obtain complementary information to further confirm material nature. Analyses were conducted with a FT-IR spectrometer (Cary 630 FT-IR Spectrometer, Agilent, USA) with ATR diamond crystal. Experimental conditions are described in Table 3.2.1-2. The ATR diamond crystal was cleaned with acetone and a background scan was performed between each sample. In order to confirm the nature of the polymers, results were compared with literature.

Table 3.2.1-2. *Instrumental conditions for FTIR-ATR analyses of single commercial polymers.*

Cary 630 FTIR Spectrometer with ATR diamond crystal	
Spectral range	650 – 4000 cm^{-1}
Background scans	32
Sample scans	32
Resolution	8 cm^{-1}

3.2.1.2.4. Thermal identification and quantification

Polymer characterisation was based on the identification of the respective thermal degradation products by matching mass spectra of NIST14 database or published literature, pyrolysis of model compounds, or mass spectrum interpretation. Additionally, comparison was made with temperature programmed Kovats' Retention Indices (RI) when available. RI were calculated using the retention times of the *n*-alkanes determined in the pyrogram of PE from the Equation 3.2.1-1

$$RI_x = 100\left(n + \frac{RT_x - RT_n}{RT_{n+1} - R\ _n}\right) \qquad \textbf{Equation 3.2.1-1}$$

RT_x, RT_n, and RT_{n+1} are the retention times of compound x, the *n*-alkane with n the carbon atoms eluting immediately before compound x, and the *n*-alkane with n + 1 carbon atoms eluting immediately after the compound x, respectively. Calibration protocols were made by pyrolysing individual polymers weighed by the microbalance of a Mettler Toledo STDA851 TGA with a sensitivity of 0.001 mg. Characteristics pyrolytic markers employed in calculations of each polymer are indicated in Table 3.2.1-4. Recovery (R) was calculated as the percentage ratio of weight calculated from the single-polymer calibration curve to the weight of the pyrolysed particle, as Equation 3.2.1-2 shows.

$$R = \frac{WEIGHT_{calculated}}{WEIGHT_{pyrolysed}} 100 \qquad \textbf{Equation 3.2.1-2}$$

Analytical standard deviations (s_{x0}) were calculated for each calibration protocol, indicating the random error of the analytical process for each polymer. s_{x0} resulted by the following equation (Equation 3.2.1-3):

$$S_{x0} = \frac{S_{xy}}{b} = \frac{\sqrt{\frac{1}{n-2}\left(SS_{yy} - \frac{SS_{yx}^2}{SS_{xx}}\right)}}{b} \qquad \textbf{Equation 3.2.1-3}$$

*w*here s_{xy} is the residual standard deviation which indicates the calibration error, b is the slope of the calibration curve, n is the number of calibration points, SS_{xx}, SS_{yy} and SS_{yx} are the Sum of Squares [33].

3.2.1.3. Results

3.2.1.3.1. Single polymer characterisation by Py-GC-MS

Pyrolyses of single polymeric material were useful to characterise polymers, confirming the expected nature and evaluating the presence of additives. Pyrograms for polymer characterisation were recorded with a preliminary oven programmed temperature, and later a more suitable one was selected for polymer mixture analysis (Section 3.2.1.2.2), to better separate polymer peaks while they were co-pyrolysed. The peaks of the resulting pyrograms were identified by the NIST14 library match and by comparison with literature [34]. Pyrolysis of each single polymer led to the typical fingerprint of the corresponding pure polymer and no additional, unexpected compounds were revealed. As Figure 3.2.1-2 shows, pyrolysis of PE, produces a characteristic fingerprint made by triplets of peaks of aliphatic hydrocarbons of increasing length, deriving from random scission and end-chain scission degradations [35,36]. In each triplet, the first eluting compound is the α,ω-alkadiene, the second one (with the highest intensity) is the α-alkene and the last one which elute is the alkane [34,35]. The *n*-alkanes are produced from C-C cleavage, then C-H cleavage is also involved for *n*-alkene and *n*-alkadiene formation [35,36]. The pattern of elution of the triplets is highlighted into the blue square in Figure 3.2.1-2. Pyrolysis of PET mainly produce aromatic compounds with carboxyl or ester groups (Figure 3.2.1-3). These compounds reflect the monomers of PET synthesis, ethylene glycol and terephthalic acid. Ester scission reaction produce carboxylic acid and olefin end groups [35,37]. C–O bonds, along the polymer chains and in side position, are most likely subject to thermal cleavage with further degradation, and benzoic acid and possibly to benzene with CO_2 release [34,38]. As Figure 3.2.1-3 shows, benzoic acid or (vinyloxycarbonyl)benzoic acid eluted as tailing peaks and this behaviour was attributed to the less affinity with the non-polar column used for the separation. Pyrolysis of PP involved consecutive reaction mechanisms, including chain scission, radical recombination, allyl chain fission, mid-chain and end-chain scission, radical addition and hydrogen transfers [39]. Figure 3.2.1-4 represents the pyrogram of PP, which is dominated by clusters of stereoisomers with increasing number of carbon atoms. Depending on the number of carbons which compose the group of compounds, they elute at different increasing retention times [34]. PP can exist in isotactic, atactic or syndiotactic form

and the same thermal degradation products are released for each form. However, relative abundances are different depending on the form and, thanks to literature comparison [34], the fingerprint of the analysed PP was attributed to isotactic PP. PS is one of the first investigated polymer by Py-GC-MS and the main thermal degradation products are fragments of the chain with one, two or three styrene units (Figure 3.2.1-5). These three compounds are highly representative of the presence of PS, and they also show a high relative intensity with respect to the other peaks (e.g., α-methyl styrene). End-chain β-scissions produce monomers (styrene). Homolytic scissions take place leading to the formation of radicals, with a methylene- or benzyl-end. These two radicals are involved in other end- or mid-chain β-scissions which also produces dimer and trimer [34,35,40]. As Figure 3.2.1-6 shown, pyrolysis of PVC mostly produces polycyclic aromatic hydrocarbons (PAH), but different reactions occur. Chain scissions and rearrangements can bring about the formation of alkenes, both linear and cyclic and hydrogen chloride [34,41]. By the way this is not the only reaction series that takes place, in fact also the formation of chlorinated hydrocarbons, such as chlorobenzene can occur even though it is not the more favourable pathway. While cyclisation occurs, monocyclic aromatics or PAH are produced [34,41]. Pyrogram of PA-6 is dominated by caprolactam which is the monomer used for its synthesis (Figure 3.2.1-7). Polymerization of caprolactam occurs in a reaction where water is added to open the caprolactam ring and then eliminated for the polycondensation step [35]. Besides the peptide bond C(O)–NH, various other bonds undergo cleavages, such as C–N, C–C(O) and C–C bonds. The cleavage of the C–N bond produces molecule with an amide and an unsaturated hydrocarbon end. Further elimination of water leads to the formation of nitriles [34,35,42].

The analysed polymers (expect for PA-6) derived from commercial products. For this reason, it was expected to find signals of additives which are typically present (such as stabilisers for polyolefins or plasticiser for PVC). Analysis by Py-GC-MS did not reveal their presences, maybe because they were present in low concentration (< 1 %).

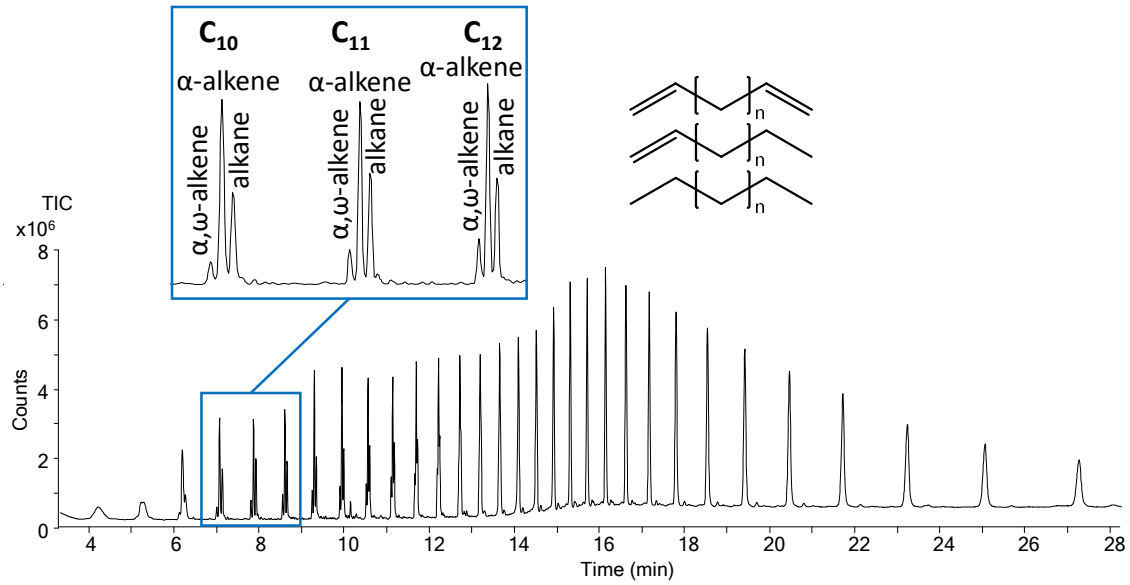

Figure 3.2.1-2. *TIC pyrogram from pyrolysis of HDPE bottle cap (Figure 3.2.1-1a).*

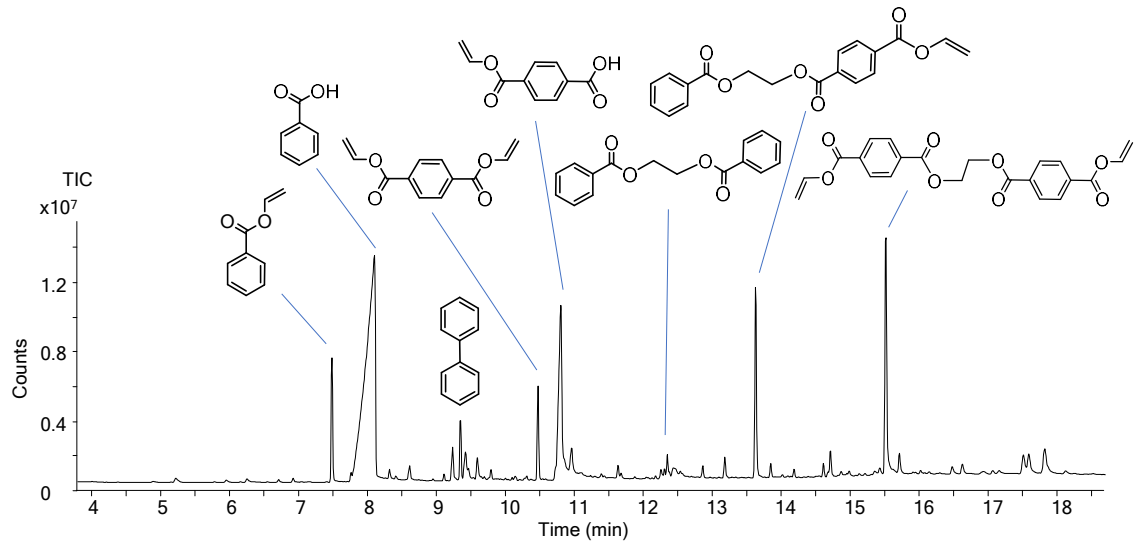

Figure 3.2.1-3. *TIC pyrogram from pyrolysis of PET disposable plastic clear bottle (Figure 3.2.1-1b).*

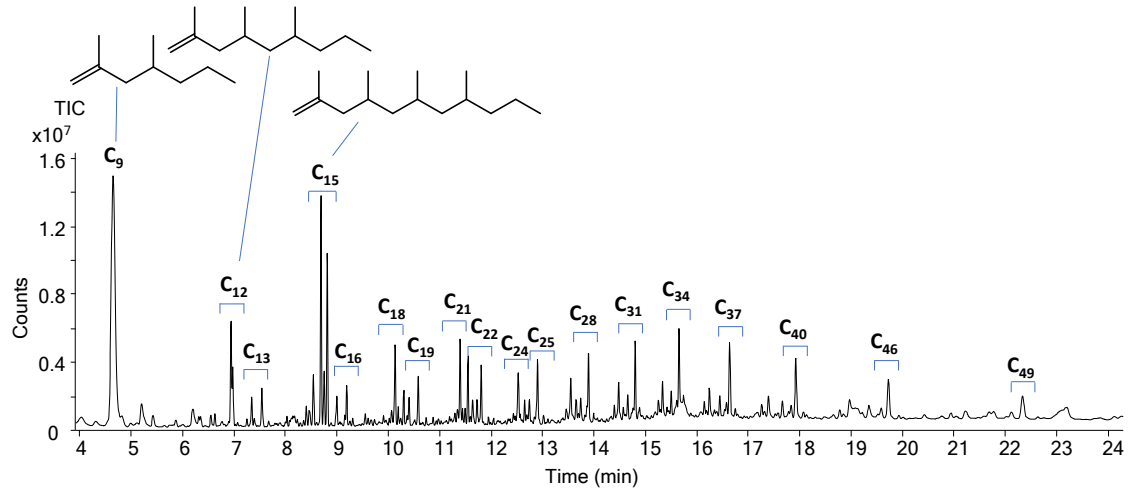

Figure 3.2.1-4. *TIC pyrogram from pyrolysis of PP lid of a food container (Figure 3.2.1-1c).*

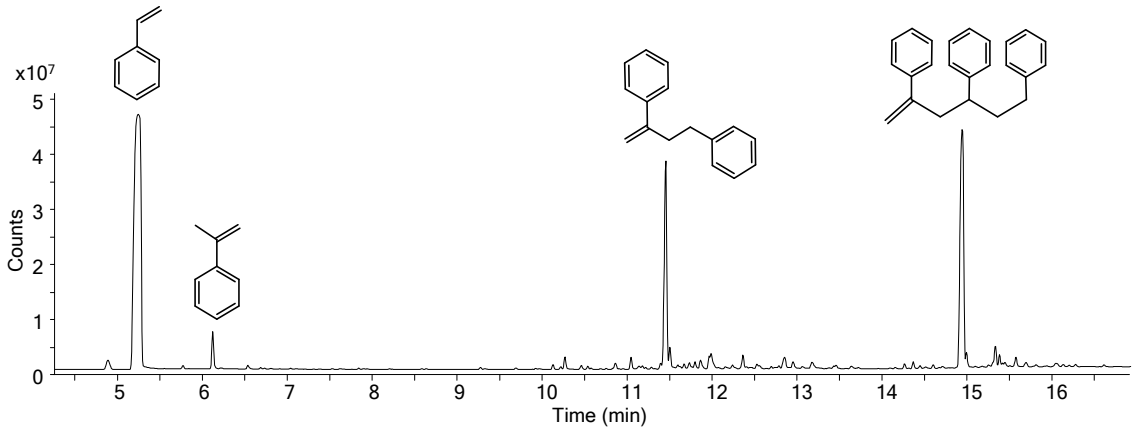

Figure 3.2.1-5. *TIC pyrogram from pyrolysis of PS disposable glass (Figure 3.2.1-1d).*

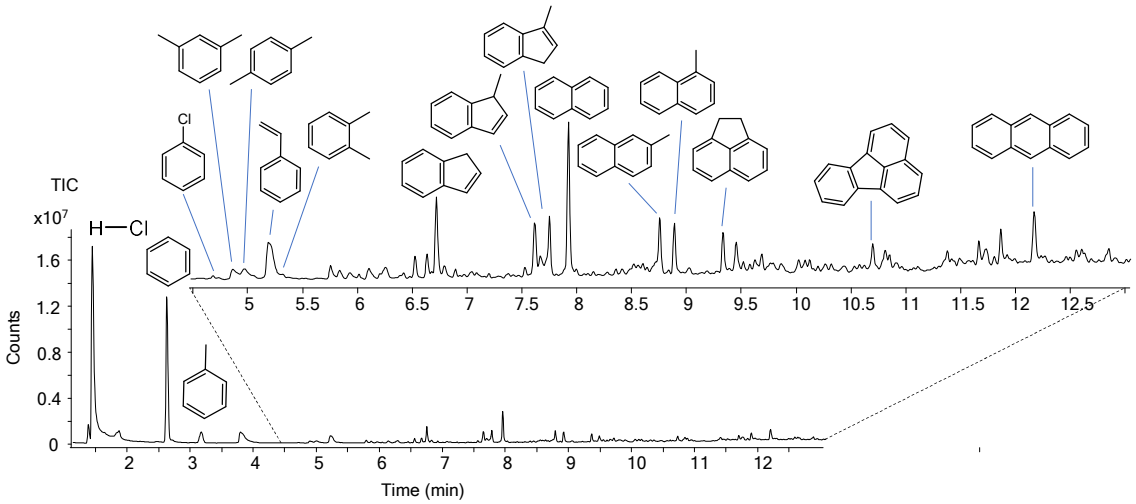

Figure 3.2.1-6. *TIC pyrogram from pyrolysis of PVC pipe connector (Figure 3.2.1-1e).*

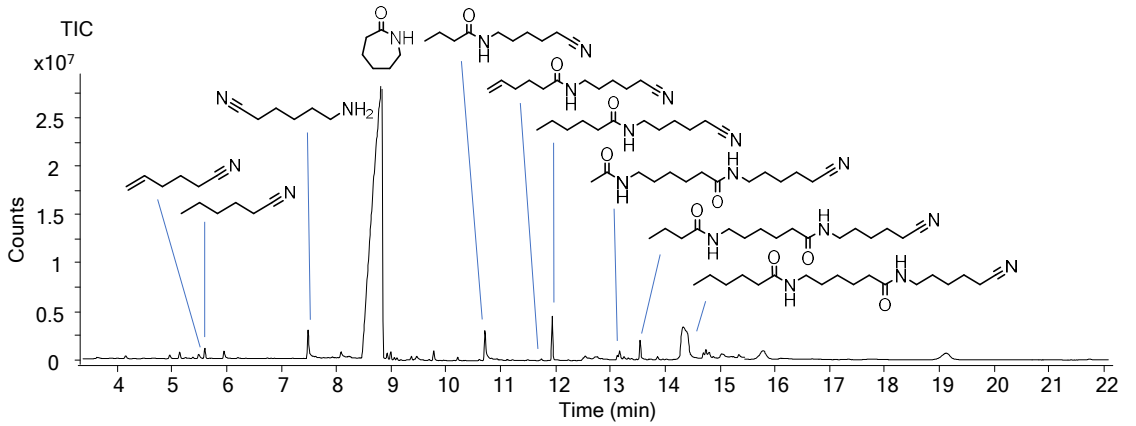

Figure 3.2.1-7. *TIC pyrogram from pyrolysis of PA-6 standard pellet (Figure 3.2.1-1f).*

3.2.1.3.2. Single polymer characterisation by FTIR-ATR

In addition to the comparison of pyrograms with literature [34], the identity of the polymers was also confirmed by FTIR spectra, obtained with a Cary 630 FTIR spectrometer with an ATR diamond crystal in the 650 – 4000 cm^{-1} range [43]. IR spectra are shown in Figures 3.2.1-8, 3.2.1-9, 3.2.1-10, 3.2.1-11, 3.2.1-12 and 3.2.1-13 for HDPE, PET, PP, PS, PVC and polyamides, respectively. Main signals for each polymer were confirmed by literature comparison ad bands are expressed in Table 3.2.1-3. As thermal analyses revealed, no additives were identified in the analysed spectra, except for PVC that presented a small broad peak in the 1765 cm^{-1}. This band is typical of commercial PVC resins and it is attributed to C=O groups introduced into the polymer chain in processing steps [44] (the signal of the C=O stretching of phthalates falls around 1730 cm^{-1}). However, the pyrograms did not reveal the presence of these compound, probably because their very low concentration.

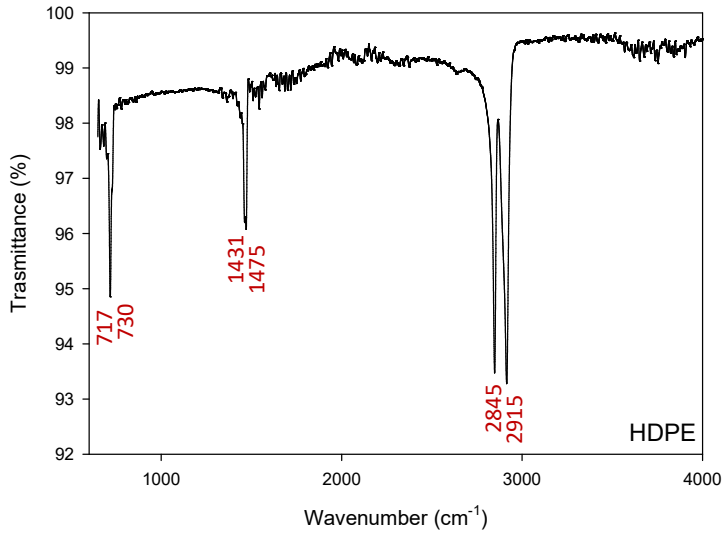

Figure 3.2.1-8. *IR spectrum recorded for HDPE bottle cap (Figure 3.2.1-1a).*

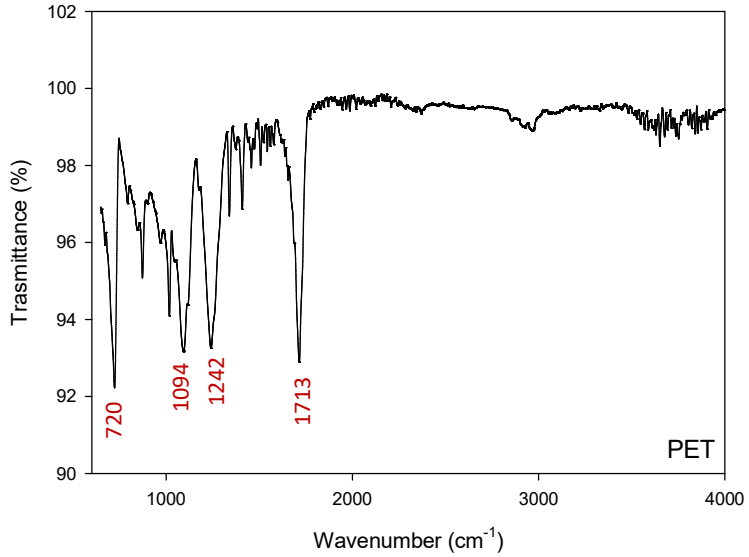

Figure 3.2.1-9. *IR spectrum recorded for PET disposable plastic clear bottle (Figure 3.2.1-1b).*

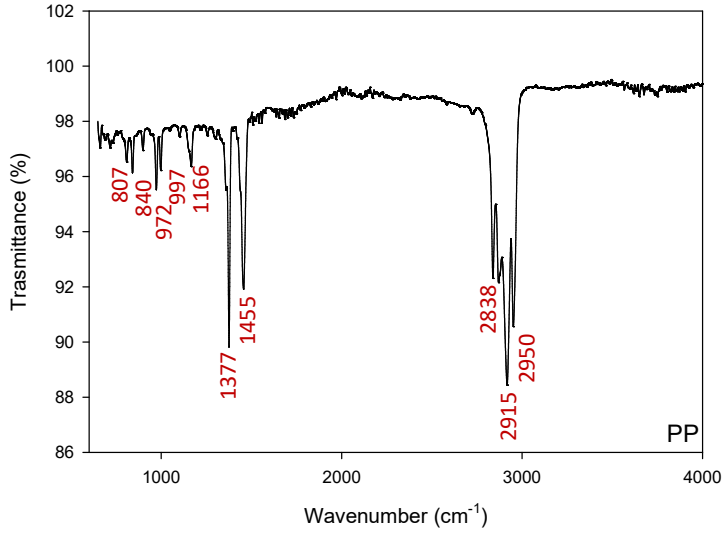

Figure 3.2.1-10. *IR spectrum recorded for PP lid of a food container (Figure 3.2.1-1c).*

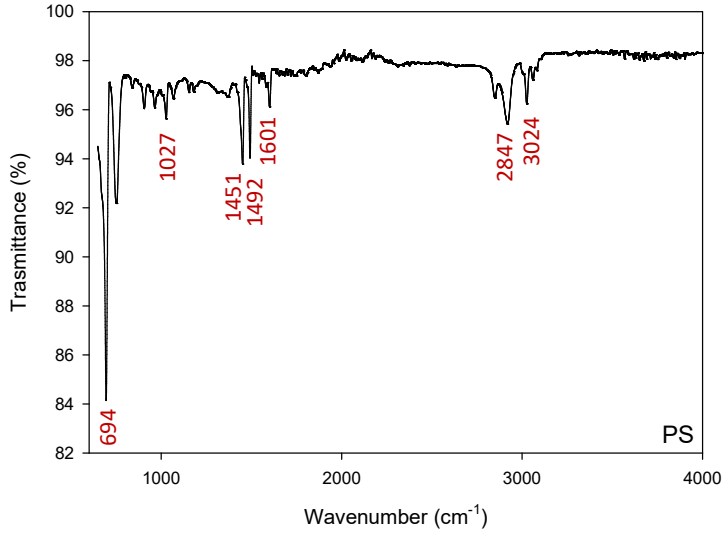

Figure 3.2.1-11. *IR spectrum recorded for PS disposable glass (Figure 3.2.1-1d).*

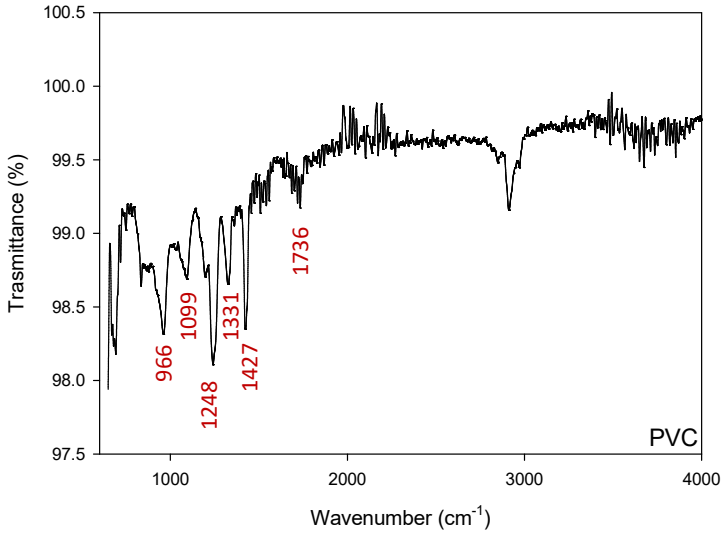

Figure 3.2.1-12. *IR spectrum recorded for PVC pipe connector (Figure 3.2.1-1e).*

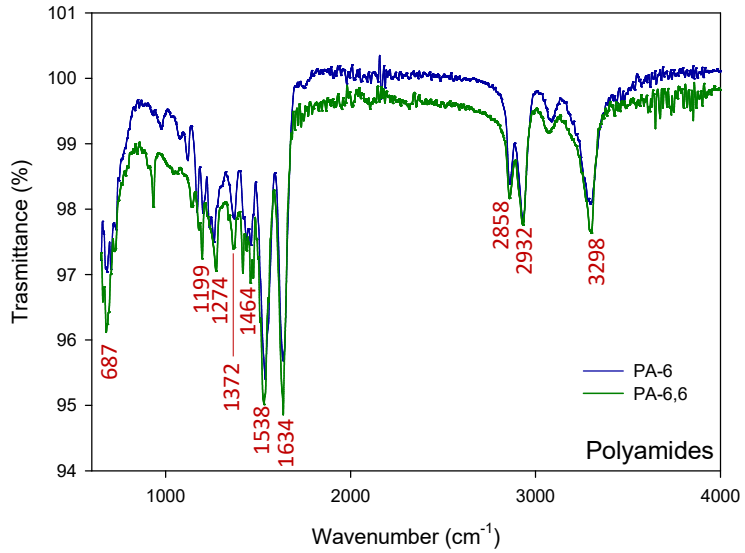

Figure 3.2.1-13. *IR spectra recorded for PA-6 standard pellet and PA-6,6 tie wrap (Figure 3.2.1-1 f and g, respectively).*

Table 3.2.1-3*. IR spectra characterisation from FTIR-ATR data (wavenumbers and bond type assignment) and comparison with literature. Wavenumber referred to IR spectra in Figure 3.2.1-8 (HDPE), Figure 3.2.1-9 (PET), Figure 3.2.1-10 (PP), Figure 3.2.1-11 (PS), Figure 3.2.1-12 (PVC) and Figure 3.2.1-13 (polyamides).*

Wavenumber (cm^{-1})	Assignment	Reference
HDPE		
717	C–H_2 rock	[43,45–47]
730	C–H_2 rock	
1431	CH_2 bending	
1475	CH_2 bending	

2845	C–H stretching	
2915	C–H stretching	
PET		
720	Aromatic CH out-of-plane bend	[43,45,47,48]
1094	C–O stretching	
1242	C–O stretching	
1713	C=O stretching	
PP		
807	CH_2 rock, C-C stretching, C–CH stretching	[43,45–47]
840	CH_2 rock, C–CH_3 stretching	
972	CH_3 rock, C-C stretching	
997	CH_3 rock, CH_3 bending, CH bending	
1166	CH bending, CH_3 rock, C–C stretching	
1377	CH_3 bending	
1455	CH_2 bending	
2838	C-H stretching	
2915	C-H stretching	
2950	C-H stretching	
PS		
694	Aromatic CH out-of-plane bend	[43,45–47]
1027	Aromatic CH bending	
1451	CH_2 bending	
1492	Aromatic ring stretching	
1601	Aromatic ring stretching	
2847	C–H stretching	
3024	Aromatic C–H stretching	
PVC		
966	CH_2 rock	[43,44,46,47]
1099	C–C stretching	
1248	CH bending	
1331	CH bending	
1427	CH_2 bending	
1736	C–O stretching of phthalates	
Polyamides		
687	NH bending, C=O bending	[43,46,47,49]
1099	CH_2 bending	
1274	NH bending, C–N stretching	
1372	CH_2 bending	
1464	CH_2 bending	
1538	NH bending, C-N stretching	
1634	C=O stretching	

2858	CH stretching
2932	CH stretching
3298	N–H stretching

3.2.1.3.3. Calibrations of single polymers

Calibration curves were created on single polymers (Figure 3.2.1-14), choosing one representative thermal degradation product (marker) for each polymer. Area integrations were performed by extracting the current for specific fragment ions of the mass spectra of each marker (Table 3.2.1-4). For the quantification of MPs in environmental samples, internal standardisation is preferable because it helps in standardise chromatographic variations, especially on longer time periods. Anyway, the study intended to evaluate the possible interactions occurring when different polymers were pyrolysed and no real samples were taken into account. Theoretical analyses works is less complex system than applicated methods, therefore external calibration was considered enough accurate. Polyolefins (PE, PP and PS) and PA-6 showed good linearity within the investigated range resulting in $R^2 > 0.99$ (Figure 3.2.1-14 a, d, e and g, respectively and calibration details in Table 3.2.1-4). PVC and PET curves were subjected to greater s_{x0} (Table 3.2.1-4), nevertheless correlation results were satisfactory in comparison with literature [14,50,51]. In particular, given the poor linearity obtained for PET calibration with vinilybenzoate (Figure 3.2.1-14c), calculations were repeated for divilynterephthalate (Figure 3.2.1-14b), obtaining good correlation.

Table 3.2.1-4. *Calibration data obtained from Py-GC-MS of single polymeric materials [52]. Retention indices RI experimental and RI_{lit} from literature [34].*

Polymer	Marker	*m/z*	RI	RI_{lit}	a	b	R^2	s_{x0}
PE	n-tetradec-1-ene	55	1392	1392	$5.4\ 10^2$	$1.1\ 10^3$	0.996	2.7
PET	vinyl benzoate	105	1137	1143	$2.7\ 10^3$	$-2.3\ 10^4$	0.878	25
PET	divinyl terephthalate	175	1570	1577	$3.5\ 10^3$	$-1\ 10^4$	0.958	14
PP	2,4-dimethyl-1-heptene	43	837	845	$8.5\ 10^3$	$6.1\ 10^4$	0.993	3.4
PS	2,4-diphenyl-1-butene	208	1729	1749	$3.4\ 10^3$	$1.3\ 10^4$	0.993	5.4
PVC	2-methylnaphtalene	142	1293	1320	$2.9\ 10^2$	7.5 10	0.944	11
PA-6	caprolactam	113	1277	1265	$2.9\ 10^3$	$1.7\ 10^4$	0.992	6

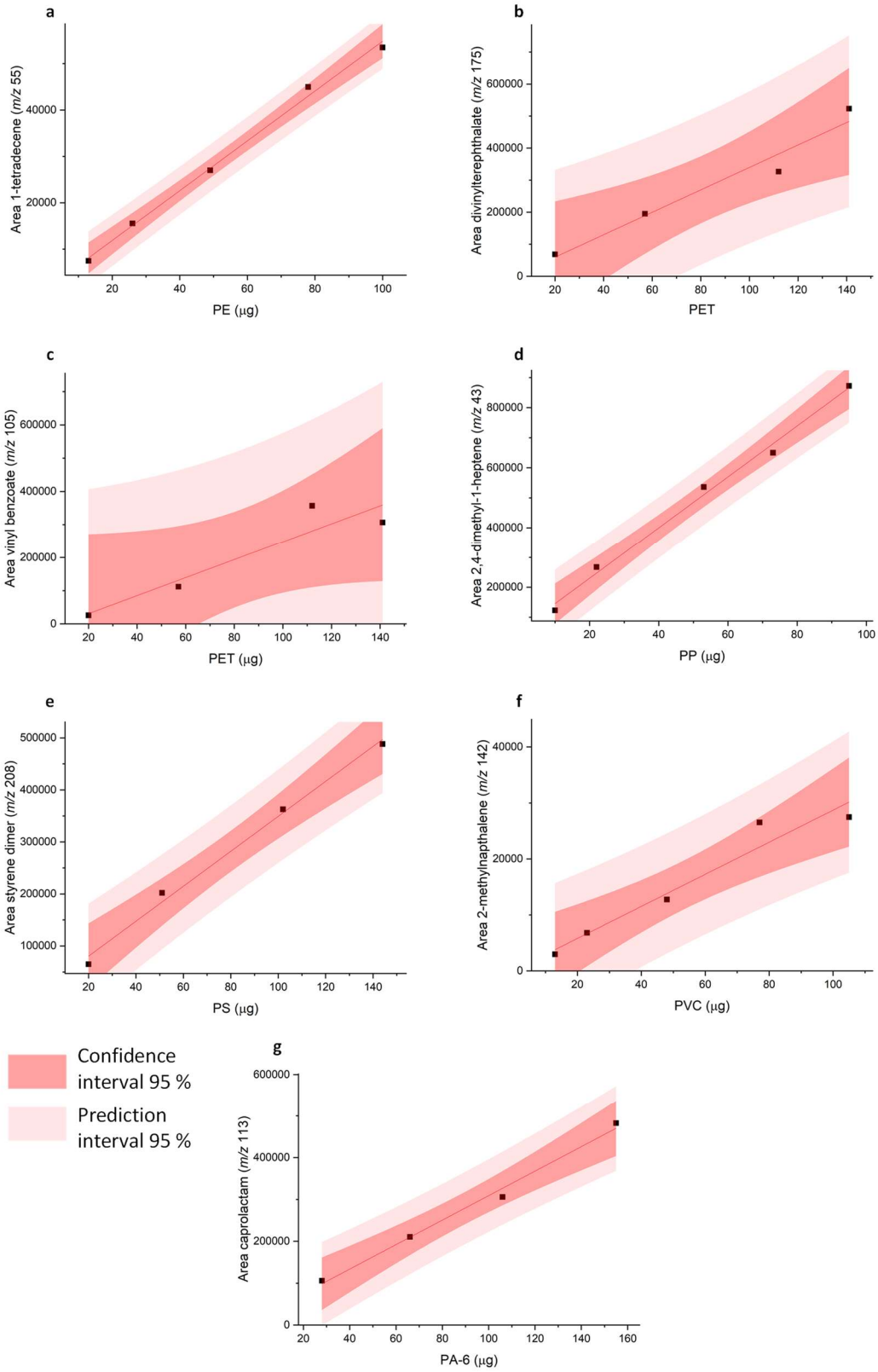

Figure 3.2.1-14. *Calibration curves of commercial items: HDPE (a), PET (b and c), PP (d), PS (e), PVC (f), PA-6 (g). Areas of pyrolytic markers were integrated at specific m/z.*

3.2.1.3.4. Py-GC-MS of polymer mixtures

Figure 3.2.1-15 shows the pyrogram obtained from Py-GC-MS of a mixture of plastic particles of different polymers (PE, PP, PS, PVC, PET, PA-6, PA-6,6). From the comparison between the pyrograms of polymer mixtures and the pyrograms of each single polymer, the production of additional peaks was highlighted. In addition to the typical pyrolysis products of the investigated polymers [34], new peaks were revealed produced by nitrogen-bearing aromatic compounds (Table 3.2.1-5) and chlorinated benzoic acid derivatives (Table 3.2.1-6). These new pyrolysis products were observed when particles of PET were co-pyrolysed with particles of PA or PVC and were attributed to secondary reactions in the polymer melt or vapour phase. Pyrolysis products indicative of secondary reactions were not identified in the case of PE, PP and PS in accordance to literature [20]. The presence of chlorinated pyrolysis products of PP (2-chloro-2-phenyl propane, 2-chloro-2-methyl propane, 2-chloro-2-methyl pentane) were suggested from the pyrolysis of municipal waste plastic mixtures [25], but these products could not be identified in the pyrograms of our study. In accordance with our results, it was reported that PVC did not affect the thermal behaviour of polyolefins [24]. Besides qualitative features, the mutual interactions between polymers can affect quantitative analysis as highlighted by Matsueda et al. [20]. In order to investigate this latter aspect, calibration curves were produced by pyrolysing single polymers. Particle weights were selected within the calibration ranges typically reported in the literature (0.1 – 1070 µg) [8,11,12,15]. The results are summarised in Table 3.2.1-4. These calibration curves were utilised for calculating the quantity of each polymer particle in mixtures, and the differences between expected and measured values were expressed as recovery R (Figure 3.2.1-16). Recoveries were acceptable for polyolefins (mean ± RSD (n = 3): PE 96 % ± 4 %, PP 97 % ± 1 %, PS 104 % ± 11 %, PVC 108 % ± 14 %, RSD = relative standard deviation). This finding would indicate that interactions between polyolefins were minimal. This observation apparently contrasts with studies performed on mixtures of polyolefins with PS [29] and mixtures of PE, PP, PS, PVC and PET [30] were important changes of the pyrolytic behaviour of polymers were observed in comparison to isolated species. Williams and Williams reported a much higher concentration of aromatic compounds in the pyrolysis oil of PE/PS and PP/PS mixtures in comparison to single polymers, while a strong decrease of benzene concentration was observed in PVC/PS mixtures in comparison to PVC [29]. Similarly, an increase of styrene and other aromatic compounds in pyrolysis oils from mixtures of PE/PP/PS/PVC/PET in comparison to those of individual polymers was observed by Muhammad et al. [30]. However, these studies employed a fixed-bed gas-purged pyrolytic reactor [29] and two-stage fixed bed pyrolysis-catalytic reactor [30] where interactions are supposed to be more significant with

respect to flash pyrolysis, due to a higher residence time. In agreement with this interpretation, not important changes were found by Predel and Kaminsky [31] in the pyrolytic behaviour of PE, PP and PS mixtures. When these polymers were individually pyrolysed and co-pyrolysed in binary and ternary mixtures under flash pyrolysis conditions, no significant variations were identified, except for PP/PS pyrolysis where an enhanced production of unsaturated waxes was revealed for compounds with a number of C > 30, mostly dienes [31]. In comparison to polyolefins, the recoveries of PET and PA-6 were less satisfactory in terms of both mean values and variability (RSD). In the case of PET, the recovery was 123 % ± 30 % when using vinyl benzoate as pyrolytic marker, and 76 % ± 48 % with divinyl terephthalate. PA-6 presented low recovery and high variability (63 % ± 32 %). The difference from polyolefins could be due to the poor calibration data for PET (Table 3.2.1-4) that exhibited the lowest determination coefficients R^2 and highest s_{x0}. The poor calibration behaviour of PET was also reported in the literature, mostly in the absence of an internal standard [9,10,13,19]. However, deviations could also be caused by possible interactions between polymers as demonstrated in the case of PU with PET and PA-6 [20]. Co-pyrolysis experiments with PVC and PA-6 showed that HCl evolved from PVC increased the pyrolytic yield of aliphatic nitriles and favoured the depolymerisation of PA-6 into caprolactam [24,28]. The formation of 6-chlorohexanenitrile was also reported as pyrolysis product from PVC-PA-6 co-pyrolysis [28]. Instead, the pyrolytic behaviour of PA-6,6 did not appear to be influenced by PVC [24]. Apparently, these interactions did not affect quantitative results of PVC and PA microplastics in mixtures [20]. While interactions between PVC and PA have been described in the literature, there are few articles on the interactions between PVC and PET [23], and no published studies dealing with the interactions between PET and PA to the best of our knowledge. Therefore, our attention was focused to the co-pyrolysis of PET particles with polyamides (PA-6 and PA-6,6) and PVC.

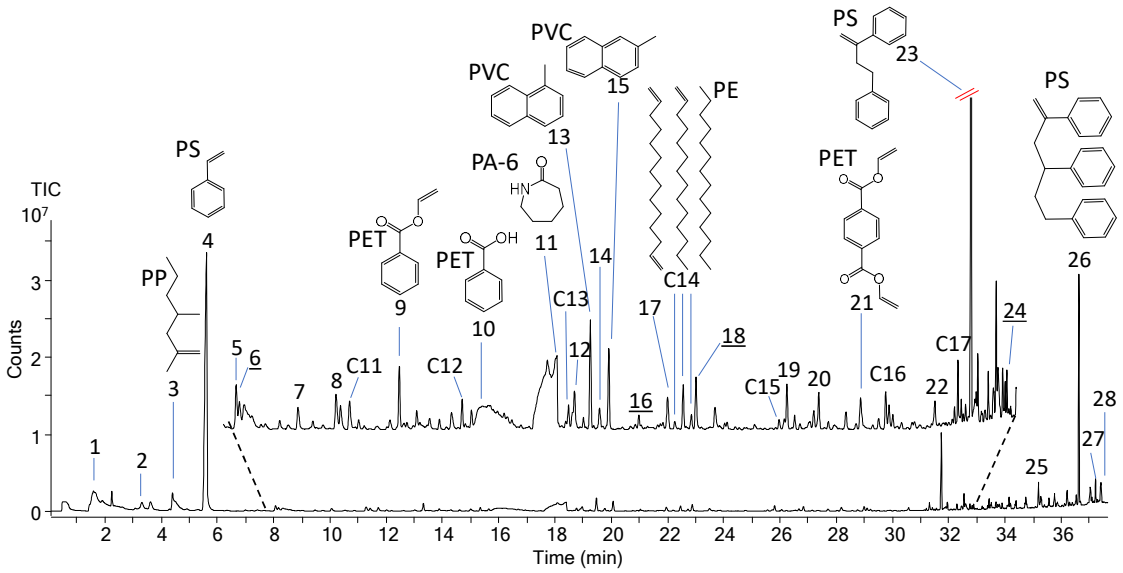

Figure 3.2.1-15. *Pyrogram from a mixture of plastic particles (PE, 14 µg; PP, 13 µg; PS, 12 µg; PET, 12 µg; PA-6, 13 µg; PA-6,6, 10 µg; PVC, 10 µg) Peak numbers refer to compounds listed in Table 3.2.1-5. Cx: alkadiene, alkene, alkane triplets with x carbon atoms (PE). Peak numbers underlined: products not found in the pyrograms of single polymers [52].*

Table 3.2.1-5. *GC-MS data and structural attribution of peaks labelled in the pyrogram of Figure 3.2.1-15 obtained from Py-GC-MS of polymer mixture [52].*

#	Compound	RI	*m/z*	Polymers
1	benzene	–	51, 52, 78	PVC (PET)
2	cyclopentanone	–	41, 55, 84	PA-6,6
3	2,4-dimethyl-1-heptene	837	43, 70, 126	PP
4	styrene	898	51, 78, 104	PS
5	α-methylstyrene	982	103, 117, 118	PS
6	benzonitrile	993	50, 76, 103	PET+PA
7	indene	1043	63, 115, 116	PVC
8	2,4,6-trimethyl-1-nonene	1079	41, 69, 168	PP
9	vinylbenzoate	1137	77, 105, 148	PET
10	benzoic acid	1214	77, 105, 122	PET
11	caprolactam	1277	55, 84, 113	PA-6
12	2-methylnaphthalene	1296	115, 141, 142	PVC
13	2,4,6,8-tetramethyl-1-undecene	1307	43, 69, 154	PP
14	1-methylnaphthalene	1313	115, 141, 142	PVC
15	2,4,6,8-tetramethyl-1-undecene	1324	55, 69, 154	PP
16	benzamide	1357	77, 105, 121	PET+PA-6,6
17	diphenyl	1379	76, 153, 154	PET
18	2-chloroethylbenzoate	1415	105, 122, 184	PVC+PET
19	n-pentadec-1-ene	1497	43, 55, 210	PE
20	2,4,6,8,10-pentamethyl-1-tridecene	1527	43, 69, 196	PP

21	divinyl terephthalate	1567	76, 104, 175	PET
22	1,3-diphenylpropane	1659	92, 105, 196	PS
23	styrene dimer	1726	91, 104, 208	PS
24	unknown	1863	175, 211, 213	PVC?+PET?
25	ethandiol dibenzoate	2190	77, 105, 227	PET
25	1,4-benzenedicarboxylic acid, di-2-chloroethyl ester	2190	166, 211, 213	PVC+PET
26	styrene trimer	2510	91, 117, 312	PS
27	2-(benzoyloxy) ethylvinylterephthalate	2662	105, 149, 297	PET
28	unknown	2980	105, 211, 213	PVC+PET

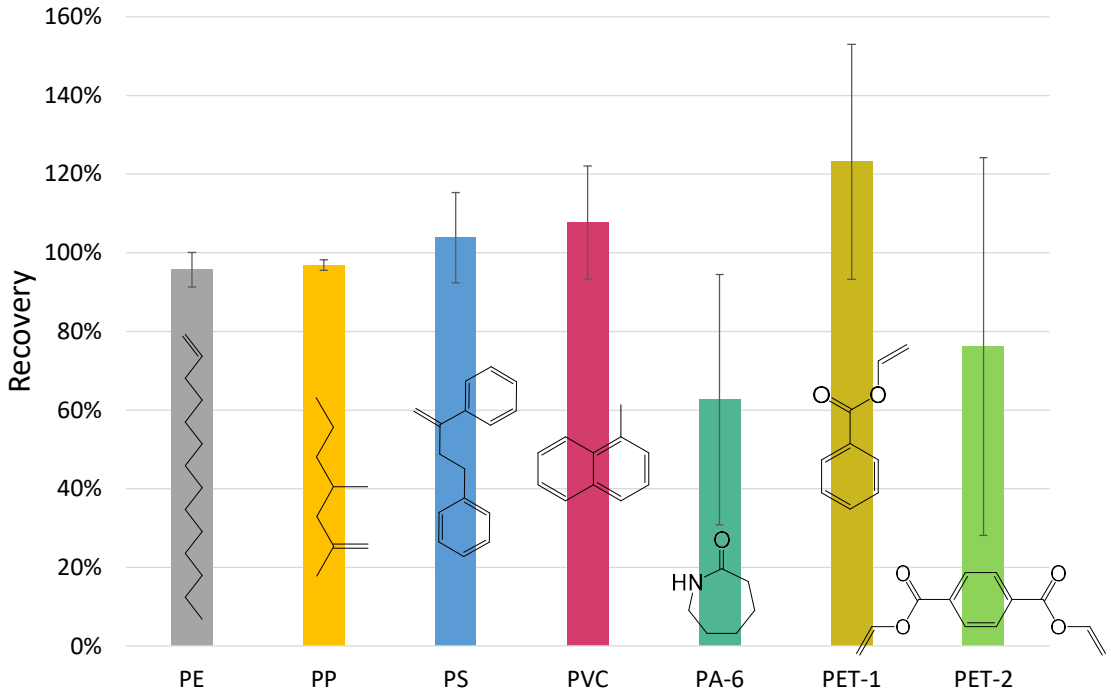

Figure 3.2.1-16. *Recovery values from Py-GC-MS of polymer particle mixtures using the calibration protocols reported in Table 3.2.1-4; PET-1 marker: vinyl benzoate, PET-2 marker: divinyl terephthalate [52].*

3.2.1.3.4.1. Py-GC-MS of PET with PA

Py-GC-MS of PET produced a pyrogram characterised by several peaks (Figures 3.2.1-3 and 3.2.1-17a) identified by their known GC-MS characteristics [34]. Although benzoic acid was the predominant pyrolysis product, its poor chromatographic behaviour in GLC with non-polar stationary phase precluded us from choosing it as a suitable pyrolytic marker. Moreover, when it was used as a pyrolytic marker by other authors, it produced non-linear calibration curves in polymer mixtures attributed to secondary reactions [20]. Vinyl terephthalate and divinyl terephthalate produced calibration plots with a better linearity in comparison to benzoic acid

[20]. Vinyl benzoate was also used as a pyrolytic marker for PET [11]. The pyrolyzates of PA-6 (Figures 3.2.1-7 and 3.2.1-17b) were dominated by caprolactam in accordance with literature [53,54]. When particles of PET and PA-6 were co-pyrolysed, variations in the retention behaviour of benzoic acid and caprolactam were observed in the resulting pyrograms (Figure 3.2.1-17c). The retention time of benzoic acid shifted with a concurrent reverse of the shape of peak tail. This change was noticed when benzoic acid was pyrolysed in the presence of caprolactam under the same conditions. Figure 3.2.1-18 shows five different pyrolysis of 50 µg of benzoic acid (red peak), with an increasing amount of caprolactam (blue peak), from 5 to 75 µg. It is possible to see that when benzoic acid is higher than caprolactam in ration 10:1 (a), the two peaks are separated. When caprolactam amount is increased, and the ratio is reduced, the shape of benzoic acid peak is modified up to the full inversion of the tail of the peak. This behaviour was attributed to interactions between these two compounds inside the Py-GC system that along with reactions leading to benzonitrile could be responsible for the observed low recoveries (Figure 3.2.1-16). Benzonitrile and 4-cyanobenzoic acid were identified as new pyrolysis products from the co-pyrolysis of PET and PA-6 (Figure 3.2.1-17c and Table 3.2.1-6). In order to gather some information about their formation, benzoic acid was pyrolysed individually and in the presence of aliphatic amines, typical pyrolysis products of polyamides. Py-GC-MS of pure benzoic acid produced benzene, diphenyl and occasionally benzophenone (data not shown). Benzene and diphenyl can be formed from phenyl radical produced by the cleavage of the carbon-carbon single bond of benzoic acid [55]. An anionic mechanism of decarboxylation involving the phenyl anion was proposed for the formation of benzene in the case of sodium, potassium and calcium benzoates [56]. These reactions are favoured by experimental conditions (presence of water or catalysts) and hence could be of relevance in the analysis of MP mixtures. In fact, benzene is a common pyrolytic marker of PVC and its production from PET pyrolysis may interfere with the quantitation of PVC. Interestingly, thermal degradation products of benzoic acid such as diphenyl [13] and benzophenone [32] have been used as pyrolytic markers for the analysis of PET MPs. Pyrolysis of a mixture of benzoic acid and 1-hexanamine brought about the formation of the *N*-hexylbenzamide, in addition to the obvious volatilisation of benzoic acid and 1-hexanamine (Figure 3.2.1-19a). Benzonitrile could not be revealed. The production of benzonitrile was revealed when benzoic acid was co-pyrolysed with hexan-1,6-diamine (Figure 3.2.1-19b). The *N*-hexylbenzamide was also tentatively identified (Figure 3.2.1-19b). A possible mechanism that explains the formation of the above-mentioned products is the following: the nitrogen of alkylamine reacts with the carbon of carbonyl group of the benzoic acid forming the corresponding alkylamide which is thermally decomposed into the corresponding nitrile derivative (Figure 3.2.1-20). It is long known that nitriles are thermal decomposition products of

amides [57]. Benzonitrile was revealed from the reaction of benzoic acid with hexan-1,6-diamine, but not with 1-hexanamine even though both generated N-hexylamide. A possible explanation is that *N*-hexylbenzamide was volatilised faster than its decomposition occurred, while the less volatile products from hexan-1, 6-diamine (e.g., hexyl-bis-benzamide) remained long enough in the hot zone to undergo thermal degradation. Hexanamine and hexan-1, 6-diamine are pyrolysis products of PA-6,6 (Figure 3.2.1-21a). Concordantly with the results from the analyses of low molecular weight compounds described above, the co-pyrolysis of PET and PA-6,6 yielded benzonitriles and amides as relevant pyrolysis products, not present in the pyrograms of the isolated polymer particles (Figure 3.2.1-21b). Because aromatic compounds are not formed from the pyrolysis of PA, and this latter is the source of nitrogen atoms, it is evident that aromatic compounds with nitrogen-containing functional groups are derived from the interaction between PET and PA. In the case of PA-6,6, pyrolysis products from secondary reactions that were tentatively identified included: benzonitrile, methylbenzonitrile, ethylbenzonitrile, dicyanobenzene, benzamide, cyanobenzoic acid, benzamide, N-hexylbenzamide (Table 3.2.1-6). Benzoic acid derivatives substituted with a nitrile group exhibited mass spectra with an intense peak at *m/z* 130 (4-formylbenzonitrile ion) and *m/z* 102 (benzonitrile ion), thus these ions can be used to verify PET-PA co-presence in the MP mixture (Figure 3.2.1-20). Some of these products were identified by library matching, others could not be assigned, but their GC-MS data are reported in Table 3.2.1-6. Interestingly, benzamide and its N-alkyl series from methyl to hexyl were revealed (mass spectra characterised by base peak at *m/z* 105, molecular ion and loss of alkyl radical) supporting a chain scission mechanism from the longer alkyl chain of the amide precursor. All together these results suggest that a possible route towards the formation of nitriles involves the formation of amides (Figure 3.2.1-20). The nucleophilic attack of amines to the carbonyl group of benzoic/terephthalic acid leading to amides could occur in the vapour phase between low molecular weight pyrolysis products or in the melt between oligomers or polymer chains (e.g., terminal NH_2 group of PA-6,6 and esters of benzoic acids). Py-GC-MS of PET particle physically separated by the particle of PA-6 with a quartz filter produced benzonitrile; benzonitrile and amides were revealed by a similar experiment with PET and PA-6,6. These results demonstrated that secondary products can be observed even when the particles are physically separated. The presence of ε-caprolactam, a typical pyrolysis product of PA-6, in the pyrolyzates of standard PA-6,6 has been reported [34,53], but in our case it could be due to the co-presence of the two polymers in the commercial specimen.

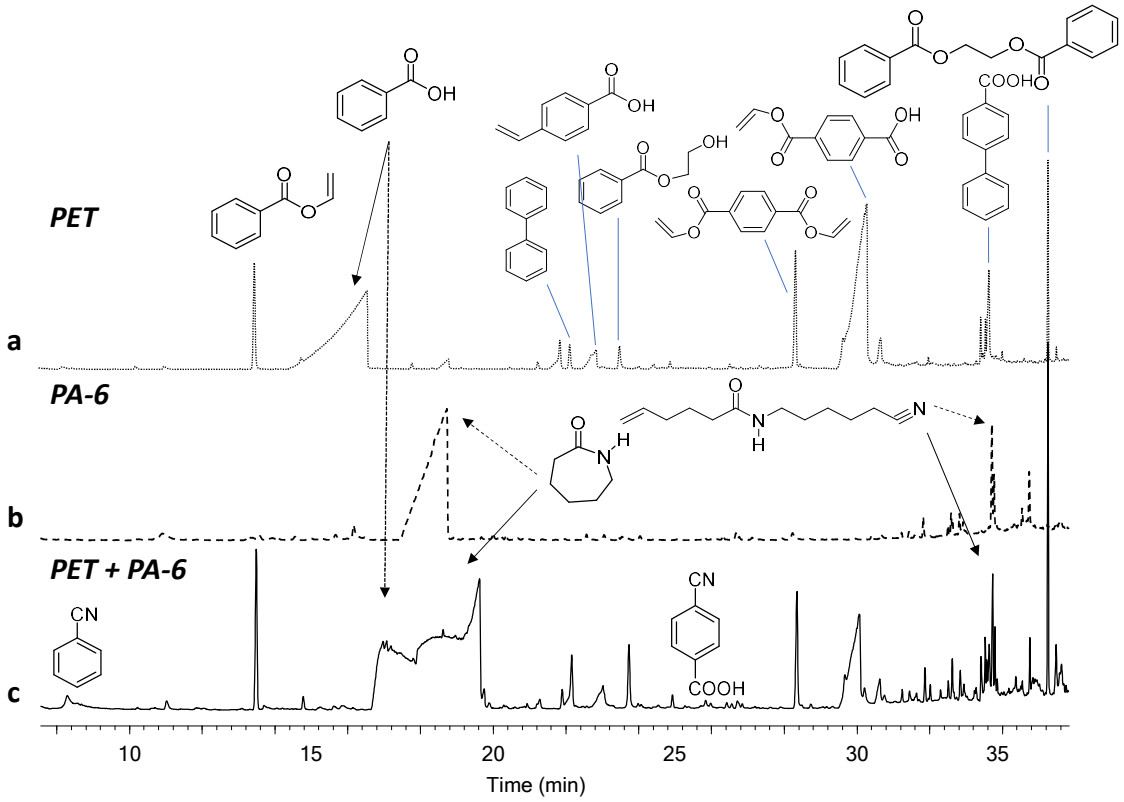

Figure 3.2.1-17. *Pyrograms obtained from Py-GC-MS of particles of (a) PET, (b) PA-6, (c) PET (50 µg) and PA-6 (48 µg) [52].*

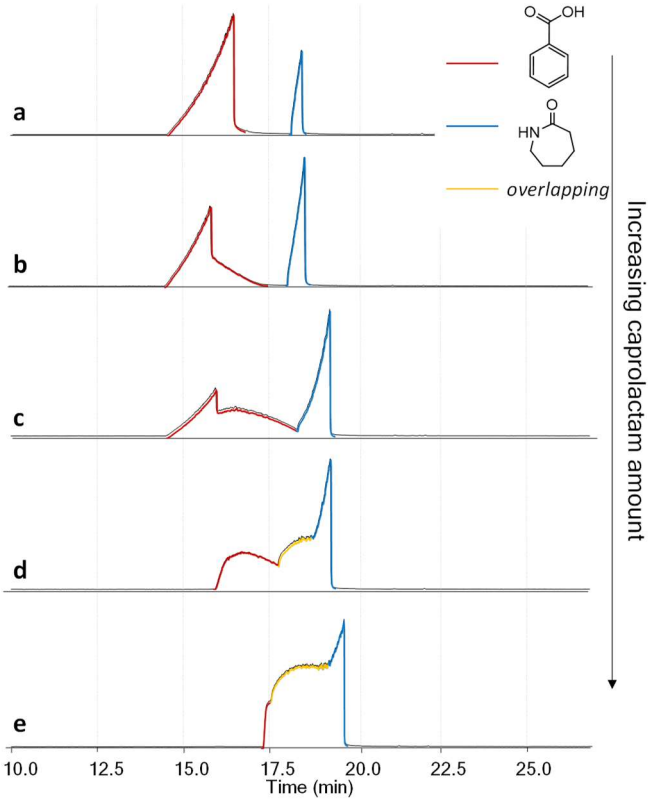

Figure 3.2.1-18. *Pyrograms of 50 ug of benzoic acid with increasing amount of caprolactam: 5 µg (a), 10 µg (b), 25 µg (c), 50 µg (d) and 75 µg (e).*

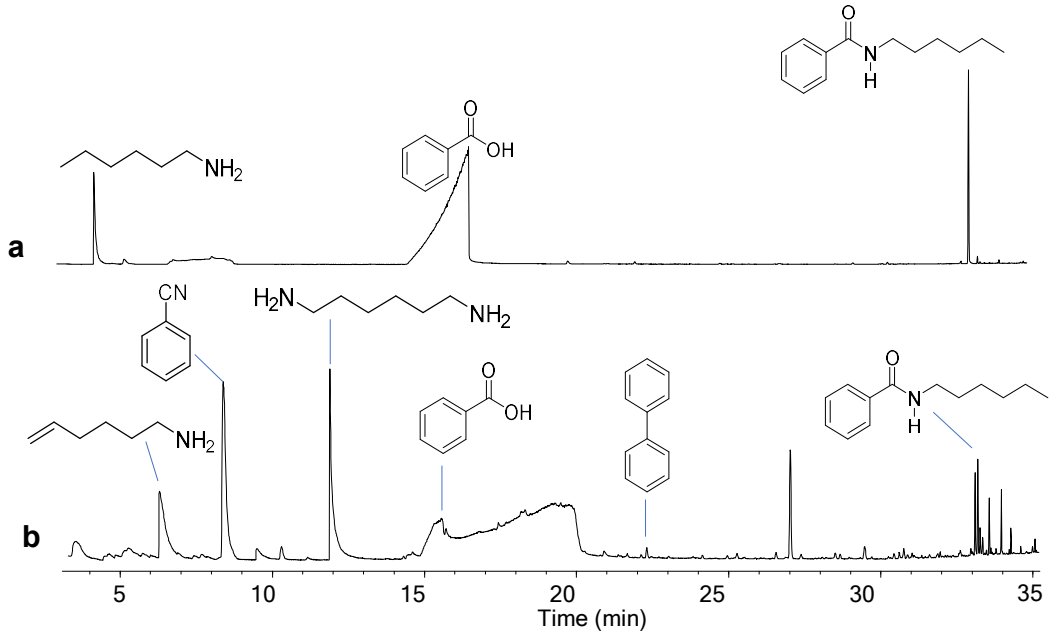

Figure 3.2.1-19. *Pyrograms obtained from Py-GC-MS of benzoic acid with (a) hexan-1-amine and (b) hexane-1,6-diamine [52].*

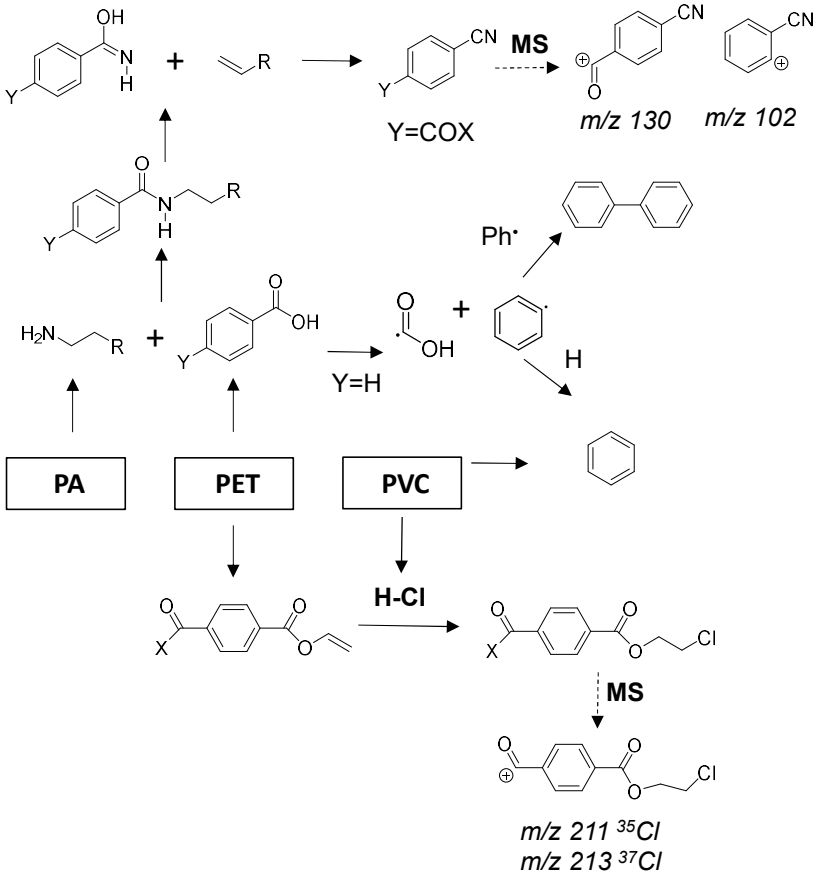

Figure 3.2.1-20. *Scheme summarising the formation of secondary products from the pyrolysis of PET with PA and PVC. The structure and m/z values of relevant ions in the mass spectrum are reported [52].*

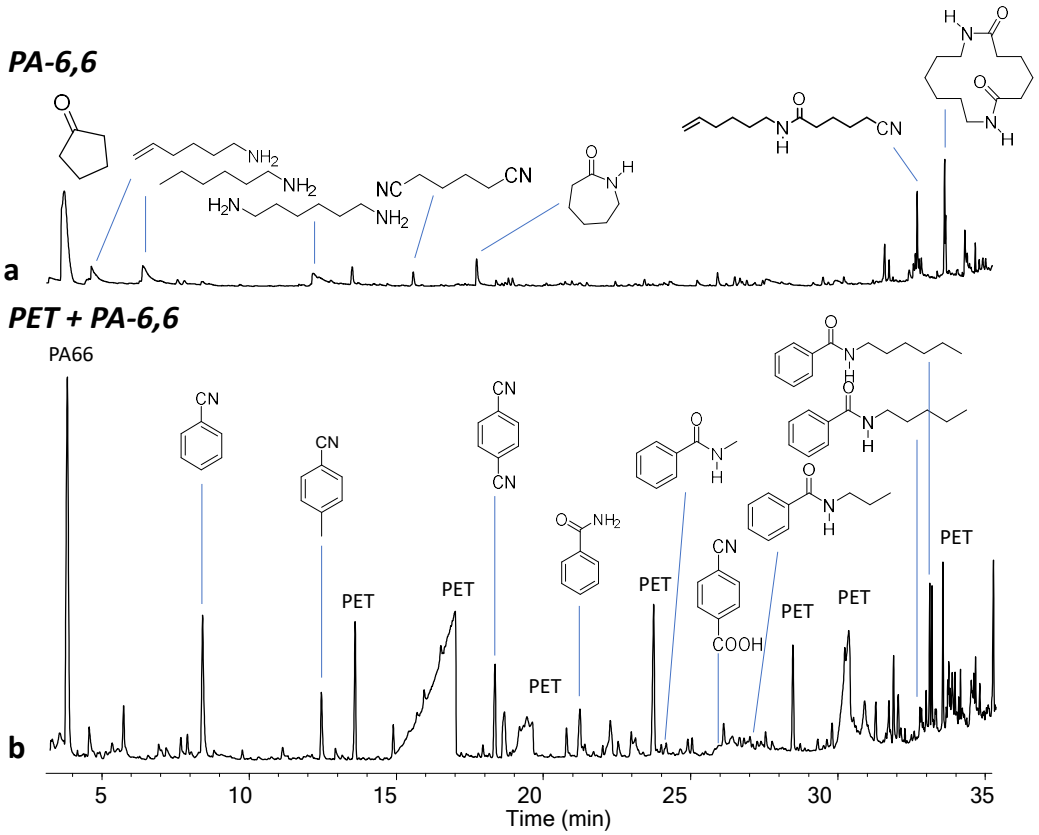

Figure 3.2.1-21. *Pyrograms obtained from Py-GC-MS of particles of (a) PA-6,6, (b) PET (71 µg) and PA-6,6 (63 µg) [52].*

3.2.1.3.4.2. Py-GC-MS of PET with PVC

Co-pyrolysis of PET and PVC particles resulted in the formation of chlorinated derivatives of benzoic and terephthalic acids as secondary pyrolysis products (Figure 3.2.1-22). The identification of some compounds was based on comparison with the mass spectra reported by Kulesza and German (2003) [27] who investigated the co-pyrolysis of PVC and PET. Specifically, the 2-chloroethyl esters of benzoic acid, 4-methylbenzoic acid and 1,4-benzenedicarboxylic acid (Table 3.2.1-6). The 2-chloroethyl ester of 4-acetylbenzoic acid was tentatively identified from the interpretation of the mass spectrum: molecular ion at *m/z* 226 (*m/z* 228 ^{37}Cl isotopic ion) and fragment ions from the loss of methyl radical at *m/z* 211 (*m/z* 213 ^{37}Cl isotopic ion), loss of C_2H_2ClO radical at *m/z* 147, loss of vinyl chloride from the rearrangement with H transfer at *m/z* 164. This compound was reported as a pyrolysis product from Py-GC-MS of 1/1 PVC/PET mixture even though the mass spectrum was not reported [26]. The cluster of chlorine isotopes differing of two relative mass units with the characteristic 100:33 relative abundances in the mass spectrum was fundamental for the assignment of mono-chlorinated species. The chlorinated compounds reported in Figure 3.2.1-22 and Table 3.2.1-6 exhibited mass spectra with at least

one identifiable isotopic cluster of chlorine. The ions at *m/z* 211 and 213 with about 100 and 33 relative abundances represented a typical situation attributed to the ions $C_{10}H_8{}^{35}ClO^+$ and $C_{10}H_8{}^{37}ClO^+$, respectively. The structural unit is the 2-chloroethyl ester of 4'-formyl benzoic acid ion (see Figure 3.2.1-20). The chloroethyl unit can be thought as virtually formed by the addition of HCl evolved by the thermal dehydrochlorination of PVC to the vinyl group of the pyrolysis products of PET (vinyl ester of benzoic acid and terephthalic acid). Benzoyl chloride and chlorobenzoic acid were also revealed, the latter compound in agreement with Czégény et al. (2012) [26]. All these compounds, reported in Table 3.2.1-6, were not detected in the pyrogram of PVC or PET single particles. However, two unknown compounds displaying the ions *m/z* 211 and 213 (100:32 abundance ratio) were observed at RI 1863 and 2980, respectively, in the pyrograms of mixtures (Table 3.2.1-5), PVC/PET (peaks 15 and 20 of Figure 3.2.1-22) and occasionally in the pyrograms of PVC and PET. The origin and structure of these compounds could not be assigned. The possible chlorination of additives like diesters of *o*-phthalic acid cannot be excluded, but difficult to explain as phthalates are generally esters of saturated alcohol without aliphatic double bonds capable to add HCl. Besides, phthalates were not detected in the IR spectra. At this stage of the investigation, the origin of these two compounds remained uncertain and only tentatively attributed to secondary reactions. These two compounds as well as those listed in Table 3.2.1-6 were observed when Py-GC-MS was conducted on the particles of PET and PVC physically separated by a quartz filter indicating that physical contact is not necessary for polymer interaction and secondary reactions may occur in the gas phase. The presence of chlorinated derivatives of benzoic or benzenedicarboxylic acids was not reported in the literature dealing with the analysis of polymer mixtures by THM-TMAH. The use of TMAH, which is quite common in the analysis of MPs, has probably the effect of reducing PET-PVC interactions due to the neutralisation of HCl and the formation of methyl ester in place of vinyl esters.

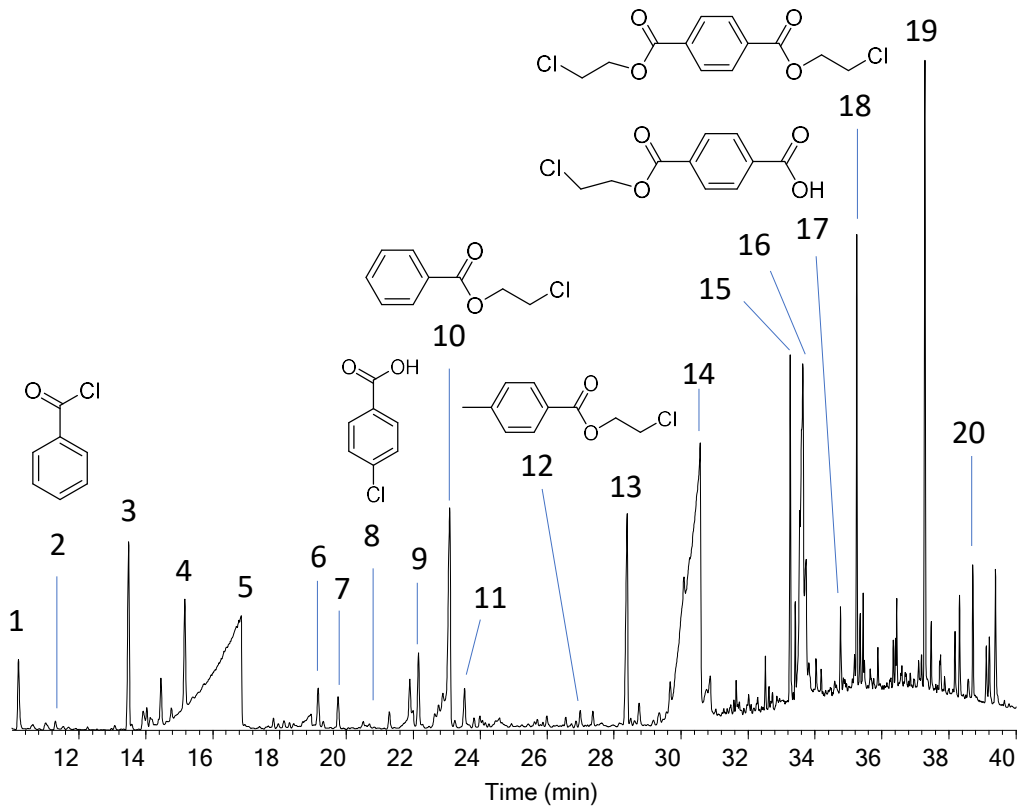

Figure 3.2.1-22. *Pyrogram obtained from Py-GC-MS of PET (121 µg) and PVC (114 µg) 1: indene (PVC); 2: benzoylchloride (PET+PVC); 3: vinylbenzoate (PET); 4: naphthalene (PVC); 5: benzoic acid (PET); 6: 2-methylnaphthalene (PVC); 7: 1-methylnaphthalene (PVC); 8: 4- chlorobenzoic acid (PET+PVC); 9: diphenyl (PET and PVC); 10: 2-chloroethylbenzoate (PET+PVC); 11: 2-hydroxyethylbenzoate (PET); 12: 4-methylbenzoic acid, 2-chloroethylester (PET+PVC); 13: divinylterephthalate (PET); 14: terephthalic acid, monovinylester (PET); 15: unknown (m/z 104, 149?, 175, 211, 213, Table 3.2.1-5); 16: terephthalic acid (PET); 17: diphenylcarboxyilic acid (PET) 1,4-benzenedicarboxylic acid (PET)+terephthalic acid, mono-2-chloroethyl ester (PET+PVC); 18: terephthalic acid, di-2-chloroethyl ester (PET+PVC), overlaps with 1,2-ethandiolbenzoate; 19:2-(benzoyloxy)ethylvinylterephtalate (PET); 20: unknown (m/z 77, 105, 211, 213,Table 3.2.1-5) [52].*

Table 3.2.1-6. *GC-MS data and tentative structural attribution of pyrolysis products derived from polymer interactions between PET and PA or PVC. Rt: retention time (minutes); RI: retention index, RI_{lit}: retention index from PubChem, n.f. not found. m/z: mass to charge ratio of relevant ions, bold base peak, italics molecular ion. ID, identification by MS comparison with library (XX % match), [XX] literature, INT. mass spectrum interpretation [52].*

Compound	Rt	RI	RI_{lit}	*m/z*	Polymers	ID
benzonitrile	8.28	993	937–940	50, 76, 103	PET+PA	97 %
benzylchloride	9.16	1020	978–1479	65, 91, 126, 128	PET+PVC	93 %
benzoyl chloride	11.3	1083	1037–1095	51, 77, 105, 140, 142	PET+PVC	96 %

methylbenzonitrile	12.31	1111	1071	90, 117	PET+PA-6,6	95 %
ethylbenzonitrile	15.82	1208	n.f.	89, 103, 116, 131	PET+PA-6,6	87 %
1,4-benzenedicarbonitrile	18.21	1274	n.f.	50, 64, 101, 128	PET+PA-6,6	95 %
4-chlorobenzoic acid	20.68	1344	1336	111, 139, 141, 156, 158	PET+PVC	91 %
benzamide	21.1	1357	1339–1344	51, 77, 105, 121	PET+PA-6,6	94 %
N-methyl benzamide	22.4	1394	1390–1404	77, 105, 134, 135	PET+PA-6,6	88 %
2-chloroethyl benzoate	23.09	1415	1366–2159	51, 77, 105, 122, 184, 186	PET+PVC	[27]
N-ethylbenzamide	23.85	1438	n.f.	77, 105, 148, 149	PET+PA-6,6	INT.
ethyl 4-cyano benzoate	24.03	1443	n.f.	102, 130, 147, 175	PET+PA-6,6	90 %
4-methylbenzamide	24.76	1465	n.f.	65, 91, 119, 135	PET+PA-6,6	92 %
4-cyanobenzoic acid	25.6	1491	n.f.	102, 130, 147	PET+PA-6,6 PET+PA-6	87 %
N-propylbenzamide	26.89	1529	1526	51, 77, 105, 134, 162, 163	PET+PA-6,6	INT.
4-methyl benzoic acid,2-chloroethyl ester	26.99	1532	n.f.	65, 91, 119, 198, 200	PET+PVC	[27]
3,4-dichlorobenzoic acid	27.21	1538	n.f.	145, 147, 173, 175, 190, 192	PET+PVC	83 %
N-butylbenzamide	30.08	1637	1642	51, 77, 105, 134, 135, 177	PET+PA-6,6	INT.
N-pentylbenzamide	31.92	1743	n.f.	51, 77, 105, 134, 148, 162, 191	PET+PA-6,6	INT.

4-acetyl benzoic acid, 2-chloroethyl ester (#)	32.72	1817	n.f.	147, 164, 211, 213, 226, 228	PET+PVC	[26] INT.
Benzamide derivative	32.96	1844	n.f.	51, 77, 105, 130, 162	PET+PA-6,6	INT.
N-hexylbenzamide	33.04	1853	n.f.	77, 105, 135, 148, 162, 176, 205	PET+PA-6,6	92 %
1,4-benzenedicarboxylic acid, 2-chloroethyl ester, ethyl ester (§)	33.59	1922	n.f.	149, 166, 194, 211, 213, 256, 258	PET+PVC	[27]
1,4-benzenedicarboxylic acid, mono-2-chloroethyl ester (§)	33.64	1929	n.f.	65, 121, 149, 166, 228, 230	PET+PVC	[27]
unknown	34.52	2066	n.f.	102, 130	PET+PA-6,6	
unknown	35.01	2156	n.f.	102, 130	PET+PA-6,6	
1,4-benzenedicarboxylic acid, di-2-chloroethyl ester (*)	35.25	2202	n.f.	149, 166, 211, 213, 290, 292, 294	PET+PVC	[27]

3.2.1.4. Conclusions

This study evidenced that secondary pyrolysis products can be produced from Py-GC-MS of mixtures of plastic particles. PET resulted the most critical polymer as benzoic acid and its derivatives, such as vinyl esters, can be involved in various reactions leading to new products. Nitrogen-containing aromatic compounds, such as nitriles and amides, are indicative of interactions between PET and polyamides, in particular PA66. Nitriles are probably generated by the dehydration of amides in turn generated by reactions with alkyl(di)amines and benzoic acid derivatives. The occurrence of PET-PA66 interactions can be monitored in the MS-pyrograms by selecting the ions at *m/z* 102 and 130. Chlorinated pyrolysis products of PET are formed from the addition of HCl to the double bond of the vinyl ester of benzoic and terephthalic

acids. The occurrence of PET-PVC interactions can be monitored in the MS-pyrograms by selecting the ions at *m/z* 211 and 213. The results of this study did not provide firm evidence that these secondary reactions were responsible of the deviations observed in quantitative analysis, however, they highlighted the role they may play in method optimisation. It is expected that two main procedures adopted in the determination of microplastic by analytical pyrolysis may reduce the extent of secondary reactions: the use of TMAH (e.g., neutralisation of HCl, methylation of benzoic acid) and dilution with a solid material. While this latter method has been proved to be effective in reducing secondary reactions in recent publications, polymer interactions in the presence of TMAH is a topic worth of consideration in future studies.

References

[1] A.A. Horton, A. Walton, D.J. Spurgeon, E. Lahive, C. Svendsen, Microplastics in freshwater and terrestrial environments: Evaluating the current understanding to identify the knowledge gaps and future research priorities, Science of The Total Environment. 586 (2017) 127–141. https://doi.org/10.1016/j.scitotenv.2017.01.190.

[2] N.B. Hartmann, T. Hüffer, R.C. Thompson, M. Hassellöv, A. Verschoor, A.E. Daugaard, S. Rist, T. Karlsson, N. Brennholt, M. Cole, M.P. Herrling, M.C. Hess, N.P. Ivleva, A.L. Lusher, M. Wagner, Are we speaking the same language? Recommendations for a definition and categorization framework for plastic debris, Environ. Sci. Technol. 53 (2019) 1039–1047. https://doi.org/10.1021/acs.est.8b05297.

[3] Y.K. Müller, T. Wernicke, M. Pittroff, C.S. Witzig, F.R. Storck, J. Klinger, N. Zumbülte, Microplastic analysis – Are we measuring the same? Results on the first global comparative study for microplastic analysis in a water sample, Anal Bioanal Chem. 412 (2020) 555–560. https://doi.org/10.1007/s00216-019-02311-1.

[4] R. Peñalver, N. Arroyo-Manzanares, I. López-García, M. Hernández-Córdoba, An overview of microplastics characterization by thermal analysis, Chemosphere. 242 (2020) 125170. https://doi.org/10.1016/j.chemosphere.2019.125170.

[5] N. Yakovenko, A. Carvalho, A. ter Halle, Emerging use thermo-analytical method coupled with mass spectrometry for the quantification of micro(nano)plastics in environmental samples, TrAC Trends in Analytical Chemistry. 131 (2020) 115979. https://doi.org/10.1016/j.trac.2020.115979.

[6] J. La Nasa, G. Biale, D. Fabbri, F. Modugno, A review on challenges and developments of analytical pyrolysis and other thermoanalytical techniques for the quali-quantitative determination of microplastics, Journal of Analytical and Applied Pyrolysis. 149 (2020) 104841. https://doi.org/10.1016/j.jaap.2020.104841.

[7] Y. Picó, D. Barceló, Pyrolysis gas chromatography-mass spectrometry in environmental analysis: Focus on organic matter and microplastics, TrAC Trends in Analytical Chemistry. 130 (2020) 115964. https://doi.org/10.1016/j.trac.2020.115964.

[8] A. Gomiero, K.B. Øysæd, L. Palmas, G. Skogerbø, Application of GCMS-pyrolysis to estimate the levels of microplastics in a drinking water supply system, Journal of Hazardous Materials. 416 (2021) 125708. https://doi.org/10.1016/j.jhazmat.2021.125708.

[9] C. Dibke, M. Fischer, B.M. Scholz-Böttcher, Microplastic mass concentrations and distribution in German bight waters by pyrolysis–gas chromatography–mass spectrometry/thermochemolysis reveal potential impact of marine coatings: Do ships leave skid marks?, Environ. Sci. Technol. 55 (2021) 2285–2295. https://doi.org/10.1021/acs.est.0c04522.

[10] M. Fischer, I. Goßmann, B.M. Scholz-Böttcher, Fleur de Sel – An interregional monitor for microplastics mass load and composition in European coastal waters?, Journal of Analytical and Applied Pyrolysis. (2019). https://10.1016/j.jaap.2019.104711 (accessed September 9, 2021).

[11] E.D. Okoffo, F. Ribeiro, J.W. O'Brien, S. O'Brien, B.J. Tscharke, M. Gallen, S. Samanipour, J.F. Mueller, K.V. Thomas, Identification and quantification of selected plastics in biosolids by pressurized liquid extraction combined with double-shot pyrolysis gas chromatography–mass spectrometry, Science of The Total Environment. 715 (2020) 136924. https://doi.org/10.1016/j.scitotenv.2020.136924.

[12] A. Gomiero, K.B. Øysæd, T. Agustsson, N. van Hoytema, T. van Thiel, F. Grati, First record of characterization, concentration and distribution of microplastics in coastal sediments of an urban fjord in south west Norway using a thermal degradation method, Chemosphere. 227 (2019) 705–714. https://doi.org/10.1016/j.chemosphere.2019.04.096.

[13] F. Ribeiro, E.D. Okoffo, J.W. O'Brien, S. Fraissinet-Tachet, S. O'Brien, M. Gallen, S. Samanipour, S. Kaserzon, J.F. Mueller, T. Galloway, K.V. Thomas, Quantitative analysis of selected plastics in high-commercial-value Australian seafood by pyrolysis gas chromatography mass spectrometry, Environ. Sci. Technol. 54 (2020) 9408–9417. https://doi.org/10.1021/acs.est.0c02337.

[14] M. Fischer, B.M. Scholz-Böttcher, Microplastics analysis in environmental samples – Recent pyrolysis-gas chromatography-mass spectrometry method improvements to increase the reliability of mass-related data, Anal. Methods. 11 (2019) 2489–2497. https://doi.org/10.1039/C9AY00600A.

[15] M. Fischer, B.M. Scholz-Böttcher, Simultaneous trace identification and quantification of common types of microplastics in environmental samples by pyrolysis-gas chromatography–mass spectrometry, Environ. Sci. Technol. 51 (2017) 5052–5060. https://doi.org/10.1021/acs.est.6b06362.

[16] G. Dierkes, T. Lauschke, S. Becher, H. Schumacher, C. Földi, T. Ternes, Quantification of microplastics in environmental samples via pressurized liquid extraction and pyrolysis-gas chromatography, Anal Bioanal Chem. 411 (2019) 6959–6968. https://doi.org/10.1007/s00216-019-02066-9.

[17] S. Primpke, M. Fischer, C. Lorenz, G. Gerdts, B.M. Scholz-Böttcher, Comparison of pyrolysis gas chromatography/mass spectrometry and hyperspectral FTIR imaging spectroscopy for the analysis of microplastics, Anal Bioanal Chem. 412 (2020) 8283–8298. https://doi.org/10.1007/s00216-020-02979-w.

[18] R. Becker, K. Altmann, T. Sommerfeld, U. Braun, Quantification of microplastics in a freshwater suspended organic matter using different thermoanalytical methods – Outcome of an interlaboratory comparison, Journal of Analytical and Applied Pyrolysis. 148 (2020) 104829. https://doi.org/10.1016/j.jaap.2020.104829.

[19] Z. Steinmetz, A. Kintzi, K. Muñoz, G.E. Schaumann, A simple method for the selective quantification of polyethylene, polypropylene, and polystyrene plastic debris in soil by pyrolysis-gas chromatography/mass spectrometry, Journal of Analytical and Applied Pyrolysis. 147 (2020) 104803. https://doi.org/10.1016/j.jaap.2020.104803.

[20] M. Matsueda, M. Mattonai, I. Iwai, A. Watanabe, N. Teramae, W. Robberson, H. Ohtani, Y.-M. Kim, C. Watanabe, Preparation and test of a reference mixture of eleven polymers with deactivated inorganic diluent for microplastics analysis by pyrolysis-GC–MS, Journal of Analytical and Applied Pyrolysis. 154 (2021) 104993. https://doi.org/10.1016/j.jaap.2020.104993.

[21] S. Kumagai, T. Yoshioka, Latest trends in pyrolysis gas chromatography for analytical and applied pyrolysis of plastics, Analytical Sciences. advpub (2020). https://doi.org/10.2116/analsci.20SAR04.

[22] M. Blazsó, B. Zelei, E. Jakab, Thermal decomposition of low-density polyethylene in the presence of chlorine-containing polymers, Journal of Analytical and Applied Pyrolysis. 35 (1995) 221–235. https://doi.org/10.1016/0165-2370(95)00910-7.

[23] Z. Czégény, E. Jakab, M. Blazsó, Thermal decomposition of polymer mixtures containing poly(vinyl chloride), Macromolecular Materials and Engineering. 287 (2002) 277–284. https://doi.org/10.1002/1439-2054(20020401)287:4<277::AID-MAME277>3.0.CO;2-#.

[24] Z. Czégény, M. Blazsó, Thermal decomposition of polyamides in the presence of poly(vinyl chloride), Journal of Analytical and Applied Pyrolysis. 58–59 (2001) 95–104. https://doi.org/10.1016/S0165-2370(00)00152-2.

[25] T. Bhaskar, Md.A. Uddin, K. Murai, J. Kaneko, K. Hamano, T. Kusaba, A. Muto, Y. Sakata, Comparison of thermal degradation products from real municipal waste plastic and model mixed plastics, Journal of Analytical and Applied Pyrolysis. 70 (2003) 579–587. https://doi.org/10.1016/S0165-2370(03)00027-5.

[26] Zs. Czégény, E. Jakab, M. Blazsó, T. Bhaskar, Y. Sakata, Thermal decomposition of polymer mixtures of PVC, PET and ABS containing brominated flame retardant: Formation of chlorinated and brominated organic compounds, Journal of Analytical and Applied Pyrolysis. 96 (2012) 69–77. https://doi.org/10.1016/j.jaap.2012.03.006.

[27] K. Kulesza, K. German, Chlorinated pyrolysis products of co-pyrolysis of poly(vinyl chloride) and poly(ethylene terephthalate), Journal of Analytical and Applied Pyrolysis. 67 (2003) 123–134. https://doi.org/10.1016/S0165-2370(02)00057-8.

[28] F. Kubatovics, M. Blazsó, Thermal decomposition of polyamide-6 in the presence of PVC, Macromolecular Chemistry and Physics. 201 (2000) 349–354. https://doi.org/10.1002/(SICI)1521-3935(20000201)201:3<349::AID-MACP349>3.0.CO;2-Y.

[29] P.T. Williams, E.A. Williams, Interaction of plastics in mixed-plastics pyrolysis, Energy Fuels. 13 (1999) 188–196. https://doi.org/10.1021/ef980163x.

[30] C. Muhammad, J.A. Onwudili, P.T. Williams, Thermal degradation of real-world waste plastics and simulated mixed plastics in a two-stage pyrolysis–catalysis reactor for fuel production, Energy Fuels. 29 (2015) 2601–2609. https://doi.org/10.1021/ef502749h.

[31] M. Predel, W. Kaminsky, Pyrolysis of mixed polyolefins in a fluidised-bed reactor and on a pyro-GC/MS to yield aliphatic waxes, Polymer Degradation and Stability. 70 (2000) 373–385. https://doi.org/10.1016/S0141-3910(00)00131-2.

[32] T. Ishimura, I. Iwai, K. Matsui, M. Mattonai, A. Watanabe, W. Robberson, A.-M. Cook, H.L. Allen, W. Pipkin, N. Teramae, H. Ohtani, C. Watanabe, Qualitative and quantitative analysis of mixtures of microplastics in the presence of calcium carbonate by pyrolysis-GC/MS, Journal of Analytical and Applied Pyrolysis. 157 (2021) 105188. https://doi.org/10.1016/j.jaap.2021.105188.

[33] M. Reichenbächer, J.W. Einax, Challenges in analytical quality assurance, Springer Science & Business Media, 2011.

[34] S. Tsuge, H. Ohtani, C. Watanabe, Pyrolysis–GC/MS data book of synthetic polymers - Pyrograms, thermograms and MS of pyrolyzates, Elsevier, 2012.

[35] S.C. Moldoveanu, Analytical pyrolysis of synthetic organic polymers, Elsevier, Amsterdam Oxford, 2005.

[36] Supriyanto, P. Ylitervo, T. Richards, Gaseous products from primary reactions of fast plastic pyrolysis, Journal of Analytical and Applied Pyrolysis. 158 (2021) 105248. https://doi.org/10.1016/j.jaap.2021.105248.

[37] N. Dimitrov, L. Kratofil Krehula, A. Ptiček Siročić, Z. Hrnjak-Murgić, Analysis of recycled PET bottles products by pyrolysis-gas chromatography, Polymer Degradation and Stability. 98 (2013) 972–979. https://doi.org/10.1016/j.polymdegradstab.2013.02.013.

[38] A. Brems, J. Baeyens, C. Vandecasteele, R. Dewil, Polymeric cracking of waste polyethylene terephthalate to chemicals and energy, Journal of the Air & Waste Management Association. 61 (2011) 721–731. https://doi.org/10.3155/1047-3289.61.7.721.

[39] T.M. Kruse, H.-W. Wong, L.J. Broadbelt, Mechanistic modeling of polymer pyrolysis: Polypropylene, Macromolecules. 36 (2003) 9594–9607. https://doi.org/10.1021/ma030322y.

[40] J. Huang, X. Li, H. Meng, H. Tong, X. Cai, J. Liu, Studies on pyrolysis mechanisms of syndiotactic polystyrene using DFT method, Chemical Physics Letters. 747 (2020) 137334. https://doi.org/10.1016/j.cplett.2020.137334.

[41] J. Zhou, G. Liu, S. Wang, H. Zhang, F. Xu, TG-FTIR and Py-GC/MS study of the pyrolysis mechanism and composition of volatiles from flash pyrolysis of PVC, Journal of the Energy Institute. 93 (2020) 2362–2370. https://doi.org/10.1016/j.joei.2020.07.009.

[42] M. Herrera, G. Matuschek, A. Kettrup, Main products and kinetics of the thermal degradation of polyamides, Chemosphere. 42 (2001) 601–607. https://doi.org/10.1016/S0045-6535(00)00233-2.

[43] M.R. Jung, F.D. Horgen, S.V. Orski, V. Rodriguez C., K.L. Beers, G.H. Balazs, T.T. Jones, T.M. Work, K.C. Brignac, S.-J. Royer, K.D. Hyrenbach, B.A. Jensen, J.M. Lynch, Validation of ATR FT-IR to identify polymers of plastic marine debris, including those ingested by marine organisms, Marine Pollution Bulletin. 127 (2018) 704–716. https://doi.org/10.1016/j.marpolbul.2017.12.061.

[44] M. Beltran, A. Marcilla, Fourier transform infrared spectroscopy applied to the study of PVC decomposition, 33 (1997) 1135–1142. https://doi.org/10.1016/S0014-3057(97)00001-3.

[45] R. Chércoles Asensio, M. San Andrés Moya, J.M. de la Roja, M. Gómez, Analytical characterization of polymers used in conservation and restoration by ATR-FTIR spectroscopy, Anal Bioanal Chem. 395 (2009) 2081–2096. https://doi.org/10.1007/s00216-009-3201-2.

[46] G.A.L. Verleye, N.P.G. Roeges, M.O.D. Moor, Easy identification of plastics and rubbers, iSmithers Rapra Publishing, 2001.

[47] I. Noda, A.E. Dowrey, J.L. Haynes, C. Marcott, Group frequency assignments for major infrared bands observed in common synthetic polymers, in: J.E. Mark (Ed.), Physical Properties of Polymers Handbook, Springer, New York, NY, 2007: pp. 395–406. https://doi.org/10.1007/978-0-387-69002-5_22.

[48] K. Nishikida, J. Coates, Infrared and Raman analysis of polymers, in: H. Lobo, J. Bonilla (Eds.), Handbook of Plastics Analysis, CRC Press, 2003. https://doi.org/10.1201/9780203911983.ch7.

[49] G. Rotter, H. Ishida, FTIR separation of nylon-6 chain conformations: Clarification of the mesomorphous and γ-crystalline phases, Journal of Polymer Science Part B: Polymer Physics. 30 (1992) 489–495. https://doi.org/10.1002/polb.1992.090300508.

[50] M. Fischer, B.M. Scholz-Böttcher, Simultaneous Trace Identification and Quantification of Common Types of Microplastics in Environmental Samples by Pyrolysis-Gas Chromatography–Mass Spectrometry, Environ. Sci. Technol. 51 (2017) 5052–5060. https://doi.org/10.1021/acs.est.6b06362.

[51] I. Goßmann, M. Halbach, B.M. Scholz-Böttcher, Car and truck tire wear particles in complex environmental samples – A quantitative comparison with "traditional" microplastic polymer mass loads, Science of The Total Environment. 773 (2021) 145667. https://doi.org/10.1016/j.scitotenv.2021.145667.

[52] I. Coralli, V. Giorgi, I. Vassura, A.G. Rombolà, D. Fabbri, Secondary reactions in the analysis of microplastics by analytical pyrolysis, Journal of Analytical and Applied Pyrolysis. 161 (2022) 105377. https://doi.org/10.1016/j.jaap.2021.105377.

[53] H. Ohtani, T. Nagaya, Y. Sugimura, S. Tsuge, Studies on thermal degradation of aliphatic polyamides by pyrolysis-glass capillary chromatography, Journal of Analytical and Applied Pyrolysis. 4 (1982) 117–131. https://doi.org/10.1016/0165-2370(82)80003-X.

[54] S.V. Levchik, E.D. Weil, M. Lewin, Thermal decomposition of aliphatic nylons, Polymer International. 48 (1999) 532–557. https://doi.org/10.1002/(SICI)1097-0126(199907)48:7<532::AID-PI214>3.0.CO;2-R.

[55] K. Winter, D. Barton, The thermal decomposition of benzoic acid, Can. J. Chem. 48 (1970) 3797–3801. https://doi.org/10.1139/v70-641.

[56] R. Dabestani, P.F. Britt, A.C. Buchanan, Pyrolysis of aromatic carboxylic acid salts: Does decarboxylation play a role in cross-linking reactions?, Energy Fuels. 19 (2005) 365–373. https://doi.org/10.1021/ef0400722.

[57] D. Davidson, M. Karten, The pyrolysis of amides, J. Am. Chem. Soc. 78 (1956) 1066–1068. https://doi.org/10.1021/ja01586a051.

3.2.2. Determination of polyurethanes within microplastics in complex environmental samples by analytical pyrolysis

Selected for forefront paper on Analytical and Bioanalytical Chemistry (2023).

3.2.2.1. Introduction

Polyurethanes (PURs) consist of a wide group of polymers defined by the presence of the urethane bond. Depending on the required polymer type, diisocyanates and polyols are differently coupled during the synthesis, resulting in a manifold number of possible PUR structures, forms and properties. The diisocyanates used in PUR synthesis can be classified as aliphatic or aromatic. For the most widely used PURs, starting molecules are limited to a small number of monomers for both group. Diisocyanates affect the reactivity and curing properties of PURs: the aliphatic ones are mostly employed in applications where transparency and colour are highly desired, e.g., coatings. Aromatic diisocyanates are part of the majority of foams and elastomers [1–3]. The other reactants, the polyols, can be classified in polyethers, polyesters, acrylics, polycarbonate, triols, etc. Many molecules can be included in each category; therefore, a huge number of compounds can be used as polyol. Molecular weights, functionalities and molecular structures of polyol chains are important parameters in formulations, defining physical properties such as the flexibility [1]. According to Plastic Europe, the European demand of PUR was about 8 % of the whole plastic demand in 2020. It was on the fifth position after polyethylene, polypropylene, polyvinylchloride and polyethylene terephthalate (PE, PP, PVC and PET, respectively) which mainly represent packaging, buildings and synthetic fibres [4]. The compositional versatility of PURs results in their wide range of applications. Foams (flexible and rigid) cover more than 60 % of the PUR produced in Europe, Middle East and Africa (EMEA) in 2017, followed by coating (14 %), elastomers (8 %), adhesives and sealants (6 %) and binders (4 %) [5].

PURs are basically present in every aspect of our everyday life; therefore, it is easy to understand why they are included among the commonly investigated polymers in the analysis of environmental microplastics (MPs). Figure 3.2.2-1 intends to summarise the complexity of this polymer class depending on the chemicals that constitute the structure and the fields of application. In the analysis of MPs, pyrolysis gas-chromatography-mass spectrometry (Py-GC-MS) is gaining interest and an ever-increasing number of studies on environmental MPs is published. Many of these are focused on polymers which derive from packaging or disposable items, such as PE, PP, PET and polystyrene (PS) [6–12]. Nowadays, the investigation and

quantification of MPs in environmental matrices is already extended to many other polymers [13,14]. Moreover, mass-related results obtained by thermal methods need to be extended from single pure polymers (used for the quantification) to clusters containing same basic polymers (in real samples). Each cluster includes, not only the respective pure polymer, but also its copolymers, polymer-containing formulations and even related polymers that release corresponding, characteristic indicator ion(s) during pyrolysis [15–17]. PURs are not always considered in the analysis of environmental MPs. One possible reason of this exclusion is the complexity of the analytical investigation. Spectroscopical methods, e.g., FTIR, focus the shared urethane bond signal for characterization, which is often clustered with other polymers due to overlaps in complex mixtures [17,18]. The analysis of such a heterogeneous polymer class by thermal methods, e.g., Py-GC-MS, is further challenging due to the lack of a unique degradation product that allows identification and quantification of all PURs at once. Moreover, analytical difficulties have been encountered in PUR identification and quantification by Py-GC-MS. One of the main pyrolytic indicators of PUR is the diisocyanate involved in the urethane bond. Matsueda et al. (2021) noticed that the diisocyanate can be easily hydrolysed to a diamine depending on the matrix [19]. The formation of isomers of amine-diisocyanate was noticed in the analysis of PUR foams and paintings by La Nasa et al. (2018) [20]. The formation of new or different peaks leads to difficulties in the identification of PUR, but also to errors in its quantification.

Although the analysis of PUR-MPs is challenging, the assessment of relevance, sources and fate of PURs in the environment is of great importance to understand their contribution to global MP pollution. The main aim of this study is to increase the knowledge of this relevant but diverse polymer class, to get analytically hold of its environmental occurrences as microparticles. This project intended to provide comprehensive information about different commonly used PURs under defined Py-GC-MS conditions, unreactive and under methylating conditions with tetramethylammonium hydroxide (TMAH). The PURs were compared with respect to their thermal fragmentation behaviour. The aim was to clarify whether (i) it is possible to make a reliable statement on the PUR content in environmental samples based on a few, characteristic thermal decomposition products and (ii) which restrictions are required in this context. The superordinate goal was also to integrate a reliable analysis of PURs into an already existing Py-GC-MS method for the simultaneous analysis of plastics. Finally, the information gathered from Py-GC-MS of model PURs was applied to evaluate MP contamination by PUR and other polymers in a urban environment close to an industrial area.

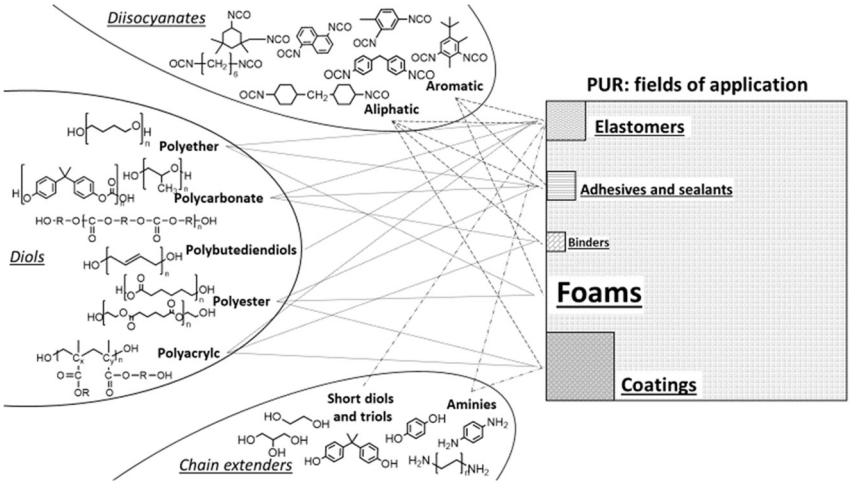

Figure 3.2.2-1. *Combinations of monomers (diisocyanates, diols and chain extender) for the formulation of different PUR types. Area of the squares of each field of application reflects its relative proportion of production.*

3.2.2.2. Experimental

3.2.2.2.1. PUR samples

Four standard MDI-PURs varying in chemical composition (named as MDI-PUR_A, MDI-PUR_B, MDI-PUR_C, MDI-PUR_D, Table 3.2.2-1 and Figure 3.2.2-2) were kindly provided by Frontier Lab (Japan) and GEBA GmbH (Germany), whereas a commercial TDI-PUR was selected among items of daily use. Particles of each polymer were prepared by using a scalpel blade and they were directly inserted into the pyrolysis cups (Eco-Cup LF, Frontier Lab). Particles were weighted using a Cubis Ultramicro balance (MSE2.7S-000-DM, Sartorius, Germany) with a readability 0.0001 mg and repeatability 0.00025 mg. The particles were placed into the cups and covered by a glass fiber filter (1 µm pore size, Ø 6 mm punched from Ø 4.7 cm Whatman, pre-treated at 400 °C for 4 h) in order to avoid their loss during sample preparation and analysis. Polymers were individually analysed to understand their respective thermal degradation behaviour by direct pyrolysis and thermochemolytic conditions. Analyses with and without TMAH were also performed by adding MDI- and TDI-PUR particles (≈ 25 µg) as well as PET (≈ 10 µg) to 10 mg of a representative solid matrix (coastal sediment fully processed for MP analysis: density separation and enzymatic digestion, according to Fischer and Scholz-Böttcher, 2019 [21]) (exact weights in Table 3.2.2-7). The sediment matrix was finely grained in an agate ball mill to guarantee a high degree of homogeneity. Accordingly, identical matrix background during the respective pyrolysis experiments was ensured. Additionally, quantification performance of the different PURs was evaluated by internal standardization and calibrations.

Table 3.2.2-1. *Standard MDI-PURs with description and main properties or application extracted from related data sheets. A, B, C were kindly provided by Frontier Lab (Japan) and D was kindly provided by Geba GmbH (Germany) [22].*

Standard polymer	Abbreviation	Description	Characteristics or applications
E359	A	-	-
Elastollan® 590 A	B	Thermoplastic polyester polyurethane	Tyres and inner tubes, sports shoes
Elastollan® C85A10	C	Thermoplastic polyester polyurethane elastomer	Outstanding mechanical properties Very good damping behaviour Good rebound Very good wear resistance
Desmovit® DP LFC 3379	D	Thermoplastic polyester polyurethane	Electrical and electronical

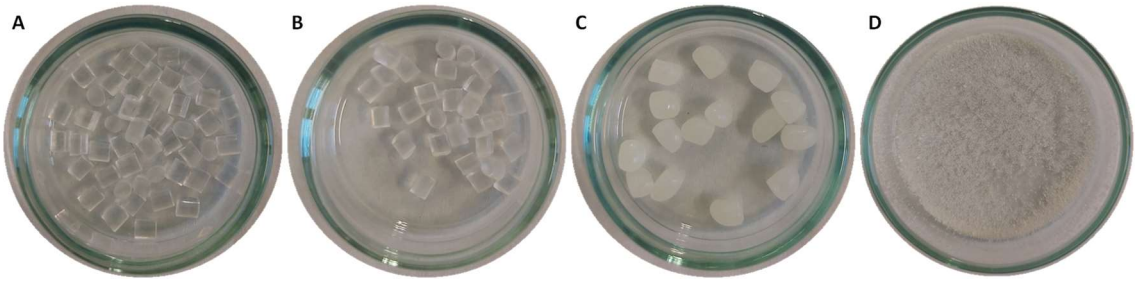

Figure 3.2.2-2. *Particle appearance of standard MDI-PURs before the preparation for the analysis by Py-GC-MS [22].*

3.2.2.2.2. Py-GC-MS and thermochemolysis

Analyses were performed using a multi-shot pyrolyzer (EGA/PY-3030D Frontier Lab) interfaced to a GC-MS system (6890 N and MSD 5973 Agilent Technology). Each sample was spiked with two solutions of internal standards (IS): 20 µL of 20 µg mL^{-1} TOHA, 20 µg mL^{-1}, cholanic acid 40 µg mL^{-1}, in *n*-hexane, and 20 µL of deuterated polystyrene (d-PS), 125 µg mL^{-1} in DCM, were added directly into each pyrolysis cup [21] (where TOHA = 9-tetradecyl-1,2,3,4,5,6,7,8-octahydro anthracene, DCM = dichloromethane). When experiments required thermochemolysis conditions, 20 µL of TMAH (25 % in methanol, Sigma Aldrich) were also added into pyrolysis cups. After solvent evaporation (both with and without TMAH), an auto-shot sampler (AS-1020E, Frontier Lab) was charged with the sample cups, which automatically fell into the pyrolysis chamber one at time.

Table 3.2.2-2. *Instrumental conditions for Py-GC-MS analyses.*

Pyrolyzer	**Multi-Shot Pyrolyzer (EGA/PY-3030D) - Frontier Lab**	
	Furnace temperature	590 °C
	Interface temperature	230 °C
Gas chromatograph	**Agilent 6890 N**	
	Pre-column	Trajan 064062, 3 m, 0.25 mm ID, VSPD tubing
	Column	DB-5MS-column Agilent J&W, 30 m, 0.25 mm ID, 0.25µm film
	Carrier gas	He
	Column flow	1.2 mL min^{-1}
	Split	1:12.5
	Injector	300 °C
Oven programmed temperature	Initial temperature	35 °C
	Temperature hold time	2 min
	Temperature rate	4 °C min^{-1}
	Maximum temperature	310 °C
	Temperature hold time	60 min
Mass spectrometer	**Agilent MSD 5973**	
	MS source temperature	230 °C
	MS quad temperature	150 °C
	Mass scan	50 – 550 *m/z*
	Scan rate	2.91 scan s^{-1}
	Ionization energy	70 eV

3.2.2.2.3. Statistics

Linear regression models were elaborated for four chemically different MDI-PURs, with the aim to understand if significant differences occurred in their calibrations. The slopes of the obtained regression curves were submitted to the one-way ANOVA to test their parallelism, with a significance level $\alpha = 0.05$.

3.2.2.2.4. Sampling campaign

To prevent any secondary contamination during sampling, only plastic free and pre-cleaned (pre-washed with pre-filtered ethanol, 0.3 µm pore size) equipment was used, such as glass containers, aluminium foil, wooden toothpicks, stainless steel spoons and spatulas. No synthetic cloth or face mask was worn during sampling. Immediately after sampling, the samples were stored in glass ware, protected with aluminium foil and transported to the laboratory. The

sampling took place in the mid-sized city of Oldenburg (Germany), in November 2021. Five road dust (RD) samples were collected at public drain covers and sampling started from the North, continuing contra clockwise around the plant (Figure 3.2.2-3, black arrows: RD from 1 to 5). It was not possible to sample on the east side of the plant because of the lack of public drains for the presence of the railway (orange line in Figure 3.2.2-3). Spider webs (SW) were sampled at covered places at bus stops (under the protecting roof) or at a pylon of the railway (Figure 3.2.2-3, white arrows: SW from 1 to 3). Only three suitable sampling points were found close to the plant and a transect was drawn in the southern side moving from West to East (white dotted line in Figure 3.2.2-3). In each sampling point (SW-1 – 3) one single spider web was collected by rolling it un in a toothpick. The sampling area was located at about 4 km from the one of a previous study by Goßmann et al. 2022, where road dusts and spiderwebs were analysed as well [16]. This latter paper is going to be used as a reference for a more comprehensible discussion of the results of the present study.

Detailed information about each sampling point is summarised in Table 3.2.2-3. Road dust collection was bounded to the presence of public drains. Anyway, many sampling points were present to choose from. RD-1 was selected because this area was characterised by trucks transit (Figure 3.2.2-4, RD-1). RD-2 and RD-3 were both on the west side of the plant, but they were located in two different environments: RD-2 was located in a parking area, whereas RD-3 was a little further away from the plant and close to the back of a shopping centre (Figure 3.2.2-4, RD-3). Reasonably, in the case that the plant was a PUR emission source, these two points should have slightly different PUR concentration, but possibly highly different polymer compositions in background. The last two sampling points were on the south side of the plant. They were very close to each other, but RD-4 was in the close vicinity of a storage area of the plant, whereas RD-5 was a drain on the street (Figure 3.2.2-4, RD-4 and RD-5). It was expected that the two sampling points had very similar results, with sightly differences in backgrounds. Spider webs collection was highly influenced by the presence of sampling points covered enough to allow the formation of aged spider webs. For this reason, only 3 sampling points were suitable to the test: two bus stops, Nordstraße and Schulstraße, and the pylon of the railway (Figure 3.2.2-5).

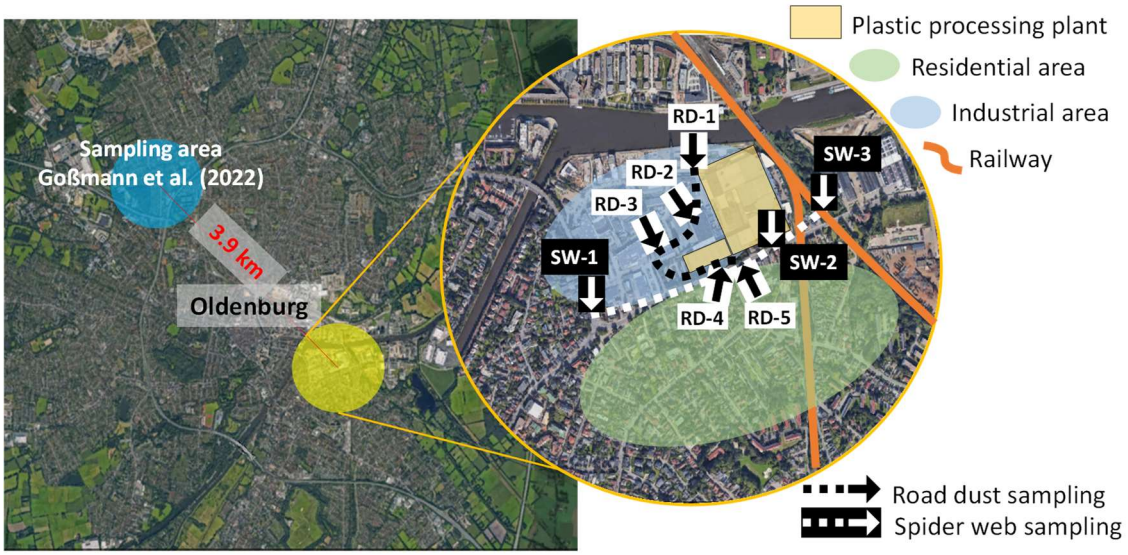

Figure 3.2.2-3. *Sampling area (yellow area), relative position with respect to reference study (blue area) and selected sampling points. Black arrows represent the sampling points of road dust samples at public drains, starting from the northernmost (RD-1) and moving on the black dotted line until RD-5. White arrows show the sampling points of spider webs samples, starting from the westernmost (SW-1) and moving on the white dotted line until SW-3 [22].*

Table 3.2.2-3. *List of sampling point with related description, coordinates and type of collected matrix [22].*

Name	Sampling point	Description	Coordinates (° N, ° E)	Collected matrix
RD-1	Public drain	Area of trucks transit	53.138931, 8.231458	Road Dust
RD-2	Public drain	Parking area	53.137987, 8.231197	Road Dust
RD-3	Public drain	Area close to the back of a shopping centre	53.136664, 8.232141	Road Dust
RD-4	Public drain	Storage area of the plant	53.136937, 8.229880	Road Dust
RD-5	Public drain	Drain on the street	53.136757, 8.232146	Road Dust
SW-1	Bus stop	Nordstraße bus stop	53.135528, 8.227446	Spider Web
SW-2	Bus stop	Schulstraße bus stop	53.137246, 8.234439	Spider Web
SW-3	Pylon	Railway pylon	53.138337, 8.236724	Spider Web

Figure 3.2.2-4. *Sampling point for the collection of road dusts [22].*

Figure 3.2.2-5*. Sampling point for the collection of spider webs [22].*

3.2.2.2.5. Sample pre-treatment

After the sampling campaign, all samples were stored in cleaned glass bottles, covered with aluminium foil. Then, they were dried in an oven at 90 °C for three days. According to literature, no PUR degradation was expected below 290 °C [23,24]. The road dusts were homogenized in an agate ball mill (Pulverisette 5, Fritsch, GmbH) and transferred into a 1 mm analytical stainless-steel sieve (Ø 10 cm, Retsch) to eliminate particles > 1 mm. Dried spider webs were cleaned up, by manually removing part of insects or rocks with the help of tweezers and a binocular microscope. Road dust pre-treatments were initially performed on 10 mg of dried sample, then the amount of sample was doubled to 20 mg and two replicates were performed with this weight. Conversely, the spider webs collected in each sampling point were processed as a single sample. Each sample was transferred in an Erlenmeyer flask, where an advanced oxidation process, using Fenton reagent (iron sulphate and hydrogen peroxide 30 % v/v), was performed to eliminate the accompanying organic matter [14,16,25]. The remaining sample was filtered on a glass fiber filter (Ø 13 mm, 0.3 µm pore size, Pall Life Sciences; pre-treated in a muffle furnace at 400 °C for 4 h). With respect to the study of Goßmann et al. (2022) [16], the pore size of glass fiber filter was reduced, from 1 µm to 0.3 µm. By folding the entire glass fiber filter, the resulting filter cake was transferred into a pyrolysis cup for the analysis. Laboratory procedural blanks were performed in parallel to each set of samples, including all preparation steps, to monitor any potential secondary MP contamination. Analogous to the entire sample preparation procedural blanks (n = 4) were performed and analysed. In case of any observed polymer related signal the results (mean) were subtracted from sample signals on a raw data basis. Subtraction was performed considering the ratios of the peak areas of each respective polymer marker to the IS area.

3.2.2.3. Results

3.2.2.3.1. Selection of PURs

The identification of few characteristic thermal degradation products which are representative of such a heterogeneous class of polymers was not an easy task and two aspects were considered in this study. The first one was the pyrolytic identification. Direct pyrolysis of PURs leads to the formation of peaks related to both the diisocyanate and the polyol used in the polymer synthesis. Nowadays, studies which have included PUR in the analyses of MPs focused on the pyrolytic markers deriving from one diisocyanate, namely methylene diphenyl

diisocyanate (MDI) [13,19,21]. Thermal degradation of the structural unit of diisocyanates typically produces one prominent peak while polyols, are often fragmented into many peaks of lower intensities [26]. Thus, the detection of pyrolysis markers from the diisocyanate portion is more favourably placed than those from polyol for the analysis of PURs. For this reason, the study focused on pyrolytic indicators of diisocyanates as representative for the presence of the related PURs. In addition to the advantage of the high peak intensity, the choice to focus only on thermal indicators of diisocyanates (excluding those from polyols) also reduces the number of peaks that can be detected while analysing different PURs. The second important aspect was related to the environmental occurrence of PUR in form of microparticles; therefore, it was reasonable to focus on polymer types that are the most probably found in the environment. The production data put the spotlight on foams, which cover more than 60 % of the produced PUR . Due to the areas of applications, foams are usually positioned in indoor environments (e.g., mattress) or in even more hidden and enclosed places (e.g., cavity wall) where they are not subjected to strong environmental degradation induced by wind, rain or sun. For this reason, their occurrence in the environment in form of MP may be not fully representative of the whole PUR class. When looking at polymer types that are the most probable to be degraded from daily use, elastomers must be included. Elastomers compose the majority of PUR that we use in our everyday life such as artificial leather bags, jackets, and shoes. Considering PUR foams and elastomers, the largest portion is made by aromatic diisocyanates, with methylene diphenyl diisocyanate (MDI) and toluene diisocyanate (TDI) the most widely use. Actually, MDI and TDI are the diisocyanates which are the most representative in the whole PUR's world. In fact, they are not only employed in foams and elastomers synthesis, but they also constitute most of PUR adhesives and sealants and a part of hydro repellent coatings [1–3]. From this viewpoint, MDI and TDI-PUR should reasonably cover the most significate and representative portion of the whole PURs to be expected as microparticles in the environment.

3.2.2.3.2. PUR characterisation Py-GC-MS and TMAH-Py-GC-MS

Standard MDI-PURs were analysed to highlight differences in their pyrograms and, in order to estimate the extent of the MDI and TDI PUR daily use, several commercial items were analysed. Table 3.2.2-4 shows the PUR items and the related diisocyanates identified by Py-GC-MS. Twelve items were analysed and two of them were TDI-PUR. TDI-PUR characterisation was performed with and without and main thermal degradation indicators are showed in Figure 3.2.2-6. 2,5-toluene diamine (TDA) was the main indicator in direct pyrolysis, whereas two different

methylated form of the diamine were recognised with TMAH: N^1,N^4,N^4,2-tetramethylbenzene-1,4-diamine (Me_3-TDA) and (N^1,N^1,N^4,N^4,2-pentamethylbenzene-1,4- diamine, Me_4-TDA.

Table 3.2.2-4. *List of pyrolysed PUR-commercial items and chemical identification of the related diisocyanate [22].*

Commercial items	PUR chemical identification
Artificial leather from jacket	MDI-PUR
Artificial leather from backpack	MDI-PUR
Commercial insulation foam A	MDI-PUR
Kitchen sponge	TDI-PUR
Foam covering of bike handlebar	MDI-PUR
Insulating material from sandwich panel	MDI-PUR
Insulation foam from a door	MDI-PUR
Packing foam	MDI-PUR
Mattress	MDI-PUR
Gasket from roof window	MDI-PUR
Commercial insulation foam B	MDI-PUR
Bumper sponge	TDI-PUR

Direct pyrolysis. As expected from the pyrolysis of both MDI and TDI-PURs, diisocyanate portions produced one main peak, whereas polyols produced many peaks of low intensities (Figures 3.2.2-7, 3.2.2-8, 3.2.2-9 and 3.2.2-10). Both for MDI and TDI-PUR, direct pyrolysis led to the formation of a diamine from the starting diisocyanate: 4,4'-methylendiphenyl diamine (MDA) and 2,5-toluene diamine (TDA), respectively. MDI-PUR is a polymer already investigated among MPs of the reference study [16], whereas TDA was recognized as main marker of the thermal degradation of commercial items. As mentioned above, the pyrolysis of PUR should release the starting diisocyanate [26], but experimental conditions affect the composition of pyrolyzates. Matsueda et al. (2021) noticed interactions in pyrolytic response of MDI-PUR due to the presence of inorganic diluents. They found out that a quantitative conversion of MDI to MDA occurred when MDI-PURs were pyrolyzed in presence of inorganic materials containing surfaces hydroxy groups [19]. Related to these findings, the identification of MDA and TDA in the present study can be attributed to the influence of the glass fiber filter. Moreover, environmental degradation may also lead to changes of form and properties of PURs [27], and the diisocyanate content may be partially converted in diamine [20,28,29]. PUR-microparticles from environmental samples could be affected by degradation at different degrees, inevitably leading to errors in quantification by Py-GC-MS.

TMAH-Thermochemolysis. Pyrolytic indicators under the thermochemolysis conditions were adopted from the pyrolysis of the previously analysed polymers with the addition of TMAH [21]. 4,4'-methylenebis-N,N-dimethyl benzeneamine (Me_4-MDA) was recognized as main indicator for MDI-PUR in accordance with literature [13]. In case of thermochemolysis of TDI-PUR, N^1,N^4,N^4,2-tetramethylbenzene-1,4-diamine (Me_3-TDA) was tentatively identified from the mass spectra of the main peak (*m/z* 149 base peak, loss of methyl radical from the molecular ion at *m/z* 164; mass spectrum reported in Figure 3.2.2-6. The partial methylation of the TDA was attributed to the *ortho* position of the amine that defined a less favourable condition to the addition of $-CH_3$ on nitrogen, due its steric hinderance. The fully methylated form of TDA was identified (N^1,N^1,N^4,N^4,2-pentamethylbenzene-1,4-diamine, Me_4-TDA; *m/z* 163 base peak, molecular ion at *m/z* 178, mass spectrum in Figure 3.2.2-6), but the intensity of the peak was very low. In fact, it was necessary to extract the ion chromatogram at *m/z* 178 to identify the peak. All the obtained markers are listed in Table 3.2.2-6. Thermochemolysis conditions led to a good identification of the two PUR types generating reproducible peaks. TMAH addition is usually convenient in the pyrolysis of MPs from environmental samples because it simultaneously allows the protection of active groups from matrices and polymers, the improvement in detection sensitivity of polar polymers like PET and PC [21,30,31] and the minimisation of polymer interactions [32]. Unfortunately, the TMAH reaction negatively affects the detection sensitivity of PUR if only standards are examined. TDI- and MDI-PUR were analysed in particles of comparable weight (see Figure 3.2.2-11) both in direct pyrolysis and under thermochemolysis conditions. Figure 3.2.2-11a shows the extracted ion chromatograms (EICs) at the specific *m/z* for the selected markers and an overall loss in sensitivity resulted, both for Me_4-MDA and Me_3-TDA, due to TMAH reactions. The comparability of the pyrograms was confirmed by the peak area ratio with IS. In Figure 3.2.2-11a these influences are highlighted, showing the comparison between Py-GC-MS (in blue) and thermochemolysis conditions (in red), both for MDI- and TDI-PUR analysis. Furthermore, without TMAH peak shape of both MDA and TDA were greater than the respective methylated compounds. This effect could have a negative impact on the detection sensitivity of PURs in environmental samples.

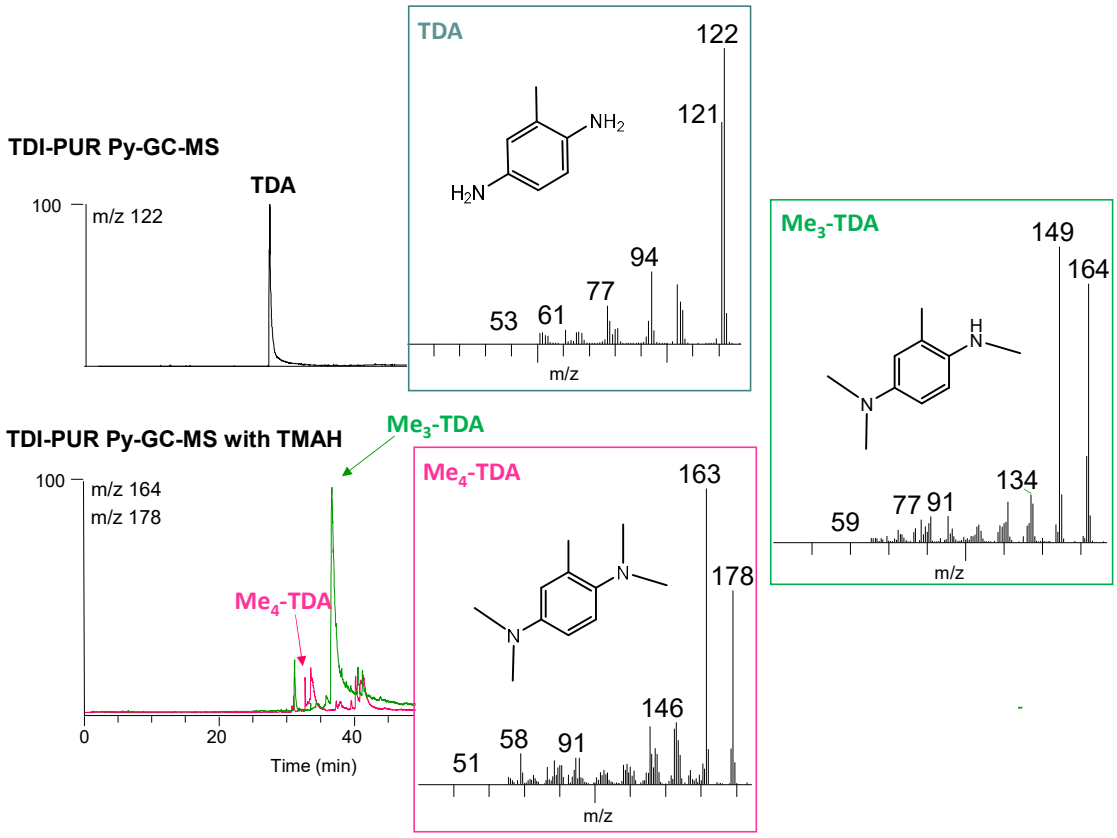

Figure 3.2.2-6. *Characterisation of TDI-PUR from commercial items by Py-GC-MS, with and without TMAH. Extracted ion chromatograms are shown to highlight main markers: without TMAH, TDA at m/z 122; with TMAH Me₃-TDA at m/z 164 and Me₄-TDA at m/z 178 [22].*

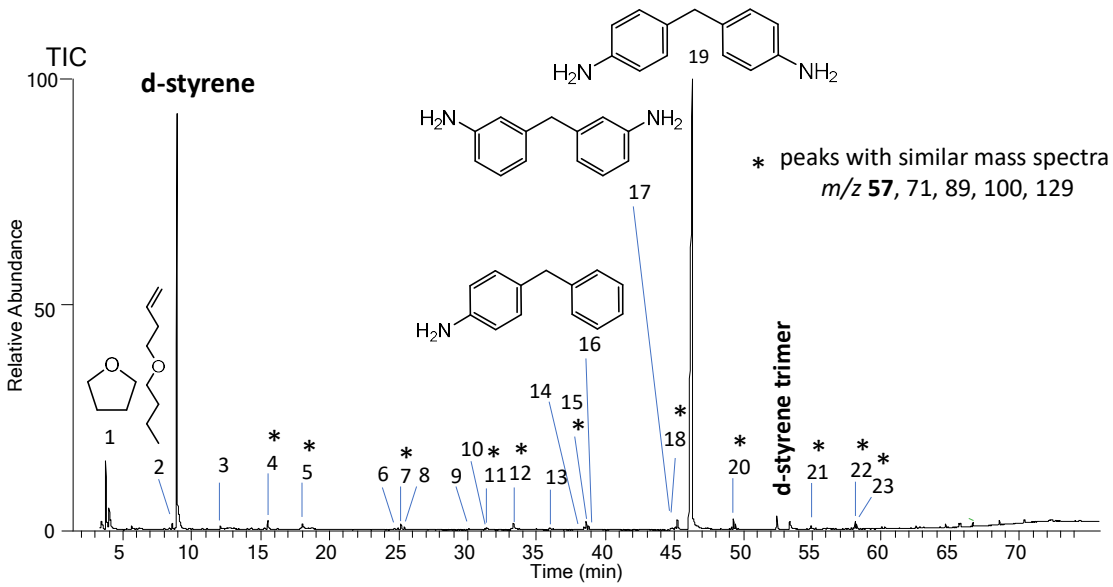

Figure 3.2.2-7. *TIC pyrogram from Py-GC-MS analysis of standard MDI-PUR_**A**. References of peaks numbers to Table 3.2.2-5 [22].*

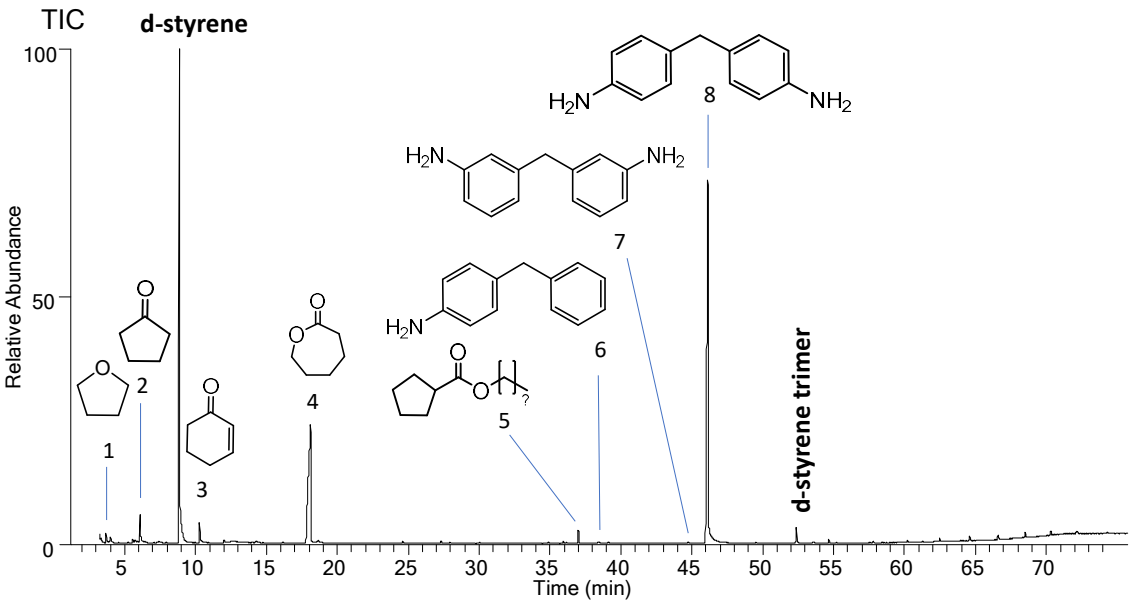

Figure 3.2.2-8. *TIC pyrogram from Py-GC-MS analysis of standard MDI-PUR_**B**. References of peaks numbers to Table 3.2.2-5 [22].*

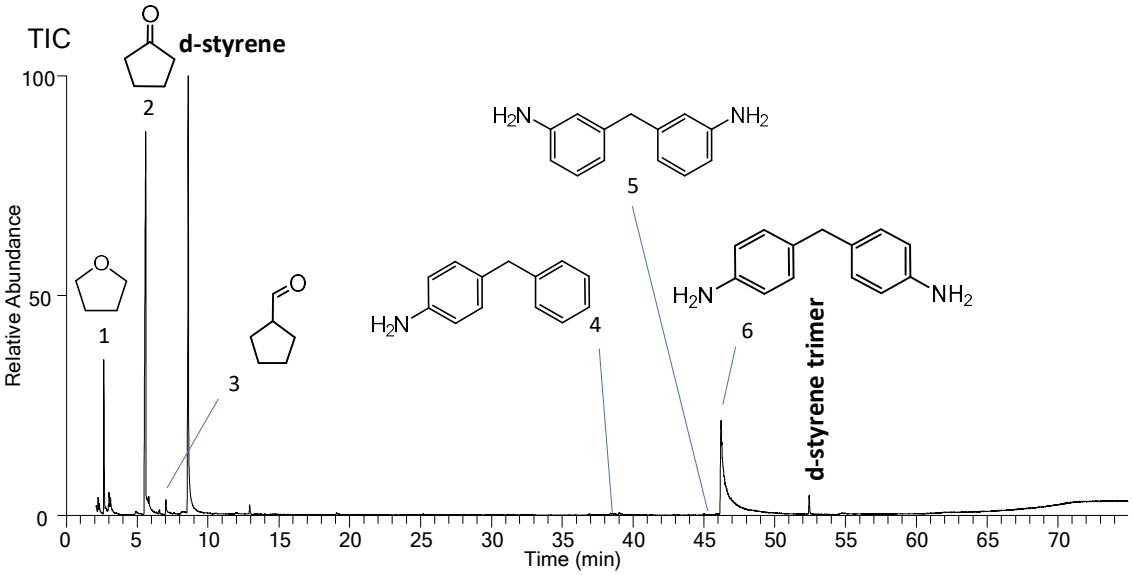

Figure 3.2.2-9. *TIC pyrogram from Py-GC-MS analysis of standard MDI-PUR_**C**. References of peaks numbers to Table 3.2.2-5 [22].*

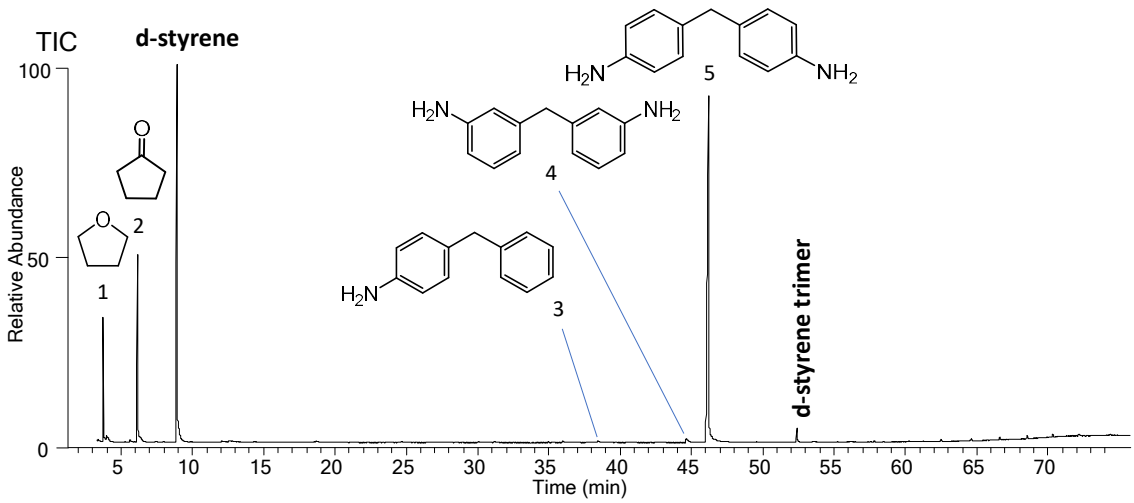

Figure 3.2.2-10. *TIC pyrograms from Py-GC-MS analysis of standard MDI-PUR_**D**. References of peaks numbers to Table 3.2.2-5 [22].*

Table 3.2.2-5. *Chemical identification of peaks from MDI-PURs analysis by Py-GC-MS. Reference number (#) to pyrograms in Figures 3.2.2-7, 3.2.2-8, 3.2.2-9 and 3.2.2-10 [22].*

#	Compound	*m/z*
MDI-PUR_A		
1	tetrahydrofuran	71, *72*
2	4-butoxy-1-butene	57, 85, 87
3	unknown	
4	*	57, 71, 85, 100
5	*	57, 71, 89, 103
6	unknown	55, 127
7	*	57, 71, 89, 100, 129
8	*	57, 71, 85, 100, 129, 145
9	unknown	
10	unknown	70, 82, 113, 196
11	*	57, 71, 85, 100, 129, 145
12	*	55, 71, 85, 100, 129, 143
13	unknown	98, 112, 140, 224
14	unknown	55, 98, 127, 136, 220
15	*	55, 73, 85, 129
16	4-(phenylmethyl)-benzenamine	106, 152, 165, 183
17	3-3'-methylendianiline	106, 180, 182, 197, *198*
18	*	55, 71, 73, 85, 100, 129
19	4,4'-methylendianiline	106, 180, 182, 197, *198*
20	*	55, 71, 73, 85, 100, 129, 197
21	*	55, 71, 73, 85, 100, 129
22	*	55, 71, 73, 85, 100, 129, 207
23	*	55, 71, 73, 85, 100, 129, 207

MDI-PUR_B		
1	tetrahydrofuran	71, *72*
2	cyclopentanone	55, 84
3	2-cyclohexen-1-one	68, 96
4	ε-Caprolactone	55, 70, 85, 114
5	cyclopentanecarboxylic acid, n-yl ester	55, 69, 97, 115
6	4-(phenylmethyl)-benzenamine	106, 152, 165, 183
7	3-3'-methylendianiline	106, 180, 182, 197, *198*
8	4,4'-methylendianiline	106, 180, 182, 197, *198*
MDI-PUR_C		
1	tetrahydrofuran	71, *72*
2	cyclopentanone	55, 84
3	cyclopentanecarboxaldehyde	57, 69, 82, 98
4	4-(phenylmethyl)-benzenamine	106, 152, 165, 183
5	3-3'-methylendianiline	106, 180, 182, 197, *198*
6	4,4'-methylendianiline	106, 180, 182, 197, *198*
MDI-PUR_D		
1	THF	71, *72*
2	cyclopentanone	55, *84*
4	4-(phenylmethyl)-benzenamine	106, 152, 165, 183
3	3,3'-methylenedianiline	77, 93, 106, 180, *198*
5	4,4'-methylendianiline	77, 93, 106, 180, *198*

Table 3.2.2-6. *Summary of main thermal degradation products from Py-GC-MS analysis of MDI-PUR and TDI-PUR, without and with TMAH addition [22].*

	MDI-PUR	**TDI-PUR**	
Py-GC-MS			
Marker	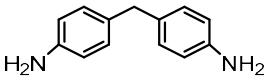 MDA	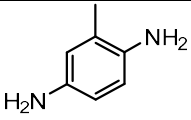 TDA	
m/z	198	122	
RT (min)	44.75	27.47	
TMAH-Py-GC-MS		*Partially methylated form*	*Fully methylated form*
Marker	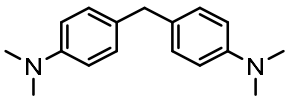 Me_4-MDA	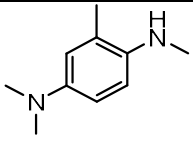 Me_3-TDA	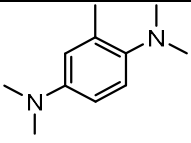 Me_4-TDA
m/z	254	164	178
RT (min)	52.60	35.38	33.42

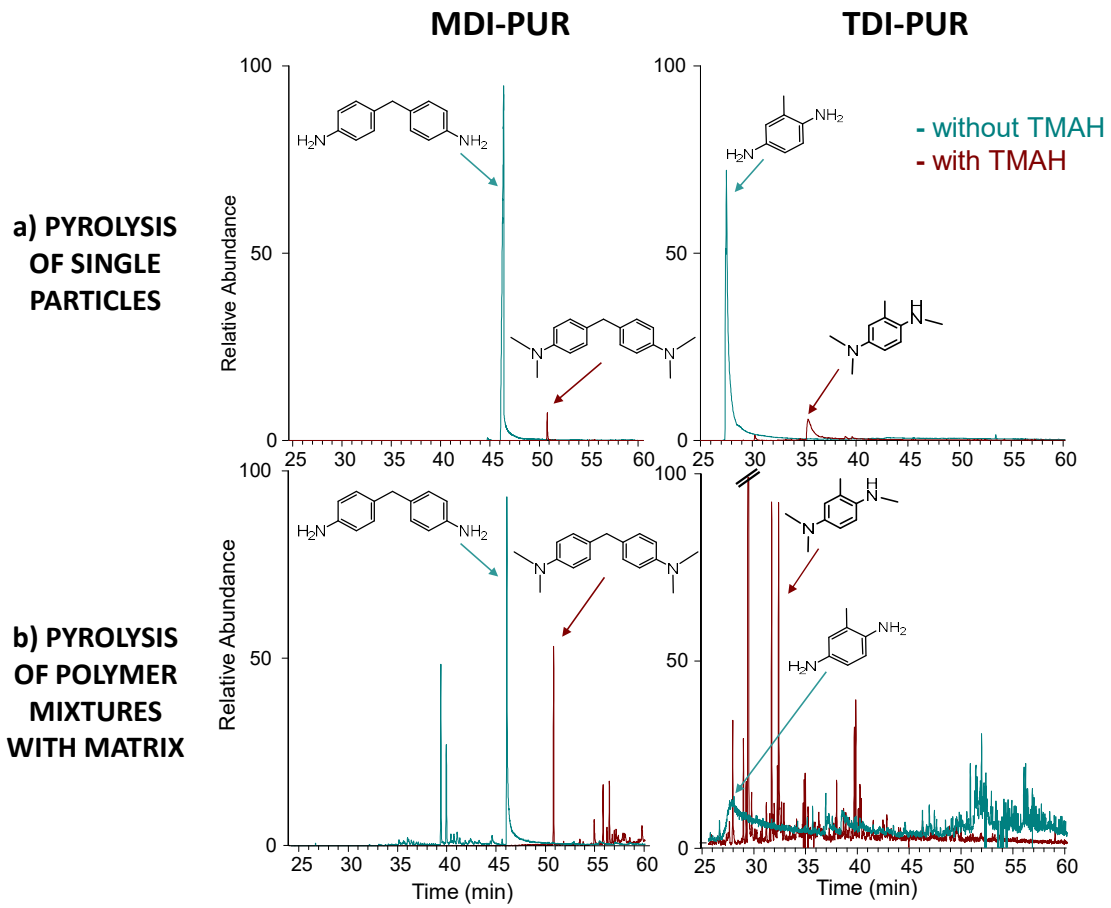

Figure 3.2.2-11. *EICs from Py-GC-MS analysis of MDI-PUR (on the left) and TDI-PUR (on the right) both with and without TMAH (red line and blue line, respectively). EIC at m/z 198 for MDA, m/z 254 for Me4-MDA, m/z 122 for TDA and m/z 164 for Me3-TDA. Comparison between analyses of single PUR particles (a) and PUR mixture with a sediment matrix (b). Weights of pyrolyzed particles: (a) MDI-PUR 54.3 µg and 53.3 µg, TDI-PUR 34.9 µg and 36.8 µg (b) MDI-PUR 24.7 µg and 26.4 µg, TDI-PUR 25.5 µg and 24.5 µg, without and with TMAH, respectively [22].*

3.2.2.3.3. PUR characterization by Py-GC-MS and TMAH-Py-GC-MS in the presence of a matrix

However, the use of TMAH might be crucial in the analysis of environmental MPs. In the perspective of environmental investigation, it is important to take into account that residual matrix may be present in the analysed sample despite the application of an intensive sample pre-treatment to reduce accompanying inorganic and organic matrices. Compounds deriving from pyrolysis of any organic matter affect the quality of the resulting pyrogram, producing noise and generating molecules with active groups (e.g., hydroxyl groups) that can potentially promote secondary reactions [32]. In this context it is expected that the presence of TMAH during pyrolysis prevents a large share of these reactions. As a result of thermal methylation, the reactivity of polar groups, either in the matrix or generated during pyrolysis, is reduced [33].

Furthermore, TMAH achieves concrete benefits in polymer identification and quantification [31]. In order to evaluate MP pollution, it is important to include and simultaneously detect as many polymers as possible in the investigation, not only PURs. The use of TMAH enhances the chromatographic separation behaviour and elution of less volatile and polar polymers, allowing a great increase in sensitivity for the quantification of crucial polymers (e.g., PET) [21,30,31].

To clarify the role of TMAH in PUR identification and analysis within environmental MPs, experiments were conducted to investigate the pyrolysis behaviour of PURs in the presence of a natural, environmental matrix. For this purpose, exactly weighed particles of MDI-PUR, TDI-PUR and PET (considered a widespread, representative MP) were added to a sediment matrix after appropriate pre-treatments for MP analysis. Samples were analysed with and without TMAH (more details Table 3.2.2-7). Main results are presented in Figure 3.2.2-12 and Figure 3.2.2-13. The absence of pyrolysis markers of MDI and TDI-PUR in the pure sediment was verified (Figure 3.2.2-13). In the presence of TMAH, the markers of all the three polymers were detectable (Figure 3.2.2-13), whereas without TMAH the identification of TDI-PUR and PET could not be confirmed. The chromatographic elution of TDA marker was not appropriate to TDI-PUR identification and some important markers from PET were missing (e.g., divinyl terephthalate) (Figure 3.2.2-12). As expected from the pyrolysis of isolated, single PUR particles (Figure 3.2.2-11a), the intensity of MDI-PUR marker peak was lower when measured with TMAH, compared to the direct pyrolysis. However, the difference of intensities of the respective signals between direct and TMAH pyrolysis was greatly reduced in the presence of a matrix (Figure 3.2.2-11b). These findings evidence the effect of the accompanying matrix, highlighting that the associated interactions/reactions with polymer decomposition products negatively affect polymer investigation in direct pyrolysis. It is assumed, that reactive matrix compounds are “deactivated”/derivatized by TMAH, opposing the loss of signals and, accordingly, the noticeable reduction in detection sensitivity. These observations support the hypothesis that, besides the significant improve of detection sensitivity for some polymers, the addition of TMAH to pyrolysis greatly reduces the interactions of pyrolytic MP analytes with the remaining organic matrix of environmental samples and the associated negative effects on analytical results. In conclusion pyrolysis with TMAH should be favoured for MP analysis from complex environmental samples.

Table 3.2.2-7. *Sample preparation for matrix effect analyses. IS (20 µL of d-PS 125 µg mL^{-1} in DCM) was also added to each analysis [22].*

Sample	Sediment (mg)	MDI-PUR (µg)	TDI-PUR (µg)	PET (µg)	TMAH
a-1	10	-	-	-	-
a-2	10	-	-	-	20 µL
b-1	10	24.7	25.5	9.9	-
b-2	10	26.4	24.5	9.8	20 µL

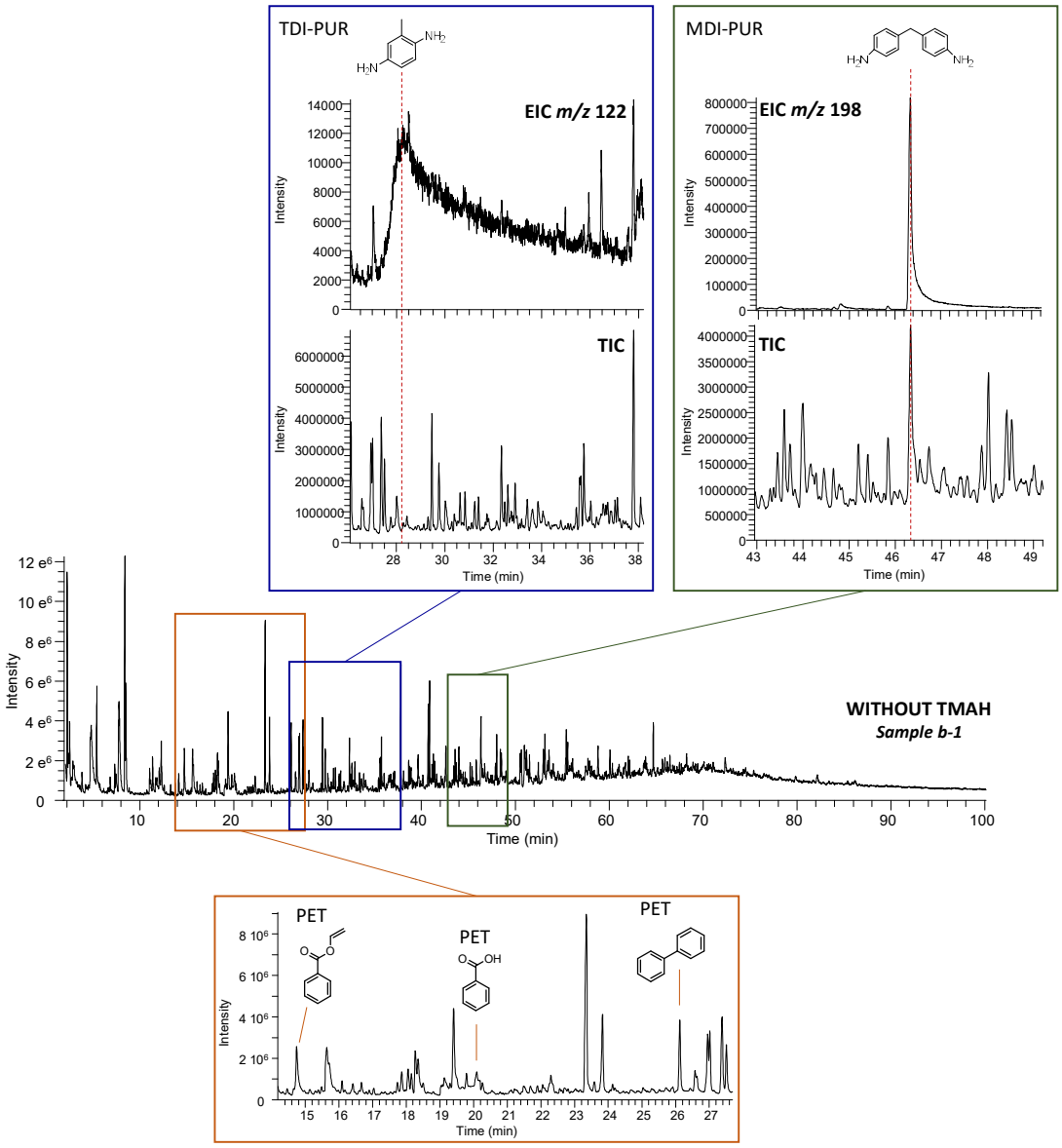

Figure 3.2.2-12. *TIC from pyrolysis without TMAH of pre-treated sediment samples spiked with MDI-PUR, TDI-PUR and PET (sample b-1 from Table 3.2.2-7). Blue and green frames show extracts of TIC and EICs for TDI-PUR and MDI—PUR identification, respectively. Red dotted lines indicate the RT [22].*

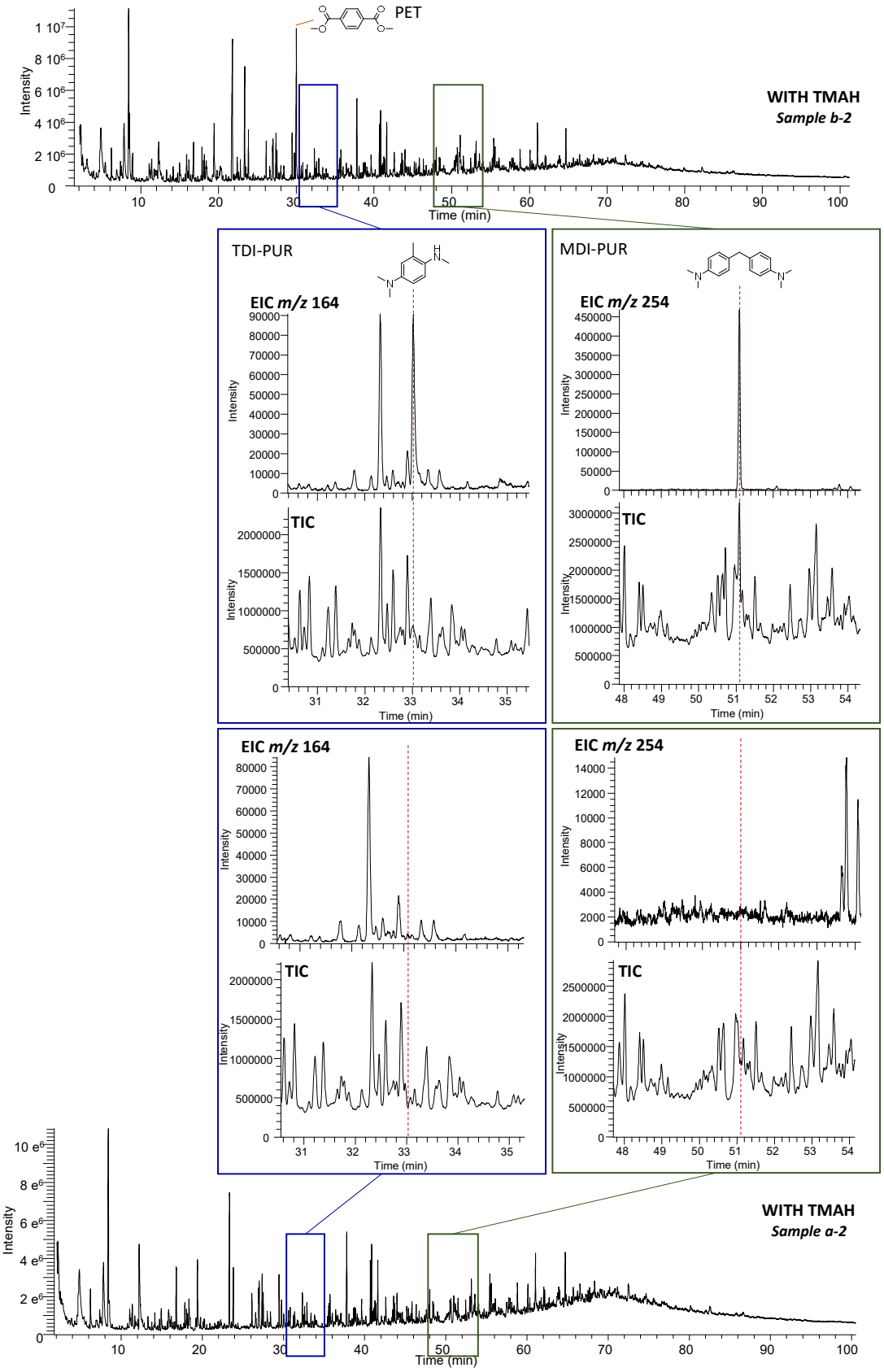

Figure 3.2.2-13. *Comparison of TIC from pyrolysis with TMAH of pre-treated sediment samples (sample b-2 above and sample a-2 below, from Table 3.2.2-7, with spiked polymers and without, respectively). Blue and green frames show extracts of TIC and EICs for TDI-PUR and MDI-PUR identification, respectively. Red dotted lines indicate the RT [22].*

3.2.2.3.4. Calibration results

Calibration curves were created with four different MDI-PUR standards (MDI-PUR_A, B, C and D) and one commercial TDI-PUR by TMAH-Py-GC-MS. Tested polymers showed good linearities with all three different IS (d-PS, TOHA, cholanic acid) and d-PS was the one selected to carry on with polymer quantification. Peak areas (A) were determined by integration of the peak in the extracted ion chromatogram of a single specific ion. Calibration protocol was constructed in the form of the Equation 3.2.2-1

$$\frac{A_x}{A_{IS}} = a + b\,W_x \qquad \textbf{Equation 3.2.2-1}$$

A_x is the peak area of the pyrolytic marker of interest, integrated at a specific *m/z* (254 and 164 for MDI and TDI-PUR, respectively, see Table 3.2.2-6). A_{IS} is the peak area of the internal standard (IS) applied in the calculation, integrated at the related *m/z*, W_x the weight (µg) of the pyrolysed polymer; *a* is the intercept and *b* the slope (sensitivity). The selected was the deuterated polystyrene (d-PS) and the indicator used in calibrations was the deuterated styrene trimer at *m/z* 98. Regression parameters obtained with d-PS-IS are listed in Table 3.2.2-8.

As Figure 3.2.2-15a, c, e, g shows, over the whole calibration range (0.7 – 39.8 µg) good regression models were obtained for all the investigated polymers (R^2 = 0.942 – 0.944). An exception was MDI-PUR_A (R^2 = 0.715) which exhibited a typical "plateau behaviour" over 20 µg (Figure 3.2.2-15a, Table 3.2.2-8). Nevertheless, by limiting the mass range to 1 – 20 µg, results changed and all polymers, including MDI-PUR_A, showed satisfactory linearity (Figure 3.2.2-15b, d, f, h and Table 3.2.2-8). These results suggested that MDI-PURs, although of partly different chemically constituents and resulting structure, may behave comparably during pyrolysis and result into similar yields of respective indicator molecule/ion.

TDI-calibration curve was constructed from a commercial kitchen sponge (Figure 3.2.2-14). R^2 showed good correlation (Table 3.2.2-8), but the loss in sensitivity due to the derivatisation led to the impossibility to detect the investigated marker under 9 µg.

Considering a signal to noise ratio (S/N) ratio of 3 as the limit of detection (LOD) and an S/N ratio of 10 as the limit of quantification (LOQ), the S/N ratios were calculated for the lowest points of the calibration curves to indicate how far the calibration ranges were from those limits. Interestingly, they showed almost the same S/N of around 30 related to ≈ 1 µg polymer weight, although polymer structures of the investigated MDI-PURs differed. An exception was MDI-PUR_A that showed only half of the sensitivity for the same polymer mass (S/N = 15). The detection sensitivity of TDI was substantially lower, 9 µg polymer had an S/N ratio of 32. The

sensitivity might represent a great obstacle in the trace analysis of PURs. Main regression parameters are summarized in Table 3.2.2-8.

Table 3.2.2-8. *Regression parameters for standard MDI-PURs calibrations within the two mass ranges, 1 - 40 µg and 1 - 20 µg. The table includes coefficient of determination (R^2), process standard deviation (s_{x0}, calculated by the residual standard deviation of a linear regression to the slope [34], intercept (a), slope (b) and points used for the calibration (n) [22].*

	1 – 40 µg					**1 – 20 µg**					**Lowest point (µg)**	**S/N lowest point**
	R^2	s_{x0}	a	b	n	R^2	s_{x0}	a	b	n		
MDI-PUR_A	0.715	9.7	-	-	10	0.923	2.6	-0.04	0.04	8	0.8	15
MDI-PUR_B	0.944	3.4	-0.06	0.05	10	0.905	2.9	0.04	0.04	8	0.7	32
MDI-PUR_C	0.942	3.9	-0.15	0.06	10	0.944	2.1	-0.09	0.05	8	0.7	30
MDI-PUR_D	0.962	3.1	0.02	0.04	10	0.961	1.6	-0.04	0.05	8	1.1	33
TDI-PUR	0.936	3.3	-0.1	0.03	13						9.3	32

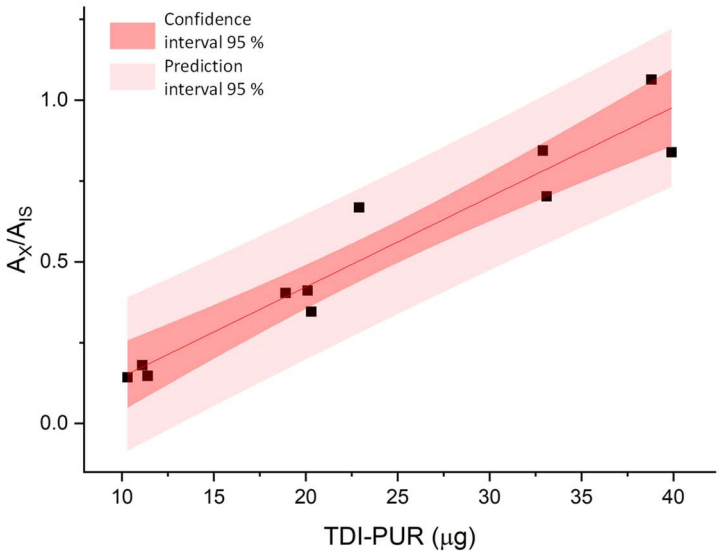

Figure 3.2.2-14. *Calibration curves elaborated for TDI-PUR from a commercial item. A_X =area of Me_3-TDA at m/z 164, internal standard: IS = d-PS, A_{IS}= area od deuterated styrene trimer at m/z = 98 [22].*

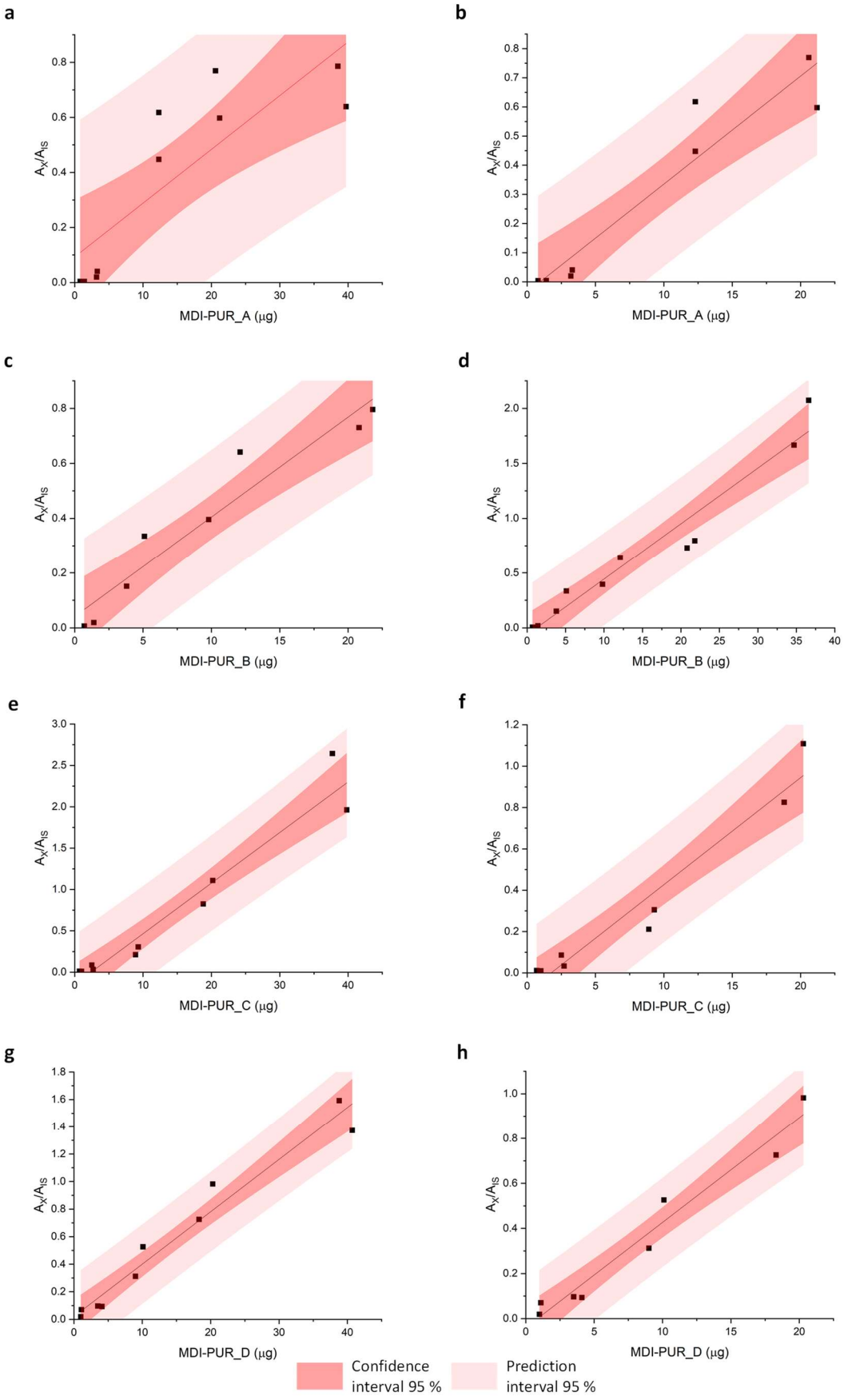

Figure 3.2.2-15. *Calibration curves elaborated in the 1-40 µg (a, c, e, g) and 1-20 µg (b, d, f, h) mass range for four different standard MDI-PUR (MDI-PUR_A, B, C, D) A_X =area of Me_4-MDA at m/z 254, internal standard: IS = d-PS, A_{IS}= area of deuterated styrene trimer at m/z = 98 [22].*

3.2.2.3.5. Statistics

In the context of MPs quantification in the environment, calibrations play a fundamental role. Even though specific pyrolytic markers were selected as representative of the related diisocyanate-PUR subclasses (e.g., MDI or TDI), the quantification can be challenging. Given the huge number of possible PUR structures, the use of one standard polymer for the quantification of the whole subclass might lead to mistakes. To assess the feasibility of a generalization with respect to PUR quantification in environmental samples we applied statistics. In this section, only calibrations based on d-PS internal standardization are considered. In analytical pyrolysis, the slope and the intercept represent the linear relationship between the independent variable, polymer weight, and the dependent one, pyrolytic response. These two parameters are fundamental in regression model description, and they indicate the quantification behaviour of a calibration. In particular, when two mathematical functions are parallel (same angular coefficients), those functions are said to be mathematically similar [35]. It is plausible to conclude that, based on the same thermal degradation indicator (e.g., Me_4-MDA for MDI-PURs), different PURs can be assumed as one when their regressions have the same slopes. Equations of MDI-PUR_A, B, C, D calibrations were considered to perform parallelism tests in order to understand if statistically significant differences occurred within their angular coefficients. One-way ANOVA test was elaborated to solve the problem, comparing the effect of four different polymer structure (MDI-PUR_A, B, C, D) on the pyrolytic response of Me_4-MDA (considered in area ratio with IS, d-PS). Curves for both mass ranges are shown in Figure 3.2.2-16. The test was performed on both regression models in the 1 – 40 µg (number of considered curves, k = 3. MDI-PUR_A was excluded due to its poor linearity in the range) and 1 – 20 µg (k = 4) mass ranges. ANOVA revealed a statistically significant difference in pyrolytic response of Me_4-MDA of at least two MDI-PURs ($F_{2, 24}$ = 7.8, α = 0.05) when calibrations were elaborated in the 1 – 40 µg mass range. On the other hand, when the mass range was reduced to 1 – 20 µg not statistically differences were revealed ($F_{3, 24}$ = 2.7, α = 0.05). Data and obtained results for the two tests are summarised in Table 3.2.2-9. These results indicated that, within a limited mass range, a reliable mass estimation of the total MDI-PURs is possible just using one thermal decomposition product (Me_4-MDA). Results are almost independent of the polymer used for calibration and accordingly regardless of the whole MDI-PUR structures.

As a result of the comparison, MDI-PUR_D was selected for the further calibration, in order to maintain the same polymer used for quantification in the reference study [16].

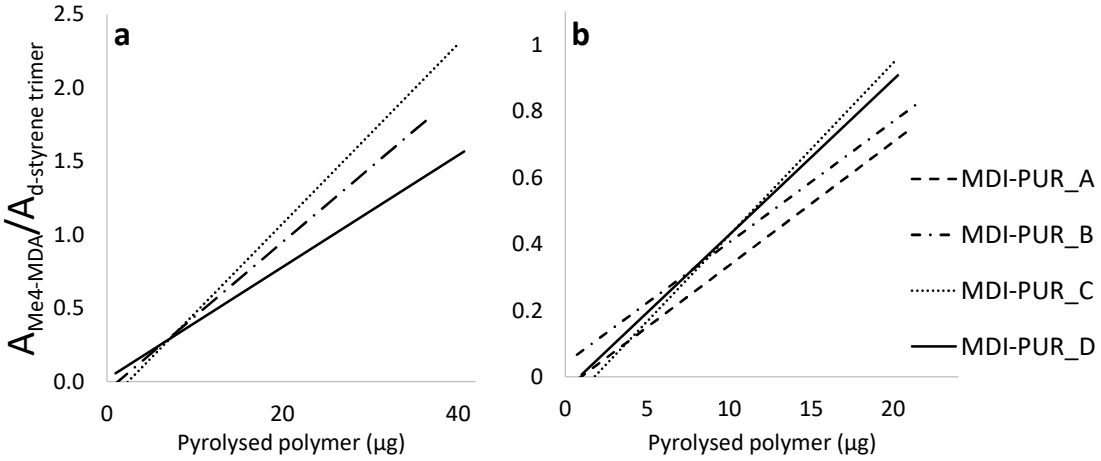

Figure 3.2.2-16. *Comparison of calibration curves elaborated from different MDI-PUR standards (A, B, C, D) in two different mass ranges, 1 - 40 µg (a) and 1 - 20 µg (b) [22].*

Table 3.2.2-9. *Data and results of ANOVA tests on calibrations on two different mass ranges (1 - 40 µg and 1 - 20 µg). Deviations, degrees of freedom (df), variances (S^2), number of total observation (N) and number of considered calibrations (k) calculated as preliminary data. Value of observed and tabulated F-statistics (F_{OBS} and F_{TAB}, respectively) resulting from the test with α = 0.05 [22].*

Mass range	**1 – 40 µg**			**1 – 20 µg**		
	Deviation	df	S^2	Deviation	df	S^2
Error between angular coefficients	0.53	2	0.263	0.08	3	0.025
Error within each curve	0.80	24	0.033	0.23	24	0.009
N	30			32		
k	3			4		
α	0.05			0.05		
F_{OBS}	7.8			2.7		
F_{TAB}	3.4			3.0		

3.2.2.3.6. Particle size effect

The particle size has considerable relevance in thermal analyses. The same temperature applied on different size particles may lead to non-identical heating rate in diverse parts of the same particle (e.g., the surface and the centre), resulting in different pyrolysis yield [36,37]. The issue may be even more important when a surface related chemical reaction (thermochemolysis) is included. Given that regression models and ANOVA tests showed an influence of pyrolytic behaviour of MDI-PURs related to the mass of pyrolysed polymer (over 20 µg), the assessment of possible particle size effects was necessary aluminium a first set of experiment one single large particle (LP) was individually pyrolysed and a second set was prepared to pyrolyse several

(4 or 5) small particles (SP) in the 5 – 10 µg mass range. MDI-PUR_D was excluded from these experiments, because it was only provided in small particles and no large enough LP could be obtained, whereas the others were in pellet form (Figure 3.2.2-2). In the second set, the pyrolyzed sample was made by assembling 4 – 5 small particles (SP, < 100 µm) that in total weighted 40 µg. The weight of each SP ranged between 5 – 10 µg. MDI-PUR_D was excluded from the first set of experiments, because it was available already grinded in SP, whereas the others were in pellet form (Figure 3.2.2-2). An estimation of LP size is provided in Figure 3.2.2-17. Two replicate analyses were performed both for LP and SP of MDI-PUR_A, B, C and for SP of MDI-PUR_D. Pyrolytic behaviour was investigated by the ratio of Me_4-MDA area by the one of deuterated styrene trimer (from d-PS) as IS, both extracted for the specific target ion (*m/z* 254 and *m/z* 98, respectively). Apparently, it was not possible to identify a univocal trend shared among all MDI-PURs. Results were transferred to a bubble chart (Figure 3.2.2-18) for an adequate visualization. The vertical Y-axis reflects the ratio *y/x*: *y* is the peak area ratio of Me_4-MDA to IS, both extracted and integrated at the specific target ion (*m/z* 254 and *m/z* 98, respectively); *x* is the exact weight of the pyrolyzed polymer. The same variables (*x* and *y*) were used to build up regression models. When *y* is normalized on *x*, the ratio explains the function that correlates the two variables. Therefore, for each MDI-PURs, LP and SP bubbles (black and white, respectively) are overlapped when the two conditions are identified by the same function. In particular, the position of the bubble explains the mean value of normalized *y* for each MDI-PUR and the size of the bubble describes the relative standard deviation (RSD%). Hence, the larger the bubble the higher the variability.

The bubbles of the four standard MDI-PURs have different relative positions (Figure 3.2.2-18) Accordingly, they are described by different functions, showing different pyrolytic behaviour. For MDI-PUR_A and MDI-PUR_C, the black bubbles (LP) and the white bubbles (SP)overlap even though they are not exactly centred in the same point. In both cases, RSD% (reflected by the diameter) increased when polymers were pyrolyzed in SP (from 17 % to 42 % for MDI-PUR_A and from 25 % to 42 % for MDI-PUR_C), suggesting that no significant size dependence can be detected here. The larger standard deviation observed for the small particles might be related to a surface effect. Interestingly, results for MDI-PUR_B were totally different. In this case, black and white bubbles did not overlap. This indicates that two different functions describe the respective pyrolytic behaviours of the two particle sizes (LP and SP). In contrast, the RSD% calculated for LP and SP analysis (accordingly the bubble size) were comparable, 12 % and 17 % respectively. In this case, particle size seemed to highly affect the pyrolytic response of the polymers. Finally, results for SP of MDI-PUR_D were reported. In comparison with other MDI-PURs, the related bubble is placed in an intermediate position, with an RSD% of 14 %.

These results underline the highly variable and hardly predictable pyrolytic behaviour of MDI-PURs most likely related to the polymer structures and the investigated mass range. Assuming that PUR particles from a wide variety of sources and sizes may be present in environmental samples, a unified behaviour is assumed for their analysis.

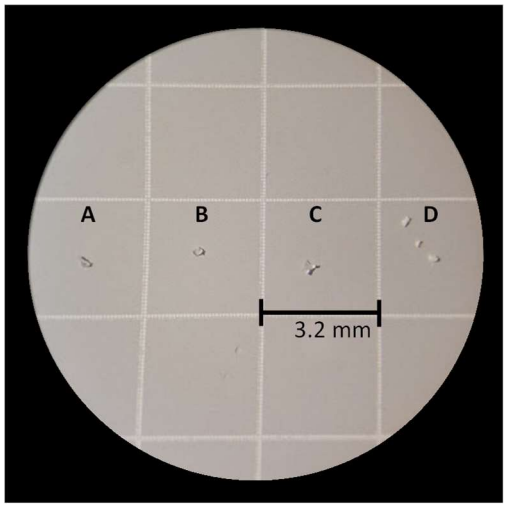

Figure 3.2.2-17. *40 µg particles dimension for each standard MDI-PUR (A, B, C and D). MDI-PUR_D was provided in small particles, whereas MDI-PUR_A, B and C were cut from pellet (Figure 3.2.2-2) [22].*

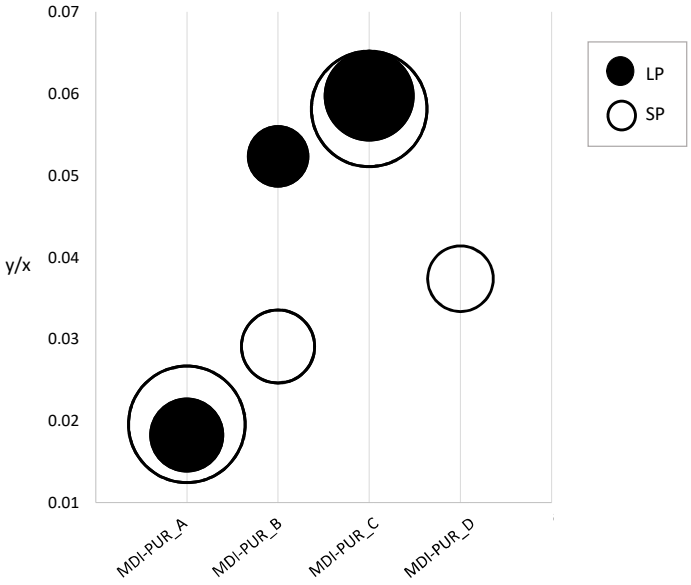

Figure 3.2.2-18. *Bubble chart of results obtained from Py-GC-MS analysis of large and small particles (LP and SP, respectively) of three different MDI-PURs (MDI_PUR_A, B, C and D). y indicates the ratio of Me4-MDA area by the one of deuterated styrene trimer as IS, both extracted for their specific target ion (m/z 254 and m/z 98, respectively) and x is the pyrolyzed polymer weight (µg). MDI-PUR_D was investigated for SP only [22].*

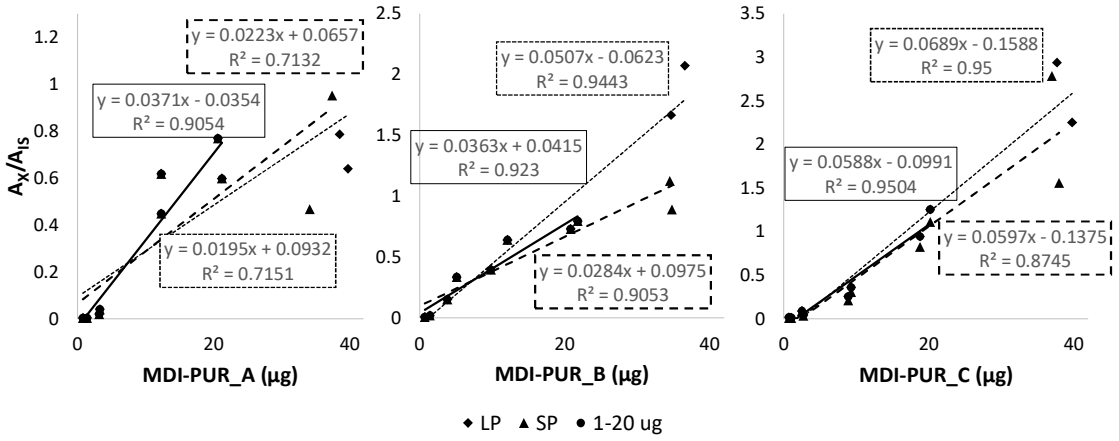

Figure 3.2.2-19. *Comparison of calibration curves constructed in the 1 – 40 µg mass range with large and small particles (LP and SP, respectively) and in the 1 – 20 µg range. Investigated polymers, standard MDI-PURs [22].*

3.2.2.3.7. Environmental occurrence

Despite the high production and the wide variety of application fields, discrete sources for PURs in environmental compartments are not easily predictable. Regarding environmental matrices of previous investigations, MDI-PUR could be detected only sporadically [13,16]. In order to obtain suitable environmental samples that could be assumed to also contain PUR, road dusts and spider webs were collected in close vicinity to a plastic processing plant in the mid-sized city of Oldenburg (Germany). While road dust represents the washout of urban particulates in general, spider webs are an appropriate tool to reflect the airborne particulate load [16].

Qualitative detection Chemically oxidative pre-treated road dust and spider web samples from the vicinity of a polymer processing factory were analysed with respect to their potential PUR content. The analytical strategy was based on the information collected during the preceding characterization phase. The pyrograms generated by thermochemolysis of the entire samples were investigated by extracting the PUR target ions applied for the preparation of calibration curves at the related retention time (RT) (Table 3.2.2-8). In order to broaden information about MPs contamination, other polymer clusters indicated by prefix “C-” were investigated, according to the quantification method used by Goßmann et al (2022) [16] (details about polymer clusters and their thermal degradation indicators in Table 3.2.2-10).

Me_4-MDA was detected in all samples, except for SW-3, confirming the presence of C-MDI-PUR MPs in the surroundings of the factory as a potential emission source. The absence of C-MDI-PURs in SW-3 may be related to the sampling point itself. SW-3 was located at a pylon of the railways; therefore, the collected spider web was much less protected from environmental influences compared to SW-1 and SW-2. These sampling points were located at bus stops, where

the platform roof guarantees a safe barrier. This lack of a full coverage over the sampling point may cause a shorter lifespan, for example because of the cleaning of spider webs during rain events. More likely, the reason for the absence of C-MDI-PURs in this web sample is related to the position of the sampling point. Sampling was performed beyond the railway line (Figures 3.2.2-3 and 3.2.2-5 and Table 3.2.2-3). Here the high train frequency might work as an impediment in the microparticles pathway, acting in the way that emissions from the potential PUR source are too much dispersed to be trapped by the spider webs. A more detailed discussion is elaborated in quantitative section.

Me_3-TDA was not detected in any of these samples. A peak with a very similar mass spectrum was found at a RT 3 minutes earlier than expected. In GC analyses, RT is a basic parameter to assign a compound in unknown samples. However, the co-elution of accompanying matrix related compounds of variable polarities might affect the elution behaviour, causing slight changes in RT. In order to solve the doubt, the fully methylated form of the compound (Me_4-TDA) was investigated in the same pyrograms. It was absent as well, suggesting that TDI-PURs were not present in the given samples. Given that the pyrolytic behaviour in sediment matrix was tested (Figure 3.2.2-13, Table 3.2.2-7), the absence of TDI-PUR markers indicates that the suspected emission source does not process this polymer type, justifying its absence in the form of microparticles. However, despite LOD was not calculated, similar S/N ratios were found for ≈ 9 µg and ≈ 1 µg of Me_3-TDA and Me_4-MDA, respectively, suggests a lower sensitivity for TDI-PUR with respect to MDI-PUR.

Quantification. C-MDI-PURs were quantified using the calibration curve of the standard MDI-PUR_D, in the 1 – 20 µg range, the same standard MDI-PUR used in the reference study [16]. The derived results are summarised in the histograms and pie charts in Figure 3.2.2-20 for RD and Figure 3.2.2-21 for SW. Here, concentrations of other polymer clusters at the respective sampling points are given as well. Concentrations of C-MDI-PURs in road dust were calculated from triplicate analyses for each sampling point (RD-1 – 5). Mean concentrations and standard deviations are shown in the histogram in Figure 3.2.2-20. Polymer concentrations were related to weight of dried road dust and C-MDI-PUR ranged between 82 and 131 µg g^{-1} with satisfactory RSD% from 14 to 29 % (Table 3.2.2-11). Considering that sampling points were selected in the vicinity of the potential PUR emission source, no strong variation of C-MDI-PUR within the area was expected. Nevertheless, the total amount of investigated polymers was not homogeneous. Pie charts in Figure 3.2.2-20 show the MPs composition, considering the investigated polymers (C-MDI-PUR, C-PE, C-PP, C-PET, C-PS, C-PVC, C-PMMA, C-PC, CTT and TTT, polymer explanation and more details in Table 3.2.2-10.

Polyamides were included among the investigated polymers, but the related markers were absent in pyrograms. The size of each pie chart is proportional to the total amount of polymers per sample type quantified at the respective locations (full quantitative results Table 3.2.2-11). The signal of some polymers ranged below the LOQ or showed a high RSD%. Those polymers were excluded from pie charts, but their occurrence is shown in the labels close to the charts in Figure 3.2.2-20. However, the qualitative composition of quantified MPs, other than C-PUR, was homogeneous. It showed a clearly related pattern (Table 3.2.2-11) and, excluding tire wear particles, C-PET and C-PVC were predominant. It is already known that quantification of C-PVC is challenging. Pyrolysis products suitable for quantification rely in particular on PAHs, which might be assigned to other organic matter [13,15,26]. Samples were pre-treated by Fenton's reaction that ensured a substantial degradation of low molecular and most of polymeric organic matter. However, it was shown recently that treated polymeric residues of some particular soot types have the ability to release PAHs and consequently interfere with results [16]. Goßmann et al (2022) evaluated the amount of PAHs generated by potential contamination sources (diesel, charcoal and wood stove soot) in the context of urban and congested traffic areas. Those results were used to estimate a correction factor for a restricted, semi quantitative determination of *C-PVC indicated by an asterisk. Assuming an overall qualitative composition of urban soot, also considering the closeness of the two sampling areas, the same correction factor was applied in the present study. Despite the overall comparable MPs composition, each sampling point reflected site-specific conditions. Further details on sites and polymer concentrations are given in Figure 3.2.2-4 and Table 3.2.2-3 and polymer concentrations are expressed in Table 3.2.2-11. The lowest amount of polymers and relative predominance of CTT was detected in RD-1, which represented the road entering the plant. RD-2 showed the greatest variety of polymer types. This might be related to the broad parking area that allows wind circulation on one hand, and to the directly adjacent high building of the plant on the other hand, which acts as a barrier causing particle deposition. RD-3 showed the highest quantified polymer amount (Figure 3.2.2-20). A nearby shopping centre, with comparatively high traffic volume and the use of diverse polymers, might act as a possible explanation. Finally, RD-4 and RD-5, only few meters apart from each other, resulted in comparable polymer pattern with similar MPs concentrations, except for tire particles and *C-PVC (Table 3.2.2-11). The fact that RD-5 shows higher overall TTT and CTT concentrations could be a result of the close main street.

Spider webs were represented by one single sampling each, and the polymers quantified herein were referred to the total weight the respective sample. MDI-PUR contaminated samples reflected a coherent, relative position to the potential MDI-PUR source (production plant). SW-2 was the closest to the source and showed the highest concentration of C-MDI-PUR, followed

by SW-1 with 0.12 µg mg^{-1} and 0.08 µg mg^{-1} spider web, respectively (Figure 3.2.2-21). As suspected earlier, the absence of C-MDI-PUR in SW-3 is plausibly attributed to its sampling point behind the railway. This assumption is strengthened by the absence of other polymers (C-PE, C-PP, C-PMMA, C-PS, CTT and TTT) quantified in SW-1 and SW-2 and the overall very low total polymer content restricted to C-PET and *C-PVC only (Figure 3.2.2-21). In particular, the divergent, non-comparable sampling conditions prevented meaningful data comparison here.

According to studies of Goßmann et al (2021 and 2022), C-MDI-PURs were not detected in road dusts and spider webs collected in urban traffic and residential areas of the same city [14,16]. The closest sampling point was approximately 1.5 km as the crow flies of the area discussed here. These former results and the observations of the presented study, lead to the general outcome that a detectable presence of C-MDI-PUR in environmental samples seems to be highly dependent on the proximity to potential sources/emitters, like a production plant in the given case.

Table 3.2.2-10. *List of characteristic thermal degradation indicators (markers) selected for the quantification of the detected polymer clusters, according to Goßmann et al. (2022). Pyrograms were extracted at the specific target ion (m/z) for data elaborations [22].*

Abbreviation	Cluster associated compounds	Selected markers	*m/z*
C-PE	High-density and low-density polyethylene, PE-containing copolymers and rubbers, ethylene-vinyl acetate (EVA), ethylene-propylene diene monomer (EPDM) rubber	α,ω-Alkanes (average C_{16}-C_{26})	82
C-PP	Polypropylene, EPDM rubber	2,4-Dimethylhept-1-ene	70
C-PET	Polyethylene terephthalate, polybutylene terephthalate	Dimethyl terephthalate	163
***C-PVC**	Polyvinylchloride (hard and plasticised), chlorinated PE, chlorinated rubber	Naphthalene	128
C-PS	Polystyrene, PS-containing copolymers (ABS, SAN),PS- or acryl styrene binders, varnish	2,4,6-Triphenyl-1-hexene	91
C-PC	Polycarbonate, epoxide resin	2,2-Bis(4'-methoxy-phenyl)propane	241
C-PMMA	Polymethyl methacrylate, polyalkylated methacrylate, acryl-containing binder	Methyl methacrylate	100
CTT	Car tyre tread	Cyclohexenxlbenzene	104
TTT	Truck tire tread, bus tire tread	2,4-Dimethyl-4-vinylcyclohexene	202

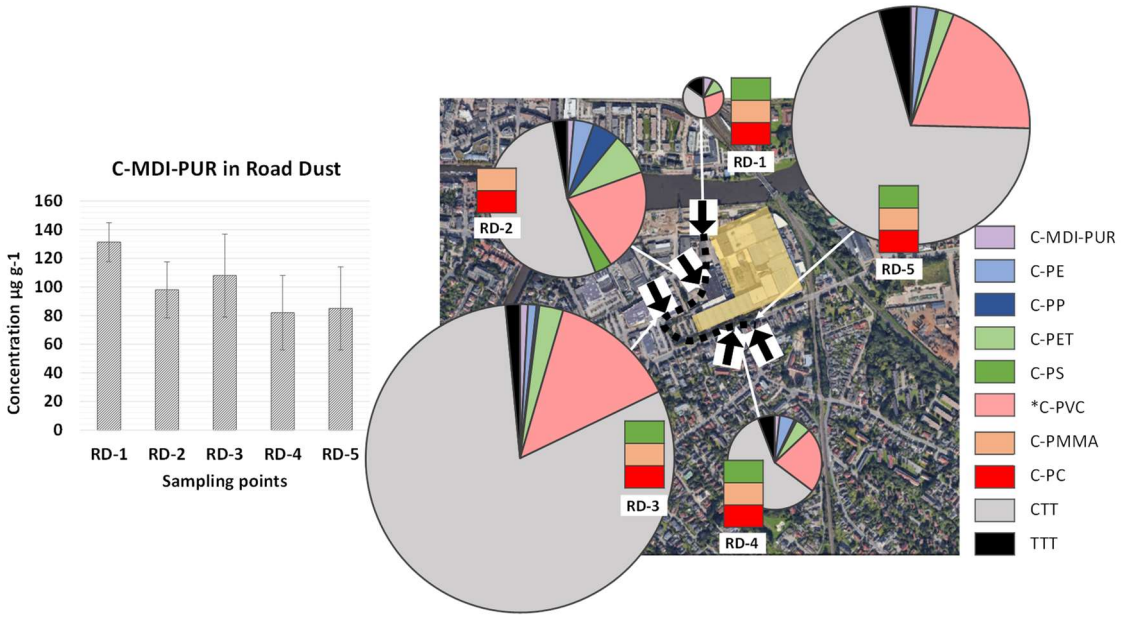

Figure 3.2.2-20. *On the left, histogram showing concentration of C-MDI-PURs at RD-1, RD-2, RD-3, RD-4 and RD-5 in dried road dust samples with error bar for standard deviation. On the right, pie charts showing the relative distribution of C-MDI-PURs compared to other analysed polymer clusters in road dust for the same sampling points [22].*

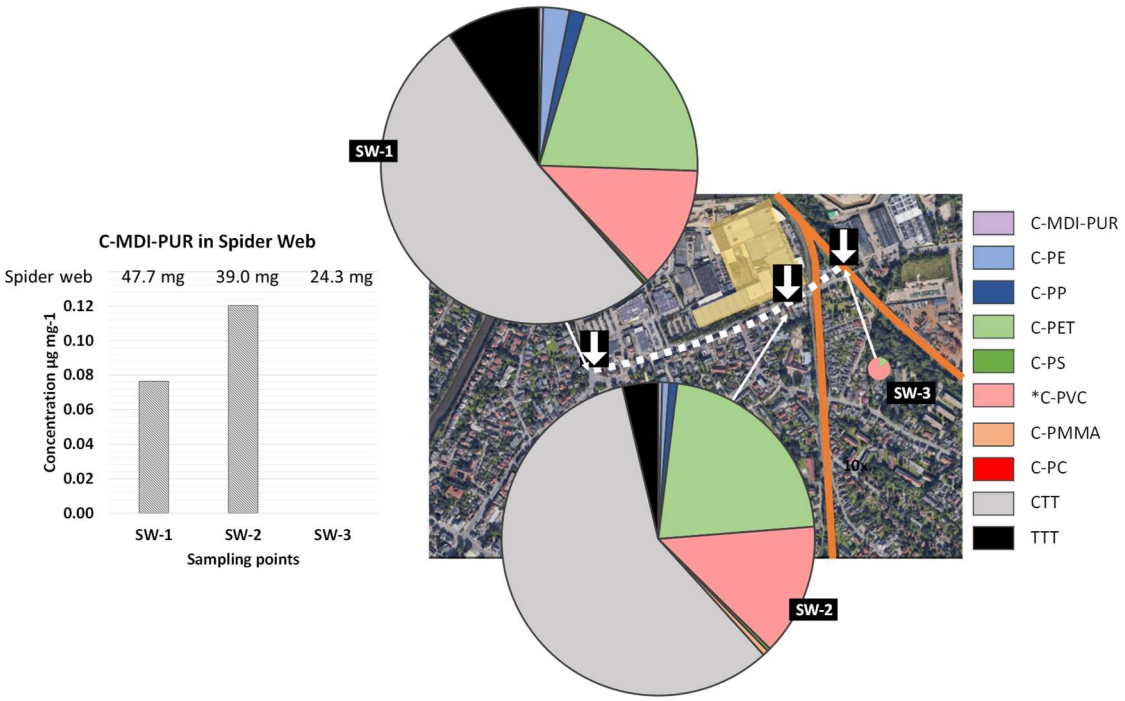

Figure 3.2.2-21. *On the left, histogram showing concentration of C-MDI-PURs SW-1, SW-2 and SW-3 in dried spider web samples. On the right, pie charts showing the relative distribution of C-MDI-PURs compared to other analysed polymer clusters in spider webs for the same sampling points [22].*

Table 3.2.2-11. *Concentrations (µg g^{-1}) and standard deviations (n = 3) obtained for each polymer cluster in road dusts at each sampling point (RD-1 – 5) and concentrations (µg mg^{-1}) obtained for each polymer cluster in spider webs at each sampling point (SW-1 – 3). Some polymer clusters were qualitatively identified but their occurrence under the limit of quantification (< LOQ) [22].*

	Concentrations ± standard deviations (µg g^{-1})					**Concentrations (µg mg^{-1})**		
	RD-1	RD-2	RD-3	RD-4	RD-5	SW-1	SW-2	SW-3
C-MDI-PUR	131 ± 14	98 ± 20	108 ± 29	82 ± 26	85 ± 29	0.08	0.07	0.00
C-PE	15 ± 2	295 ± 59	118 ± 13	242 ± 29	272 ± 11	0.50	0.13	0.00
C-PP	< LOQ	393 ± 109	38 ± 9	42 ± 13	29 ± 16	0.30	0.15	0.00
C-PET	192 ± 49	617 ± 149	328 ± 64	248 ± 78	223 ± 73	3.90	4.05	0.20
***C-PVC**	496 ± 148	1521 ± 216	1750 ± 222	1051 ± 106	2020 ± 227	2.33	2.53	1.23
C-PS	< LOQ	255 ± 64	•	< LOQ	< LOQ	0.06	0.06	0.00
C-PC	< LOQ	< LOQ	< LOQ	< LOQ	< LOQ	0.00	0.00	0.00
C-PMMA	< LOQ	< LOQ	< LOQ	< LOQ	< LOQ	0.03	0.11	0.00
CTT	645 ± 128	3804 ± 672	10566 ± 1515	2779 ± 482	7280 ± 722	9.72	10.78	0.00
TTT	264 ± 19	214 ± 39	199 ± 60	274 ± 48	448 ± 67	1.80	0.68	0.00

• RSD > 35 %

3.2.2.4. Conclusions

In the context of MPs pollution, the given study intended to provide thermoanalytical, mass related information about the complex polymer group of PURs, representing 8 % of European annual plastic demand. This had the particular aim of analysing this heterogeneous group in environmental samples. Due to the highly diversified structures of PURs, a univocal identification of the whole group is not possible by thermal analysis of complex samples. Diisocyanates have shown to be key indicators of the related PUR-subclass (e.g., MDI for MDI-PURs or TDI for TDI-PURs), but experimental conditions may affect their pyrolytic behaviour. Specifically, the formation of diamines can be promoted by interactions with inorganic matrices or by the environmental degradation of the material, leading to possible errors in polymer quantification by Py-GC-MS. However, this problem is overcome when thermochemolysis is associated to Py-GC-MS, where main indicators are methylated form of diamines. Even though thermochemolysis conditions strongly affect the sensitivity of the analysis of MDI- and TDI-PURs when individually pyrolysed, the use of TMAH showed to be basically advantageous in the simultaneous investigation of a broad variety of polymers in complex environmental matrices. In addition to greatly increased detection sensitivity for ester- and ether-based plastics, the thermochemolytic

process also has the positive side effect to minimize matrix interferences and secondary reactions for analytes e.g., PURs. The study showed that when Py-GC-MS is associated to thermochemolysis, one thermal degradation indicator can be used to identify the whole aromatic PUR subclass (e.g., Me_4-MDA for MDI-PURs and Me_3-TDA for TDI-PURs, respectively), regardless of the heterogeneity of the PUR structures. Regression models for thermal decomposition products of both TDI and MDI-PURs provided satisfactory correlation results for single polymers. Moreover, promising results were obtained when regressions of chemically different MDI-PURs were compared. ANOVA showed that, within a limited mass-range, no significant differences occurred in calibration sensitivities of different MDI-PURs. This enables a reliable mass estimation of total MDI-PURs as a cluster, regardless of chemical heterogeneity.
Environmental investigations under the same analytical conditions confirmed the capability of the method to investigate C-MDI-PURs as a representative polymer cluster within others. Results showed that C-MDI-PURs detection in urban context is strongly related to the presence of an emission source. Road dust and spider webs were confirmed to be suitable sample types for the simultaneous investigation of MPs, reflecting the contamination level of the sampling area.
Thermal analysis showed a trustworthy analytical role in the context of tracking and characterizing MP pollution. Despite the challenges defined by the heterogeneity of this broad class of contaminants, Py-GC-MS is gaining more and more consents, providing reliable characterization and mass quantification of different polymers. The study highlighted the potential of thermochemolysis-Py-GC-MS for the investigation of PURs subclasses within MPs, providing information that support the possibility for a reliable statement on the PUR content in environmental samples based on a few, characteristic thermal decomposition products.

References

[1] M. Szycher, Structure – Property relations in polyurethanes, Routledge Handbooks Online, 2012. https://doi.org/10.1201/b12343-4.

[2] A.S. Dutta, Polyurethane foam chemistry, in: Recycling of Polyurethane Foams, Elsevier Inc., 2018. https://doi.org/10.1016/B978-0-323-51133-9.00002-4.

[3] K.C. Frisch, D. Klempner, 24 - Polyurethanes, in: G. Allen, J.C. Bevington (Eds.), Comprehensive Polymer Science and Supplements, Pergamon, Amsterdam, 1989: pp. 413–426. https://doi.org/10.1016/B978-0-08-096701-1.00165-8.

[4] Plastics - the Facts 2021 • Plastics Europe, 2021. https://plasticseurope.org/knowledge-hub/plastics-the-facts-2021/.

[5] Polyurethanes chemicals and products in Europe, Middle East & Africa (EMEA), 2018, (2018).

[6] Z. Steinmetz, A. Kintzi, K. Muñoz, G.E. Schaumann, A simple method for the selective quantification of polyethylene, polypropylene, and polystyrene plastic debris in soil by pyrolysis-gas chromatography/mass spectrometry, Journal of Analytical and Applied Pyrolysis. 147 (2020) 104803. https://doi.org/10.1016/j.jaap.2020.104803.

[7] G. Liu, J. Wang, M. Wang, R. Ying, X. Li, Z. Hu, Y. Zhang, Disposable plastic materials release microplastics and harmful substances in hot water, Science of The Total Environment. 818 (2022) 151685. https://doi.org/10.1016/j.scitotenv.2021.151685.

[8] M. Huber, V.-M. Archodoulaki, E. Pomakhina, B. Pukánszky, E. Zinöcker, M. Gahleitner, Environmental degradation and formation of secondary microplastics from packaging material: A polypropylene film case study, Polymer Degradation and Stability. 195 (2022) 109794. https://doi.org/10.1016/j.polymdegradstab.2021.109794.

[9] Y.Y. Hee, K. Weston, S. Suratman, The effect of storage conditions and washing on microplastic release from food and drink containers, Food Packaging and Shelf Life. 32 (2022) 100826. https://doi.org/10.1016/j.fpsl.2022.100826.

[10] H. Bouwmeester, P.C.H. Hollman, R.J.B. Peters, Potential health impact of environmentally released micro- and nanoplastics in the human food production chain: Experiences from nanotoxicology, Environ. Sci. Technol. 49 (2015) 8932–8947. https://doi.org/10.1021/acs.est.5b01090.

[11] D.K.A. Barnes, F. Galgani, R.C. Thompson, M. Barlaz, Accumulation and fragmentation of plastic debris in global environments, Philosophical Transactions of the Royal Society B: Biological Sciences. 364 (2009) 1985–1998. https://doi.org/10.1098/rstb.2008.0205.

[12] S.J. Lim, Y.-K. Park, H. Kim, J. Kwon, H.M. Moon, Y. Lee, A. Watanabe, N. Teramae, H. Ohtani, Y.-M. Kim, Selective solvent extraction and quantification of synthetic microfibers in textile laundry wastewater using pyrolysis-gas chromatography/mass spectrometry, Chemical Engineering Journal. 434 (2022) 134653. https://doi.org/10.1016/j.cej.2022.134653.

[13] M. Fischer, I. Goßmann, B.M. Scholz-Böttcher, Fleur de Sel – An interregional monitor for microplastics mass load and composition in European coastal waters?, Journal of Analytical and Applied Pyrolysis. (2019). https://10.1016/j.jaap.2019.104711 (accessed September 9, 2021).

[14] I. Goßmann, M. Halbach, B.M. Scholz-Böttcher, Car and truck tire wear particles in complex environmental samples – A quantitative comparison with “traditional” microplastic polymer mass loads, Science of The Total Environment. 773 (2021) 145667. https://doi.org/10.1016/j.scitotenv.2021.145667.

[15] C. Dibke, M. Fischer, B.M. Scholz-Böttcher, Microplastic mass concentrations and distribution in German bight waters by pyrolysis–gas chromatography–mass spectrometry/thermochemolysis reveal potential impact of marine coatings: Do ships leave skid marks?, Environ. Sci. Technol. 55 (2021) 2285–2295. https://doi.org/10.1021/acs.est.0c04522.

[16] I. Goßmann, R. Süßmuth, B.M. Scholz-Böttcher, Plastic in the air?! – Spider webs as spatial and temporal mirror for microplastics including tire wear particles in urban air, Science of The Total Environment. 832 (2022) 155008. https://doi.org/10.1016/j.scitotenv.2022.155008.

[17] L. Roscher, M. Halbach, M.T. Nguyen, M. Hebeler, F. Luschtinetz, B.M. Scholz-Böttcher, S. Primpke, G. Gerdts, Microplastics in two German wastewater treatment plants: Year-long effluent analysis with FTIR and Py-GC/MS, Science of The Total Environment. 817 (2022) 152619. https://doi.org/10.1016/j.scitotenv.2021.152619.

[18] S. Primpke, M. Wirth, C. Lorenz, G. Gerdts, Reference database design for the automated analysis of microplastic samples based on Fourier transform infrared (FTIR) spectroscopy, Anal Bioanal Chem. 410 (2018) 5131–5141. https://doi.org/10.1007/s00216-018-1156-x.

[19] M. Matsueda, M. Mattonai, I. Iwai, A. Watanabe, N. Teramae, W. Robberson, H. Ohtani, Y.-M. Kim, C. Watanabe, Preparation and test of a reference mixture of eleven polymers with deactivated inorganic diluent for microplastics analysis by pyrolysis-GC–MS, Journal of Analytical and Applied Pyrolysis. 154 (2021) 104993. https://doi.org/10.1016/j.jaap.2020.104993.

[20] J. La Nasa, G. Biale, B. Ferriani, M.P. Colombini, F. Modugno, A pyrolysis approach for characterizing and assessing degradation of polyurethane foam in cultural heritage objects, Journal of Analytical and Applied Pyrolysis. 134 (2018) 562–572. https://doi.org/10.1016/j.jaap.2018.08.004.

[21] M. Fischer, B.M. Scholz-Böttcher, Microplastics analysis in environmental samples – Recent pyrolysis-gas chromatography-mass spectrometry method improvements to increase the reliability of mass-related data, Anal. Methods. 11 (2019) 2489–2497. https://doi.org/10.1039/C9AY00600A.

[22] I. Coralli, I. Goßmann, D. Fabbri, B.M. Scholz-Böttcher, Determination of polyurethanes within complex environmental microplastics by analytical pyrolysis, Accepted to Analytical and Bioanalytical Chemistry. (2023).

[23] D. Allan, J. Daly, J.J. Liggat, Thermal volatilisation analysis of TDI-based flexible polyurethane foam, Polymer Degradation and Stability. 98 (2013) 535–541. https://doi.org/10.1016/j.polymdegradstab.2012.12.002.

[24] H. Mikulcic, Q. Jin, H. Stančin, X. Wang, S. Li, H. Tan, N. Duić, Thermogravimetric analysis investigation of polyurethane plastic thermal properties under different atmospheric

conditions, J. Sustain. Dev. Energy Water Environ. Syst. 7 (2019) 355–367. https://doi.org/10.13044/j.sdewes.d6.0254.

[25] A.S. Tagg, J.P. Harrison, Y. Ju-Nam, M. Sapp, E.L. Bradley, C.J. Sinclair, J.J. Ojeda, Fenton's reagent for the rapid and efficient isolation of microplastics from wastewater, Chem. Commun. 53 (2017) 372–375. https://doi.org/10.1039/C6CC08798A.

[26] S. Tsuge, H. Ohtani, C. Watanabe, Pyrolysis–GC/MS data book of synthetic polymers - Pyrograms, thermograms and MS of pyrolyzates, Elsevier, 2012.

[27] M. Rutkowska, K. Krasowska, A. Heimowska, I. Steinka, H. Janik, Degradation of polyurethanes in sea water, Polymer Degradation and Stability. 76 (2002) 233–239. https://doi.org/10.1016/S0141-3910(02)00019-8.

[28] A. Lattuati-Derieux, S. Thao-Heu, B. Lavédrine, Assessment of the degradation of polyurethane foams after artificial and natural ageing by using pyrolysis-gas chromatography/mass spectrometry and headspace-solid phase microextraction-gas chromatography/mass spectrometry, Journal of Chromatography A. 1218 (2011) 4498–4508. https://doi.org/10.1016/j.chroma.2011.05.013.

[29] M. Mutsuga, M. Yamaguchi, Y. Kawamura, Quantification of isocyanates and amines in polyurethane foams and coated products by liquid chromatography–tandem mass spectrometry, Food Sci Nutr. 2 (2014) 156–163. https://doi.org/10.1002/fsn3.88.

[30] J. La Nasa, G. Biale, D. Fabbri, F. Modugno, A review on challenges and developments of analytical pyrolysis and other thermoanalytical techniques for the quali-quantitative determination of microplastics, Journal of Analytical and Applied Pyrolysis. 149 (2020) 104841. https://doi.org/10.1016/j.jaap.2020.104841.

[31] M. Fischer, B.M. Scholz-Böttcher, Simultaneous trace identification and quantification of common types of microplastics in environmental samples by pyrolysis-gas chromatography–mass spectrometry, Environ. Sci. Technol. 51 (2017) 5052–5060. https://doi.org/10.1021/acs.est.6b06362.

[32] I. Coralli, V. Giorgi, I. Vassura, A.G. Rombolà, D. Fabbri, Secondary reactions in the analysis of microplastics by analytical pyrolysis, Journal of Analytical and Applied Pyrolysis. 161 (2022) 105377. https://doi.org/10.1016/j.jaap.2021.105377.

[33] J.M. Challinor, A pyrolysis-derivatisation-gas chromatography technique for the structural elucidation of some synthetic polymers, Journal of Analytical and Applied Pyrolysis. 16 (1989) 323–333. https://doi.org/10.1016/0165-2370(89)80015-4.

[34] M. Reichenbächer, J.W. Einax, Challenges in analytical quality assurance, Springer Science & Business Media, 2011.

[35] W.C. Smith, G.S. Sittampalam, Conceptual and statistical issues in the validation of analytic dilution assays for pharmaceutical applications, J Biopharm Stat. 8 (1998) 509–532. https://doi.org/10.1080/10543409808835257.

[36] S. Zhou, M. Garcia-Perez, B. Pecha, A.G. McDonald, R.J.M. Westerhof, Effect of particle size on the composition of lignin derived oligomers obtained by fast pyrolysis of beech wood, Fuel. 125 (2014) 15–19. https://doi.org/10.1016/j.fuel.2014.01.016.

[37] A. Mlonka-Mędrala, A. Magdziarz, T. Dziok, M. Sieradzka, W. Nowak, Laboratory studies on the influence of biomass particle size on pyrolysis and combustion using TG GC/MS, Fuel. 252 (2019) 635–645. https://doi.org/10.1016/j.fuel.2019.04.091.

3.2.3. Analysis of seawater leachates from bioplastics: an analytical pyrolysis and GC-MS study

Data published on Environmental Pollution (2023). DOI: 10.1016/j.envpol.2022.120951

3.2.3.1. Introduction

The issue of ocean plastic pollution represents a global concern for its potential impact on ecosystems' health [1]. After their first introduction in society, plastics produced enormous benefits. However, now that the amount of plastic is greatly increasing and plastic wastes are not properly managed, a negative impact on ecosystems is occurring. About 8 Mt of plastics are estimated to enter the environment every year [2] and in 2018, European Commission reported that 70 – 80 % of the marine litter was represented by plastics [3]. Well before being degraded, plastics are fragmented to micro and nano plastics, with higher potential to bioaccumulate and cause detrimental health effects in marine species [4–8]. The formation of micro and nano particles is not the unique matter of concern. Plastic fragmentation and weathering may facilitate the leaching of chemical additives, e.g., compounds intentionally mixed with polymeric matrixes during manufacturing to confer the final product specific requirements [9–11]. Additives are polymer- and function-specific, and include plasticizers, flame retardants, stabilizers, antioxidants, pigments, biocides, etc. Their presence can vary from relatively low to significant amounts (from 0.05 wt% for antioxidants up to 70 wt% for phthalate esters in flexible PVC), according to their function [12]. Most of these additives are not bound to the polymer structures, therefore they can migrate into the aquatic environment with consequent risk of exposure for wildlife and humans [13,14]. Plastic leachates represent complex mixtures of additives released by plastics in the surrounding environment, including marine water. Among organic additives, bisphenols, phthalates, brominated flame retardants, organotin compounds, alkylphenols, formaldehyde, antimicrobials and azocolorants are included [12,15]. Many of the above chemicals are known or suspected Endocrine Disrupting Chemicals (EDCs), for example compounds able to interfere at different levels of the endocrine regulation inducing multiple adverse effects [16–19]. Trace metals represent a prominent group of inorganic additives, often demonstrated as hazardous to human and environmental health [20]. In addition, further intentionally and non-intentionally added substances, including unreacted monomers and side or breakdown products, do occur in plastic items [21]. Recent reports using experimentally produced plastic leachates have shown that plastics can release a variety of organic and inorganic additives into seawater within 1 – 14 days [22,23], providing evidence that plastic

additive leachates are chemically complex, and can affect marine organisms' growth, development and survival. To tackle the long-term persistence of conventional plastics, bioplastics are promoted as an alternative to conventional plastics.

Bioplastics commonly encompass a diverse family of polymeric materials that originate from biomass and/or are biodegradable. Confusion usually occurs among bio-, bio-based and biodegradable plastics [24,25]. Bio-based plastics are those containing organic carbon of renewable origin from the natural environment, while biodegradable plastics are made of polymers susceptible to mineralization into CO_2, biomass and water by biological activity [26,27]. Three main groups can be recognised: (I) Bio-based or partially bio-based plastics, such as bio-based polyethylene (bio-PE) or polyethylene terephthalate (bio-PET) (so-called drop-in solutions), that are not biodegradable as they respective fossil-based polymers; (II) Bio-based and biodegradable plastics, such as polylactic acid (PLA), poly(hydroxyalkanaoate) (PHA), polybutylene succinate (PBS), and starch blends; (III) Biodegradable plastics based on fossil resources, mostly polyesters, such as poly(butylene adipate-co-terephthalate) (PBAT). Bioplastics made of these polyesters can be manufactured in forms of composites, as for instance PBAT/PLA and PBAT/starch. It is worth to mention that some biodegradable plastics do not degrade in industrial or natural settings (e.g., plastics suitable to industrial composting) [28]. The market share of bioplastics is relatively low compared to conventional thermoplastics; however, it is steeply increasing worldwide after new law regulations have been approved in many countries [29]. Although most studies have shown no harmful effects from degradation of biodegradable polymers [30], very little is known on the bioplastic chemical safety, the chemical nature of compounds included in the items, and the potential toxicity of the leachates for ecosystem and human health. It has been reported that bioplastics contain similar additives as their conventional counterparts [31] and may be similarly toxic [31,32]. Bioplastics undergo ageing processes mediated by abiotic and biotic agents (mechanical abrasion, thermal degradation, hydrolysis, photo-oxidation, biodegradation) that can deeply affect the properties of the polymer matrix, with consequent additive release. Moreover, bioplastics are more vulnerable to degradation with respect to conventional plastics, thus can produce microplastics or release associated toxic chemicals more readily [24].

In general, hidden compromises and vagueness are found in the information provided by the manufacturers both for bioplastic item composition as well as for their degradation due to environmental agents [30,33], which hampers establishing correlations between exposure and potential biological effects. To get this type of information for bioplastics, a research effort focusing on both chemical and biological aspects is needed [34].

The present work investigated the biological responses in mussels, *Mytilus galloprovincialis* exposed to seawater leachates from different types of bioplastics. Mussels of the genus *Mytilus* are worldwide considered as a suitable sentinel organism for biomonitoring the effects of contaminants in coastal waters [35]. Leachates were experimentally produced and chemically characterized in terms of inorganic and organic chemical content to identify possible relationships with biological effects. The screening of a wide range of leachate concentrations was performed for the impairment of mussel gamete fertilization, embryonic development, and larvae survival and motility. An array of cellular, biochemical and physiological responses (biomarkers) was also investigated to evaluate adult mussel health status after in vivo exposure to the leachates. Results were supported by chemical investigations of organic and inorganic compounds in leachates and the characterisation of the starting bioplastics by analytical pyrolysis.

3.2.3.2. Experimental

3.2.3.2.1. Starting materials

Starting materials were prepared from commercial items and provided in particles with ≈ 0.5 cm size (Figure 3.2.3-1) by the research group on *Health and Environmental Physiology* of the University of Bologna at the Campus of Ravenna, in order to compare chemical and physiological results with previous studies [20,22]. Three different types of bioplastics were analysed to get information about their leaching behaviour: (I) bio-based plastic from compostable bag for organic wastes (Bio-PL), of unknown nature material, but labelled as suitable to industrial composting; (II) polylactic acid from a disposable item (PLA), 100 % bio-based and biodegradable; (III) bio-polyethylene terephthalate (Bio-PET) from a disposable bottle, partially bio-based and non-biodegradable. Finally, tire rubber (TR) from bicycle tire was used as positive control, given for the high number of studies on the toxicity of tire leachates to water organisms [20,22,23]. Artificial seawater (ASW), prepared according to ASTM (2004) as previously described by Capolupo et al. (2020) [20], was used to simulate leachates in marine environment [20,22].

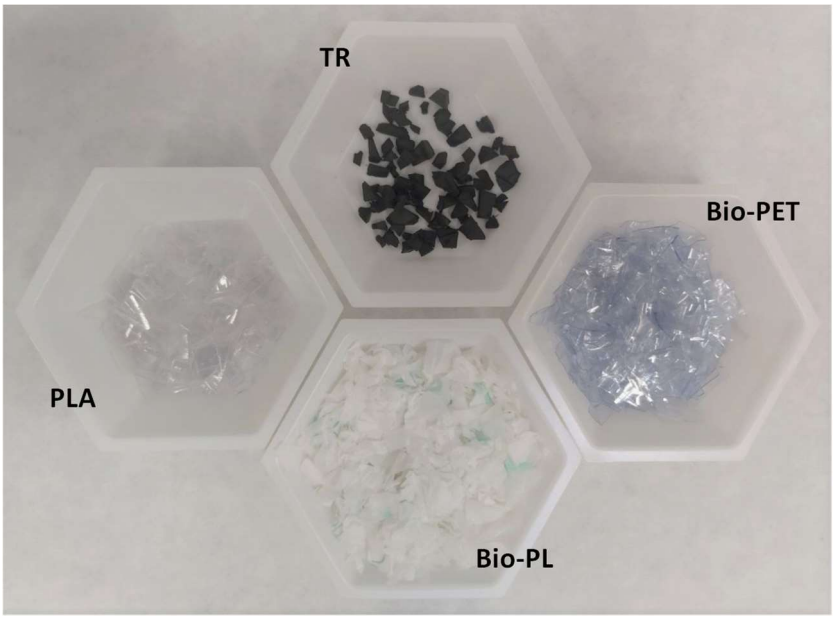

Figure 3.2.3-1. *Starting materials, TR, PLA, Bio-PL and Bio-PET. Each weighting boat contains 2.8 g of polymer.*

3.2.3.2.2. Material characterisation

The chemical identity of the commercial bioplastic items was investigated by analytical pyrolysis (Py-GC-MS) and infrared spectroscopy (ATR-FTIR). This step was crucial because polymers which compose the materials may be not fully described in their labels, leading to mistakes in leachates' investigation. As an example, bottles labelled as PLA resulted to contain other polymers and only a low content of PLA, after analysis by Py-GC-MS and ATR-FTIR [36].

3.2.3.2.2.1. Py-GC-MS

The solid plastic materials were pyrolysed with a Multi-Shot Pyrolizer (EGA/PY-3030D Frontier Lab, Japan) interfaced to a GC coupled with MS (7890B and 5977B Agilent Technology, USA). Instrumental conditions are summarised in Table 3.2.3-1. Materials were cut into very tiny pieces (0.14 ± 0.02 mg) with a scalpel and introduced into a stainless-steel cup (Eco-cup LF, Frontier Lab);

3.2.3.2.2.2. FTIR-ATR

Solid plastic materials were cut in small fragments with the help of a scalpel and spectroscopic analyses were conducted with a FT-IR spectrometer (Cary 630 FT-IR Spectrometer, Agilent, USA) with ATR diamond crystal. Experimental conditions are described in Table 3.2.3-2. The ATR diamond crystal was cleaned with acetone and a background scan was performed between each sample. In order to confirm the nature of the polymers, results were compared with literature.

Table 3.2.3-1. *Instrumental conditions for Py-GC-MS analyses.*

Pyrolyzer	**Multi-Shot Pyrolyzer (EGA/PY-3030D) - Frontier Lab**	
	Furnace temperature	500 °C
	Interface temperature	280 °C
Gas chromatograph	**Agilent 7890B**	
	Column	HP-5ms Ultra Inert Agilent 19091S-433UI 30 m x 250 µm x 0.25 µm
	Carrier gas	He
	Column flow	1 mL min^{-1}
	Split	1:100
	Injector	280 °C
Oven programmed temperature	Initial temperature	40 °C
	Temperature hold time	2 min
	Temperature rate	20 °C min^{-1}
	Maximum temperature	305 °C
	Temperature hold time	12 min
Mass spectrometer	**Agilent 5977B**	
	MS source temperature	230 °C
	MS quad temperature	150 °C
	Mass scan	35 – 600 *m/z*
	Ionization energy	70 eV

Table 3.2.3-2. *Instrumental conditions for FTIR-ATR analyses.*

Cary 630 FTIR Spectrometer with ATR diamond crystal	
Spectral range	650 – 4000 cm^{-1}
Background scans	32
Sample scans	32
Resolution	8 cm^{-1}

3.2.3.2.3. Leachate procedure

A first batch of seawater leachates was initially prepared by the research group on *Health and Environmental Physiology* of the University of Bologna at the Campus of Ravenna, which utilised the same sample batch for biological tests. Leachates were produced ASW, prepared according to ASTM (2004) as previously described by Capolupo et al. (2020) [20]. Briefly, the selected materials (Figure 3.2.3-1) were added to ASW at a final concentration of 80 g L^{-1}. Samples were

placed in a rotating incubator (125 rpm) at RT (≈ 20 °C) for 14 days in the dark to allow for chemical leaching. Leachates were then passed through a sterile filter (0.2 mm Nalgene®) to eliminate particles and kept in darkness at 4 °C until use. Glass or polytetrafluoroethylene materials were utilised whenever feasible, laboratory items were rinsed with acetone (pico-grade, LGC Standards) and glassware annealed at 200 °C for ≥3 h. To complete chemical analyses, a second batch of leachates from the same starting materials was necessary. Leachate were produced following the same procedure, but with some difference in laboratory materials [20]. Four centrifuge tubes (Argos TC5000, 50 mL, polypropylene, conical natural) were filled with artificial water and starting materials reaching concentrations of 80 g L^{-1} (Bio-PET, PLA, Bio-PL) and one further tube was filled with artificial water only to control the procedure (blank). Tubes were installed on a Rotator Drive STR4 and subjected to a rotational rate of 60 rpm for 14 days at room temperature (≈ 18 °C), in dark. Samples were then filtered with a vacuum filtration apparatus using a cellulose nitrate filter (Sartorius 1140-4-N) with 0.2 µm particle retention. Leachates were poured in the same centrifuge tubes used for the leachate procedure ad they were stored in dark at -20 °C prior to extraction. Before the extraction procedure, samples were transferred in a fridge at 4 °C, waiting for the sample melting and then transferred at room temperature.

Biological tests were performed on the first batch of leachates only, as well as analyses of metals. Semi-quantitative chemical analyses of organic compounds were carried out on the second batch of samples, after the qualitative confirmation of chemical composition of leachates by comparison with the first sample batch.

3.2.3.2.4. Analysis of organic compounds by leachate extractions

Leachate extractions were arranged to perform chemical analyses by GC-MS. For the first qualitative analyses (on the first batch of leachates), 2 mL of samples were used for the extraction, then the volume was increased to 6 mL (from the second batch of samples) to obtain more reliable quantitative results. Anyway, the same extraction procedure was applied. Seawater leachates (2 mL or 6 mL from each starting material, bioplastics and rubber) were introduced into 10 mL-glass centrifuge tubes, acidified to pH 3 with HCl 0.1 M and extracted with 1 mL of ethyl acetate. Tri-*tert*-butylbenzene (TTB) was used as IS and 5 µL of 1.0 mg mL^{-1} solution in ethyl acetate was added to each sample. Glass tubes were previously covered with aluminium foil in order to avoid the contact between the organic solvent and polypropylene-caps. Samples were extracted in a Rotator Drive STR4 at ≈ 20 rpm for 20 minutes, then they were centrifuged at 3100 rpm for 15 min to separate the two phases. The organic supernatant was withdrawn

with a Pasteur pipette and transferred into an 8-mL glass vial. The procedure was repeated three times obtaining 3 mL of extracted organic phase for each sample. Anhydrous sodium sulphate was used to eliminate residual water in the extracted sample. A Buchner apparatus was installed with a glass filter (Whatman, 0.2 µm particle retention). 3 g of anhydrous sodium sulphate was added on the filter and the extracted sample was gently poured on the salt, allowing a slow contact with the residual water. The vial containing the sample was rinsed three times with ethyl acetate and the rinsing solvent was each time transferred into the filtration apparatus, still switched off. After 5 minutes of contact with the salt, the solution was filtered switching on the apparatus, then the funnel was rinsed three times with ≈ 1 mL of ethyl acetate. The dehydrated sample was recovered rinsing the whole apparatus 3 times and concentrated to about 500 µL by N_2 flow. The sample was then fully transferred into a GC vial, previously weighted. The weight of the sample was calculated by difference (Table 3.2.3-3) in order to know the exact volume of sample, which was estimated assuming the sample as ethyl acetate (density = 902 kg m^{-3}). Therefore, it was also possible to estimate the exact amount of IS injected in each analysis. Three replicate analyses were performed on each leachate sample (#1, #2 and #3) and parallel samples were prepared with ASW only, as procedural blank.

Table 3.2.3-3. *Extracted seawater in ethyl acetate (weight and volume) and amount of IS injected in each GC-MS run.*

	Sample (mg)	Volume (µL)	TTB injected (ng)
Blank#1	411	456	11.01
Bio-PL#1	420	465	10.78
TR#1	433	480	10.45
PLA#1	486	539	9.31
PET#1	388	430	11.66
Blank#2	371	411	12.19
Bio-PL#2	445	494	10.16
TR#2	438	485	10.34
PLA#2	442	490	10.23
PET#2	413	457	10.96
Blank#3	404	447	11.21
Bio-PL#3	400	444	11.30
TR#3	419	464	10.80
PLA#3	426	472	10.62
PET#3	315	349	14.38

3.2.3.2.4.1. GC-MS

Analyses were performed using an auto injector Shimadzu AOC-20i and instrumental conditions are shown in Table 3.2.3-4.

Table 3.2.3-4. *Instrumental conditions for GC-MS analyses.*

Gas chromatograph	**Shimadzu GC-2010**	
	Column	Zebron ZB-35 30 m x 250 µm x 0.25 µm
	Carrier gas	He
	Column flow	1.1 mL min^{-1}
	Injection volume	1 µL
	Injector	250 °C
	Splitless	
Oven programmed temperature	Initial temperature	40 °C
	Temperature hold time	2 min
	Temperature rate	10 °C min^{-1}
	Maximum temperature	320 °C
	Temperature hold time	6 min
Mass spectrometer	**Shimadzu GCMS-QP2010S**	
	MS source temperature	230 °C
	MS quad temperature	240 °C
	Mass scan	35 – 500 *m/z*
	Ionization energy	70 eV
	Solvent delay	3 min

Data for the semi-quantitative analysis were collected by integrating the peaks in TIC (total ion current) chromatograms. A pure quantitation was not performed because not all the analytes were commercially available for calibration. The amount of the compounds (μg_x) was calculated by assuming unitary relative factor compared to the IS using the Equation 3.2.3-1.

$$\mu g_x = \frac{A_x}{A_{IS}} \mu g_{IS} \qquad \textit{Equation 3.2.3-1}$$

where μg_{IS} is the quantity of injected TTB-IS, which was calculated for each sample on the basis of the final volume of the extracted sample (Table 3.2.3-3); A_x and A_{IS} refer to the peak areas of compound x and TTB-IS respectively. In the absence of pure standard analytes, the calculated concentrations are semi-quantitative and the identification was based on NIST14 MS library match tentative. These calculations were elaborated on the second batch of leachates, whereas the first batch of leachates (used for biological tests and analysis of metals) was only qualitatively analysed to confirm the presence of tentatively identified components.

3.2.3.2.4.2. Silylation procedure

Silylation was performed on extracted samples to obtain further qualitative information. To evaluate the extent of the derivatisation, tridecanoic acid (TDA) was used as procedural IS, preparing a 1.0 mg mL^{-1} solution in ethyl acetate. To derivatise the extracted compounds, 200 µL seawater extracted samples was introduced into a 1.5 mL amber vial, added with 5 µL of TDA-IS solution and silylated with 200 µL of BTSFA. The vial was immersed in a water bath for 2 h, maintaining the temperature at 60 °C with a heating plate. Aliquots of all samples were subjected to silylation (including procedural blanks, from ASW samples) and solutions were analysed by GC-MS, immediately after the end of the reaction. The same experimental conditions showed in Section 0 were applied to silylated samples, increasing the solvent delay from 3 to 9 min.

3.2.3.2.5. Analysis of metals

Analyses of metals were performed by the research group on *Health and Environmental Physiology* of the University of Bologna at the Campus of Ravenna, under the supervision of Prof. Elena Fabbri (Department of Biological, Geological, and Environmental Sciences) [23,37].
For trace metals assessment, leachate samples (from the first sample batch) were diluted in MilliQ water before internal standards (^{103}Rh and ^{115}In) were added. Analysis was performed using an Agilent 8800 Triple Quadrupole ICP-MS (ICP-QQQ) equipped with a SPS 4 Autosampler, and quantification performed using standards from Inorganic Ventures.

3.2.3.2.6. Biological tests

Biological tests (on the first leachates batch) were performed by the research group on *Health and Environmental Physiology* of the University of Bologna at the Campus of Ravenna, under the supervision of Prof. Elena Fabbri (Department of Biological, Geological, and Environmental Sciences) [23,37].

3.2.3.2.6.1. Mussel early life stages endpoints

Early life stages endpoints investigated in this work encompassed mussel gamete fertilization, embryotoxicity, larvae motility and survival. Biological effects of 11 different leachate concentrations were assessed in vitro, ranging from 100 % (no dilution) to 0.6 % (167 times dilution) leachate concentrations in seawater. All experiments were carried out in quadruplicate (n = 4) and parallel samples were run as controls (filtered ASW).

Fertilization and embryo-larval development

The effect of bioplastic leachates on gamete fertilization was evaluated as previously reported by Capolupo et al. (2020) [20], by exposing sperms to the leachates (100 % – 0.6 % concentration) for 1 h prior to add eggs in 1:5 proportion as in ASTM (2004) [38]. The reaction was blocked after 30 min by adding calcium buffered formalin (4 %). The acute embryotoxicity test [38] was adapted to 96 microwell plates [39] to screen the impact of bioplastic leachates on *M. galloprovincialis* embryo-larval development. Prior to leachate exposure, mussel oocytes were fertilized by mixing eggs and spermatozoa at a 1:5 ratio in 96-well plates. Fifty eggs/well were used for fertilization test. After microscopical verification of (> 90 %) fertilization success, embryos (50 embryos/well) were exposed for 48 h to different dilutions of bioplastic leachates; the test was blocked as above described, and samples examined at 40× magnification using an inverted microscope. Normally developed larvae showing the typical "D-shaped" veliger stage in the absence of developmental failures (e.g., uncomplete shell, protruding velum) were identified. According to ASTM (2004), the test was considered acceptable if showing > 70 % of normal D-veligers.

Larvae motility and survival

D-shaped larvae obtained by egg fertilization were reared until 5 days post fertilization in laboratory conditions and then exposed to the leachates in 96-well microplates at a density of 50 larvae/well, as previously described [12]. Results were recorded up to 48 h (motility) and 216 h (mortality) following the criteria previously reported by Sprung (1984) [40].

3.2.3.2.6.2. Adult mussel exposure and biomarker evaluation

Experimental design

Adult mussels (*M. galloprovincialis*) were purchased from a mussel farm (Cesenatico, Italy) and acclimated in controlled laboratory conditions (filtered seawater, 16 °C, 14 h:10 h light/dark conditions) for four days before experimental treatment. Ten mussels were then placed in aquaria (3 per experimental condition) each containing 10 L of filtered seawater, and exposed to 0.6 % concentration of leachate (167 x dilution of the original leachates) for seven days in line with previous experimental exposure using thermoplastic leachates [22].

All leachates were tested in triplicate, each aquarium representing a single experimental replicate (n = 3). Aquaria for control condition with only filtered seawater were run in parallel (n = 3). The exposure was performed in controlled conditions of temperature (16 – 18 °C), photoperiod 14 h:10 h light/dark) and feeding (1200 cells/mL of the green alga *Nannochloropsis*

oculata), as previously described by Capolupo et al. (2021) [22]. Leachates and food were daily renewed after water change.

Biomarker analysis

After exposure, mussel tissues were dissected and, depending on the parameter to be tested, frozen in liquid N_2 then stored at -80 °C, or immediately used for analysis. A battery of nine biomarkers was assessed following the OSPAR 2013 protocol [35], namely lysosome membrane stability (LMS), lysosome/cytosol ration (LYS/CYT), neutral lipid (NL), malondialdehyde (MDA), and lipofuscin (LF) accumulation, and lysozyme (LYZ), catalase (CAT), glutathione S-transferase (GST), and acethylcholinesterase (AChE) activities. Haemocytes were collected from 4 mussels per vessel and LMS evaluated by the Neutral Red Retention Assay (NRRA) [41]. LYS/CYT, NL and LF accumulation were assessed on 10 µm cryo-sections of mussel digestive glands as published by Capolupo et al. (2021) [22]. Enzymatic assays were performed in pools of digestive glands and/or gills taken from 6 mussels per vessel (18 mussels per experimental condition). After homogenization and centrifugation, specific assays were conducted spectrophotometrically [22]. Gills homogenates were used for determination of AChE activity; after incubation with 0.5 mM acetylthiocholine iodide and 0.33 mM 5.50-dithiobis-2-nitrobenzoic acid (DTNB) changes in absorbance were followed at 405 nm for 10 min [42]. Serum LYZ activity was measured as previously described Capolupo et al. (2021) [43], following for 10 min the decrease in absorbance due to the LYZ effect on *Micrococcus lysodeikticus*.

3.2.3.3. Results

The need to obtain public information on the composition of plastics was stressed [44], even more when proposing bioplastics as safer alternative to conventional plastics ([45,46]). Effect-based approaches are needed to assess the overall toxicity of plastic items, which consider known and unknown additives released by plastic items, including NIAS, and their effects as mixtures. To the best of our knowledge only two investigations are available that report on bioplastic leachates composition and their biological effects on marine organisms, e.g., marine bacteria [32] and sea urchin larvae [47]. Zimmermann et al. (2020) [32] applied methanol extraction and 1 h-sonication in order to obtain leachates from several bioplastics; a large number of different compounds (> 1000 chemicals each in 80 % of the samples) including toxic chemicals were found in the bioplastics and plant-based items examined, including erucamide, Irganox 1076, tris (2-nonylphenyl) phosphate, etc. which also occurred in petroleum-based

plastics. The Authors also showed that commercial bio-based and/or biodegradable items may cause toxicity similar to the conventional ones. Uribe-Echeverría and Beiras (2022) [47] investigated the chemical composition of leachates obtained in seawater (24 h) from 3 different bioplastics: polyhydroxybutyrate resin (PHB), polylactic acid cups (PLA) and polylactic acid/polyhydroxyalkanoate items (PLA/PHA). Unexpectedly, a wide range of additives was found in PHB including chlorinated (1-chloro-tetradecane), brominated (dodecyltrimethylammonium bromide) and iodinated (1-iodo-hexadecane) biocides. A few chemicals were released from PLA (oxo-methanol benzoate, 1,5-dimethyl-1H-pyrazole-3,4-diamine) and PLA/PHA (including isocrotonic and crotonic acid, and 2-pentenoic acid) items. The mixture toxicity for sea urchin larvae fertilization and development was observed after exposure to PHB leachates, while PLA and PLA/PHA were ineffective. Complementary to the above studies, the present experiments aimed to analyse the chemicals released by bioplastic items after incubation for 14 days in seawater. Impairment of biological endpoints were evaluated after exposure of both early-larval stages and adult mussels to the leachates. Data were compared with control sample (seawater, incubated in parallel) and a positive sample represented by tire rubber leachate.

3.2.3.3.1. Material characterisation by Py-GC-MS

Py-GC-MS and ATR-FTIR were used to confirm the chemical identity of the polymers composing the commercial materials. As an example of the importance of this analytical check, Klein et al. (2021) found that bottles labelled as PLA resulted to contain other polymers after analysis by Py-GC-MS and ATR-FTIR [36].

Bio-PET and PLA are common polymers and the chemical composition of the pyrolyzates was confirmed by literature comparison [48]. The obtained pyrograms are shown in Figure 3.2.3-2 for Bio-PET and in Figure 3.2.3-3 for PLA and characteristic peaks are summarised in Table 3.2.3-5. Pyrolysis of Bio-PET led to the formation of the same pyrolyzates as fossil-based PET, many oxygenated aromatic compounds, derivative of benzoic and terephthalic acid (Figure 3.2.3-2). The label of the Bio-PET bottle stated that 30 % of the package comes from recycled PET, but Py-GC-MS cannot differentiate between virgin and recycled PET, since they qualitatively generate the same pyrolyzates [49].

Lactides (meso and D,L forms) were the main pyrolysis products of PLA. These compounds derive from the lactic acid (L and D), the starter of PLA polymerisation which can take place by direct condensation or through the formation of lactides (ring opening polymerisation) [50]. Besides to lactides, in PLA pyrograms (Figure 3.2.3-3) some fragments of lactic acid are present, such as

acetaldehyde, 2,3-petadione and acrilyc acid and they all were confirmed by Tsuge et al. (2012) [48].

Bio-PL and TR were provided from commercial items without chemical specification, therefore their pyrolysis led to highly informative results on their chemical structures. Identification of materials which compose Bio-PL was more challenging and analyses of an additional polymer were necessary. The presence of both meso-lactide and D,L-lactide in the pyrolyzate suggested the presence of PLA (Figure 3.2.3-4). PLA is 100 % compostable in industrial composting facilities, therefore it is plausible to find it in compostable plastic bag for organic wastes. Several peaks not associated to PLA were tentatively identified as butenyl esters of adipic and terephthalic acid [51]. These pyrolysis products are consistent as building block of polybutylene adipate terephthalate (PBAT, Figure 3.2.3-5), produced from the polycondensation of 1-4-butanediol with adipic acid and terephthalic acid [52]. PBAT is used in packaging technology, in combination with other polyesters blended with starch to improve properties and reduce costs while maintaining biodegradability [52]. The polymer was pyrolysed under the same conditions and the products evolved from PBAT were consistent with those found in the pyrogram of Bio-PL. In particular, a cyclic molecule virtually derived from the condensation of the monobutylester of adipic acid, the 1,6-dioxacyclododecane-7,12-dione (peak #7 in Figure 3.2.3-4) was tentatively identified by NIST14 library and literature comparison [51]. PBAT is used in packaging technology as a potential substitute of high density polyethylene for especially for waste bags, food containers and film wraps [53]. Thanks to its physical properties which include flexibility, good tear resistance and biodegradability, it is an attractive polymer used alto in combination with other polyester or with thermoplastic starch to improve the mechanical properties [52,54,55]. However, pyrolysis markers of starch were not detected indicating that this compostable plastic bag was not based on starch. In order to better understand how the provided Bio-PL was representative of the biodegradable plastic bags for organic wastes, four further commercial bags were analysed (data not shown). All the items were accompanied by certified labels, indicating to be biodegradable in industrial composting, according to standard ISO 14855 [56,57]. Interestingly, despite different chemical compositions resulted from the pyrograms, the presence of a peak tentatively attributed to 1,6-dioxacyclododecane-7,12-dione was found in all the samples, confirming the relevance of this compound.

Finally, pyrogram of TR was featured by limonene and 2,4-dimethyl-4-vinylcyclohexene typical markers of attributed to polyisoprene rubber [48,58,59] (Figure 3.2.3-6). Py-GC-MS can also provide information about the presence of organic additives [60] and, besides thermal degradation products of the rubber, two main additives were be identified evolved by volatilisation, namely benzothiazole and 1,2-dihydro-2,2,4-trimethyl quinoline [58,61].

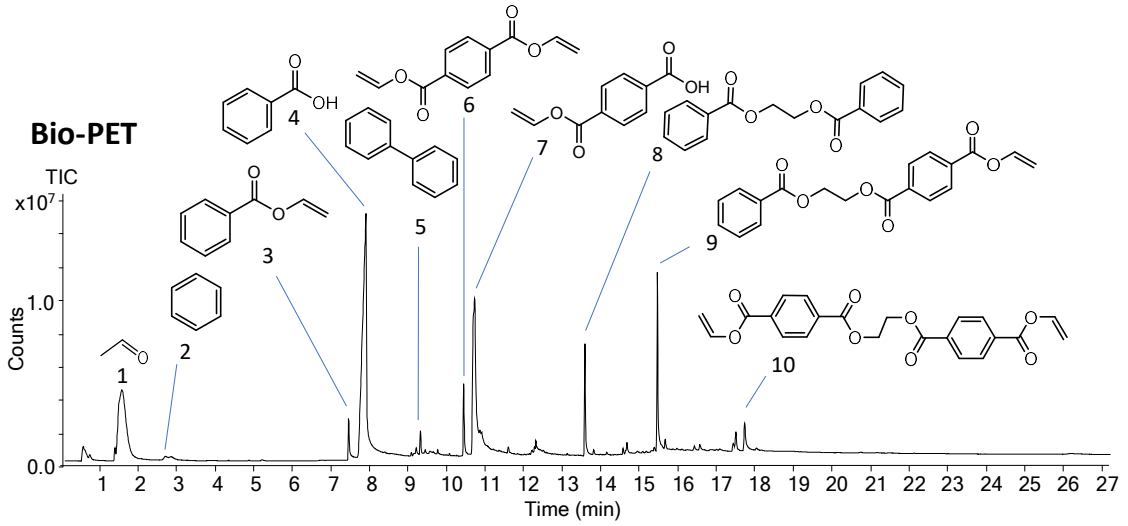

Figure 3.2.3-2. *Pyrogram do form Bio-PET Py-GC-MS (T_{Py} = 500 °C). Peak numbers refer to Table 3.2.3-5, Bio-PET section [37].*

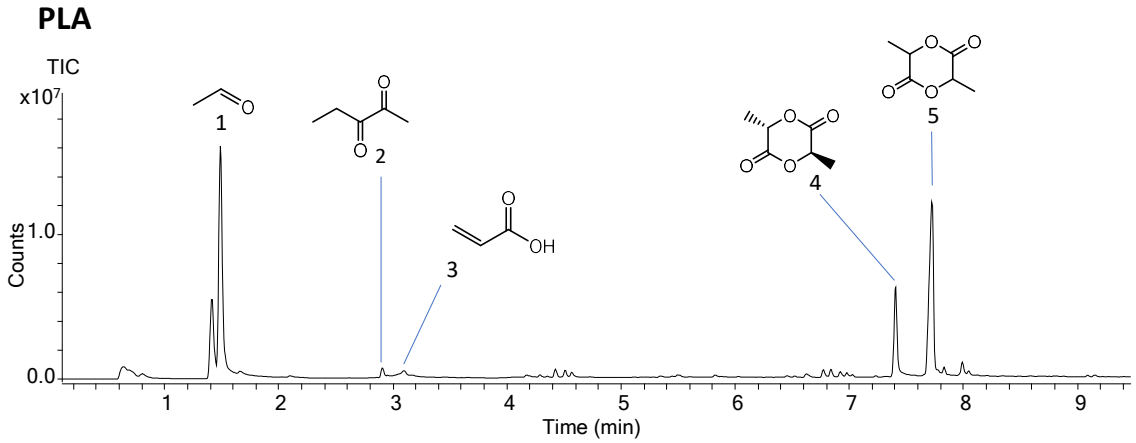

Figure 3.2.3-3. *Pyrogram do form PLA Py-GC-MS (T_{Py} = 500 °C). Peak numbers refer to Table 3.2.3-5, PLA section [37].*

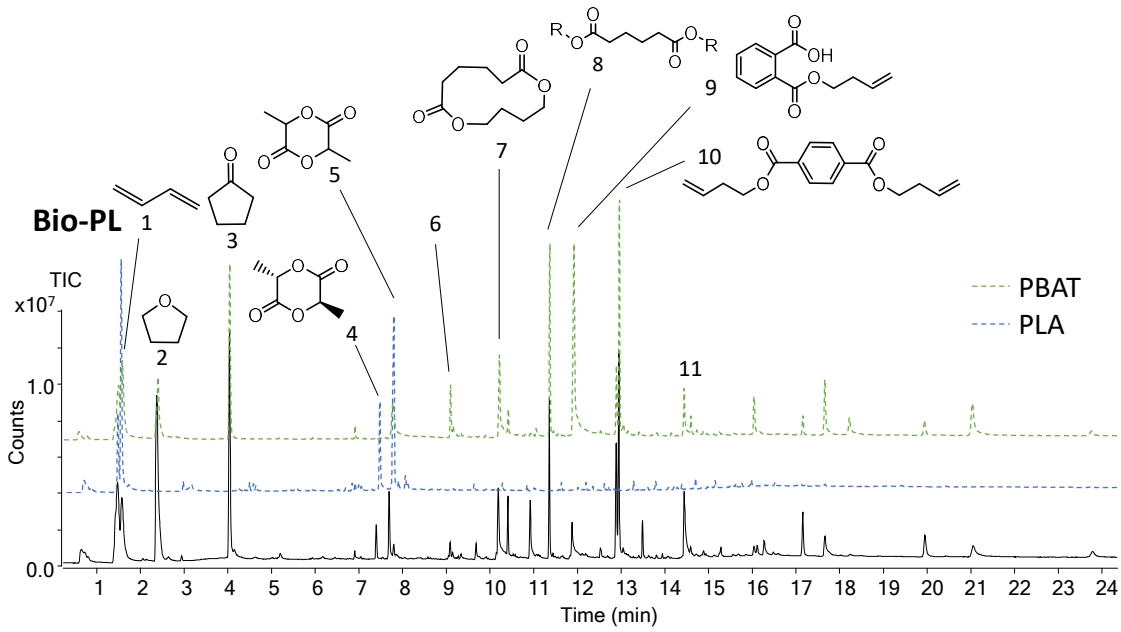

Figure 3.2.3-4. *Pyrogram do form Bio-PL Py-GC-MS (T_{Py} = 500 °C). Peak numbers refer to Table 3.2.3-6, Bio-PL section [37]. R = -H or -C_4H_6.*

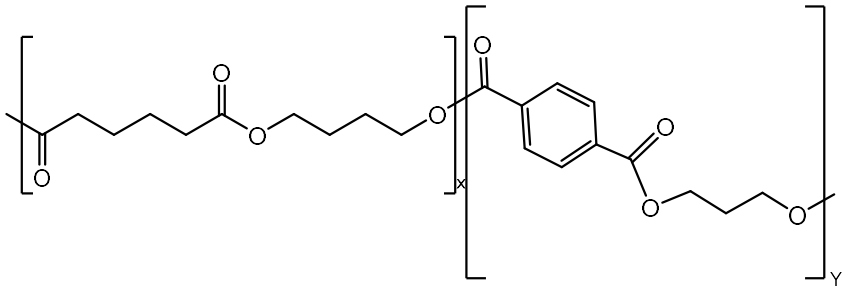

Figure 3.2.3-5. *PBAT structure [37].*

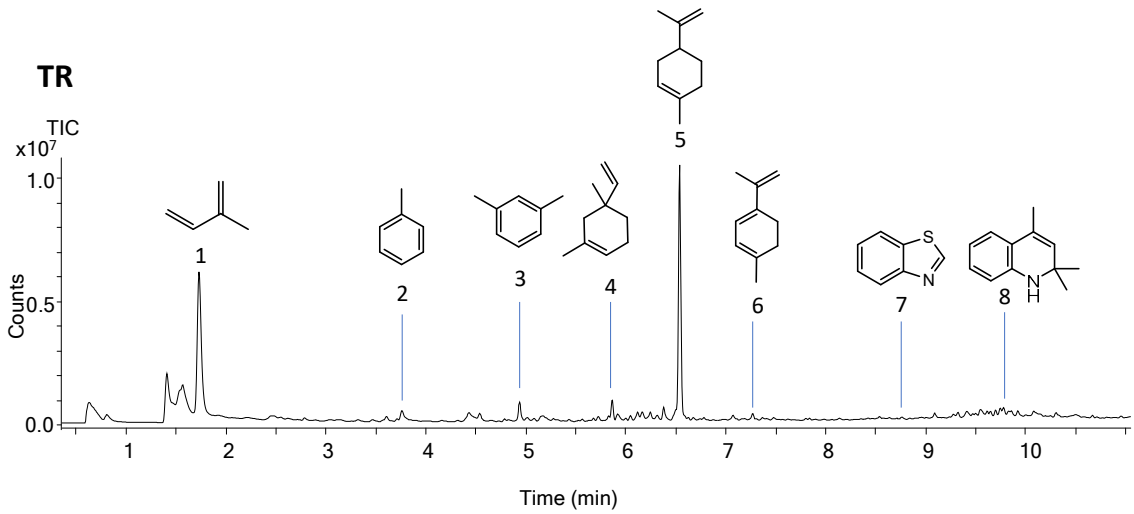

Figure 3.2.3-6. *Pyrogram do form TR Py-GC-MS (T_{Py} = 500 °C). Peak numbers refer to Table 3.2.3-6, TR section [37].*

Table 3.2.3-5. *Polymer characterisation from Py-GC-MS data (RT retention time, m/z, base peak in bold), attribution from literature. Reference numbers (#) to Figure 3.2.3-2 and Figure 3.2.3-3.*

#	Compound	*m/z*	RT (min)	Reference
Bio-PET				
1	acetaldehyde	43, 44	1.5	[48]
2	benzene	44, 51, 78	2.7	[48]
3	vinyl benzoate	51, 77, 105	7.5	[48]
4	benzoic acid	77, 105, 122	7.9	[48]
5	diphenyl	76, 128, 154	9.3	[48]
6	divinyl terephthalate	76, 104, 175, 218	10.5	[48]
7	4-(vinyloxycarbonyl) benzoic acid	65, 121, 149, 192	10.7	[48]
8	ethan-1,2-diyl dibenzoate	77, 105, 227	13.6	[48]
9	2-(benzoyloxy)ethyl vinyl terephthalate	105, 149, 297	15.5	[48]
10	ethan-1,2-diyl divinyl diterephthalate	104, 162, 325, 367	17.7	[48]
PLA				
1	acetaldehyde	43, 44	1.5	[48]
2	2,3-pentadione	43, 57, 74, 100	2.9	[48]
3	acrylic acid	45, 55, 72	3.2	[48]
4	meso-lactide	45, 56	7.4	[48]
5	D,L-lactide	45, 56, 70	7.7	[48]

Table 3.2.3-6. *Pyrogram characterisation from Py-GC-MS data (RT retention time, m/z, base peak in bold), comparison with literature or NIST14 library (NIST) for the attribution to specific polymers. Reference numbers (#) to Figure 3.2.3-6 and Figure 3.2.3-4.*

#	Compound	*m/z*	RT (min)	Attribution	Reference
Bio-PL					
1	1,3 butadiene	39, 54	1.6	PBAT	NIST
2	tetrahydrofuran	42, 72	2.4	PBAT	[51]
3	cyclopentanone	41, 55, 84	4.0	PBAT	[51]
4	meso-lactide	45, 56	7.4	PLA	[48]
5	D,L-lactide	45, 56, 70	7.7	PLA	[48]
6	benzoic acid derivative	54, 77, 105, 135	9.1	PBAT	NIST
7	1,6-dioxacyclododecane-7,12-dione	55, 84, 100, 129	10.4	PBAT	[51]
8	butenyl adipate derivative	55, 101, 111, 129	11.4	PBAT	NIST
9	2-((but-3-enyloxy) carbonyl) benzoic acid	54, 104, 121, 149	11.9	PBAT	[51]
10	terephthalic acid di(but-3-enyl) ester	54, 149, 203	13.0	PBAT	NIST
11	unknown	54, 149, 221	15	PBAT	NIST

TR					
1	isoprene	39, 53, 67	1.7	PI rubber	[48,58,59]
2	toluene	65, 91	3.8	PI rubber	[48,58,59]
3	m-xylene	77, 91, 106	4.9	PI rubber	[48,58,59]
4	2,4-dimethyl-4-vinylcyclohexene	68, 93, 121, 136	5.9	PI rubber	[48,58,59]
5	limonene	68, 93, 121, 136	6.5	PI rubber	[48,58,59]
7	p-mentha-1,3,8-triene	91, 119, 134	7.3	PI rubber	[48,58,59]
8	benzothiazole	69, 108, 135	8.7	additive	[58]
9	1,2-dihydro-2,2,4-trimethyl quinoline	115, 158, 173	9.8	additive	[61]

3.2.3.3.2. Material characterisation by FTIR-ATR

The spectroscopic analysis was selected as complementary of the thermal one for the confirmation and characterisation of the starting materials.

Being Bio-PET and PLA commercial common polymers, their spectroscopic behaviour was compared with IR spectra from literature [62,63] and results obtained by Py-GC-MS were confirmed. The obtained IR spectra are shown Figure 3.2.3-7 for Bio-PET and Figure 3.2.3-8 for PLA, and characteristic peaks are summarised in Table 3.2.3-7. In the case of Bio-PET, the peaks at 720 cm^{-1} (aromatic out of plane), 1094 and 1242 cm^{-1} (C-O stretching), 1713 cm^{-1} (C=O stretching) [62]; for PLA, 872 cm^{-1}, 1184 cm^{-1} (O-C-O stretching), 1748 cm^{-1} (C=O stretching) [63]. No additives were detected in the spectra.

Bio-PL and TR were analysed to attribute polymer composition to their spectra and, again, pyrolytic results were confirmed. In order to understand the chemical composition of Bio-PL, the IR spectra of the sample (Figure 3.2.3-9) was compared with the one recorded for PLA and PBAT (Figure 3.2.3-10). In addition to CH_2 (724 cm^{-1}), the phenylene stretching group (1017 cm^{-1}), the C-O stretching (1266 cm^{-1}) and the C=O groups stretching (1717 cm^{-1}) were revealed, suggesting again the presence of PBAT, but also the one of PLA could not be excluded [64].

Finally, Tire rubbers are complex matrices, containing carbon black, fillers, vulcanizers and other additives. The spectra in Figure 3.2.3-11 was hardly comprehensible due to ATR diamond which is a not suitable crystal of the instrument to analyse black material [65]. Anyway, the identifiable peaks revealed the nature of the sample as isoprene rubber (Table 3.2.3-8), also according with its pyrogram. The pure rubber content is often low compared to the total mass of the other ingredients and the spectrum is mostly determined by the presence of recurring structure [66].

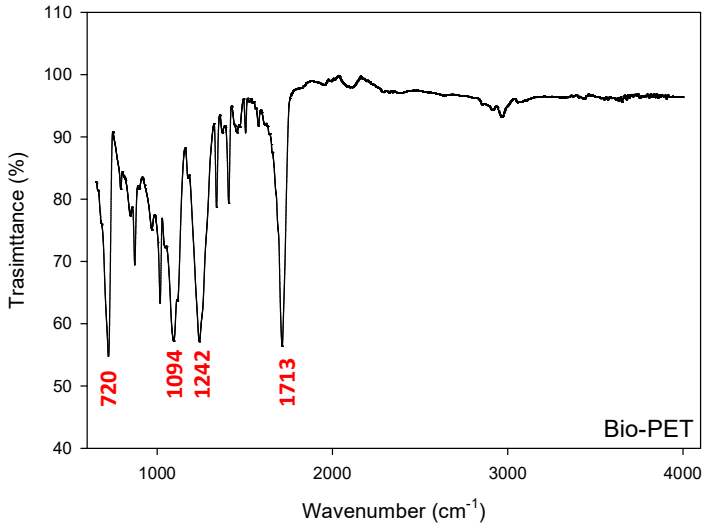

Figure 3.2.3-7. *IR spectrum from FTIR-ATR analysis of Bio-PET. Peak assignment in Table 3.2.3-7, Bio-PET section [37].*

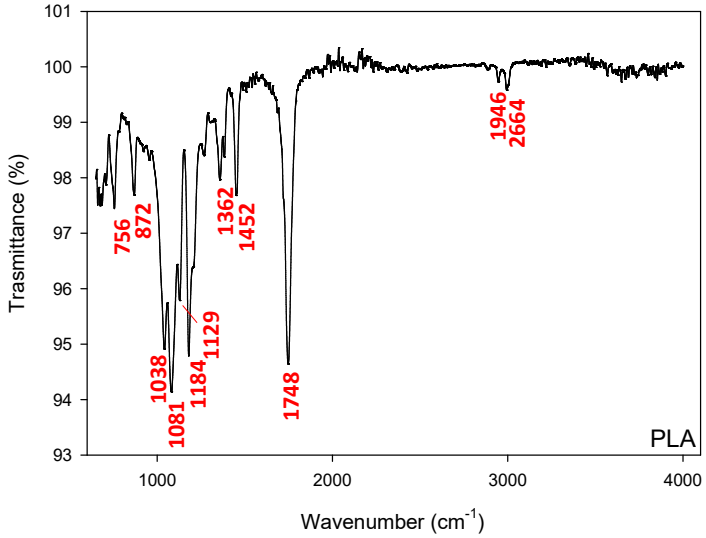

Figure 3.2.3-8. *IR spectrum from FTIR-ATR analysis of PLA. Peak assignment in Table 3.2.3-7, PLA section [37].*

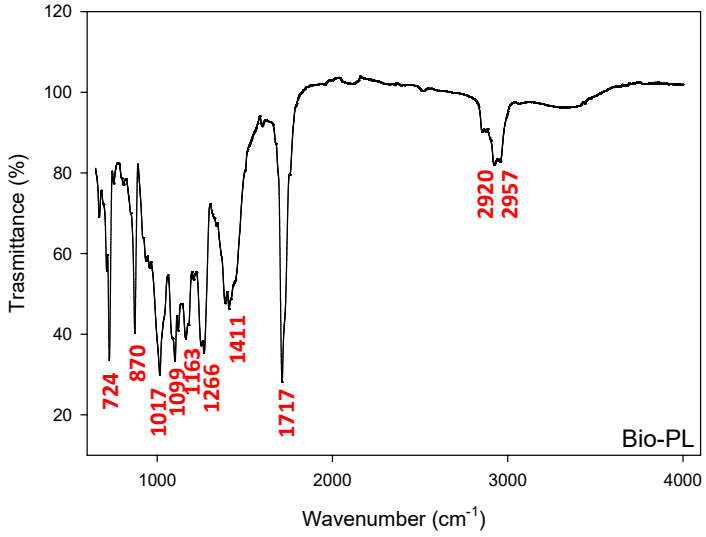

Figure 3.2.3-9. *IR spectrum from FTIR-ATR analysis of Bio-PL. Peak assignment in Table 3.2.3-8, Bio-PL section [37].*

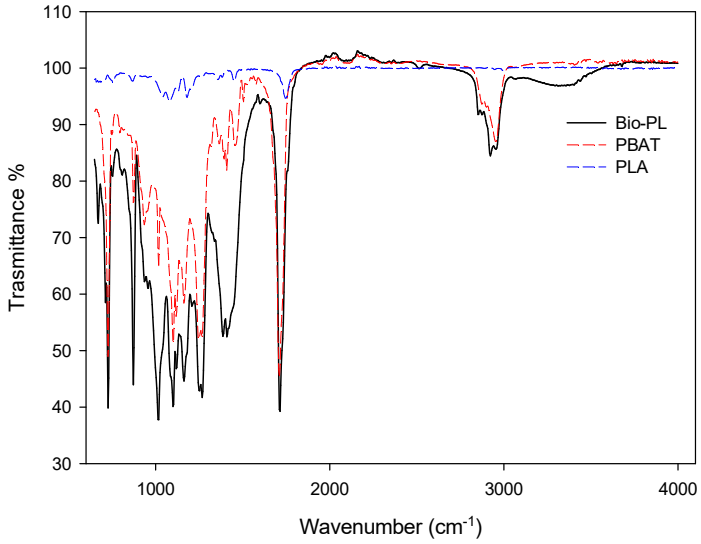

Figure 3.2.3-10. *Comparison of IR spectra from FTIR-ATR analysis of Bio-PL (black), PBAT (red) and PLA (blue). Peak assignment in Table 3.2.3-8, Bio-PL section [37].*

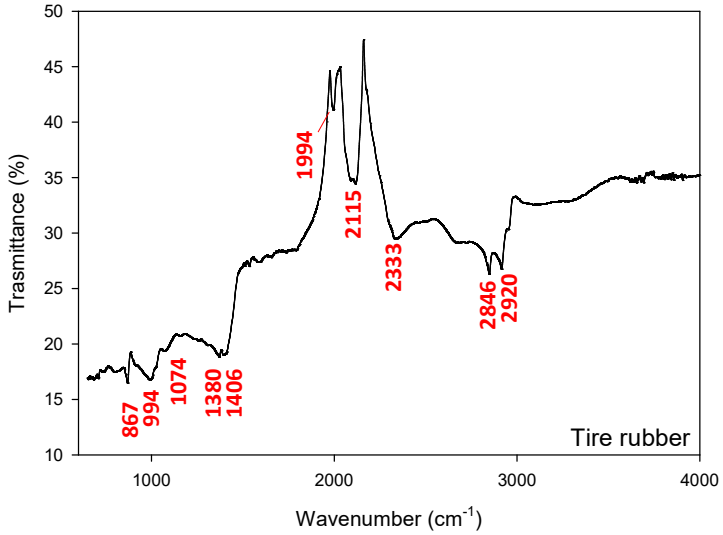

Figure 3.2.3-11. *IR spectrum from FTIR-ATR analysis of TR. Peak assignment in Table 3.2.3 8, TR section [37].*

Table 3.2.3-7. *IR spectra characterisation from FTIR-ATR data (wavenumbers and bond type assignment) and comparison with literature.*

Wavenumber (cm^{-1})	Assignment	Reference
PET		
720	Aromatic out plane bending of C-H	[62]
1092	C-O stretching	[62]
1241	C-O stretching	[62]
1713	C=O stretching	[62]
PLA		
757	alpha-CH_3	[63]
872	O-CH-CH_3	[63]

1184	C-O-C stretching	[63]
1362	CH_3 symmetric bending	[63]
1452	CH_3 asymmetric bending	[63]
1748	C=O stretching	[63]

Table 3.2.3-8. *IR spectra characterisation from FTIR-ATR data (wavenumbers and bond type assignment), comparison with literature for the attribution to specific polymers.*

Wavenumber (cm^{-1})	Assignment	Attribution	Reference
Bio-PL			
724	$-CH_2-$ group(s)	PBAT	[64]
1017	phenylene group stretching	PBAT	[64]
1266	C-O in ester linkage	PBAT	[64]
1717	C=O in ester linkage	PBAT	[64]
TR			
1388			[66]
1076	C-S-C stretching vibration	Vulcanised natural rubber	[66]
2330	S-H stretching vibration	Vulcanised natural rubber	[66,67]
2846	CH_3 symmetric stretching	Natural rubber	[66,67]
2920	CH_3 symmetric stretching	Natural rubber	[66,67]

3.2.3.3.3. Leachates extraction and silylated results

In this section seawater leachate extracted in ethyl acetate are chemically investigated and discussed. Identified compounds, target ions (*m/z*), retention time (RT) and semi-quantitative results are showed in tables with reference numbers (#) to figures. Peak identification was mainly based on NIST08 library and match percentages are showed in the table (% NIST). Mean concentration values were calculated on results obtained for the three replicate extractions. Silylated extracts (-SIL) were analysed to obtain qualitative additional results thanks to the formation of trimethyl silyl (TMS) compounds. These results were useful to confirm the GC-MS and PY-GC-MS results and to get additional information on seawater leachates. GC-MS analyses were performed by untargeted methods and operated in TIC acquisition. Semi-quantitative results are related to the second batch of leachates produced with the method in Section 3.2.3.2.3, but qualitative chemical composition was confirmed by the comparison by the analysis of leachates from the first sample batch, which was used for biological tests.

3.2.3.3.3.1. Bio-PET

No peaks were identified in the chromatograms of the extracted samples of Bio-PET leachates, neither with nor without silylation. The good recovery of the procedural IS (TTB for simple extraction, TDA for silylates samples) confirming that the method was correctly performed. Probably, the level of detection was not fitted for the investigated leaching systems.

3.2.3.3.3.2. PLA

In PLA seawater leachate extracted in ethyl acetate it was no possible to identify peaks which differ from the blank. However, the presence of TTB-IS confirmed that the method was correctly carried out. Nevertheless, after silylation important peaks were recognised (Figure 3.2.3-12), such as lactic acid TMS ether and lactic acid dimer bis TMS (with TMS corresponding to trimethyl silyl, Table 3.2.3-9). Lactic acid and its dimer could be formed by abiotic degradation of PLA or they could be originally present in the plastic material. As discussed above, oligomers could be formed in the synthesis of polyesters, remaining in the final materials with a potential to migrate. According to literature results, lactic acid was detected by GC-MS after silylation of lyophilised mineral aqueous phase incubated with biodegradable mulch blends containing PLA [68]. Moreover, lactic acid, lactide and oligomers have been found in food stimulants in contact with PLA [69,70].

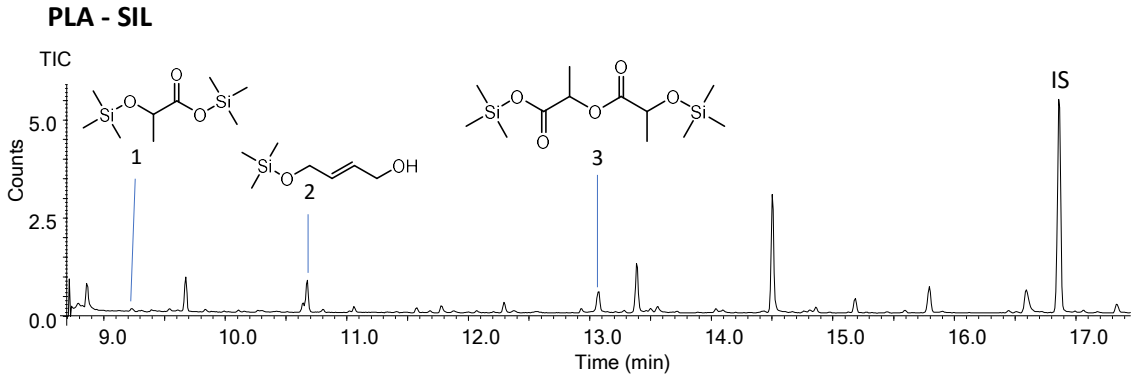

Figure 3.2.3-12. *TIC chromatogram from GC-MS analysis of silylated seawater leachate from PLA extracted with ethyl acetate. IS = TMS tridecanoate. Reference number to Table 3.2.3-9, PLA section [37].*

Table 3.2.3-9. *Tentative identification, GC-MS data (RT retention time, m/z, base peak in bold) from seawater leachates from PLA without and with silylation (PLA-SIL). Comparison with NIST08 library (% Match) and mean concentration ± standard deviation and RSD of leachate compounds. Reference numbers (#) to Figure 3.2.3-12.*

#	Compound	*m/z*	% Match	RT (min)
PLA-SIL				
1	lactic acid 2TMS derivative	73, 103, 117, 147	81 %	9.39
2	2-butene-1,4-diol TMS derivative	75, 129, 175	81 %	10.58
3	lactic acid dimer bis TMS	73, 147, 219, 291	92 %	13.06

3.2.3.3.3.1. Bio-PL

Leachates from Bio-PL (Figure 3.2.3-13) were peculiar being enriched by several compounds, structurally related to the PBAT backbone. Specifically, 1-(2-butoxyethoxy) ethanol, di(2-butoxyethoxy) adipate, bis[2-(2-butoxyethoxy) ethyl] adipate (peaks #3 #8 #11 in Figure 3.2.3-13, measured 16 ± 2 mg L^{-1}, 11.8 ± 0.8 mg L^{-1} and 5.8 ± 0.3 mg L^{-1} in Table 3.2.3-10, respectively) have chemical structures compatible with that of the polymer. It is worthwhile noting the presence of 1,6-dioxacyclododecane-7,12-dione (peak #7 in Figure 3.2.3-13) as second most abundant product, with a calculated concentration of 12 ± 2 mg L^{-1} (Table 3.2.3-10). This product was also observed in the pyrolyzates of Bio-PL (peak #7 in Figure 3.2.3-4) and other biodegradable plastic bags. The cyclic derivative, 1,6-dioxacyclododecane-7,12-dione, is quoted by ECHA web site, because it was notified for the *Classification, Labelling and Packaging of substances and mixtures Regulation* (CLP Regulation). Notifications are expressed by manufacturer or importer companies and are required for "*hazardous substances, as such or in mixtures, as well as for all substances subject to registration, regardless of their hazard*" [71]. 1,6-dioxacyclododecane-7,12-dione was imputed by companies to be possibly harmful if swallowed and to potentially cause serious eye, skin and respiratory irritations [71]. However, the compound is not registered to REACH (EU regulation n. 1907/2006) yet being under pre-registration process. 1,6-dioxacyclododecane-7,12-dione was observed in literature by other authors in different contexts. It was found in high concentration in the water leachates obtained from weathered and original plastic bags, analysed by GC-MS [72] and it was also reported among the chemicals migrated into water from infant teether toys by GC-Orbitrap-MS [73]. Interestingly, it was also found as a potential migrant into isooctane from polyurethane adhesives in laminates typical of food packaging by HS-SPME-GC-MS [74] or into air from

volatilisation from materials based on polyurethanes [75,76]. Here, 1,6-dioxacyclododecane-7,12-dione was presumed to be a NIAS associated to the polyester-based portion of polyurethane, consisting of adipic acid (1,6-hexane dioic acid) and 1,4-butanediol being found from the processing of polyurethane. Again, 1,6-dioxacyclododecane-7,12-dione was identified along with other cyclic esters among the chemicals that migrated from adhesives of food packaging materials into a solid food simulant (Tenax® poly(2,6-dipheny-*p*-phenyleneoxide) [77]. In general, cyclic oligomers are inevitably formed from polyester manufacturing probably through a "back-biting" mechanism of the polymer backbone [78]. Linear and cyclic oligomers of PBAT with several repeating units were detected by LC-MS after extraction with organic solvents or food stimulants [78–81].

After the silylation of the extract from Bio-PL leachate, new interesting peaks were found. The presence of 1,4-butanediol bis TMS ether (peak #14 in Figure 3.2.3-14 and Table 3.2.3-10) was an additional confirmation of the nature of the polymer, since 1,4-butanediol is one of the starting monomers of PBAT. Similar to our finding, 1,4-butanediol was identified by Serrano-Ruìz et al. (2020) upon silylation of the compounds migrated into a water mineral phase from bioplastic materials containing PBAT [68]. 2-(2-butoxyethoxy)ethoxy in the form of TMS ether was tentatively identified by mass spectrum and chromatographic elution (peak #17 in Figure 3.2.3-14 and Table 3.2.3-10). Lactic acid dimer bis TMS ether (peak #18 in Figure 3.2.3-14 and Table 3.2.3-10) was detected in accordance to Py-GC-MS and ATR-FTIR (Sections 3.2.3.3.1 and 3.2.3.3.2, respectively). These substances are presumably components of the polymer mixture (PLA and PBAT) composing the compostable plastic bag. PBAT/PLA materials met the international compostable criteria, however, the two polymers have different solubility properties so that compatibilizers could be present as additives along with plasticisers [52].

From the available data, we cannot argue if NIAS were originally present in the material or they have been formed by degradation during the leaching procedure. Canellas et al. 2015 proposed that cyclic esters can be neo-formed compounds derived from the cyclisation of 1,4-butandiol and adipic acid identified among the identified compounds migrated from food packaging [77]. However, some of them are known to be additives. As mentioned above, above, cyclic esters could be originally present in the manufact being formed in the synthesis of the polyesters. For instance, the bis(2-(2-butoxyethoxy) ethyl adipate is known to be a plasticiser for PBAT and PLA can be enhanced thanks to the addition of this plasticizer [82]. Moreover, 2-(2-butoxyethoxy) ethanol is known to be a solvent mainly employed in adhesives even for food packaging materials [83]. This substance was described as a potent "off odorant" of the plastic smell and it was found both in water samples and in fish meat and skin samples of rainbow trout species from aquaculture farming [84,85]. Probably, its occurrence was related to bacterial activity or

actual plastic leaching in the farm waters [84,85]. Similarly, monomer (lactic acid, lactide) and oligomers of PLA were observed to migrate in food stimulants [70,78]. Oligomers of adipic acid and 1,4-butandiol from PBAT were found in aqueous leachates of microplastics prepared from bioplastic-based shampoo bottles [36]. However, these leachates had almost no adverse effects on *L.variegatus* freshwater oligochaete. Finally, 1,4-butanediol was also identified among the substances migrated from biodegradable food packaging [77].

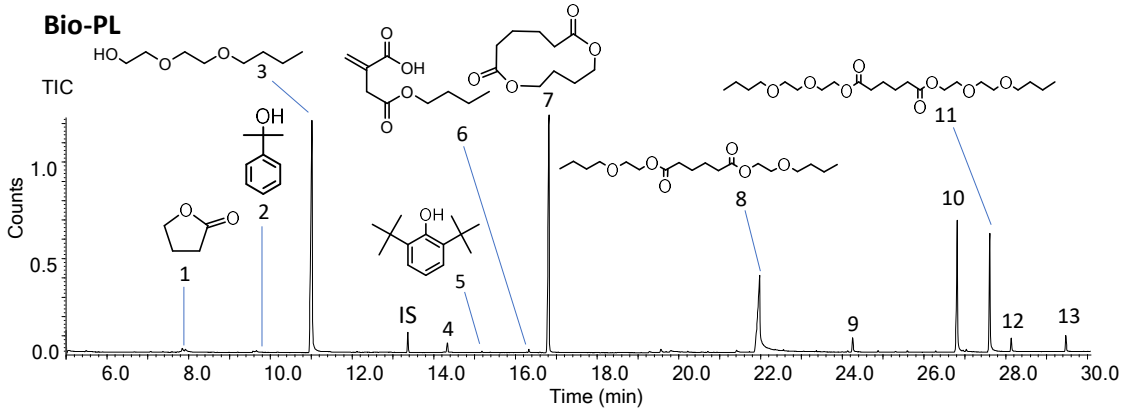

Figure 3.2.3-13. *TIC chromatogram from GC-MS analysis of seawater leachate from Bio-PL extracted with ethyl acetate. IS = TTB. Reference number to Table 3.2.3-10, Bio-PL section [37].*

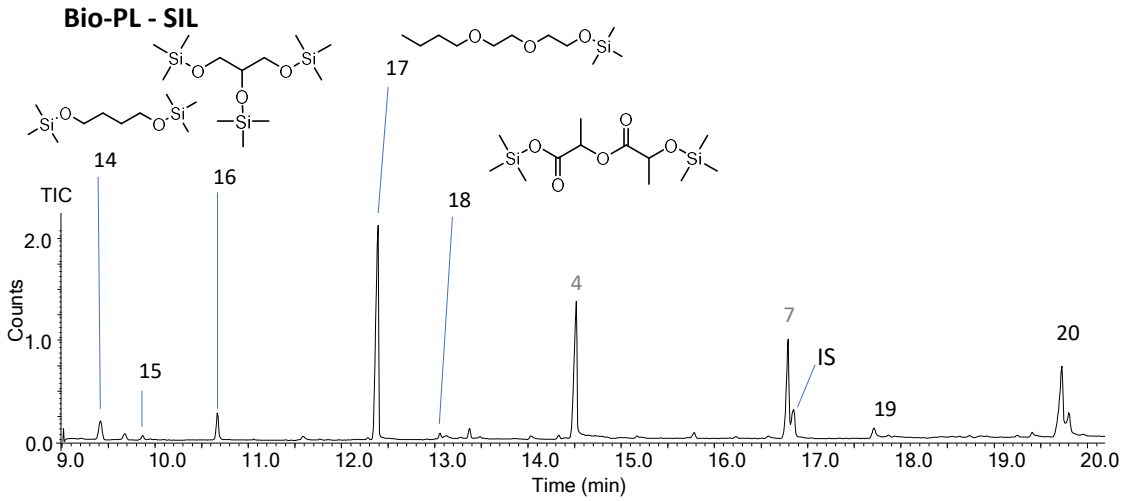

Figure 3.2.3-14. *TIC chromatogram from GC-MS analysis of silylated seawater leachate from Bio-PL extracted with ethyl acetate. IS = TMS tridecanoate. Reference number to Table 3.2.3-10, Bio-PL-SIL section [37].*

Table 3.2.3-10. *Tentative identification, GC-MS data (RT retention time, m/z, base peak in bold) from seawater leachates from Bio-PL without and with silylation (Bio-PL-SIL). Comparison with NIST08 library (% Match) and mean concentration ± standard deviation and RSD of leachate compounds. Reference numbers (#) to Figure 3.2.3-13 and Figure 3.2.3-14.*

#	Compound	*m/z*	% Match	RT (min)	Conc ± st. dev (mg L^{-1})	RSD %
	Bio-PL					
1	butyrolactone	42, 56, ***86***	93 %	7.9	0.20 ± 0.05	24 %
2	dimethyl benzene methanol	43, 77, 105, 121	81 %	9.7	0.12 ± 0.02	15 %
3	1-(2-butoxyethoxy) ethanol	45, 57, 75, 87, 132	96 %	11.0	16 ± 2	10 %
4	unknown	42, 54, 101, 142		14.3	0.41 ± 0.01	1 %
5	2,6-di-*tert*-buthylphenol	57, 191, 206	77 %	15.2	0.06 ± 0.01	22 %
6	2-(2-butoxy-2-oxoethyl) acrylic acid	41, 57, 86, 113	92 %	16.3	0.13 ± 0.01	6 %
7	1,6-dioxacyclododecane-7,12-dione	55, 84, 100, 129	95 %	16.8	12 ± 2	15 %
8	di(2-butoxyethoxy) adipate	57, 111, 129, 173	80 %	21.9	11.8 ± 0.8	7 %
9	unknown	55, 73, 99, 116		24.3	0.82 ± 0.05	6 %
10	unknown	55, 71, 101, 127		26.8	6.6 ± 0.3	13 %
11	bis[2-(2-butoxyethoxy) ethyl] adipate	57, 111, 129, 173	84 %	27.7	5.8 ± 0.3	5 %
12	unknown	55, 101, 111, 127		28.1	0.76 ± 0.05	7 %
13	unknown	55, 71, 111, 129		29.5	0.79 ± 0.04	5 %
	Bio-PL-SIL					
14	1,4-butanediol bis (TMS) ether	73, 116, 147	95 %	9.4		
15	unknown	73, 103, 117, 131		9.9		
16	tris TMS ether of glycerol	73, 147, 205, 218	89 %	10.7		
17	2-(2-butoxyethoxy)ethoxy TMS ether	73, 101, 117, 147	93 %	12.4		
18	lactic acid dimer bis TMS ether	73, 117, 191, 219, 291	92 %	13.1		
19	unknown	73, 147, 173		17.7		
20	unknown	73, 111, 145, 201		19.7		

3.2.3.3.3.2. TR

TR was utilised as positive control for the high number of studies on the toxicity of tire leachates to water organisms [20]. In fact, several compounds were released in the ASW. The chromatogram obtained from the GC-MS analysis of seawater extract of TR is shown in Figure 3.2.3-15. Benzothiazole (peak #3 in Figure 3.2.3-15 and Table 3.2.3-11) was the highest concentrated compound with a concentration of 1.06 ± 0.07 mg L^{-1}. Together with dicyclohexylamine (peak #6 in Figure 3.2.3-15 and measured at 0.06 ± 0.02 mg L^{-1}, Table 3.2.3-11), it was found in particle tire leachates in citrate buffered water at pH 5.2 [86]. In another study, the elutriates of sediments containing tire and road wear particles were subjected to toxicity tests and aniline resulted among the potential toxicants for aquatic organisms, while 2-mercaptobenzothiazole, dicyclohexylamine, were not found at detectable levels [87]. Anyway, N-cyclohexyl formamide, N-cyclohexyl-acetamide and 2(3H)-benzothiazolone were found (peaks #4, #5 and #8, respectively). These compounds, together with 2-mercaptobenzothiazole, benzothiazole derivatives and other amines derivatives, have been found to derive from the breakdown of vulcanization accelerators during vulcanisation [88]. Finally, 2,6-di-*tert*-buthylphenol (peak #7) was found at relatively low concentration (0.05 ± 0.01 mg L^{-1}), with respect to other leachates. The presence of this compound is ascribable to phenolic antioxidant usually employed in rubber [89–91].

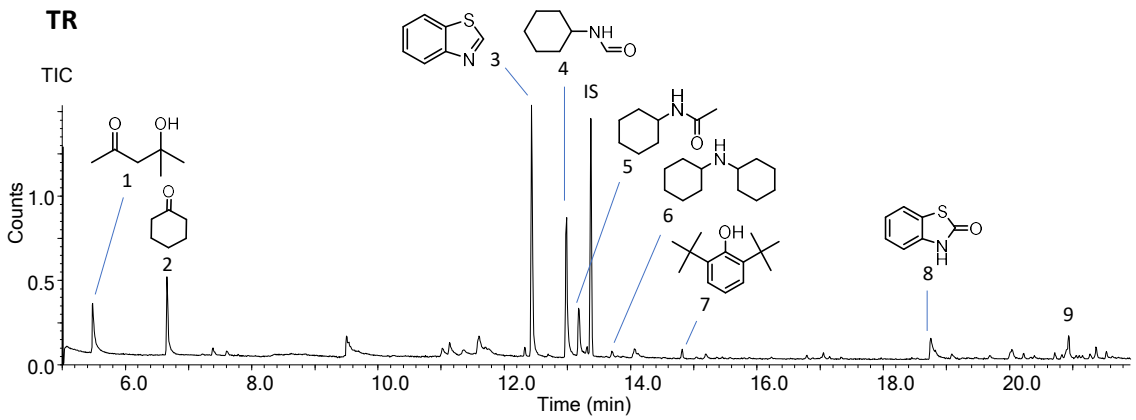

Figure 3.2.3-15. *TIC chromatogram from GC-MS analysis of seawater leachate from TR extracted with ethyl acetate. IS = TTB. Reference number to Table 3.2.3-11, TR section [37].*

Table 3.2.3-11. *Tentative identification, GC-MS data (RT retention time, m/z, base peak in bold) from seawater leachates from PLA without and with silylation (PLA-SIL). Comparison with NIST08 library (% Match) and mean concentration ± standard deviation and RSD of leachate compounds. Reference numbers (#) to Figure 3.2.3-15.*

#	Compound	*m/z*	% Match	RT (min)	Conc ± st. dev (mg L^{-1})	RSD %
	TR					
1	4-methyl-4-hydroxy-2-pentanone	43, 59, 101	96 %	5.5	0.40 ± 0.08	21 %
2	cyclohexanone	42, 55, 69, 98	94 %	6.7	0.37 ± 0.03	7 %
3	benzothiazole	69, 82, 108, 135	91 %	12.4	1.06 ± 0.07	7 %
4	N-cyclohexyl formamide	46, 56, 67, 84	94 %	13.0	0.77 ± 0.08	11 %
5	N-cyclohexyl-acetamide	56, 60, 98, 141	92 %	13.2	0.29 ± 0.04	13 %
6	dicyclohexylamine	43, 56, 138	75 %	13.7	0.06 ± 0.02	39 %
7	2,6-di-*tert*-buthylphenol	57, 191, 206	77 %	15.2	0.05 ± 0.01	23 %
8	2(3H)-benzothiazolone	96, 123, 151	74 %	18.8	0.23 ± 0.02	9 %
9	unknown	57, 86, 113, 170		20.9	0.14 ± 0.03	19 %

3.2.3.3.4. Biological impact of leachates

In this section results obtain from biological experiments carried out by the research group on *Health and Environmental Physiology* of the University of Bologna at the Campus of Ravenna, under the supervision of Prof. Elena Fabbri (Department of Biological, Geological, and Environmental Sciences) are summarised [37].

3.2.3.3.4.1. Mussel early life stages endpoints

Only leachates from TR significantly reduced the rate of egg fertilization starting from 4 % concentration, with an EC50 of 12.55 % concentration. Embryo development was the most affected endpoint (Figure 3.2.3-16), in agreement with previous results on embryos exposed to additives from conventional plastics [20]. Leachates from Bio-PL and TR induced significant effects already at 0.6 % (Bio-PL) and 2 % (TR) leachate concentration. Leachates from PLA and Bio-PET also significantly impaired the physiological larvae development with a consistent effect from 6 % (PLA) and 10 % (Bio-PET) concentrations. The adverse outcome might be related to the sensitivity of embryos to the metals found in the leachates (Table 3.2.3-12). The co-occurrence

of BPA in all the leachates was also assessed and its presence may also contribute to the final outcomes (data not shown, more details in Capolupo et al. (2023) [37]).

Several NIAS associated to the chemical structure of the polyester (monomers and oligomers of PLA and PBAT) were found in the leachates, as described in sections above. As discussed above, this finding agreed with literature as far as the susceptibility of these compounds to migrate out of the polymeric material into the surroundings medium is concerned. Water leachates from microplastics of bioplastic, presumably containing monomers/oligomers of different polyesters (among which PBAT) mixed with starch, resulted to have almost no adverse effects on *L. variegatus* freshwater oligochaete; however, toxicity was observed in the case of methanolic extracts, that represented a worst situation, not extendible to environmental conditions [92]. It is worth underlining the ubiquity of the cyclic ester 1,6-dioxacyclododecane-7, 12-dione in the mixture of compounds prone to be released from bioplastics containing PBAT. This cyclic ester was a major compound in the leachates of Bio-PL, but no information on its toxicity to marine organisms is available in published studies. Significantly reduced motility (at 48 h) was observed in larvae exposed to TR leachates within a concentration range of 20 – 100 %; significantly reduced larvae survival (at 216 h) was caused by TR leachates in the range 10 – 100 %, with EC50 values of 17.3 % and 11.9 %, respectively. Other leachates were ineffective on survival, and PLA and Bio-PL only reduced motility at the highest concentrations tested.

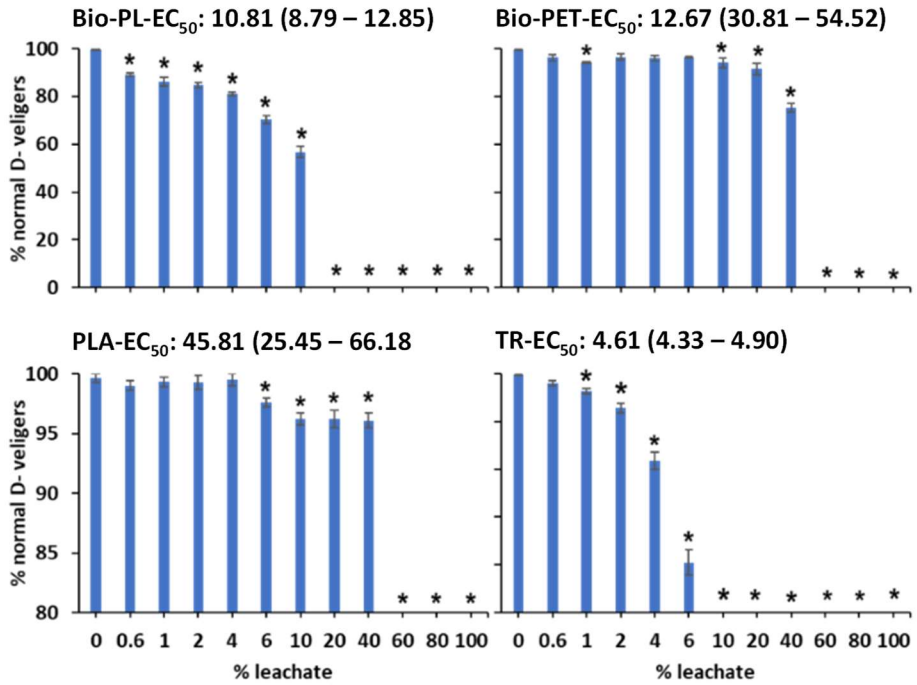

Figure 3.2.3-16. *Mean percentage of Mytilus galloprovincialis normal D-veliger larvae after 48 h exposure to leachates from bioplastics (Bio-PL, Bio-PET, PLA) and conventional tire rubber (TR). Data are expressed as mean ± SEM (n = 5, SEM: standard error mean). Asterisks indicate significant differences compared to the control (p < 0.05, One way ANOVA, Dunnett's post-hoc comparison). EC50 values (95% C.I.) are also reported [37].*

3.2.3.3.4.2. Biomarker evaluation in adult mussels

Biological effects of 0.6 % leachate concentrations were assessed after in vivo exposure of mussels for 7 days (Figure 3.2.3-17), and a significant LMS reduction was found in haemocytes withdrawn from mussels exposed Bio-PL and TR leachates (Figure 3.2.3-17-A). LMS decreased also after PLA and Bio-PET leachate exposure, without reaching significance. LMS reduction in haemocytes is the most sensitive biomarker of stress in mussels [41]. Its reduction reflects the loss of membrane integrity and the impairment of lysosome functionality and is in fact an early warning signal for pathologies in *Mytilus* spp. [93,94]. LMS has been correlated with animal scope for growth and total oxyradical scavenging capacity, and inversely correlated with protein catabolism, lipofuscin and neutral lipid accumulation, lysosomal swelling, and DNA damage [95]. Significant reduction of LMS has been previously reported after mussel exposure to leachates from conventional plastics [43] and other chemical insults such as polycyclic aromatic hydrocarbons, pesticides and metals [96] including conventional and emerging contaminants such as BPA [97]. Trace metals such as copper, zinc and lead are among the contaminants provoking destabilization of lysosome membranes [98], and these occur in TR and Bio-PL leachates (Table 3.2.3-12). Copper is much higher than in control water also in leachates from Bio-PET and PLA (Table 3.2.3-12). Other compounds found in the leachates could also affect LMS, alone or in combination. As previously shown, LMS is reduced also after mussel exposure to microplastics [17,22,99]. Whether the microplastics ingested do have time enough to release additives along the digestive tract before elimination [100] is not known yet, however it is a challenging issue in wildlife as in humans. Overall, LMS is a useful biomarker to highlight the occurrence of low concentrations of organic and inorganic contaminants in water either alone or in mixtures. Reduction of LMS often leads to lysosome increase in size and fusions [101,102]. The increase of the lysosomal volume is a condition predictive of impairment of viability and functionality of digestive gland cells [103]. The increasing size of the lysosome compartment (LYS) with respect to cytosol (CYT) has been measured in mussels exposed to leachates. LYS/CYT ratios were significantly higher than in controls in mussels exposed to TR, Bio-PL and PLA (Figure 3.2.3-17-B). Metals occurring in the leachates could be in part responsible for this effect. In fact, Cu and other metals produced lysosome enlargement and organelle fusion, with a mechanism at least in part mediated by a calcium dependent-phospholipase A2 stimulation [104]. High LYS/CYT ratio was measured in mussels which accumulated Cu and Zn from coastal lagoon waters [105]. These metals occur in all tested leachates at concentrations that in some cases are significantly higher than control water. Lysosomotropic effects could however be induced in mussels by further chemical additives or NIAS, whose properties are not known, at present. All

leachates significantly enhanced the NL content in mussels with respect to the controls (Figure 3.2.3-17-C), except for PLA ($p = 0.054$). NL increases in digestive gland indicate lipidosis, a metabolic disorder consequence either of reduced lipid utilization or decrease in fatty acid processing [94]. NL accumulation in mussels was also provoked by exposure to leachates from conventional plastics [22], and by other water pollutants in laboratory [97] as well as in field condition [105,106]. Similarly, field exposure to metals that are also present in the leachates analysed in the present work, were found to increase NL content in mussel digestive gland lysosomes [107–109]. Reactive oxygen species (ROS) production is a known effect of pollutants [110] able to induce lipid peroxidation [102]. The products of lipid peroxidation are effectively sequestered by lysosomes, among these MDA, as intermediate compounds with respect to the final products represented by LF [111]. In particular, LF are insoluble aggregates made of lipid peroxidation residues which bind to food degradation by-products, oxidized proteins, carbohydrates, and metals [111]. These compounds are observed in mussels in response to oxidative pollutants including metals [112]. LF content in digestive glands was increased significantly after 1-week exposure to 0.6 % leachates from TR and Bio-PL (Figure 3.2.3-17-D). Increases, although not significant, were noted also for PLA and Bio-PET. It has to be underlined that 1 week is a minimum time for lipofuscin accumulation [94], thus the one represented on Figure 3.2.3-17-D may not be the complete biomarker response. No significant change was instead noted for MDA content (data not shown, more details in Capolupo et al. (2023) [37]). This response was different from what expected, especially in case of moderate peroxidation as from PLA and Bio-PET, where the accumulation of LF is not significant. Such a low MDA production after exposure to Bio-PL and TR leachates could instead be ascribed to its depletion to support LF production. Increase of LF contents is correlated to the LMS decrease found in haemocytes; such a correlation was previously reported [108] and confirms the relationship between oxidative stress and lysosomal disorders [93]. Overall, biomarkers of lysosomal dysfunction in mussels are predictors for pathology and have ecosystem relevance [14,93], thus emphasising the importance of considering (bio)plastic leachates among the environmental hazards. Leachate potential to trigger mussel antioxidant system has been evaluated addressing CAT and GST activities, in gills and digestive gland of exposed animals (Figure 3.2.3-18). The different role of the enzymes in the two tissues was confirmed, with CAT having higher basal activity in and GST showing higher activity in gills, e.g., the first tissue exposed to environmental xenobiotics [22]. CAT activity was significantly reduced by leachates from Bio-PET in gills, and enhanced by leachates from Bio-PL in digestive glands (Figure 3.2.3-18-A); GST was significantly enhanced by leachates from PLA in gills, and from Bio-PL in digestive glands (Figure 3.2.3-18-B). Previous studies reported different responses of CAT and GST, increase, decrease or no effect,

after pollutant exposure [113–116]. Cu and Zn were able to activate GST in *Mytilus* spp [105]; differently, a significant GST inhibition was reported in mussels after BPA exposure[97]. The data presently observed might be the result of opposite effects by the compounds included in the leachate mixture, or the low concentrations were not sufficient to stimulate bigger responses by the cellular defences. Bivalves, as all invertebrates, display an innate immune system to fight against pathogens and xenobiotics. Lysozyme is a bacteriolytic enzyme concurring to the immune response with the specific effect to hydrolyse the β-1,4-linked glycoside bonds of bacteria wall [117]. Lysozyme activity was found in bivalve hemolymph and tissues [118] and modulated by several contaminants [119,120]. In the present experimental trials, all leachates inhibited the lysozyme activity in exposed mussels, although only the responses to Bio-PL and TR reached statistical significance (Figure 3.2.3-18-C). A reduction of lysozyme activity is a marker of immunosuppression, thus of lower resistance to bacterial insult. Lysozyme activity was also reduced by the estrogen-like compound tributyltin [121], while increased by 17-β estradiol [122]. Suggesting that estrogen receptors may be involved in the control of enzyme activity. Although *Mytilus* spp. do not produce estradiol, they possess estrogen receptors that can be involved in this function [123]. Recent studies have shown that blood clam *Tegillarca granosa* lysozyme activity (together with some other innate immune effectors) was inhibited by BPA, microplastics and BPA plus microplastics [124]. The co-exposure of *T. granosa* to microplastics, B [a]P and E2, led to the highest reduction of lysozyme release and activity [124]. Furthermore, the leachates also contained trace metals that may affect lysozyme activity (Table 3.2.3-12). In fact, an effect of Cu on lysozyme molecular configuration was suggested many years ago from investigations on *Mytilus* haemocytes [125]. Copper was more recently reported to irreversibly inhibit chicken egg white lysozyme activity up to 80 % at 390 µM, as a consequence of binding to specific aminoacidic residues at the catalytic site of the enzyme [126]. Inhibition was also observed after exposure to Zn, Mn and Co, while Ca had no effect [126]. Cr, Ni, Cd, B, Hg, and Pb in the range 10 – 50 mM caused dose-dependent reduction of hen egg white lysozyme activity already after 4 h of exposure, and the effect remained of similar extent at 12 and 24 h [127]. The strongest effects were obtained after exposure to CrVI or Cd, which reduced the lysozyme activity to about 25 % of the control already within 4 h at the lowest concentration tested. The combination of the different compounds found in the leachates may lead to the overall reduction of lysozyme activity shown in Figure 3.2.3-18-C. AChE is an enzyme involved in nervous transmission useful as biomarker of neurotoxicity [42]. Its inhibition, typically by organophosphates, induces a protraction of the nervous stimulus [42]. In the present experimental trials, however, no change in AChE activity was detected of exposure to the different leachates at 0.6 % concentration (data not shown, more details in Capolupo et al.

(2023) [37]). In mussels AChE was found to be affected by the mixture of BPA, carbamazepine and atrazine [128], and inhibited by metals [129]; moreover, AChE inhibition by plastic leachates has recently been reported in fish [130]. The short exposure and/or the high dilution of the leachates may be the reason of the lack of effect in our experimental system, although at least BPA and trace metals occur.

Table 3.2.3-12. *Trace metals in leachates from bioplastics and tire rubber. Results are expressed in µg L^{-1} and represent the mean media ± expanded uncertainty (K = 2; df = 10) of measured levels for each treatment. ASW: artificial seawater, LOQ: limit of quantification [37].*

µg L^{-1}	ASW	Bio-PL	Bio-PET	PLA	TR	LOQ
Al	< 5	< 5	< 5	< 5	6.5 ± 0.9	5
Fe	< 5	11.1 ± 1.4	< 1	< 5	13.8 ± 1.8	5
Cu	3.1 ± 0.5	36.5 ± 5.6	16.8 ± 2.6	12.9 ± 2.0	2.8 ± 0.4	1
Zn	150 ± 46	110 ± 35	150 ± 46	82 ± 25	220 ± 69	5
Pb	< 1	2.1 ± 0.	3	< 1	< 1	1.3 ± 0.5
Hg	< 0.5	< 0.5	< 0.5	< 0.5	< 0.5	0.5
Cr	< 1	< 1	< 1	< 1	1.3 ± 0.5	1
Ni	< 1	5.0 ± 1.5	2.7 ± 0.8	< 1	< 1	1
Cd	< 1	< 1	< 1	< 1	< 1	1
As	< 1	1.9 ± 0.5	< 1	< 1	1.3 ± 0.4	1
Sb	< 1	< 1	< 1	< 1	< 1	1
Co	< 1	< 1	< 1	< 1	< 1	1
Sr	5100	4900	4800	4900	5400	1
Mn	12	12.9	18.5	18.5	26.5	1

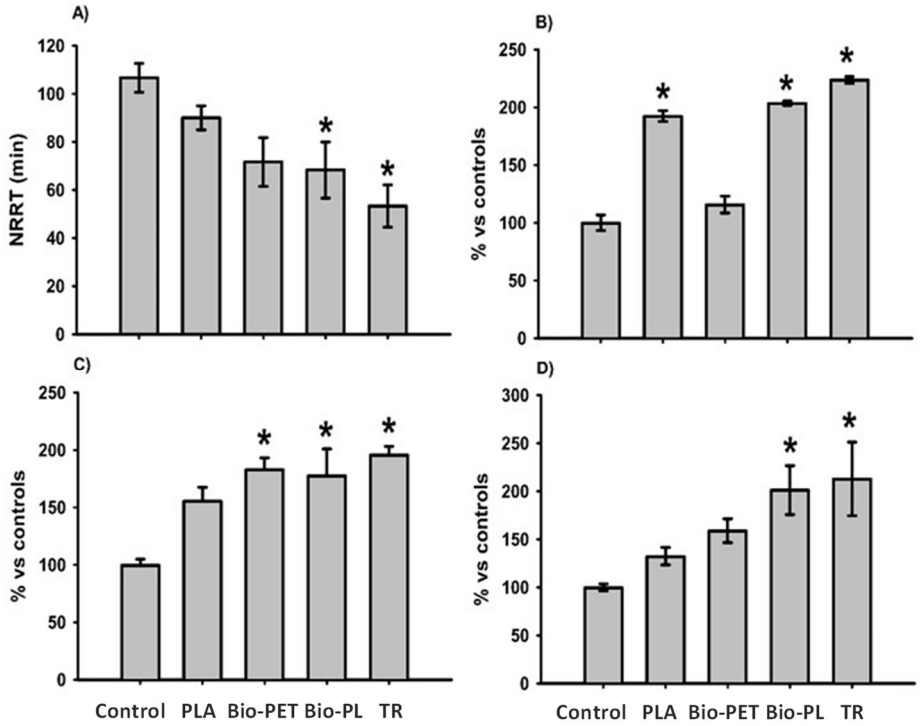

Figure 3.2.3-17. *Lysosomal parameters evaluated in adult mussels after in vivo 7-day exposure to 0.6% concentrations of bio-leachates (PLA, Bio-PET, Bio-PL) and tire rubber (TR) leachate.* ***A)*** *Lysosome membrane stability;* ***B)*** *Lysosome/Cytosol ratio;* ***C)*** *Unsaturated neutral lipid accumulation;* ***D)*** *Lipofuscin accumulation. Data are expressed as mean ± SEM (N = 3). Asterisks indicate significant differences compared to the control (p < 0.05, One-way ANOVA, Bonferroni post-hoc comparison) [37].*

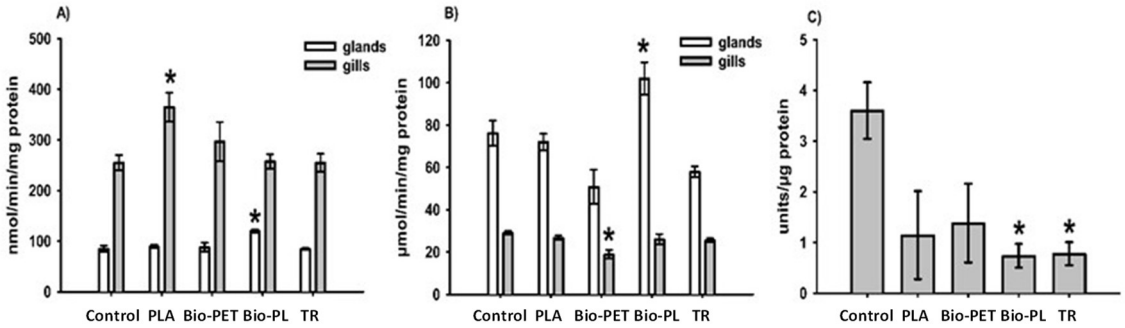

Figure 3.2.3-18. *Enzymatic activities evaluated in adult mussels after in vivo 7-day exposure to 0.6% concentrations of bio-leachates (SB, BPT, PLA) and tire rubber (TR) leachate.* ***A)*** *Catalase activity in digestive glands and gills;* ***B)*** *Glutathione-S transferase activity in digestive glands and gills;* ***C)*** *Lysozyme activity in serum. Data are expressed as mean ± SEM (N = 3). Asterisks indicate significant differences compared to the control (p < 0.05, One-way ANOVA, Bonferroni post-hoc comparison) [37].*

3.2.3.4. Conclusions

The study confirms that leachates from bioplastics do contain organic compounds (additives, non-intentionally added compounds such as oligomers) and trace metals, and exposure to leachates does affect *M. galloprovincialis* early embryo stages development and adult physiological parameters. Overall, the magnitude of the effects was different depending on the

polymer tested, possibly reflecting the different chemical composition and/or concentration of the compounds in the leachate mixtures. However, the effects of some bioplastic leachates were comparable to (or even greater than) previously tested conventional polymers. Among ontogenetic parameters, the embryo-larval development showed the greatest adverse outcomes indicating the potential of all leachates to compromise the resilience of mussel populations in the long term. The use of a 96-microwell assay allowed to test simultaneously a wide range of concentrations and demonstrate dose-dependent effects. Its application helps understanding the relationship between xenobiotic recommended for regulatory purposes. Adult physiological parameters were also affected by leachates, with highest effects observed for lysosomal and immunological biomarkers in mussels exposed to compostable bag (mixture of PBAT/PLA) bioplastic and tire rubber. Comparing with previous data, it can be observed that composition of leachates is different from different bioplastics and medium of extraction, however, no shared protocols are available for plastic leachate preparation. Furthermore, different mixtures are expected to induce different effects however full chemical characterization of (bio) plastics is not possible, yet. Although the experimental conditions are not intended to mimic real environmental situations and the investigated items are not necessarily representative of the entire class of commercialised polyesters, the results presented in this study are important as a basis to identify mechanisms of action and draw possible adverse outcome pathways that can result in disturbances at the ecosystem level. They also support the use of effect-based tests for designing new and less harmful additives in order to produce “sustainable” bioplastics. Finally, they highlight that the leaching of additives and NIAS (e.g., monomers and oligomers) and their effects on aquatic organisms need to be carefully considered when assessing the environmental impacts of plastics.

In this context, Py-GC-MS resulted a powerful technique to gather information on the chemical nature of the polymeric materials composing the commercial item. In fact, the study also underlined the challenges occurring in bioplastic leachate analysis, and a considerable limitation was ascribed to the gap of information on polymer compositions. Commercially available products do not provide information about the material sources, and producing companies are not bound to declare the packaging composition. Besides, leachate compositions can be highly variable, not only depending on the considered plastics, but also in relation with the releasing modes and surrounding medium. Therefore, untargeted analyses based on not-fully known polymers and the investigation of leachate compounds without clues on what it should be expected delineate a really difficult task. Py-GC-MS data provided helpful insights on the possible chemical compositions of leachates. In particular, about the presence of monomers and oligomers commonly present as non-intentionally added compounds. In addition to polymer

structures, the capability of Py-GC-MS to identify additives was proved and served to confirm data from leachate analysis. Target analyses together with method optimizations can supply the necessary improvement to provide reliable chemical data. Overall, the results indicate that leaching from bioplastic should not be underestimated, since the chemical nature and environmental impact of released constituents are not fully known yet.

References

[1] P. Agamuthu, S. Mehran, A. Norkhairah, A. Norkhairiyah, Marine debris: A review of impacts and global initiatives, Waste Manag Res. 37 (2019) 987–1002. https://doi.org/10.1177/0734242X19845041.

[2] J.R. Jambeck, R. Geyer, C. Wilcox, T.R. Siegler, M. Perryman, A. Andrady, R. Narayan, K.L. Law, Plastic waste inputs from land into the ocean, Science. 347 (2015) 768–771. https://doi.org/10.1126/science.1260352.

[3] B. Chatain, Parliament and Council agree drastic cuts to plastic pollution of environment, European Parliament, 2018. https://www.europarl.europa.eu/news/en/press-room/20181219IPR22301/parliament-and-council-agree-drastic-cuts-to-plastic-pollution-of-environment.

[4] D. Barceló, Y. Picó, Microplastics in the global aquatic environment: Analysis, effects, remediation and policy solutions, Journal of Environmental Chemical Engineering. 7 (2019) 103421. https://doi.org/10.1016/j.jece.2019.103421.

[5] UNEP, Microplastics: Trouble in the food chain, 2016. https://wesr.unep.org/.

[6] J.-Q. Jiang, Occurrence of microplastics and its pollution in the environment: A review, Sustainable Production and Consumption. 13 (2018) 16–23. https://doi.org/10.1016/j.spc.2017.11.003.

[7] F. Gallo, C. Fossi, R. Weber, D. Santillo, J. Sousa, I. Ingram, A. Nadal, D. Romano, Marine litter plastics and microplastics and their toxic chemicals components: the need for urgent preventive measures, Environ Sci Eur. 30 (2018) 13. https://doi.org/10.1186/s12302-018-0139-z.

[8] L. Peng, D. Fu, H. Qi, C.Q. Lan, H. Yu, C. Ge, Micro- and nano-plastics in marine environment: Source, distribution and threats — A review, Science of The Total Environment. 698 (2020) 134254. https://doi.org/10.1016/j.scitotenv.2019.134254.

[9] C. Jia, J. Luo, S. Zhang, X. Zhu, N-rich hydrochar derived from organic solvent as reaction medium generates toxic N-containing mineral in its pyrochar, Science of The Total Environment. 729 (2020) 138970. https://doi.org/10.1016/j.scitotenv.2020.138970.

[10] J. La Nasa, G. Biale, M. Mattonai, F. Modugno, Microwave-assisted solvent extraction and double-shot analytical pyrolysis for the quali-quantitation of plasticizers and microplastics in beach sand samples, Journal of Hazardous Materials. 401 (2021) 123287. https://doi.org/10.1016/j.jhazmat.2020.123287.

[11] J.H. Bridson, E.C. Gaugler, D.A. Smith, G.L. Northcott, S. Gaw, Leaching and extraction of additives from plastic pollution to inform environmental risk: A multidisciplinary review of analytical approaches, Journal of Hazardous Materials. 414 (2021) 125571. https://doi.org/10.1016/j.jhazmat.2021.125571.

[12] K. Gunaalan, E. Fabbri, M. Capolupo, The hidden threat of plastic leachates: A critical review on their impacts on aquatic organisms, Water Research. 184 (2020) 116170. https://doi.org/10.1016/j.watres.2020.116170.

[13] C.S. Kwan, H. Takada, Release of additives and monomers from plastic wastes, in: H. Takada, H.K. Karapanagioti (Eds.), Hazardous Chemicals Associated with Plastics in the Marine Environment, Springer International Publishing, Cham, 2019: pp. 51–70. https://doi.org/10.1007/698_2016_122.

[14] E.L. Teuten, J.M. Saquing, D.R.U. Knappe, M.A. Barlaz, S. Jonsson, A. Björn, S.J. Rowland, R.C. Thompson, T.S. Galloway, R. Yamashita, D. Ochi, Y. Watanuki, C. Moore, P.H. Viet, T.S. Tana, M. Prudente, R. Boonyatumanond, M.P. Zakaria, K. Akkhavong, Y. Ogata, H. Hirai, S. Iwasa, K. Mizukawa, Y. Hagino, A. Imamura, M. Saha, H. Takada, Transport and release of chemicals from plastics to the environment and to wildlife, Philos Trans R Soc Lond B Biol Sci. 364 (2009) 2027–2045. https://doi.org/10.1098/rstb.2008.0284.

[15] H. Luo, C. Liu, D. He, J. Sun, J. Li, X. Pan, Effects of aging on environmental behavior of plastic additives: Migration, leaching, and ecotoxicity, Science of The Total Environment. 849 (2022) 157951. https://doi.org/10.1016/j.scitotenv.2022.157951.

[16] S. Balbi, F. Villa, V. Mojtahed, K.T. Hegetschweiler, C. Giupponi, A spatial Bayesian network model to assess the benefits of early warning for urban flood risk to people, Natural Hazards and Earth System Sciences. 16 (2016) 1323–1337. https://doi.org/10.5194/nhess-16-1323-2016.

[17] L. Canesi, E. Fabbri, Environmental effects of BPA: Focus on aquatic species, Dose Response. 13 (2015) 1559325815598304. https://doi.org/10.1177/1559325815598304.

[18] K. Wang, T. Larkin, N. Singhal, Y. Zhao, Leachability of endocrine disrupting chemicals (EDCs) in municipal sewage sludge: Effects of EDCs interaction with dissolved organic matter, Science of The Total Environment. 742 (2020) 140366. https://doi.org/10.1016/j.scitotenv.2020.140366.

[19] Q. Chen, A. Allgeier, D. Yin, H. Hollert, Leaching of endocrine disrupting chemicals from marine microplastics and mesoplastics under common life stress conditions, Environment International. 130 (2019) 104938. https://doi.org/10.1016/j.envint.2019.104938.

[20] M. Capolupo, L. Sørensen, K.D.R. Jayasena, A.M. Booth, E. Fabbri, Chemical composition and ecotoxicity of plastic and car tire rubber leachates to aquatic organisms, Water Research. 169 (2020) 115270. https://doi.org/10.1016/j.watres.2019.115270.

[21] J. Muncke, Exposure to endocrine disrupting compounds via the food chain: Is packaging a relevant source?, Sci Total Environ. 407 (2009) 4549–4559. https://doi.org/10.1016/j.scitotenv.2009.05.006.

[22] M. Capolupo, K. Gunaalan, A.M. Booth, L. Sørensen, P. Valbonesi, E. Fabbri, The sub-lethal impact of plastic and tire rubber leachates on the Mediterranean mussel Mytilus galloprovincialis, Environmental Pollution. 283 (2021) 117081. https://doi.org/10.1016/j.envpol.2021.117081.

[23] M. Capolupo, R. Ayesha, A. Tanya, P. Valbonesi, I. Coralli, D. Fabbri, E. Fabbri, Chemical characterization and toxicity evaluation of bioplastics leachates in early larval stages and adult mussels, Mytilus galloprovincialis, (2022). https://easychair.org/smart-program/ESCPB2022/index.html.

[24] L. Wang, Y. Peng, Y. Xu, J. Zhang, C. Liu, X. Tang, Y. Lu, H. Sun, Earthworms' degradable bioplastic diet of polylactic acid: Easy to break down and slow to excrete, Environ. Sci. Technol. 56 (2022) 5020–5028. https://doi.org/10.1021/acs.est.1c08066.

[25] S. Lambert, M. Wagner, Environmental performance of bio-based and biodegradable plastics: the road ahead, Chem. Soc. Rev. 46 (2017) 6855–6871. https://doi.org/10.1039/C7CS00149E.

[26] A. Kjeldsen, M. Price, C. Lilley, E. Guzniczak, I. Archer, A review of standards for biodegradable plastics, 2022. (2022) 33.

[27] F. Razza, F.D. Innocenti, Bioplastics from renewable resources: the benefits of biodegradability, Asia-Pacific Journal of Chemical Engineering. 7 (2012) S301–S309. https://doi.org/10.1002/apj.1648.

[28] T. Haider, C. Völker, J. Kramm, K. Landfester, F. Wurm, Plastics of the future? The impact of biodegradable polymers on the environment and on society, Angewandte Chemie International Edition. 58 (2018). https://doi.org/10.1002/anie.201805766.

[29] A. Konti, D. Mamma, N. Scarlat, D. Damigos, The determinants of the growth of the European bioplastics sector –A fuzzy cognitive maps approach, Sustainability. 14 (2022) 6035. https://doi.org/10.3390/su14106035.

[30] T.P. Haider, C. Völker, J. Kramm, K. Landfester, F.R. Wurm, Plastics of the future? The impact of biodegradable polymers on the environment and on society, Angew. Chem. Int. Ed. 58 (2019) 50–62. https://doi.org/10.1002/anie.201805766.

[31] M. Lehtiniemi, S. Hartikainen, R. Turja, K.K. Lehtonen, J. Vepsäläinen, S. Peräniemi, J. Leskinen, O. Setälä, Exposure to leachates from post-consumer plastic and recycled rubber

causes stress responses and mortality in a copepod Limnocalanus macrurus, Marine Pollution Bulletin. 173 (2021) 113103. https://doi.org/10.1016/j.marpolbul.2021.113103.

[32] L. Zimmermann, S. Göttlich, J. Oehlmann, M. Wagner, C. Völker, What are the drivers of microplastic toxicity? Comparing the toxicity of plastic chemicals and particles to Daphnia magna, Environmental Pollution. 267 (2020) 115392. https://doi.org/10.1016/j.envpol.2020.115392.

[33] M. Nazareth, M.R.C. Marques, M.C.A. Leite, Í.B. Castro, Commercial plastics claiming biodegradable status: Is this also accurate for marine environments?, Journal of Hazardous Materials. 366 (2019) 714–722. https://doi.org/10.1016/j.jhazmat.2018.12.052.

[34] Y. Xia, D. Wang, D. Liu, J. Su, Y. Jin, D. Wang, B. Han, Z. Jiang, B. Liu, Applications of chitosan and its derivatives in skin and soft tissue diseases, Frontiers in Bioengineering and Biotechnology. 10 (2022). https://www.frontiersin.org/articles/10.3389/fbioe.2022.894667 (accessed October 12, 2022).

[35] OSPAR 2013 protocol - Background document and technical annexes for biological effects monitoring, Update 2013, OSPAR 2013 Protocol. (2016). www.ospar.org/documents?v=7316.

[36] K. Klein, T. Piana, T. Lauschke, P. Schweyen, G. Dierkes, T. Ternes, U. Schulte-Oehlmann, J. Oehlmann, Chemicals associated with biodegradable microplastic drive the toxicity to the freshwater oligochaete Lumbriculus variegatus, Aquatic Toxicology. 231 (2021) 105723. https://doi.org/10.1016/j.aquatox.2020.105723.

[37] M. Capolupo, A. Rafiq, I. Coralli, T. Alessandro, P. Valbonesi, D. Fabbri, E. Fabbri, Bioplastic leachates characterization and impacts on early larval stages and adult mussel cellular, biochemical and physiological responses, Environmental Pollution. 319 (2023) 120951. https://doi.org/10.1016/j.envpol.2022.120951.

[38] ASTM. Standard guide for conducting acute toxicity test starting with embryos of four species of saltwater bivalve molluscs. In: Marine Environmental Research., 2004.

[39] R. Fabbri, M. Montagna, T. Balbi, E. Raffo, F. Palumbo, L. Canesi, Adaptation of the bivalve embryotoxicity assay for the high throughput screening of emerging contaminants in Mytilus galloprovincialis, Marine Environmental Research. 99 (2014) 1–8. https://doi.org/10.1016/j.marenvres.2014.05.007.

[40] M. Sprung, Physiological energetics of mussel larvae (Mytilus edulis). II Food uptake, Mar. Ecol. Prog. Ser. 17 (1984) 295–305. https://doi.org/10.3354/meps017295.

[41] C. Martìnez-Gomez, J. Bignell, D. Lowe, Lysosomal membrane stability in mussels, (2015). https://doi.org/10.17895/ICES.PUB.5084.

[42] P. Valbonesi, G. Sartor, E. Fabbri, Characterization of cholinesterase activity in three bivalves inhabiting the North Adriatic sea and their possible use as sentinel organisms for biosurveillance programmes, Science of The Total Environment. 312 (2003) 79–88. https://doi.org/10.1016/S0048-9697(03)00227-4.

[43] M. Capolupo, P. Valbonesi, E. Fabbri, A comparative assessment of the chronic effects of micro- and nano-plastics on the physiology of the mediterranean mussel Mytilus galloprovincialis, Nanomaterials. 11 (2021) 649. https://doi.org/10.3390/nano11030649.

[44] K.J. Groh, T. Backhaus, B. Carney-Almroth, B. Geueke, P.A. Inostroza, A. Lennquist, H.A. Leslie, M. Maffini, D. Slunge, L. Trasande, A.M. Warhurst, J. Muncke, Overview of known plastic packaging-associated chemicals and their hazards, Science of The Total Environment. 651 (2019) 3253–3268. https://doi.org/10.1016/j.scitotenv.2018.10.015.

[45] C. Venâncio, I. Lopes, M. Oliveira, Bioplastics: known effects and potential consequences to marine and estuarine ecosystem services, Chemosphere. 309 (2022) 136810. https://doi.org/10.1016/j.chemosphere.2022.136810.

[46] L. Zimmermann, A. Dombrowski, C. Völker, M. Wagner, Are bioplastics and plant-based materials safer than conventional plastics? In vitro toxicity and chemical composition, Environment International. 145 (2020) 106066. https://doi.org/10.1016/j.envint.2020.106066.

[47] T. Uribe-Echeverría, R. Beiras, Acute toxicity of bioplastic leachates to Paracentrotus lividus sea urchin larvae, Marine Environmental Research. 176 (2022) 105605. https://doi.org/10.1016/j.marenvres.2022.105605.

[48] S. Tsuge, H. Ohtani, C. Watanabe, Pyrolysis–GC/MS data book of synthetic polymers - Pyrograms, thermograms and MS of pyrolyzates, Elsevier, 2012.

[49] N. Dimitrov, L. Kratofil Krehula, A. Ptiček Siročić, Z. Hrnjak-Murgić, Analysis of recycled PET bottles products by pyrolysis-gas chromatography, Polymer Degradation and Stability. 98 (2013) 972–979. https://doi.org/10.1016/j.polymdegradstab.2013.02.013.

[50] E. Castro-Aguirre, F. Iñiguez-Franco, H. Samsudin, X. Fang, R. Auras, Poly(lactic acid) – Mass production, processing, industrial applications, and end of life, Advanced Drug Delivery Reviews. 107 (2016) 333–366. https://doi.org/10.1016/j.addr.2016.03.010.

[51] E.D. Okoffo, C.M. Chan, C. Rauert, S. Kaserzon, K.V. Thomas, Identification and quantification of micro-bioplastics in environmental samples by pyrolysis–gas chromatography–mass spectrometry, Environ. Sci. Technol. 56 (2022) 13774–13785. https://doi.org/10.1021/acs.est.2c04091.

[52] J. Jian, Z. Xiangbin, H. Xianbo, An overview on synthesis, properties and applications of poly(butylene-adipate-co-terephthalate) – PBAT, Advanced Industrial and Engineering Polymer Research. 3 (2020) 19–26. https://doi.org/10.1016/j.aiepr.2020.01.001.

[53] I. Vroman, L. Tighzert, Biodegradable polymers, Materials. 2 (2009) 307–344. https://doi.org/10.3390/ma2020307.

[54] M. Dammak, Y. Fourati, Q. Tarrés, M. Delgado-Aguilar, P. Mutjé, S. Boufi, Blends of PBAT with plasticized starch for packaging applications: Mechanical properties, rheological behaviour and biodegradability, Industrial Crops and Products. 144 (2020) 112061. https://doi.org/10.1016/j.indcrop.2019.112061.

[55] F.V. Ferreira, L.S. Cividanes, R.F. Gouveia, L.M.F. Lona, An overview on properties and applications of poly(butylene adipate-co-terephthalate) – PBAT based composites, Polymer Engineering & Science. 59 (2019) E7–E15. https://doi.org/10.1002/pen.24770.

[56] ISO 14855-1:2012. Determination of the ultimate aerobic biodegradability of plastic materials under controlled composting conditions – Method by analysis of evolved carbon dioxide – Part 1: General method, 2012. https://www.iso.org/cms/render/live/en/sites/isoorg/contents/data/standard/05/79/57902.html (accessed October 26, 2022).

[57] ISO 14855-2:2018. Determination of the ultimate aerobic biodegradability of plastic materials under controlled composting conditions – Method by analysis of evolved carbon dioxide – Part 2: Gravimetric measurement of carbon dioxide evolved in a laboratory-scale test, 2018. https://www.iso.org/cms/render/live/en/sites/isoorg/contents/data/standard/07/20/72046.html (accessed October 26, 2022).

[58] L. Gueissaz, G. Massonnet, Study on the discrimination of tires using chemical profiles obtained by Py-GC/MS, Journal of Analytical and Applied Pyrolysis. 124 (2017) 704–718. https://doi.org/10.1016/j.jaap.2016.11.024.

[59] F. Xu, B. Wang, D. Yang, X. Ming, Y. Jiang, J. Hao, Y. Qiao, Y. Tian, TG-FTIR and Py-GC/MS study on pyrolysis mechanism and products distribution of waste bicycle tire, Energy Conversion and Management. 175 (2018) 288–297. https://doi.org/10.1016/j.enconman.2018.09.013.

[60] F. Akoueson, C. Chbib, S. Monchy, I. Paul-Pont, P. Doyen, A. Dehaut, G. Duflos, Identification and quantification of plastic additives using pyrolysis-GC/MS: A review, Science of The Total Environment. 773 (2021) 145073. https://doi.org/10.1016/j.scitotenv.2021.145073.

[61] B. Ibrahim, A. Wiranata, A. Malik, The effect of addition of antioxidant 1,2-dihydro-2,2,4-trimethyl-quinoline on characteristics of crepe rubber modified asphalt in short term aging and long term aging conditions, Applied Sciences. 10 (2020) 7236. https://doi.org/10.3390/app10207236.

[62] M.R. Jung, F.D. Horgen, S.V. Orski, V. Rodriguez C., K.L. Beers, G.H. Balazs, T.T. Jones, T.M. Work, K.C. Brignac, S.-J. Royer, K.D. Hyrenbach, B.A. Jensen, J.M. Lynch, Validation of ATR FT-IR to identify polymers of plastic marine debris, including those ingested by marine

organisms, Marine Pollution Bulletin. 127 (2018) 704–716. https://doi.org/10.1016/j.marpolbul.2017.12.061.

[63] Y. Cai, J. Lv, J. Feng, Spectral characterization of four kinds of biodegradable plastics: poly (lactic acid), poly (butylenes adipate-co-terephthalate), poly (hydroxybutyrate-co-hydroxyvalerate) and poly (butylenes succinate) with FTIR and Raman spectroscopy, J Polym Environ. 21 (2013) 108–114. https://doi.org/10.1007/s10924-012-0534-2.

[64] K. Elfehri Borchani, C. Carrot, M. Jaziri, Biocomposites of Alfa fibers dispersed in the Mater-Bi® type bioplastic: Morphology, mechanical and thermal properties, Composites Part A: Applied Science and Manufacturing. 78 (2015) 371–379. https://doi.org/10.1016/j.compositesa.2015.08.023.

[65] J. Seelenbinder, Rapid identification of o-rings, seals and gaskets using the handheld Agilent 4100 ExoScan FTIR, in: Materials Testing and Research Solutions from Agilent - Polymers and Rubbers Application Compendium, Agilent Technologies Danbury, CT, USA, 2010: p. 216.

[66] S. Gunasekaran, R.K. Natarajan, A. Kala, FTIR spectra and mechanical strength analysis of some selected rubber derivatives, Spectrochimica Acta Part A: Molecular and Biomolecular Spectroscopy. 68 (2007) 323–330. https://doi.org/10.1016/j.saa.2006.11.039.

[67] R. Zhang, H. Wang, J. Ji, Z. Suo, Z. Ou, Influences of different modification methods on surface activation of waste tire rubber powder applied in cement-based materials, Construction and Building Materials. 314 (2022) 125191. https://doi.org/10.1016/j.conbuildmat.2021.125191.

[68] H. Serrano-Ruíz, J. Eras, L. Martín-Closas, A.M. Pelacho, Compounds released from unused biodegradable mulch materials after contact with water, Polymer Degradation and Stability. 178 (2020) 109202. https://doi.org/10.1016/j.polymdegradstab.2020.109202.

[69] N. Zhang, F. Bi, F. Xu, H. Yong, Y. Bao, C. Jin, J. Liu, Structure and functional properties of active packaging films prepared by incorporating different flavonols into chitosan based matrix, International Journal of Biological Macromolecules. 165 (2020) 625–634. https://doi.org/10.1016/j.ijbiomac.2020.09.209.

[70] R.E. Conn, J.J. Kolstad, J.F. Borzelleca, D.S. Dixler, L.J. Filer, B.N. LaDu, M.W. Pariza, Safety assessment of polylactide (PLA) for use as a food-contact polymer, Food Chem Toxicol. 33 (1995) 273–283. https://doi.org/10.1016/0278-6915(94)00145-e.

[71] ECHA, ECHA Substance Infocard - 1,6-dioxacyclododecane-7,12-dione, European Chemical Agency. (2021). https://echa.europa.eu/it/substance-information/-/substanceinfo/100.011.174.

[72] E. Balestri, V. Menicagli, V. Ligorini, S. Fulignati, A.M. Raspolli Galletti, C. Lardicci, Phytotoxicity assessment of conventional and biodegradable plastic bags using seed

germination test, Ecological Indicators. 102 (2019) 569–580. https://doi.org/10.1016/j.ecolind.2019.03.005.

[73] Y. Liu, L. Tong, N. Si, J. Xing, Q. Zhang, Q. Ma, Q. Lv, Non-targeted identification of unknown chemical hazardous substances in infant teether toys by gas chromatography-Orbitrap high resolution mass spectrometry, Ecotoxicology and Environmental Safety. 224 (2021) 112676. https://doi.org/10.1016/j.ecoenv.2021.112676.

[74] J.S. Félix, F. Isella, O. Bosetti, C. Nerín, Analytical tools for identification of non-intentionally added substances (NIAS) coming from polyurethane adhesives in multilayer packaging materials and their migration into food simulants, Anal Bioanal Chem. 403 (2012) 2869–2882. https://doi.org/10.1007/s00216-012-5965-z.

[75] B. Thiébaut, A. Lattuati-Derieux, M. Hocevar, L.-B. Vilmont, Application of headspace SPME-GC-MS in characterisation of odorous volatile organic compounds emitted from magnetic tape coatings based on poly(urethane-ester) after natural and artificial ageing, Polymer Testing. 26 (2007) 243–256. https://doi.org/10.1016/j.polymertesting.2006.10.006.

[76] M. Watanabe, C. Nakata, W. Wu, K. Kawamoto, Y. Noma, Characterization of semi-volatile organic compounds emitted during heating of nitrogen-containing plastics at low temperature, Chemosphere. 68 (2007) 2063–2072. https://doi.org/10.1016/j.chemosphere.2007.02.022.

[77] E. Canellas, P. Vera, C. Nerín, UPLC–ESI-Q-TOF-MSE and GC–MS identification and quantification of non-intentionally added substances coming from biodegradable food packaging, Anal Bioanal Chem. 407 (2015) 6781–6790. https://doi.org/10.1007/s00216-015-8848-2.

[78] C. Zhang, E. Zhang, Z. Guo, C. Ouyang, C. Lu, X. Zeng, J. Li, Detection and control of cyclic esters in biodegradable polyesters, Advanced Industrial and Engineering Polymer Research. (2022). https://doi.org/10.1016/j.aiepr.2022.07.001.

[79] J. Song, A. Šišková, M.G. Simons, W.J. Kowalski, M.M. Kowalczuk, O.F. van den Brink, LC-multistage mass spectrometry for the characterization of poly(butylene adipate-co-butylene terephthalate) copolyester, J. Am. Soc. Mass Spectrom. 22 (2011) 641–648. https://doi.org/10.1007/s13361-010-0071-y.

[80] M. Aznar, S. Ubeda, N. Dreolin, C. Nerín, Determination of non-volatile components of a biodegradable food packaging material based on polyester and polylactic acid (PLA) and its migration to food simulants, Journal of Chromatography A. 1583 (2019) 1–8. https://doi.org/10.1016/j.chroma.2018.10.055.

[81] J. Osorio, M. Aznar, C. Nerín, C. Elliott, O. Chevallier, Comparison of LC-ESI, DART, and ASAP for the analysis of oligomers migration from biopolymer food packaging materials in food (simulants), Anal Bioanal Chem. 414 (2022) 1335–1345. https://doi.org/10.1007/s00216-021-03755-0.

[82] D.Y. Kim, J.B. Lee, D.Y. Lee, K.H. Seo, Plasticization effect of poly(lactic acid) in the poly(butylene adipate–co–terephthalate) blown film for tear resistance improvement, Polymers. 12 (2020) 1904. https://doi.org/10.3390/polym12091904.

[83] E. Canellas, M. Aznar, C. Nerín, P. Mercea, Partition and diffusion of volatile compounds from acrylic adhesives used for food packaging multilayers manufacturing, Journal of Materials Chemistry. 20 (2010) 5100–5109. https://doi.org/10.1039/C0JM00514B.

[84] M.A.A. Mahmoud, A. Buettner, Characterisation of aroma-active and off-odour compounds in German rainbow trout (Oncorhynchus mykiss). Part I: Case of aquaculture water from earthen-ponds farming, Food Chemistry. 210 (2016) 623–630. https://doi.org/10.1016/j.foodchem.2016.05.030.

[85] M.A.A. Mahmoud, A. Buettner, Characterisation of aroma-active and off-odour compounds in German rainbow trout (Oncorhynchus mykiss). Part II: Case of fish meat and skin from earthen-ponds farming, Food Chemistry. 232 (2017) 841–849. https://doi.org/10.1016/j.foodchem.2016.09.172.

[86] B. Seiwert, P. Klöckner, S. Wagner, T. Reemtsma, Source-related smart suspect screening in the aqueous environment: search for tire-derived persistent and mobile trace organic contaminants in surface waters, Anal Bioanal Chem. 412 (2020) 4909–4919. https://doi.org/10.1007/s00216-020-02653-1.

[87] C. Marwood, B. McAtee, M. Kreider, R.S. Ogle, B. Finley, L. Sweet, J. Panko, Acute aquatic toxicity of tire and road wear particles to alga, daphnid, and fish, Ecotoxicology. 20 (2011) 2079. https://doi.org/10.1007/s10646-011-0750-x.

[88] C. Eichler, European Union risk ssessment report - N-cyclohexylbenzothiazol-2-sulphenamide, Office for Official Publications of the European Communities, 2008.

[89] P.B. Sulekha, R. Joseph, Preparation and characterisation of novel polymer bound phenolic antioxidants and its use in natural rubber, Journal of Elastomers & Plastics. 35 (2003) 85–97. https://doi.org/10.1177/009524403031638.

[90] N. Bartsch, M. Girard, A. Wilde, T. Bruhn, O. Kappenstein, B. Vieth, C. Hutzler, A. Luch, Thermal stability of polymer additives: Comparison of decomposition models including oxidative pyrolysis – Polymer additives in decomposition models, J Vinyl Addit Technol. 25 (2019) E12–E27. https://doi.org/10.1002/vnl.21654.

[91] C.M. Reddy, J.G. Quinn, Environmental chemistry of benzothiazoles derived from rubber, Environ. Sci. Technol. 31 (1997) 2847–2853. https://doi.org/10.1021/es970078o.

[92] K. Klein, D. Hof, A. Dombrowski, P. Schweyen, G. Dierkes, T. Ternes, U. Schulte-Oehlmann, J. Oehlmann, Enhanced in vitro toxicity of plastic leachates after UV irradiation, Water Research. 199 (2021) 117203. https://doi.org/10.1016/j.watres.2021.117203.

[93] M.N. Moore, J.I. Allen, A. McVeigh, J. Shaw, Lysosomal and autophagic reactions as predictive indicators of environmental impact in aquatic animals, Autophagy. 2 (2006) 217–220. https://doi.org/10.4161/auto.2663.

[94] A. Viarengo, D. Lowe, C. Bolognesi, E. Fabbri, A. Koehler, The use of biomarkers in biomonitoring: A 2-tier approach assessing the level of pollutant-induced stress syndrome in sentinel organisms, Comparative Biochemistry and Physiology Part C: Toxicology & Pharmacology. 146 (2007) 281–300. https://doi.org/10.1016/j.cbpc.2007.04.011.

[95] M.N. Moore, M.H. Depledge, J.W. Readman, D.R. Paul Leonard, An integrated biomarker-based strategy for ecotoxicological evaluation of risk in environmental management, Mutation Research/Fundamental and Molecular Mechanisms of Mutagenesis. 552 (2004) 247–268. https://doi.org/10.1016/j.mrfmmm.2004.06.028.

[96] J.P. Shaw, M.N. Moore, J.W. Readman, Z. Mou, W.J. Langston, D.M. Lowe, P.E. Frickers, L. Al-Moosawi, C. Pascoe, A. Beesley, Oxidative stress, lysosomal damage and dysfunctional autophagy in molluscan hepatopancreas (digestive gland) induced by chemical contaminants, Marine Environmental Research. 152 (2019) 104825. https://doi.org/10.1016/j.marenvres.2019.104825.

[97] L. Canesi, L.C. Lorusso, C. Ciacci, M. Betti, M. Rocchi, G. Pojana, A. Marcomini, Immunomodulation of Mytilus hemocytes by individual estrogenic chemicals and environmentally relevant mixtures of estrogens: In vitro and in vivo studies, Aquatic Toxicology. 81 (2007) 36–44. https://doi.org/10.1016/j.aquatox.2006.10.010.

[98] L. Giamberini, J. Pihan, Lysosomal changes in the hemocytes of the freshwater mussel Dreissena polymorpha experimentally exposed to lead and zinc, Dis. Aquat. Org. 28 (1997) 221–227. https://doi.org/10.3354/dao028221.

[99] M. Sharifinia, Z.A. Bahmanbeigloo, M. Keshavarzifard, M.H. Khanjani, B.P. Lyons, Microplastic pollution as a grand challenge in marine research: A closer look at their adverse impacts on the immune and reproductive systems, Ecotoxicology and Environmental Safety. 204 (2020) 111109. https://doi.org/10.1016/j.ecoenv.2020.111109.

[100] B. Fernández, M. Albentosa, Insights into the uptake, elimination and accumulation of microplastics in mussel, Environmental Pollution. 249 (2019) 321–329. https://doi.org/10.1016/j.envpol.2019.03.037.

[101] D.M. Lowe, M.N. Moore, K.R. Clarke, Effects of oil on digestive cells in mussels: Quantitative alterations in cellular and lysosomal structure, Aquatic Toxicology. 1 (1981) 213–226. https://doi.org/10.1016/0166-445X(81)90016-3.

[102] M.N. Moore, Autophagy as a second level protective process in conferring resistance to environmentally-induced oxidative stress, Autophagy. 4 (2008) 254–256. https://doi.org/10.4161/auto.5528.

[103] A. Orbea, L. Garmendia, I. Marigómez, M. Cajaraville, Effects of the Prestige oil spill on cellular biomarkers in intertidal mussels: results of the first year of studies, Mar. Ecol. Prog. Ser. 306 (2006) 177–189. https://doi.org/10.3354/meps306177.

[104] B. Marchi, B. Burlando, M.N. Moore, A. Viarengo, Mercury- and copper-induced lysosomal membrane destabilisation depends on [Ca2+]i dependent phospholipase A2 activation, Aquatic Toxicology. 66 (2004) 197–204. https://doi.org/10.1016/j.aquatox.2003.09.003.

[105] M. Capolupo, S. Franzellitti, A. Kiwan, P. Valbonesi, E. Dinelli, E. Pignotti, M. Birke, E. Fabbri, A comprehensive evaluation of the environmental quality of a coastal lagoon (Ravenna, Italy): Integrating chemical and physiological analyses in mussels as a biomonitoring strategy, Science of The Total Environment. 598 (2017) 146–159. https://doi.org/10.1016/j.scitotenv.2017.04.119.

[106] G. Signa, R. Di Leonardo, A. Vaccaro, C.D. Tramati, A. Mazzola, S. Vizzini, Lipid and fatty acid biomarkers as proxies for environmental contamination in caged mussels Mytilus galloprovincialis, Ecological Indicators. 57 (2015) 384–394. https://doi.org/10.1016/j.ecolind.2015.05.002.

[107] S.J. Brooks, C. Escudero-Oñate, T. Gomes, L. Ferrando-Climent, An integrative biological effects assessment of a mine discharge into a Norwegian fjord using field transplanted mussels, Science of The Total Environment. 644 (2018) 1056–1069. https://doi.org/10.1016/j.scitotenv.2018.07.058.

[108] F. Donnini, E. Dinelli, F. Sangiorgi, E. Fabbri, A biological and geochemical integrated approach to assess the environmental quality of a coastal lagoon (Ravenna, Italy), Environment International. 33 (2007) 919–928. https://doi.org/10.1016/j.envint.2007.05.002.

[109] N.N. Fokina, T.R. Ruokolainen, N.N. Nemova, I.N. Bakhmet, Changes of blue mussels Mytilus edulis L. Lipid composition under cadmium and copper toxic effect, Biol Trace Elem Res. 154 (2013) 217–225. https://doi.org/10.1007/s12011-013-9727-3.

[110] F. Regoli, M.E. Giuliani, Oxidative pathways of chemical toxicity and oxidative stress biomarkers in marine organisms, Marine Environmental Research. 93 (2014) 106–117. https://doi.org/10.1016/j.marenvres.2013.07.006.

[111] A. Terman, U.T. Brunk, Oxidative stress, accumulation of biological “garbage”, and aging, Antioxidants & Redox Signaling. 8 (2006) 197–204. https://doi.org/10.1089/ars.2006.8.197.

[112] T. Gomes, C.G. Pereira, C. Cardoso, V.S. Sousa, M.R. Teixeira, J.P. Pinheiro, M.J. Bebianno, Effects of silver nanoparticles exposure in the mussel Mytilus galloprovincialis, Marine Environmental Research. 101 (2014) 208–214. https://doi.org/10.1016/j.marenvres.2014.07.004.

[113] S.G. Cheung, P.Y. Tong, K.M. Yip, P.K.S. Shin, Chemical cues from predators and damaged conspecifics affect byssus production in the green-lipped mussel *perna viridis*, Marine and Freshwater Behaviour and Physiology. 37 (2004) 127–135. https://doi.org/10.1080/10236240410001705798.

[114] B.T.G. Gowland, A.D. McIntosh, I.M. Davies, C.F. Moffat, L. Webster, Implications from a field study regarding the relationship between polycyclic aromatic hydrocarbons and glutathione S-transferase activity in mussels, Marine Environmental Research. 54 (2002) 231–235. https://doi.org/10.1016/S0141-1136(02)00129-0.

[115] N. Petushok, T. Gabryelak, D. Pałecz, L. Zavodnik, I. Szollosi Varga, K.A. Deér, Comparative study of the xenobiotic metabolising system in the digestive gland of the bivalve molluscs in different aquatic ecosystems and in aquaria experiments, Aquatic Toxicology. 61 (2002) 65–72. https://doi.org/10.1016/S0166-445X(02)00030-9.

[116] F. Regoli, G. Frenzilli, R. Bocchetti, F. Annarumma, V. Scarcelli, D. Fattorini, M. Nigro, Time-course variations of oxyradical metabolism, DNA integrity and lysosomal stability in mussels, Mytilus galloprovincialis, during a field translocation experiment, Aquatic Toxicology. 68 (2004) 167–178. https://doi.org/10.1016/j.aquatox.2004.03.011.

[117] M. Gerdol, M. Gomez-Chiarri, M.G. Castillo, A. Figueras, G. Fiorito, R. Moreira, B. Novoa, A. Pallavicini, G. Ponte, K. Roumbedakis, P. Venier, G.R. Vasta, Immunity in Molluscs: Recognition and Effector Mechanisms, with a Focus on Bivalvia, in: E.L. Cooper (Ed.), Advances in Comparative Immunology, Springer International Publishing, Cham, 2018: pp. 225–341. https://doi.org/10.1007/978-3-319-76768-0_11.

[118] B. Myrnes, A. Johansen, Recovery of lysozyme from scallop waste, Preparative Biochemistry. 24 (1994) 69–80. https://doi.org/10.1080/10826069408010083.

[119] V. Matozzo, F. Gagné, M.G. Marin, F. Ricciardi, C. Blaise, Vitellogenin as a biomarker of exposure to estrogenic compounds in aquatic invertebrates: A review, Environment International. 34 (2008) 531–545. https://doi.org/10.1016/j.envint.2007.09.008.

[120] L. Stabili, P. Pagliara, Effect of zinc on lysozyme-like activity of the seastar Marthasterias glacialis (Echinodermata, Asteroidea) mucus, Journal of Invertebrate Pathology. 100 (2009) 189–192. https://doi.org/10.1016/j.jip.2009.01.005.

[121] V. Matozzo, M.G. Marin, Can 4-nonylphenol induce vitellogenin-like proteins in the clam Tapes philippinarum?, Environmental Research. 97 (2005) 43–49. https://doi.org/10.1016/j.envres.2004.03.002.

[122] L. Canesi, C. Ciacci, L.C. Lorusso, M. Betti, T. Guarnieri, S. Tavolari, G. Gallo, Immunomodulation by 17β-estradiol in bivalve hemocytes, American Journal of Physiology-Regulatory, Integrative and Comparative Physiology. 291 (2006) R664–R673. https://doi.org/10.1152/ajpregu.00139.2006.

[123] T. Balbi, C. Ciacci, L. Canesi, Estrogenic compounds as exogenous modulators of physiological functions in molluscs: Signaling pathways and biological responses, Comparative Biochemistry and Physiology Part C: Toxicology & Pharmacology. 222 (2019) 135–144. https://doi.org/10.1016/j.cbpc.2019.05.004.

[124] Y. Tang, Y. Han, W. Zhang, Y. Yu, L. Huang, W. Zhou, W. Shi, D. Tian, G. Liu, Bisphenol A and microplastics weaken the antimicrobial ability of blood clams by disrupting humoral immune responses and suppressing hemocyte chemotactic activity, Environmental Pollution. 307 (2022) 119497. https://doi.org/10.1016/j.envpol.2022.119497.

[125] S.A. Steinert, G.V. Pickwell, Quantitative determination of lysozyme in the hemolymph of Mytilus edulis by the enzyme-linked immunosorbent assay (ELISA), Marine Environmental Research. 14 (1984) 229–243. https://doi.org/10.1016/0141-1136(84)90080-1.

[126] E. Ko, S.-I. Ku, D. Kim, S. Shin, M. Choi, Effects of heavy metals and albumin on lysozyme activity, JABC. 61 (2018) 367–370. https://doi.org/10.3839/jabc.2018.051.

[127] M. Pazmiño, S. Monica, W. James, G. Juan, A. Jose Luis, C. Wilman, Heavy metal - Induced inhibition of enzymatic activity in hen egg white lysozyme, Asian J Pharm Clin Res. 11 (2018) 212. https://doi.org/10.22159/ajpcr.2018.v11i11.22892.

[128] G. Juhel, S. Bayen, C. Goh, W.K. Lee, B.C. Kelly, Use of a suite of biomarkers to assess the effects of carbamazepine, bisphenol A, atrazine, and their mixtures on green mussels, *Perna viridis*: Biomarkers in green mussels exposed to emerging contaminants, Environ Toxicol Chem. 36 (2017) 429–441. https://doi.org/10.1002/etc.3556.

[129] M.F. Frasco, D. Fournier, F. Carvalho, L. Guilhermino, Do metals inhibit acetylcholinesterase (AChE)? Implementation of assay conditions for the use of AChE activity as a biomarker of metal toxicity, Biomarkers. 10 (2005) 360–375. https://doi.org/10.1080/13547500500264660.

[130] M. Walpitagama, M. Carve, A.M. Douek, C. Trestrail, Y. Bai, J. Kaslin, D. Wlodkowic, Additives migrating from 3D-printed plastic induce developmental toxicity and neuro-behavioural alterations in early life zebrafish (Danio rerio), Aquatic Toxicology. 213 (2019) 105227. https://doi.org/10.1016/j.aquatox.2019.105227.

4. Conclusions

Since polymeric materials have been introduced in human life, they entailed a broad variety of benefits. Advantages were achieved in many application fields, such as industry, technology, building, agriculture, medical and biomedical engineering and so forth, exceptionally improving the quality of our life. Anyway, everything that enters the environment has the potential to modify ecosystem balances, and the same holds for polymers. The intensive production, together with the widespread applications and uses, and the imperfect waste management are leading to the continuous growth of polymers in the environment, turning them into emerging contaminants (ECs). ECs generate concern because of their persistent or pseudo-persistent behaviour and the only partial knowledge about their toxicity. In fact, the risks that most of the polymers may poses on ecosystems and human health, are still unknown or uncertified. Consequently, regulations on the emission of these classes of contaminants are on the way or sill missing. For this thesis project different polymeric ECs were investigated, including both water-soluble and water-insoluble polymers. Particular attention was paid on microplastics (MPs), because of the current emerging concern on this polymer class, but also silicones and polyester-based bioplastics were considered.

Analytical approaches on polymer investigations are several and each technique can provide different specific information, also reporting results in different quantitative units (e.g., number of particles or mass units). For this thesis the thermoanalytical technique of pyrolysis gas-chromatography and mass spectrometry (Py-GC-MS) was applied for the characterisation and quantification of polymers in contexts of environmental interest. Py-GC-MS is gaining consents in the investigation of polymers in environmental complex matrices for its capability to detect and quantify polymers in mass units. Besides its potential in polymer detection, Py-GC-MS also provides chemical and structural information, enhancing the quality of results. Hence, the aim of this thesis was to provide comprehensive information about benefits and limits of Py-GC-MS for the investigation of polymers, from their characterisation to their quantification in complex matrices.

Among water-soluble polymers, poly(dimethylsiloxanes) (PDMS) bearing polyethylene glycol (PEG) side chains were selected as analytes of interest, due to their wide employing in cosmetics and personal care products. Given the large domestic use, these polymers have the potential to continuously enter the environment from wastewaters, becoming pseudo-persistent. The

potential of Py-GC-MS for the analytical investigation of these polymers was not investigated yet. The study revealed the possibility to detect PEG-PDMS from the presence of linear dimethyl polysiloxanes in the pyrolyzates, distinguishing the occurrence of copolymers from the homopolymers (PDMS). Moreover, a novel procedure for silicones extraction from sewage sludges deriving from a wastewater treatment plant was developed. The validation of the method and its application on real matrices demonstrated that Py-GC-MS is suitable for the qualitative and quantitative investigation of PDMS and their PEG-copolymers as trace analytes in complex matrices. Anyway, it was not possible to discriminate the occurrence of PEG-PDMS from the co-presence of PEG and PDMS, given the lack of pyrolytic indicators of the copolymer. Finally, in the investigated pyrograms the occurrence of other compounds, such as galaxolide fragrance and biocide triclosan, was found, showing that Py-GC-MS can be extended to the simultaneous determination of low molecular weight substances.

Investigations of water-insoluble polymers were mainly focused on MPs. A first study aimed at the understanding of thermal behaviour of polymers while they are co-pyrolysed. The use of Py-GC-MS to the study of environmental MPs, inevitably causes the co-pyrolysis of all compounds and polymers (both matrix and analytes) that compose the sample. In the event that reactive pyrolysis products are formed, secondary reactions may occur, leading to bias in polymer identification (due to the modification of the related fingerprints) and quantification (because of the variation of relative peak areas). In the present study, common polymers were considered given their intensive production and wide reporting among environmental MPs: high-density polyethylene (HDPE), polypropylene (PP), polystyrene (PS), polyvinylchloride (PVC), polyamides (nylon-6, PA-6 and nylon-6,6, PA-6,6) and polyethylene terephthalate (PET). Polymers individually pyrolysed exhibited reproducible pyrograms, and correlation results from calibrations were comparable with literature. Anyway, the pyrolysis of polymer mixtures generated new compounds, suggesting the occurrence of secondary reactions. PET resulted the most critical polymer because of the formation of benzoic acid and its derivatives (such as vinyl esters) that can be involved in various reactions. Interactions were recognised with polyamides (PA-6 and PA-6,6) and PVC, and the study revealed the possibility to monitor the occurrence of these secondary reactions looking for specific ions in the MS-pyrograms. The ions at *m/z* 102 and 130, were identified as proxies of PET/polyamides interactions, representing benzonitrile and cyano-benzoate ions, respectively; whereas the ions at *m/z* 211 and 213, indicate the presence of chlorinated derivatives of benzenedicarboxylic acids generated from PET/PVC interactions. These interactions were supposed to be minimised in the presence of tetramethylammonium hydroxide (TMAH) as derivatisation reagent.

Moving from purely laboratory investigations to complex environmental samples, MP analysis get further complicated, due to the heterogeneity of polymer classes and the matrix effect. A second study on MPs focused on polyurethanes (PURs), being a family composed of a manifold number of polymers with different structures, forms and properties. Methylene diphenyl diisocyanate- and toluene diisocyanate-PURs (MDI-PURs and TDI-PURs, respectively) were reasonably considered as representative of the most significative portion of PURs detectable within MPs. Py-GC-MS showed that PUR subclasses can be recognised depending on the diisocyanate which compose the structure, which generate one main pyrolysis product. Nevertheless, experimental conditions may affect the pyrolytic behaviour of pyrolyzates and the formation of the diisocyanates or the related diamines can occur, leading to possible bias. This ambiguity was overcome by combining thermochemolysis to pyrolysis (TMAH-Py-GC-MS), generating the methylated diamines of the respective diisocyanates as stable indicators (4,4'-methylenebis-(N,N-dimethyl) benzeneamine and N^1,N^4,N^4,2-tetramethylbenzene-1,4-diamine for MDI and TDI-PUR, respectively). Tests on PUR particles in the presence of an environmental organic matrix evidenced interactions of the accompanying compounds with polymer decomposition products, which negatively affected polymer investigation by direct pyrolysis. These interactions were avoided in the presence of TMAH, supporting the hypothesis that thermochemolysis greatly improves analytical results in investigation of PURs, as well as other polymers within environmental MPs. Moreover, statistical elaborations on chemically different MDI-PURs by TMAH-Py-GC-MS showed that, within a limited mass-range, a reliable mass estimation of total MDI-PURs as a cluster is possible just using the calibration of one standard, regardless of chemical heterogeneity. Basing on this point, PUR content was quantified in road dusts and spider webs and, by comparison with a previous study, a strong relation between PUR occurrence and the presence of an emission source was highlighted. Across this study, Py-GC-MS and TMAH-Py-GC-MS have been confirmed to be effective techniques for the characterisation of polymers, distinguishing chemically different polymers, but also providing univocal markers to identify PUR subclasses. Moreover, the capability of analytical pyrolysis for environmental investigation was proven, providing reproducible and comparable results in space and time.

In the last study, attention was paid on bioplastics. The concern generated by the spread of plastic litter in the environment, is moving the general attention to the production of alternative, more bio-compatible materials. The market of biopolymers is more and more growing, and few studies have addressed their possible impact on ecosystems. Recent studies showed that the production of MPs from plastic fragmentation is not the only reason of concern. Experimentally produced plastic leachates have shown that plastics can release a variety of organic and

inorganic additives into seawater. Additionally, negative effects of these leachates were highlighted on growth, development and survival of marine organisms. Accordingly with biodegradable plastic concept, bioplastics may more readily release both MPs and chemical additives. Moreover, hidden compromises and vagueness are found in the information provided by the manufacturers for bioplastic commercial items composition. In this context, Py-GC-MS can be a helpful tool, supplying chemical characterisation of the materials under investigation. On the basis of a previous report on plastic leachates, a study was developed with the aim to analyse the compounds released from commercial bioplastics in marine environment. Different commercial items were considered: a bio-based PET disposable bottle (partially bio-based polymer, non-biodegradable), a polylactic acid cup (100 % biobased polymer, biodegradable) and a compostable plastic bag (unknown origin, suitable to industrial composting). The study revealed the prominent occurrence of organic compounds in leachates from biodegradable and compostable plastic. Moreover, parallel biological essay assessed that the exposure of marine organisms (*Mytilus galloprovincialis*) to bioplastic leachates affected physiological parameters with a comparable extent to (or even greater than) conventional polymers. Py-GC-MS played a fundamental role: the chemical identification of the investigated commercial bioplastic items allowed the characterisation of organic compounds in bioplastic leachates (e.g., lactic acid and 1,6-dioxacyclododecane-7,12-dione), mainly ascribable to additives and non-intentionally added compounds. The study highlighted criticisms in the analysis of bioplastics leachates, but it also underlined the importance of developing and optimising methods for the study of this type of potential contaminants.

In this PhD thesis, Py-GC-MS was proven to be a powerful technique for the fingerprinting of polymer structures of interest in environmental studies. Applications can spread from the pure characterisation of polymers to more specific purposes, such as the identification of specific markers indicating the univocal presence of polymer clusters; the highlighting of the occurrence of secondary reactions; and the reliable application as a complementary technique in untargeted analyses. Moreover, thanks to the simultaneous detection of polymers and compounds, Py-GC-MS showed its potential for quick selective quantitative analyses of different analytes. The studies also demarcated the limitations in Py-GC-MS analyses. First of all, interferences may occur during pyrolysis, producing misleading results. Matrix effects and secondary reactions may hide signals or create new peaks, modifying the polymer fingerprints and affecting quantification. Moreover, calibration may be challenging due to the difficulty to recover materials and the lack of certified standard materials. Finally, depending on the aims, Py-GC-MS could need to be complemented by other techniques to obtain full informative results. For example, in the context of MP analysis, Py-GC-MS does not provide information

about the shape of particles that can be an important parameter to identify the emission sources. With a view to the harmonisation of methods and results reporting, developments aimed at outline and solve these challenges are under study. For example, the use of derivatisation reagent (mainly, TMAH) showed its potential in the minimisation of interferences, reducing the reactivity of pyrolyzates from both matrix and polymers. Moreover, preliminary reference materials for MP calibrations were tested.

In the context of environmental investigations of polymers, several techniques are currently used and each one presents values and weakness. Presumably, the integration of different techniques is successful, but this route is not always affordable by laboratories that usually opt for the optimisation of one single approach. Reproducibility and comparability are two main purposes while developing and optimising methods, even more so within environmental investigations, where the obtained data are potentially exploited for subsequent evaluations, such as risk assessments or policy supports for the development of mitigation measures and monitoring guidelines. Even though some restrictions persist, Py-GC-MS is increasingly showing its potential fulfilling these requirements, providing reliable qualitative and quantitative results in the analysis of different polymers in complex matrices.

Acknowledgements

First of all, I would like to express my gratitude to my supervisor, Prof. Daniele Fabbri. He guided me among different research topics, transmitting his huge passion for sciences and teaching me not only chemical knowledge, but also to place trust in my ideas and work. His encouragement during all my PhD have been essential.

Secondly, I am deeply grateful to Dr. Barbara M. Scholz -Böttcher for hosting me at the Institute for Chemistry and Biology of the Marine Environment (University of Oldenburg) and supervising my study on polyurethanes in Section 3.2.1. In the context of this experience, I would like to extend my sincere thanks to Isabel Goßmann for her valuable help during my staying and beyond. Moreover, the assistance provided by Anke Müllenmeister-Sawall and all the component of the Research Group was greatly appreciated. The staying was economically supported by a grant from Marco Polo Program, for which I would like to acknowledge the University of Bologna.

I would still like to acknowledge all professors, colleagues and students which contributed to the works presented in this thesis: Prof. Ivano Vassura (University of Bologna, Department of Industrial Chemistry "Toso Montanari") for his wide availability, sharing instrumentation and knowledges, and for his highly appreciated assistances and productive discussions in laboratory; Prof. Luca Valgimigli (University of Bologna, Department of Chemistry "Giacomo Ciamician") for providing standards of polydimethylsiloxanes used for the study in Section 3.1.1; Dr. Marco Capolupo (ISPRA, Rome) for the materials used for the analysis described in Section 3.2.2; Dr. Alessandro G. Rombolà, Prof. Cristian Torri (University of Bologna, Department of Chemistry "Giacomo Ciamician"), Prof. Elena Fabbri (University of Bologna, Department of Biological, Geological, and Environmental Sciences) and Valerio Giorgi for their collaboration.

During my PhD, I had the privilege to meet and collaborate with precious people, who helped and supported me in different ways. A heartfelt thanks to Dr. Rosalinda Sciacca, Beatrice Rizzi and the other colleagues and guys of the Tecnopolo of Rimini.

Beyond the academic world, my PhD was supported by people who have surrounded me with care and love. Thanks to my Family to trust me blindly, whatever my decision is and to support every step on my way. Thanks to my Campagnole, Federica, Valentina, Alice and Emily to always be ready to lighten my mind, and so my heart.

Finally, I would like to deeply thank Andrea, bedrock of my life, pure energy of my days and clean air for my breaths.